Solution of the advection equation using finite difference schemes and the method of characteristics

Sharon Gane

A thesis submitted to the University of Glasgow in partial fulfilment of the requirements for the degree of Doctor of Philosophy

September 2000

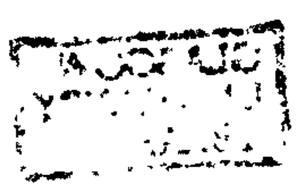

to Matt

Abstract

Numerical models are important engineering tools when considering the prediction of pollution transport in a body of water. Such a prediction is achieved by the solution of the advection-diffusion equation. At present, there exist many numerical techniques which can be used to solve the advection-diffusion equation. The major difficulty when considering undertaking such a simulation, is what method should be used to calculate the advection term. It is now accepted that the appropriate method to follow would involve, splitting up this water quality equation into two separate terms, advection and diffusion. By using this process, each term can be solved individually and the numerical difficulties associated with each term, treated separately.

This work discusses the various numerical modelling techniques which can be used to solve the advection term. Two-dimensional finite difference schemes, including QUICKEST, are compared with multi-point method of characteristics techniques. These are analysed in terms of solving advection for various distributions of concentration. The adaptation of these schemes to allow for the use of Courant numbers exceeding unity is also explored. The ultimate aim is to develop a numerical scheme which can be implemented in an industrial model.

Contents

Acknowledgements vii

Declaration viii

Chapter 1: Introduction

1.1 Introduction 2

1.2 The advection-diffusion equation 4

1.3 Thesis overview 8

1.4 References 9

Chapter 2: Literature Review

2.1 Solution of the advection-diffusion equation 11

2.1.1 The operator splitting technique 12

2.1.2 Numerical methods used to solve partial differential equations 14

2.1.2.1 Finite difference schemes 15

2.1.2.2 Methods of characteristics 24

2.2 Discussion 29

2.3 References 31

Chapter 3: One-Dimensional Finite Difference Methods

3.1 Introduction 36

3.1.1 Definitions and terms used in finite difference methods 36

3.1.2 First order upwinding 46

3.1.3 Second order central differencing 50

3.1.4 Quadratic upstream interpolation for convective kinematics (QUICK) 53

3.1.5 Quadratic upstream interpolation for convective kinematics with estimated streaming terms QUICKEST) 58

3.2 Testing of finite difference schemes using one-dimensional idealised testcases 62
3.2.1 Results for the point release of pollution 64
3.2.2 Results for the linear distribution of pollution 69
3.2.3 Results for the Gaussian distribution of pollution 73
3.3 Conclusions 76
3.4 References 81

Chapter 4: One-Dimensional Methods of Characteristics
4.1 Introduction 85
4.1.1 Basis of the method of characteristics 85
4.1.2 Linear method of characteristics 88
4.1.3 Cubic interpolation methods 89
4.1.4 Eight point method of characteristics 93
4.1.5 Six point method of characteristics 99
4.2 Testing of method of characteristics schemes using one-dimensional idealised testcases 102
4.2.1 Results for the point release of pollution 102
4.2.2 Results for the linear distribution of pollution 107
4.2.3 Results for the Gaussian distribution of pollution 111
4.3 Conclusions 115
4.4 References 117

Chapter 5: Two-Dimensional Numerical Methods
5.1 Introduction 120
5.1.1 Extension of the upwinding scheme to two-dimensions 120
5.1.2 Extension of the QUICKEST scheme to two-dimensions 123
5.1.3 Extension of the eight point method of characteristics scheme to two-dimensions 134
5.1.4 Extension of the six point method of characteristics scheme to two-dimensions 143

5.2 Comparison of the two-dimensional finite difference schemes and methods of characteristics 149
5.2.1 Diagonal testcase 149
5.2.1.1 Results using a point release 149
5.2.1.2 Results using a linear distribution 155
5.2.1.3 Results using a Gaussian distribution 162
5.2.2 Rotational flow case using a Gaussian distribution 167
5.3 Conclusions 172
5.4 References 176

Chapter 6: Inclusion of a Spatial Reachout Scheme
6.1 Introduction 179
6.2 Limitations of numerical schemes when Cr>1 180
6.3 Definition of a spatial reachout scheme 182
6.4 Testing of the spatial reachout scheme 184
6.5 Conclusions 188
6.6 References 190

Chapter 7: Implementation of the six point method of characteristics in DIADEM3D
7.1 Introduction 193
7.2 Programming the six point method of characteristics into DIADEM3D 193
7.2.1 General operation of DIADEM3D 194
7.2.2 Implementation of the six point method of characteristics 195
7.3 Application of the six point method of characteristics to the Firth of Clyde 200
7.3.1 Analysis of the model results 211
7.4 References 218

Chapter 8: Conclusions

8.1 Conclusions 220

8.2 Discussion 223

8.3 References 224

Acknowledgements

Firstly I wish to express my appreciation to the University of Glasgow for allowing me to carry out this study. I would also like thank my supervisor Professor Garry Pender for his advice during this project. I must also gratefully acknowledge the Engineering and Physical Science Research Council for providing the funding for this research.

I wish to sincerely thank Ken McColl for his incredible patience with my constant computer problems and for always fixing them. Many thanks also to Eileen, Barbara and Tessa, I appreciate all the help you gave me when I was preparing for Germany!

Also thanks to the Babtie Group Ltd for providing hydrodynamic data for this work, particularly, Yusef Kaya, James Wark and Alastair Nisbet. In addition I acknowledge, West of Scotland Water Authority, for permitting me to use data from their survey of the Firth of Clyde.

Finally thanks to Ruth, Emily, Chris, James, Alex, Samina, Graeme and everyone else who made my time in Glasgow even more fun.

Declaration

I declare that the work contained in this thesis, submitted by me for the degree of Doctor of Philosophy, is my own work, except where due reference is made to other authors, and has not been previously submitted by me for any other degree at this or any other university.

Chapter 1

Introduction

1.1 Introduction 2

1.2 The advection-diffusion equation 4

1.3 Thesis overview 8

1.4 References 9

1.1 Introduction

Public interest in the environment, and the effects society has on it, has increased in recent years. This is reflected by more stringent European legislation regarding environmental pollution which has come into effect. There are numerous directives encompassing, noise, water and air pollution, general waste management and protection of flora and fauna. These directives have compelled environmental agencies to improve existing methods of pollution management.

The issues of water pollution and waste water management are of particular significance as water is essential for life. It is widely used by society for industrial and domestic purposes most obviously in, manufacturing, sanitation, cooking, drinking and bathing. In addition, consideration must be given to marine and river environments in terms of fish and shellfish habitats. Coastal waters are also important, particularly in tourist areas, which are detrimentally affected if polluted. To this end strict regulations exist which affect how waste water treatment must be undertaken and where effluent can be discharged.

A common means of disposing of waste in the sea is by means of a long sea outfall. This transfers waste from either an industrial source or perhaps a sewage treatment plant, to a location far from the shore. The location of an outfall will affect how the waste becomes dispersed in the water, so it is important to position it where it will have the least environmental impact. The difficulty lies in how to determine the best discharge location. Civil engineering can provide an answer to this problem.

It is a role of the civil engineer to find creative solutions to the practical problems faced by society. There are two techniques which he can apply to produce an answer to the question of positioning a long sea outfall, experimental or computational modelling.

Experimental modelling plays a valuable role in hydraulic engineering because, it enables the full three dimensional flow behaviour including turbulence and mixing effects to be studied. However, there are factors which must be taken into consideration with this approach. The effect of scale is important as it is difficult to reproduce certain

parameters at a smaller scale accurately.[1] For instance the size of air bubbles or friction factors cannot be scaled down. Furthermore, laboratory modelling is costly in terms of time and resources. This is particularly significant realising that such a model is specific to a particular scenario. Altering dimensions and discharge parameters in a hydraulic model may require redesigning the model. In the case of positioning a long sea outfall, several models would have to be built to explore dispersion characteristics at different locations. This can prove costly and time consuming.

A numerical model simulates real processes by solving a set of equations, which describe any particular process. One advantage a numerical model has over an experimental model is the fact that it is considerably more portable. Many parameters can be simply adjusted in the program, which makes it very useful from an industrial perspective.[2] Several positions of an outfall can be considered and compared quickly, once the basic model has been developed. The major benefit of this is that it can then be easily adapted for another similar project. This makes it efficient in terms of both time and cost. However, it is also true that in the development of a numerical model many assumptions are made to facilitate the process, hence the mathematics can become oversimplified.[1] This is improving as approximate solution methods and our understanding of the physical processes develop, but it is still a concern.

It would be desirable, during model development, to have both a numerical model and experimental analysis for comparison and calibration purposes. Unfortunately, in practice, it is very difficult to obtain good experimental data.

This work is concerned with the development of a computational model which can be used to predict the movement of a contaminant in a body of water. It does this by solving the two-dimensional advection-diffusion equation. It includes the analysis of well known finite difference schemes, which are used as benchmark tests for the methods of characteristics.

1.2 The advection-diffusion equation

The advection-diffusion equation is used to predict the movement of a pollutant in a body of water. The accepted derivation of this simple equation is as also used by Abbott and Basco.[3] The one-dimensional form of the equation is given as equation (2.1):

$$\underset{(i)}{\frac{\partial \phi}{\partial t}} + \underset{(ii)}{u\frac{\partial \phi}{\partial x}} = \underset{(iii)}{D_x \frac{\partial^2 \phi}{\partial x^2}} \qquad (2.1)$$

Term (i) Local concentration gradient

Term (ii) Advection Term

Term (iii) Diffusion Term

The equation is based on the fundamental principle of conservation of mass. Figure (2.1) depicts a three-dimensional infinitesimal control volume of fluid, in which the pollutant is completely dissolved. Consider that the flow rate per unit area of solute into the control volume, in the x-direction, is defined as ζ.

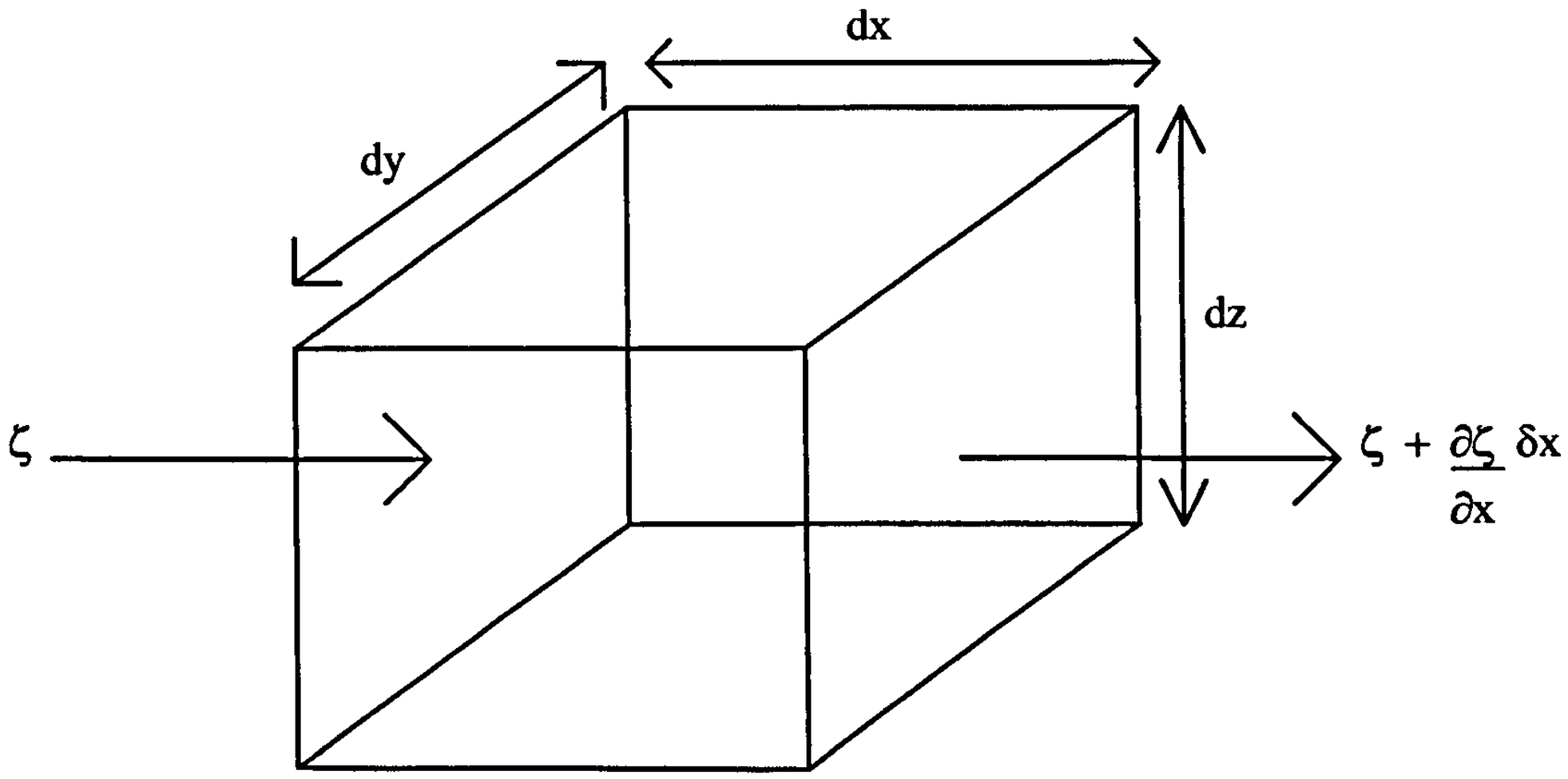

Figure (2.1): Control volume of a fluid

The total mass entering the control volume in the x-direction, M_{in}, is as given as equation (2.2), and the total mass leaving is as defined as equation (2.3),

$$M_{in} = \zeta \delta y \delta z \tag{2.2}$$

$$M_{out} = \left[\zeta + \frac{\partial \zeta}{\partial x}\delta x\right]\delta y \delta z \tag{2.3}$$

To satisfy the conservation of mass equation, the difference between the mass entering and leaving the control volume must be equal to the rate of change of mass solute within the control volume. Thus the net mass flow rate into the control volume in the x-direction M_{tx} is defined as:

$$M_{tx} = M_{in} - M_{out} \tag{2.4}$$

Substituting equations (2.2) and (2.3) into (2.4) gives:

$$M_{tx} = \zeta \delta y \delta z - \left[\zeta + \frac{\partial \zeta}{\partial x}\delta x\right]\delta y \delta z \tag{2.5}$$

which simplifies to:

$$M_{tx} = -\left[\frac{\partial \zeta}{\partial x}\delta x\right]\delta y \delta z \tag{2.6}$$

Similarly for the y and z-directions, where ξ and ε are the corresponding mass flow rates per unit area of solute:

$$M_{ty} = -\left[\frac{\partial \xi}{\partial y}\delta y\right]\delta x \delta z \tag{2.7}$$

$$M_{tz} = -\left[\frac{\partial \varepsilon}{\partial z}\delta z\right]\delta x \delta y \tag{2.8}$$

The mass flow rate has two components namely advection and diffusion. Advection is the physical process whereby the pollutant is carried downstream with the streamflow velocity. If the velocity field is constant, the pollutant does not alter in shape or peak concentration. The diffusion term describes the mixing of the pollutant in the flow by Brownian motion on a molecular scale or turbulent eddies at the macroscopic scale.

Thus:

$$\zeta = u\phi - D_x \frac{\partial \phi}{\partial x} \qquad \xi = v\phi - D_y \frac{\partial \phi}{\partial y} \qquad \varepsilon = w\phi - D_z \frac{\partial \phi}{\partial z} \tag{2.9}$$

where u,v,w are velocities in the x, y and z-directions respectively and D_x, D_y and D_z are the corresponding molecular diffusion coefficients. The factor ϕ represents the pollution concentration.

The sum of the net mass flow rates in each direction gives the total rate of change of mass of solute in the control volume:

$$\frac{\partial \phi}{\partial t} = -\frac{\partial}{\partial x}\left(u\phi - D_x \frac{\partial \phi}{\partial x}\right) - \frac{\partial}{\partial y}\left(v\phi - D_y \frac{\partial \phi}{\partial y}\right) - \frac{\partial}{\partial z}\left(w\phi - D_z \frac{\partial \phi}{\partial z}\right) \tag{2.10}$$

This can be rearranged into the common form of the three-dimensional advection-diffusion equation:

$$\frac{\partial \phi}{\partial t} + u\frac{\partial \phi}{\partial x} + v\frac{\partial \phi}{\partial y} + w\frac{\partial \phi}{\partial z} = D_x \frac{\partial^2 \phi}{\partial x^2} + D_y \frac{\partial^2 \phi}{\partial y^2} + D_z \frac{\partial^2 \phi}{\partial z^2} \tag{2.11}$$

It is obvious by inspection of equation (2.11), that the advection process is governed by the velocity. If the velocity is high then advection will dominate the pollution transport. Conversely, if the velocity is very low or static, then the diffusion process will

determine the motion of the pollutant. The proportion by which advection and diffusion contribute to the pollutant transport can be defined in terms of the Péclet number, Pe.

The Péclet number is dimensionless and is defined in one-dimension as equation (2.12). The factor L, is the length of the flow domain in metres.

$$Pe = \frac{|u|L}{D_x} \qquad (2.12)$$

At low Péclet numbers, diffusion is the dominant process. Under these circumstances, local velocity would be small compared to the co-efficient of diffusion. Correspondingly, when the value is high, advection controls the transport.

1.3 Thesis overview

The aim of this study is to analyse finite difference schemes and the method of characteristics in the solution of the advection equation.

This chapter presents the derivation of the advection-diffusion equation.

Chapter 2 discusses methods which have previously been explored and indicates some of the limitations of different schemes.

Chapter 3 explains the concept of the finite difference approach. It also includes the full derivation of four popular methods in one-dimension. These schemes are compared using idealised testcases.

Chapter 4 details the method of characteristics in one-dimension. It describes the basis of this numerical approach and includes complete derivation of four schemes. These are also compared using the same idealised tests used in Chapter 3.

Chapter 5 describes the extension of the most favourable finite difference schemes and methods of characteristics, derived in the previous chapters, from one to two dimensions. The two-dimensional methods are applied to more complicated testcases.

Chapter 6 explores the use of the spatial reachout approach to allow larger time increments to be used by the method of characteristics. This method is adapted to allow it to be applied to the QUICKEST finite difference scheme.

Chapter 7 explains how the six point method of characteristics is implemented into an existing industrial model. The procedure followed and an example of how this adapted model can be applied to a realistic test is discussed.

Whilst complementary to other work previously carried out in numerical modelling, this work is new in the increasing of the time step for the methods investigated and also in its implementation to DIADEM3D.

1.3 References

1. Falconer, R.A., "Flow and Water-Quality Modeling in Coastal and Inland Water", *Journal of Hydraulic Research*, 1992, 30(4), 437-452.

2. Greenberg, J.B., "Operator splitting methods for computation of reacting flows", *Computers & Fluids*, 1983, **11**(2), 95-105.

3. Abbott, M.B. and Basco, D.R., *Computational Fluid Dynamics; An Introduction for Engineers*. 1989: Longman Scientific and Technical.

Chapter 2

Literature Review

2.1 Solution of the advection-diffusion equation 11

2.1.1 The operator splitting technique 12

2.1.2 Numerical methods used to solve partial differential equations 14

2.1.2.1 Finite difference schemes 15

2.1.2.2 Methods of characteristics 24

2.2 Discussion 29

2.3 References 31

2.1 Solution of the advection-diffusion equation

There are a number of different numerical techniques which can be used to solve the hydrodynamic or water quality equations in any given situation. The main general categories are explicit and implicit numerical methods.

Explicit schemes use data which is already known, at the present time step, to calculate conditions at a future time. Although these methods are relatively simple to set up, the time step that can be used in the solution is governed by a stability criterion, *i.e.* the Courant number, such that for a specific spatial increment, the time step must be less than some limit imposed by this constraint. This can lead to very small time increments, which inevitably increases the computer time, so the calculation can take longer.

Implicit schemes involve the solution of equations at several points simultaneously.[1, 2] This requires that both known and unknown quantities are used in the solution process. It is a complex method to set up and, because very large matrix manipulations are necessary at each time step, the computer time per time step is high compared with explicit schemes.[3, 4] As large time increments can be used, the truncation error is larger than for explicit methods, and hence implicit methods may not give as accurate a solution to the governing equations. However, using larger time steps will also reduce overall computational time, provided the numerical scheme remains stable.

A choice must be made between, explicit schemes which have time increments limited by stability, or the more complicated but unconditionally stable implicit schemes. In this work it was important to preserve numerical stability, therefore explicit schemes were developed. The issue of the time increment connected with these methods is also addressed.

2.1.1 The operator splitting technique

When the advection-diffusion equation is used in the modelling of a river or coastal environment, it will encounter a range of velocities. As the velocity changes, the Péclet number will increase or decrease indicating that the dominant transport process in the flow is changing between advection and diffusion.[5, 6] Solution of this equation, particularly under such complex varying flow conditions, is a difficult task.

Cao and Wei[7] state that, " Any numerical algorithm which maintains a Eulerian framework has potential deficiency of numerical dispersion and may lead to an oscillating solution." This means that when the governing equations are discretised using a grid which is fixed in space, the solution can produce spurious results. It is generally accepted that these numerical instabilities arise from the solution of the advection term.[6-12] Obviously, this is a particular concern in situations where advection dominates the transport processes.[13] To limit such instabilities, it has been suggested that the advection-diffusion equation should be solved using an operator splitting technique.[6, 8, 11, 14-18]

The benefit of using an operator splitting approach is that it allows the separate solution of the advection and diffusion terms. This is an important advantage as it is difficult to find a single numerical scheme which will solve both terms with comparable accuracy.[8] Solving the terms separately allows the optimum numerical scheme to be used for each process.

Benque *et al*[14] promote the splitting up of these terms because the advection term is hyperbolic, whereas the diffusion equation is parabolic and therefore requires different numerical boundary conditions.[19, 20] This stepped approach not only separates these terms but further splits the solution into x and y-directions and also propagation. The equations are solved in succession in the order, advection, diffusion then propagation.

Holly[21] discusses a similar one-dimensional operator splitting scheme using the method of characteristics to solve the advection term. This is then used as an initial condition for the solution of the diffusion step, and subsequent source or sink terms are

solved using both the advection and diffusion fields. The calculations are sequential over a single time step.

Cao and Wei[7] also advocate this method and have developed a fractional step method based on operator-splitting in three dimensions. The advection term is solved by the method of characteristics and the diffusion term by use of an explicit finite difference scheme. This approach differs from the others mentioned as it claims to simultaneously solve advection and diffusion as opposed to sequentially. This, although complex, is much closer to the way the processes occur in reality.

Lin and Falconer[22] compared the use of an operator splitting approach with solving both advection and diffusion as part of the same equation. They use forms of the QUICKEST[23] scheme to solve the advection terms during the split tests. The results of their standard rotational testcases indicated that there was no significant difference between the results obtained using the split and non split approaches. Both were observed to be stable, non-oscillatory and to closely predict the analytical solution. A field test in the Humber Estuary was also carried out. These results demonstrated that, in this case, the operator splitting method was beneficial. This was due to the fact that the ULTIMATE[24] limiter, was applied to the advection term only, hence the extent of the limiting was independent of the physical dispersion-diffusion term.

The operator splitting approach is also used in the solution of other equations. Greenberg[25] describes the difficulty with modelling the chemistry of reacting flows. In this situation the main difficulty is "stiffness", which is caused by the wide range of time scales associated with reactive collisions between molecules. These reacting flow equations consist of both parabolic and hyperbolic terms, as does the advection-dispersion equation. He found that by splitting the equation and solving terms individually using appropriate numerical schemes, the problem of stiffness was overcome.

It is clear that in situations where the governing equations consist of a mixture of parabolic and hyperbolic terms, it is logical to use an operator splitting technique to solve the equations separately. This is particularly useful if there is a dominant process

within the equation, as in a high velocity flow where advection governs contaminant transport.

2.1.2 Numerical methods used to solve partial differential equations

It is relatively simple to model one-dimensional transport, but very difficult to model it accurately. The main reason for this has already been indicated as numerical errors stemming from the solution of the advection term in the water quality equations. To this end civil engineers have been striving to improve the approximation of this term, by developing complicated numerical schemes.

One of the most popular techniques applied to the solution of hydrodynamic and water quality equations is the finite difference method.[12, 22, 23, 26-28] This approach uses Taylor series expansions to derive finite difference representations of partial differential equations.[29-31] These finite difference equations solve the water quality equation, using values of dependant variables at specific points on a space-time grid, which represents the continuous physical domain. This technique is explained in detail in Chapter 3.

The finite element method can also be used in water quality modelling.[32-34] In this approach the domain, over which the partial differentials are applied, is split into a finite number of sub-domains. These sub-domains are termed, finite elements. The variation of a dependant variable over each element is calculated and these are used collectively to give a solution over the entire domain. This approach is more complicated than the finite difference scheme and the mathematics will not be discussed here. However, it is interesting to note that despite its relative complexity it is widely used in the solution of partial differential equations. Although it is used occasionally in pollution modelling, the more popular usage is in structural engineering.

A third commonly used approach in numerical modelling is the finite volume technique, which is viewed as a combination of the finite difference and finite element methods. Like the finite difference scheme it develops numerical equations at a specific location

on a grid, based on values at adjacent points. It also uses some of the implementation methods used in finite elements.

Another, quite different, widely used approach is the method of characteristics. This is a popular method because the equations used are fairly easy to derive and also because they exhibit the, "essential physical wave behaviour"[35], as a characteristic contains the time-space path along which information travels. They differ from finite difference approaches in that they employ interpolating polynomials to calculate the concentration at the foot of the characteristic. This value is then advected forward in time and space along a characteristic curve. A detailed analysis and derivations of various method of characteristics schemes are included in Chapter 4.

In this study the finite difference and method of characteristics approaches have been developed, analysed and compared. However, as indicated by the mention of finite elements and finite volumes, they are not the only approaches which can be used in computational fluid dynamics or numerical modelling in general.

2.1.2.1 Finite difference schemes

One of the most basic methods which utilises finite differences in the solution of hydrodynamic and water quality equations is the box model. Jeffries and Steele[36], developed a box model to predict concentrations of caesium in the Irish Sea. The sea is split into six compartments across which water transfer occurs. The solution uses a system of linear first order differential equations using a semi-implicit Crank-Nicholson scheme to represent the box model. Mean concentrations were calculated in each compartment and compared with actual data. The greatest drawback with this approach, as is often the case in water quality modelling, was simulation of the hydrodynamics. The flow pattern was altered regularly to improve correlation between predicted and actual concentrations. Forms of the box model are used in modelling of radionuclides, but seldom in general pollution modelling.[37]

Although the concept of box models is simple, it has not been pursued in numerical modelling. However, finite differences have been developed extensively.

Quadratic upstream interpolation methods

In 1979, Leonard[23] realised that the favoured upwind and central differencing finite difference schemes, used to model convection, were severely limited in their numerical accuracy. He observed that upwinding, although numerically stable, suffered from significant numerical diffusion.[38, 39] This meant that, although the predicted solution was smooth, it was squashed such that the peak was reduced and the solution spread out spatially. Central differencing was subject to numerical instability, which is observed as spurious oscillations in the solution. In fact it is stated by Abbott and Basco[31] that, in the case of advection only conditions, central differencing is unstable for all Courant numbers.

More recently, Karpik and Crockett[41] reinforced these observations with comparisons between upwinding and central differencing with other higher order schemes. In the simulation of one-dimensional advection of a Gaussian distribution, upwinding is shown to produce a stable numerical solution, however, it severely underpredicts the solution. Despite this failing it does prove to be superior to the central differencing scheme, which exhibits undershooting. Although these methods are still in use, they are generally only used as benchmark schemes for comparison with new approaches.

These inadequacies prompted Leonard[23] to develop a quadratic upstream interpolation method, which would overcome these errors and accurately solve the advection term. He first derived the one-dimensional, quadratic upstream interpolation method for convective kinematics, QUICK, which was then adapted to create QUICKEST. The latter is QUICK with estimated streaming terms and can be used to model conditions influenced by unsteady flows. Although for unsteady flows it is necessary to estimate variation in concentration through time, QUICKEST is also an improved form of the original equation in terms of numerical accuracy and dispersion.

Testing of the schemes in one-dimension showed that both QUICK and QUICKEST predicted a solution closer to the analytical result than either upwinding or central differencing. This was also confirmed in tests by Falconer and Liu[28], who compared QUICK to four other numerical schemes in a one-dimensional test. The test considered the advection process only, using, a regular grid of spacing 200m, a time step of 100s and a constant flow of 0.5m/s. The other methods included the implicit Crank-Nicholson, implicit and explicit upwinding and a six point method of characteristics approach developed by Komatsu *et al*[20]. The results after 400 time steps were analysed and it was concluded that QUICK performed better in terms of accuracy and numerical stability than all of the other schemes with the exception of the method of characteristics. Although this approach performed better, the authors advocated QUICK due to its simpler derivation and application. However, the Courant number in the test was only 0.25 and does not indicate the behaviour of the schemes at higher Courant numbers. In accordance with Leonards[23] observation of the limitation of the Courant number on QUICK, the results from Falconer and Liu[28] indicate spurious undershoot in the QUICK solution. This makes it difficult to fully appreciate why this approach was considered the optimal method in this case.

The QUICK scheme was further developed in two-dimensions by Falconer and Liu[28] and also by Kaya[42]. In the first case, QUICK was compared with experimental results of a laboratory test. This consisted of a constant inflow into a tank, which then passed over a weir. The results were encouraging and demonstrated good consistency with the actual data.

Although QUICK appeared to be a useful numerical tool, it was only applicable under certain circumstances. The flow must be constant and it was also observed that as the time step was increased, the predicted solution began to show signs of numerical diffusion and instability.[38, 39, 43] It was with this in mind that QUICKEST was developed.

QUICKEST[23] uses a more complicated derivation than its predecessor but is more flexible. It avoids the problem of numerical errors associated with QUICK, central differencing and upwinding, when considering pure advection.[39] The main advantage

is that, QUICKEST is shown to be numerically stable and accurate for Courant numbers from zero to one for convection only conditions. Additionally, the ability to apply this method to unsteady flow conditions is beneficial.[23] It is interesting to note that although QUICKEST is clearly an improvement on QUICK, it has not been as widely applied.[44] This is perhaps due to the difficulty of implementation associated with its expansion to two-dimensions. However, practical flow problems are often unsteady and multi-dimensional which makes this development essential.

In 1984, Davies and Moore[45] presented a third order accurate numerical method to solve two-dimensional flow around rectangles in infinite domains. The scheme used is a multi-dimensional form of Leonard's[23] one-dimensional QUICKEST, which as explained previously, circumvents the difficulties of instability and numerical diffusion associated with upwinding and central differencing schemes.

This version of the two-dimensional scheme is effectively the one dimensional Leonard equation, applied to all four faces of a control volume. The cross term derivatives are neglected, which reduces the temporal accuracy, but not the spatial accuracy, when calculating pure advection. However, the authors use very small time steps and hence claim, that the omission of these terms has a negligible effect on the numerical results. This concurs with Leonard[23] and Abbott and Basco[31], who both show that there is a region of stability for pure advection when using QUICKEST. If there is no physical diffusion the Courant number and thus time step must be very small. In fact the authors use a value of 0.05s, which ensured that the Courant number was always less than one, which satisfies the condition set by Leonard.

The two-dimensional QUICKEST equation, described by Davies and Moore[45], was also used by Falconer *et al*[46]. This study set out to test the QUICK, QUICKEST and third order upwinding schemes, using data from Bridlington Bay in North Yorkshire.

The bay was modelled in the first instance using a coarse grid, which was then used to obtain the boundary conditions for a much finer grid placed in the immediate vicinity of an outfall in the bay. Both QUICK and third order upwinding gave very similar results, demonstrating good correlation with the actual data. However QUICKEST did not

perform as well as expected due to the fact that the method applied by Davies and Moore[45], was followed, thereby excluding the cross-terms described by the Taylor series expansion. This strengthens the concept, that all terms from the Taylor series expansion must be used in the application of multi-dimensional QUICKEST.

This hypothesis is reinforced by further work in the extension of QUICKEST from one to multi-dimensions. Leonard and Niknafs[47] derivation stemmed from the solution of a two-dimensional third order polynomial. Ekebjærg and Justesen[48] and Vested *et al*[49] give a more complete description of their derivation, which produces the same set of equations as Leonard and Niknafs.

Ekebjærg and Justesen[48], and Vested *et al*[49] both used the same approach to extended the scheme to two and three dimensions. This required use of a control volume approach in combination with a Taylor expansion of the time derivatives. They solve for the case of pure advection, in which source terms are ignored and the flow is assumed to be steady over the control volume. The temporal derivatives are converted to spatial ones by differentiating twice with respect to time and substituting into the convection equation.

Advection terms are then discretised using central differencing and all terms from the Taylor expansion up to third order are retained. Next the authors discretise the remaining spatial derivatives using upstream centred Taylor expansions to a condition of third order accuracy.

As the scheme was explicit, a stability analysis on the extended QUICKEST scheme was executed, using Fourier series to obtain functions of the Courant numbers in the form of contour plots. It revealed that as the Courant number increased, stability decreased, as expected for explicit schemes. The influence of physical diffusion expanded the stable region to a certain extent but then restricted it. Hence it was concluded that, the length of the time step was a major factor in the stability analysis and must be limited. In fact the authors defined stability to be limited by the condition that, the sum of the Courant numbers in each direction must be less than 0.5, for the case of pure advection.

The scheme was compared with data from a groundwater flow test and found to give good correlation.

Balzano[12] has recently developed a two-dimensional scheme based on an extension of the one-dimensional QUICKEST equation. It is very similar to Leonard's equation, in fact in one-dimension the equations are the same, but it is derived in a different way. This new scheme, which is second order accurate, is known as MOSQUITO, *i.e.* modified second-order QUICKEST scheme for two-dimensional advection. As is the case for uni-dimensional QUICKEST, this new approach can be used for unsteady state problems. In tests with other time centred and implicit QUICK schemes, the new approach fared better in terms of stability. However no direct comparison was made with the original two-dimensional QUICKEST equation.

QUICKEST is also compared with other numerical schemes in the solution of the advection equation using, classical two-dimensional tests and also in the San Francisco Bay by Gross *et al.*[50] The other schemes are, upwinding, leapfrog-central[51], a multi-dimensional positive-definite advection transport algorithm (MPDATA) developed by Smolarkiewicz[52], a Eulerian-Lagrangian method (ELM) used by Casulli[53] and a Lax-Wendroff scheme called LWlim. Some details of these alternative techniques are included here.

The leapfrog-central approach as applied by Blumberg and Mellor[51], utilises central differencing in conjunction with leapfrog time stepping. This hybrid scheme produces less numerical damping when compared with forward differencing, but does exhibit grid scale oscillations in the solution, which is expected when using central differencing. The authors minimised this instability by applying an Asselin filter, which smoothes the solution.

Smolarkiewicz[52] developed a technique based on upwind differencing. Initially, upwinding is applied to solve the algorithm over the first time increment. In each subsequent iteration the upwind scheme is reapplied using a specially defined antidiffusive velocity field. This approach gives improved results in terms of numerical diffusion when compared to upwinding alone, but does produce spurious oscillations.

This problem was later addressed in 1990[54] but in this comparison the original method was used.[50]

The semi-implicit Eulerian-Lagrangian method proposed by Casulli[53] is designed such that the stability of the scheme is independent of velocity. Explicit upwinding is used to solve the velocity dominated advection term. The advantage of this approach is that larger time increments can be applied without compromising stability.

The final approach, LWlim combines a Lax-Wendroff scheme, based on work by Hirsch[55] with a flux limiter. The Lax Wendroff approach is second order accurate and, as is typically the case with schemes of this order, produces oscillations in the solution of the advection equation. To reduce these "wiggles" the flux limiter, Superbee, was developed by Roe[56]. In comparisons with upwinding and Lax-Wendroff without the limiter, this new approach gives more accurate results.

The standard cases used are, the advection of a square wave and rotation of a Gaussian cone. The first test utilised a constant velocity field of 1m/s in the x and y directions with a Courant number of 0.25. It is a complicated test due to the sharp concentration gradients involved. The LWlim approach produces the closest approximation to the analytical solution. QUICKEST, as expected, demonstrates some spurious oscillations in the result. This is a recognised disadvantage with this approach. The leapfrog and MPDATA schemes produce much more significant oscillations in the solution. The upwinding and ELM schemes produce severely diffused though stable results. However, the ELM was also applied using a Courant number of 2.5, producing a numerically accurate and stable result.

The rotational test challenged the schemes in a different way as it consisted of a spatially varying flow. However, the movement of the Gaussian cone is much easier to simulate as the concentration gradient is much less severe than the previous case. Interestingly, QUICKEST and LWlim again produced the most numerically accurate results. Further to this, it was concluded from the analysis of the San Francisco Bay that these two methods were the most favourable for the solution of the advection equation in shallow estuaries.

The preference for the QUICKEST approach is backed in a discussion by Wallis and Manson[57]. They raise the point as to why this method has not been more widely applied since its introduction by Leonard. This is a valid statement and is one of the reasons why its application is explored in this study.

Limitations of quadratic upstream interpolation methods

It has been shown in the literature that although quadratic approaches are an improvement on other lower order schemes, they do have their limitations. Their main drawback with respect to this research is the time increment. It is expected that as the scheme is explicit it will be restricted by the Courant number, which has a maximum value of unity if stability is to be maintained. This has been addressed to some extent in the literature.

Manson and Wallis[58] present an algorithm to solve pure advection when the Courant number is greater than one. The proposed scheme is called DISCUS *i.e.* domain of influence search for convective unconditional stability. It is one-dimensional and uses the QUICKEST approach in a Lagrangian treatment of advection. It differs from other Lagrangian schemes in that, it uses the method of characteristics to determine the location of the control volume as opposed to determining the grid points from which concentrations are interpolated.

The errors in numerical accuracy or diffusion stem from the number of time steps required in the calculation. Fewer interpolations produce smaller errors due to the rounding of the truncation error. This approach is similar to the spatial reachout technique adopted in some method of characteristics schemes.

This scheme was adapted to solve the two-dimensional advection-diffusion equation using a streamtube approach.[59] It may be described by considering a basic rectangular channel, which is split up into streamlines. Longitudinal advection occurs within each individual streamtube and the diffusion process takes place between streamtubes. This appears to be one dimensional advection with transverse diffusion. However, the

mathematical formulation of the scheme would enable transverse advection to be included.

A second limitation of the QUICKEST approach is the solution of sharp concentration gradients. It is not alone in this restriction and methods of overcoming this problem have been widely discussed. This has led to the development of schemes which limit oscillations in the solution and preserve monotonicity. Examples of these are universal limiters or total variation diminishing schemes, TVD.

Leonard[24, 60] derived a universal limiter technique which he applied to QUICKEST. He developed a limiter called, ULTIMATE, which basically replaces variables which would cause monotonicity to be compromised, with others which preserve it. This technique was adopted by Lin and Falconer[22, 61] in tidal modelling and also by Wallis and Manson[62] who used this limiter in conjunction with the DISCUS scheme. Comparisons of various numerical schemes with and without the limiter are discussed.

Leonard[24, 60] demonstrated that using ULTIMATE with a numerical scheme helped remove spurious oscillations from the solution. This is less significant in cases where the concentration gradient is less steep. It must also be noted that there are certain restrictions using a limiter. In the cases of ULTIMATE QUICKEST and DISCUS, diffusion of the solution is observed. This effect must be considered in addition to the improved monotonicity of the solution when considering its application.

An alternative TVD scheme is the previously mentioned Superbee limiter developed by Roe[56]. He found this to improve numerical stability when used in conjunction with the Lax Wendroff scheme. Hirsch[55] also tested this limiter, but with a second order upwinding scheme. He discussed the results of one-dimensional advection of Gaussian and square concentrations using first and second order upwinding. The latter was also tested using the minmod and van Leer limiters.

The results of both tests using upwinding gave the normal, numerically stable but diffused solution. Second order upwinding typically exhibited overshoot and undershoot of the solution. All of the limiters removed these oscillations from the

second order solution. However, the minmod approach also caused the solution to become smoothed, such that it resembled the first order upwinding result. The van Leer scheme was an improvement, but in the case of the square distribution, the extrema were not defined. Superbee simulated the closest solution to the ideal prediction. This was particularly clear in the case of the square distribution as the gradients remained steep and the oscillations were flattened. Unfortunately this is less suitable for Gaussian distributions which are more curved.

2.1.2.2 Method of characteristics

There are several methods of characteristics schemes in use. The classical scheme is the Holly-Preissmann[13] method, developed in 1977, which explicitly calculates future concentrations provided the Courant number is less than one. It solves the advection-dispersion equation in one and two dimensions using, two point, fourth order accurate, higher order interpolating polynomials. The most significant complication with this method is the fact that both concentration and the corresponding spatial derivatives must be calculated in each time step. This is relatively easy to do in one-dimension but extremely complex in two.

The one-dimensional testing of this approach for the case of pure advection, for Courant numbers less than one, showed excellent correlation with analytical solutions. The solution, although subject to some numerical diffusion, is numerically stable and accurate which are great assets for a numerical scheme.

The approach utilises concentrations and their spatial derivatives at only two points on a fixed grid, as shown in Figure (2.1). This was observed by the authors to reduce the computational time compared with other higher order schemes although if the Courant number exceeded unity the method was unstable.

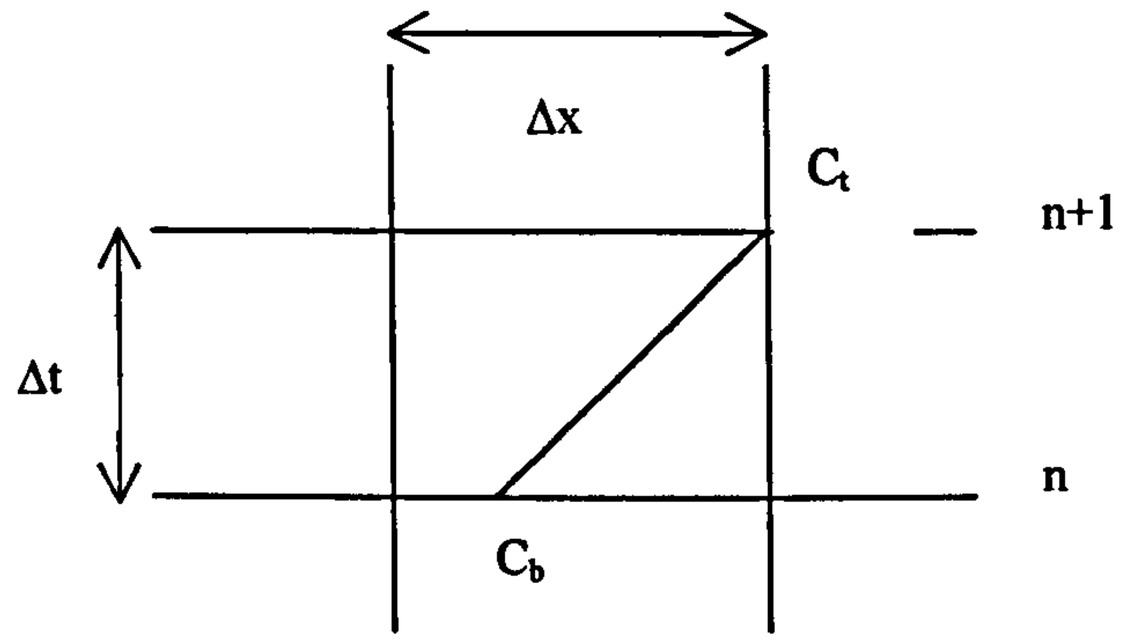

Figure (2.1) Grid used in classical 1D Holly-Preissmann scheme

As the scheme is relatively easy to derive in one-dimension, it has been further developed by other authors seeking to find a solution to the problem of the limit of the Courant number. However, development in two-dimensions has been limited and other methods have been formed, due to the difficulty of advecting both concentration and the spatial derivatives simultaneously.

In 1988, Yang and Wang[63] described an improved hybrid solution process for the advection-dispersion equation in one-dimension, based upon the Holly-Preissmann scheme. They demonstrate that this enhanced scheme can circumvent the problem of instability associated with Courant numbers greater than one.

The new scheme uses essentially the same quadratic equations used by Holly-Preissmann, but uses different Courant number based factors to allow for a varying time step. This technique is known as spatial reachout. It allows the shifting of the interpolating polynomials to new grid points based on the Courant number. This is illustrated by Figure (2.2).

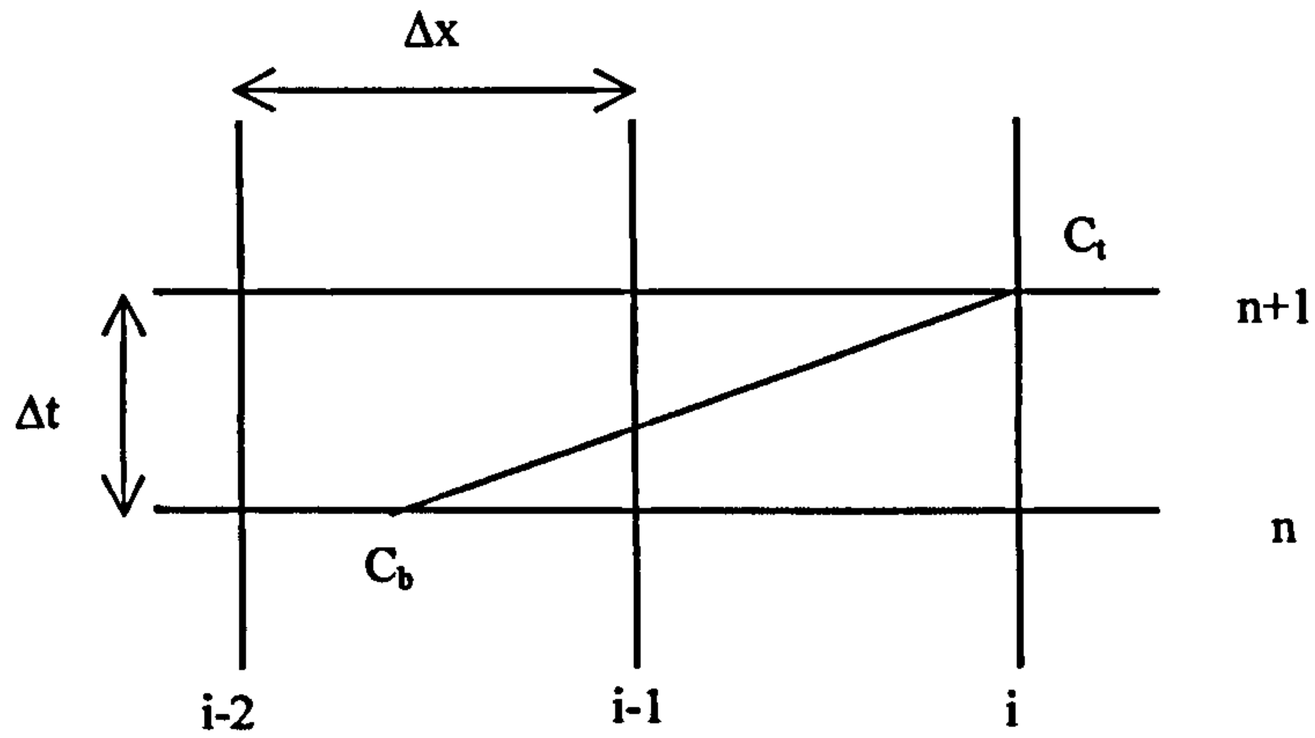

Figure (2.2) Grid used in spatial reachout scheme

The authors applied this scheme to a concentration of pollutant in an infinitely long channel. Courant numbers up to four were considered, the results of which were almost identical to the exact solution.

This scheme which alleviates the time step restriction suffered by explicit computational models, is also discussed by Chintu[3, 64]. In fact he describes, in detail, a multimode method of characteristics which allows a different scheme to be applied depending on each specific situation, contained within one numerical model. In this case the scheme uses implicit, temporal reachback, spatial reachback, spatial reachout and classical schemes.

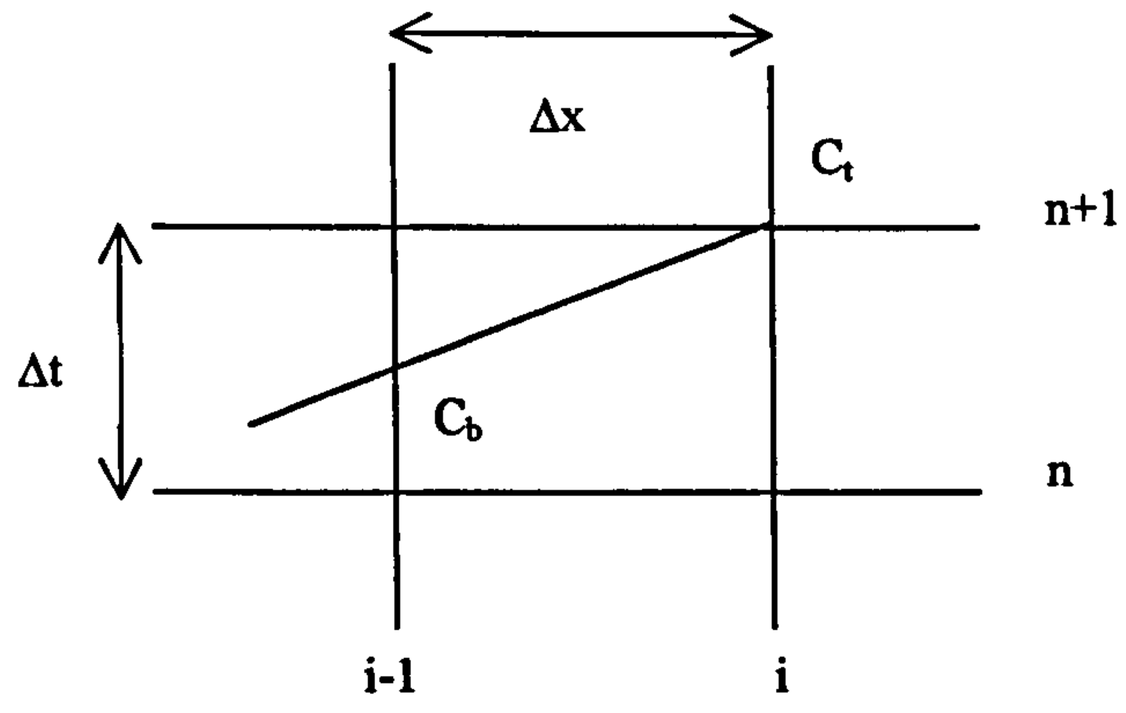

Figure (2.3) Grid used for implicit interpolation

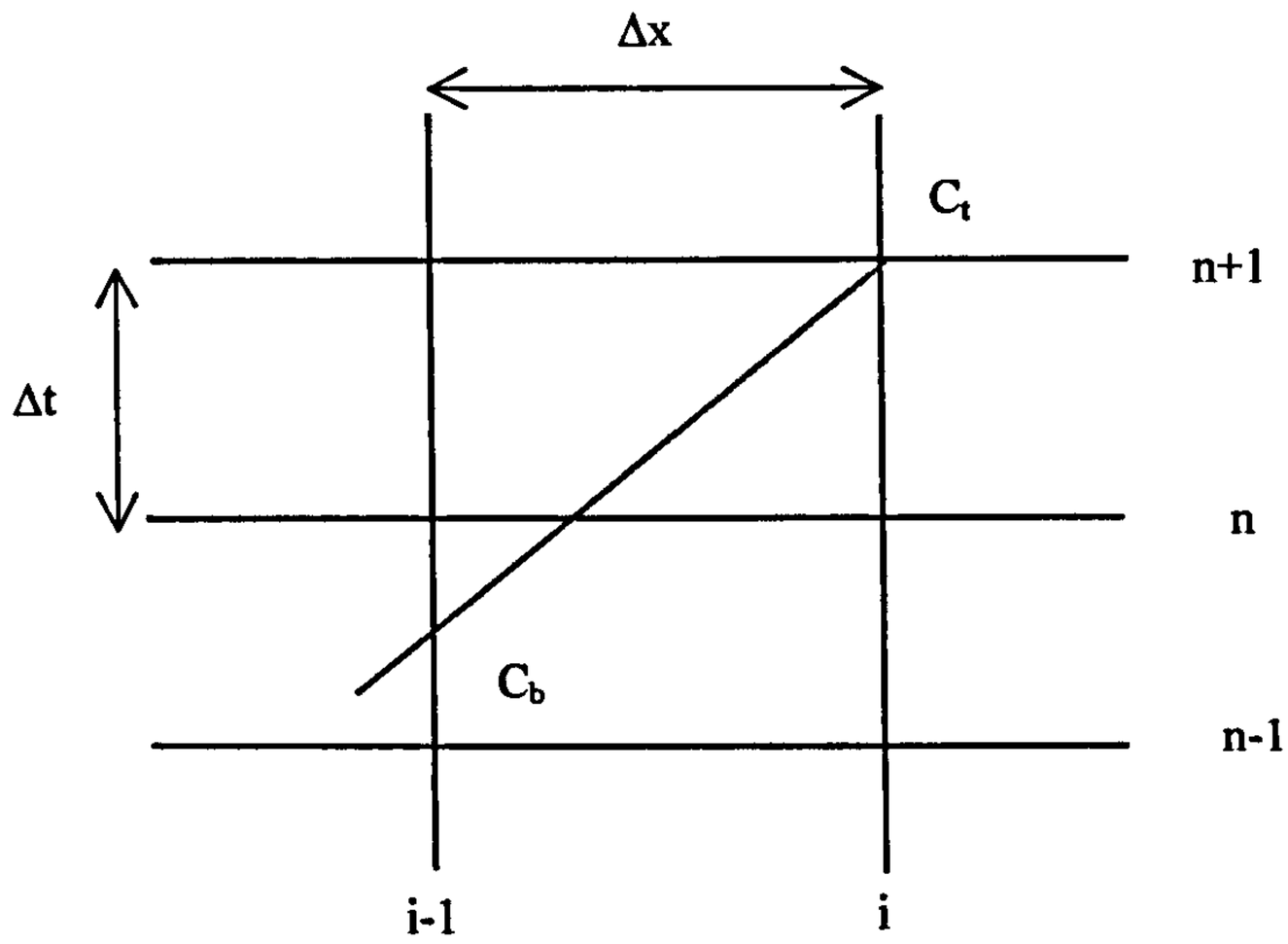

Figure (2.4) Grid used for temporal reachback interpolation

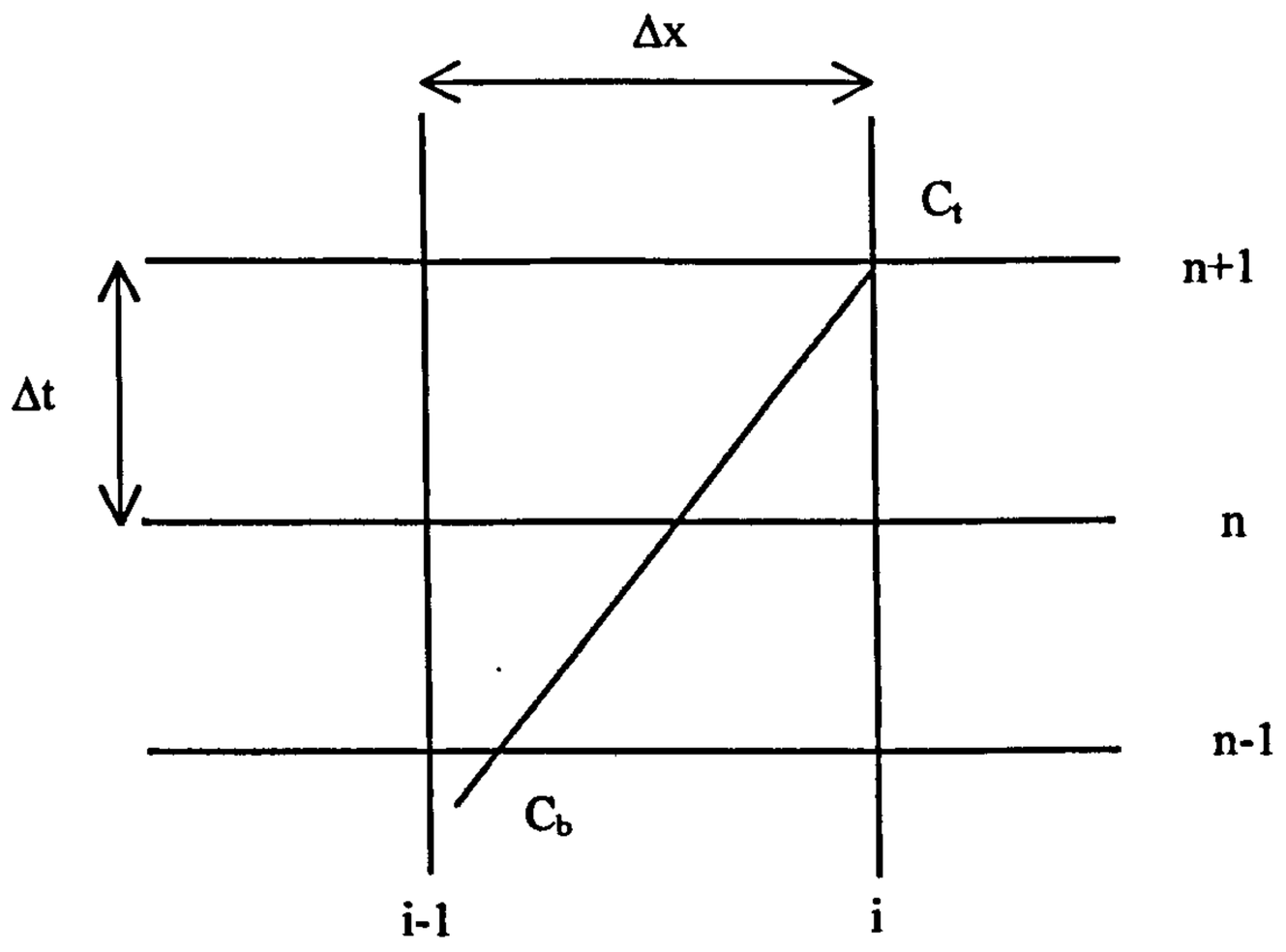

Figure (2.5) Grid used for spatial reachback interpolation

He demonstrates that the implicit mode of the scheme is best suited to higher Courant numbers and faster flow, whereas spatial reachback is optimum for very low Courant numbers. As channel flow will vary depending on the cross-section and bed formation, this illustrates the benefits of using such a hybrid scheme.

The temporal and spatial reachback approaches were also adopted by Goldberg and Wylie[35]. They address the various problems associated with the solution of the method

of characteristics using a time-line interpolation approach, to solve the linear waterhammer equations.

Reachback time-line interpolation involves the projection of a characteristic back before the current time step, Figure (2.4). This results in the reduction of numerical diffusion associated with the process of spatial interpolation. The implicit method requires projection of the characteristic into the present time interval, Figure (2.3). Implicit methods have the advantage of being very efficient in a temporal sense, because large time increments can be used. However, the use of large time steps can increase numerical diffusion and dispersion.

The general conclusion made by the authors is that the temporal reachback scheme is a viable alternative to the spatial method, as it experiences less numerical diffusion. However, the fact that the Courant restriction is relaxed in implicit schemes causes stability to be relinquished.

Glass and Rodi[65], extended the Holly-Preissmann scheme and developed the equations to derive a practical two-dimensional solution. The scheme is complex and subsequently requires high computer time when compared with upwinding and central differencing. However, the authors conclude that given the significantly improved numerical accuracy of the approach, in relation to these lower order schemes, this may be acceptable.

Despite these findings it was still accepted that this scheme was extremely complex and computationally inefficient. This prompted the development of other multi-dimensional methods of characteristics.

A new method of simulating the advection process, using eight points in one-dimension was considered by Holly and Komatsu[19]. The main difference between this eight point approach and the classical scheme was, the way in which the spatial derivatives were calculated. The equation is also solved singly which reduces the complexity and simulation time. However this method is not compact and would require sixty-four grid points in two-dimensions. Although this process is not necessarily difficult it is

cumbersome and could lead to problems in the implementation. To alleviate these problems Komatsu *et al*[20] developed a more compact six-point approach.

Komatsu *et al*[20] simulated pure advection using upwinding, Holly-Preissmann, and the six and eight point methods of characteristics, using the case of an infinitely long channel. As expected, upwinding exhibited significant numerical diffusion. However, the other schemes all showed good correlation with the actual results, for a Courant number of 0.25.

In two-dimensions the results were as shown in one-dimension, with the six-point scheme proving to be far easier to implement than either Holly-Preissmann or the eight-point scheme. When considering a non-uniform grid the results continued to be stable and so it may be concluded that this scheme is a favourable one to use.

2.2 Discussion

The literature review demonstrates that there is room for improvement in the solution of the advection equation.

The QUICKEST[23] approach is one of the most popular numerical methods used to solve the advection equation. It has been applied to many one and two-dimensional tests proving to be a highly stable and accurate scheme. However, there are obvious limitations of this finite difference scheme: underprediction of the peak, time step restrictions and simulation of sharp concentration gradients.

The numerical diffusion which occurs using QUICKEST can be addressed by considering other numerical schemes which can be used to solve the advection term. Rather than investigating other higher order finite difference equations, however, this work develops the method of characteristics.

The latter restriction appears to have been explored extensively in the literature in the development of total variation diminishing schemes. However the issue of the time increment has had limited discussion. Work by Wallis and Manson[62], presented an interesting application of the method of characteristics with QUICKEST to solve one-dimensional advection using large Courant numbers. It indicates how this time step limitation may be overcome.

Explicit forms of the method of characteristics are also restricted by the time step. Several schemes have been proposed to counteract this difficulty: implicit, spatial reachout, temporal reachback, spatial reachback. The spatial reachout technique is investigated in detail in this research. It allows the method of characteristics to remain explicit and is also a relatively straightforward technique to implement.

The time restriction is important to address because it affects two main factors in the solution of the advection term: selection of the numerical scheme and computational efficiency. Removal of the time restriction allows an explicit method to be applied using very large time steps in the same way that implicit methods can be. This is beneficial as in general, explicit schemes are simpler to derive and implement than implicit approaches. It is also true that explicit schemes are not inherently stable, however, the explicit approach discussed by Wallis and Manson[62] is. Computational efficiency would improve as large time steps allow the numerical simulation to be executed more quickly. This makes a numerical scheme much more attractive.

2.3 References

1. Roberts, D.L. and Selim, M.S., "Comparative-Study of 6 Explicit and 2 Implicit Finite-Difference Schemes For Solving One-Dimensional Parabolic Partial-Differential Equations", *International Journal For Numerical Methods in Engineering*, 1984, **20**(5), 817-844.

2. Casulli, V., "Semi-implicit finite difference methods for the two-dimensional shallow water equations", *Journal of Computational Physics*, 1989, **86**, 56-74.

3. Chintu, L., "Modelling alluvial-channel flow by multimode characteristic method", *Journal of Engineering Mechanics*, 1991, **117**, 32-53.

4. Hogarth, W.L., Noye, B.J., Stagnitti, J., Parlange, J.Y., and Bolt, G., "A Comparative-Study of Finite-Difference Methods For Solving the One-Dimensional Transport-Equation With an Initial Boundary-Value Discontinuity", *Computers & Mathematics With Applications*, 1990, **20**(11), 67-82.

5. Shlomo, P.N., "A Eulerian-Lagrangian numerical scheme for the dispersion-convection equation using conjugate space-time grids", *Journal of computational physics*, 1981, **41**, 270-294.

6. Wang, J.D., Cofershabica, S.V., and Fatt, J.C., "Finite-Element Characteristic Advection Model", *Journal of Hydraulic Engineering-Asce*, 1988, **114**(9), 1098-1114.

7. Cao, Z. and Wei, L., "An operator-splitting algorithm for advection-diffusion-reaction equation", *Journal of Hydrodynamics*, 1992, **Ser B**(1), 65-73.

8. Holly, F.M. and Usseglio-Polatera, J.M., "Dispersion Simulation in Two-Dimensional Tidal Flow", *Journal of Hydraulic Engineering-Asce*, 1984, **110**(7), 905-926.

9. Zheng, C., "Extension of the Method of Characteristics For Simulation of Solute Transport in 3 Dimensions", *Ground Water*, 1993, **31**(3), 456-465.

10. Glass, J. and Rodi, W. *An explicit Hermitian finite difference scheme for pollutant transport in transient river flows*. in *Proceedings of the 4th GAMM Conference on Numerical Fluid Mechanics*. 1981. Paris, France.

11. Komatsu, T., Ohgushi, K., and Asai, K., "Refined numerical scheme for advective transport in diffusion simulation", *Journal of Hydraulic Engineering-Asce*, 1997, **123**(1), 41-50.

12. Balzano, A., "Mosquito: An efficient finite difference scheme for numerical simulation of 2D advection", *International Journal For Numerical Methods in Fluids*, 1999, **31**(2), 481-496.

13. Holly, F.M. and Preissmann, A., "Accurate calculation of transport in two dimensions", *Journal of the Hydraulic Division, ASCE*, 1977, **103**, 1259-1277.

14. Benque, J.P., Hauguel, A., and Viollet, P.L., *Numerical models in environmental fluid mechanics; Engineering applications of computational hydraulics Vol.II Homage to Alexandre Preissmann*, ed. M.B. Abbott and J.A. Cunge. 1982: Pitman.

15. Abbott, M.B., *Computational Hydraulics; Elements of the theory of free surface flows*. Vol. 1. 1979: Pitman.

16. Li, C.W., "Advection-Dispersion Simulation By Minimization Characteristics and Alternate Direction Explicit Methods", *Applied Mathematical Modelling*, 1991, **15**(11-12), 616-623.

17. Ding, D. and Liu, P.L.F., "An Operator-Splitting Algorithm For Two-Dimensional Convection Dispersion Reaction Problems", *International Journal For Numerical Methods in Engineering*, 1989, **28**(5), 1023-1040.

18. Hasbani, Y., Livne, E., and Latteux, B., "Finite elements and characteristics applied to the advection-diffusion equations", *Computers & Fluids*, 1983, **11**, 71-83.

19. Holly Jr., F.M. and Komatsu, T. *Derivative approximations in the two-point fourth order method for pollutant transport.* in *Frontiers in Hydraulic Engineering.* 1983. MIT, MA: ASCE.

20. Komatsu, T., Holly, F.M., Nakashiki, N., and Ohgushi, K., "Numerical calculation of pollutant transport in one and two-dimensions", *Journal of Hydroscience and Hydraulic Engineering*, 1985, **3**, 15-30.

21. Holly Jr., F.M., "One-dimensional transport-dispersion and water quality models", in *Coastal, Estuarial and Harbour Engineers Reference Book*, M.B. Abbott, E. Price, and F.N. Spon, Editors. 1994. 191-198.

22. Lin, B.L. and Falconer, R.A., "Tidal flow and transport modeling using ULTIMATE QUICKEST scheme", *Journal of Hydraulic Engineering-Asce*, 1997, **123**(4), 303-314.

23. Leonard, B.P., "A stable and accurate convective modelling procedure based on quadratic upstream interpolation", *Computer methods in applied mechanics and engineering*, 1979, **19**, 59-98.

24. Leonard, B.P., "The Ultimate Conservative Difference Scheme Applied to Unsteady One-Dimensional Advection", *Computer Methods in Applied Mechanics and Engineering*, 1991, **88**(1), 17-74.

25. Greenberg, J.B., "Operator splitting methods for computation of reacting flows", *Computers & Fluids*, 1983, **11**(2), 95-105.

26. Noye, B.J. and Dehghan, M., "New explicit finite difference schemes for two-dimensional diffusion subject to specification of mass", *Numerical Methods For Partial Differential Equations*, 1999, **15**(4), 521-534.

27. Ahmad, Z., Kothyari, U.C., and Raju, K.G.R., "Finite difference scheme for longitudinal dispersion in open channels", *Journal of Hydraulic Research*, 1999, **37**(3), 389-406.

28. Falconer, R.A. and Liu, S.Q., "Modeling Solute Transport Using Quick Scheme", *Journal of Environmental Engineering-Asce*, 1988, **114**(1), 3-20.

29. Hirsch, C., *Numerical computation of internal and external flows; Part 1*, ed. Wiley. Vol. 1. 1988: Wiley.

30. Shaw, T.S., *Using Computational Fluid Dynamics*. 1992: Prentice Hall.

31. Abbott, M.B. and Basco, D.R., *Computational Fluid Dynamics; An Introduction for Engineers*. 1989: Longman Scientific and Technical.

32. Varoglu, E. and Finn, W.D.L., "A finite element method for the diffusion-convection equation with constant coefficients", *Advances in Water Resources*, 1978, **1**, 337-343.

33. Yu, F.X. and Singh, V.P., "Improved finite-element method for solute transport", *Journal of Hydraulic Engineering*, 1995, **121**(2), 145-158.

34. Hill, D.L. and Baskarone, E.A., "A monotone streamline upwind method for quadratic finite elements", *International Journal of Numerical Methods in Fluids*, 1993, **17**, 463-475.

35. Goldberg, D.E. and Wylie, E.B., "Characteristics Method Using Time-Line Interpolations", *Journal of Hydraulic Engineering-Asce*, 1983, **109**(5), 670-683.

36. Jefferies, D.F. and Steele, A.K., "Observed and predicted concentrations of caesium-137 in seawater of the Irish Sea 1970-1985", *Journal of Environmental Radioactivity*, 1989, **10**, 173-189.

37. Gurbutt, P.A. and Kershaw, P.J. *Modelling the behaviour of plutonium and americium in the Irish Sea.* in *Hydraulic and Environmental Modelling of Coastal, Estuarine and River Waters.* 1989. Bradford: Gower Technical.

38. Leonard, B.P., "Simple High-Accuracy Resolution Program For Convective Modeling of Discontinuities", *International Journal For Numerical Methods in Fluids*, 1988, **8**(10), 1291-1318.

39. Chen, Y.P. and Falconer, R.A., "Advection Diffusion Modeling Using the Modified Quick Scheme", *International Journal For Numerical Methods in Fluids*, 1992, **15**(10), 1171-1196.

40. Runchal, A.K., "Convergence and accuracy of three finite difference schemes for a two-dimensional conduction and convection problem", *International Journal of Numerical Methods in Engineering*, 1972, **4**, 541-550.

41. Karpik, S.R. and Crockett, S.R., "Semi-Lagrangian algorithm for two-dimensional advection-diffusion equation on curvilinear coordinate meshes", *Journal of Hydraulic Engineering-Asce*, 1997, **123**(5), 389-401.

42. Kaya, Y. *Some aspects of tidal flow and water quality modelling of the North Devon coastal waters.* in *Proceedings of the 2nd International Conference on Hydraulic and Environmental Modelling of Coastal, Estuarine and River Waters.* 1992.

43. Hervouet, J.M., "Application of the method of characteristics in their weak formulation to solving two-dimensional advection equations on mesh grids", in *Computational Techniques for Fluid Flow, Vol 5: Recent advances in Numerical Methods in Fluids*, C. Taylor, J.A. Johnson, and W.R. Smith, Editors. 1986, Pineridge Press: Swansea. 149-185.

44. Justesen, P., Olesen, K.W., and Vested, H.J. *High accuracy modelling of advection in two and three dimensions.* in *Procedings of the 23rd IAHR Congress.* 1989. Ottawa, Canada.

45. Davis, R.W. and Moore, E.F., "A numerical study of vortex shedding from rectangles", *Journal of Fluid Mechanics*, 1982, **116**, 475-506.

46. Falconer, R.A., Liu, S.Q., and Chen, Y. *Application of higher order accurate schemes for advective transport in a 2D water quality model.* in *Hydraulic and Environmental Modelling: Coastal waters, Procedings of the 2nd International Conference on Hydraulic and Environmental Modelling of Coastal, Estuarine and River Waters.* 1992.

47. Leonard, B.P. and Niknafs, H.S. *Cost-effective accurate coarse-grid method for highly convective multidimensional unsteady flows.* in *Procedings of the CFD symposium on aeropropulsion.* 1990. Cleveland, Ohio.

48. Ekebjaerg, L. and Justesen, P., "An Explicit Scheme For Advection Diffusion Modeling in 2 Dimensions", *Computer Methods in Applied Mechanics and Engineering*, 1991, **88**(3), 287-297.

49. Vested, H.J., Justesen, P., and Ekebjaerg, L., "Advection-Dispersion Modeling in 3 Dimensions", *Applied Mathematical Modelling*, 1992, **16**(10), 506-519.

50. Gross, E.S., Koseff, J.R., and Monismith, S.G., "Evaluation of advective schemes for estuarine salinity simulations", *Journal of Hydraulic Engineering-Asce*, 1999, **125**(1), 32-46.

51. Blumberg, A.F. and Mellor, G.L., "A description of a three-dimensional coastal ocean circulation model", in *Three-Dimensional Coastal Ocean Models*, N.S. Heaps, Editor. 1987, American Geophysical Union: Washington. 1-16.

52. Smolarkiewicz, P.K., "A Fully Multidimensional Positive Definite Advection Transport Algorithm With Small Implicit Diffusion", *Journal of Computational Physics*, 1984, **54**(2), 325-362.

53. Casulli, V. and Cheng, R.T., "Stability Analysis of Eulerian-Lagrangian Methods For the One-Dimensional Shallow-Water Equations", *Applied Mathematical Modelling*, 1990, **14**(3), 122-131.

54. Smolarkiewicz, P.K. and Grabowski, W.W., "The multidimensional positive definite advection transport algorithm: nonoscillatory option", *Journal of Computational Physics*, 1990, **86**, 355-375.

55. Hirsch, C., *Numerical computation of internal and external flows; Part 2*, ed. Wiley. Vol. 2. 1988: Wiley.

56. Roe, P.L., "Some contributions to the modelling of discontinuous flows", in *Large Scale Computations in Fluid Mechanics ; Lectures in Applied Mathematics*. 1985. 163-193.

57. Wallis, S.G. and Manson, J.R., "Evaluation of advection schemes for estuary transport - Discussion", *Journal of Hydraulic Engineering-Asce*, 2000, **126**(4), 314-314.

58. Manson, J.R. and Wallis, S.G., "An accurate numerical algorithm for advective transport", *Communications in Numerical Methods in Engineering*, 1995, **11**(12), 1039-1045.

59. Manson, J.R. and Wallis, S.G., "Accurate simulation of transport processes in two-dimensional shear flow", *Communications in Numerical Methods in Engineering*, 1998, **14**(9), 863-869.

60. Leonard, B.P. and Niknafs, H.S., "Sharp Monotonic Resolution of Discontinuities Without Clipping of Narrow Extrema", *Computers & Fluids*, 1991, **19**(1), 141-154.

61. Lin, B. and Falconer, R.A., "Modeling Sediment Fluxes in Estuarine Waters Using a Curvilinear Coordinate Grid System", *Estuarine Coastal and Shelf Science*, 1995, **41**(4), 413-428.

62. Wallis, S.G. and Manson, J.R., "Accurate numerical simulation of advection using large time steps", *International Journal For Numerical Methods in Fluids*, 1997, **24**(2), 127-139.

63. Yang, J.C. and Wang, J.Y., "Numerical solution of dispersion equation in one dimension", *Journal of the Chinese Institute of Engineers*, 1988, **11**, 379-383.

64. Chintu, L., "Comprehensive method of characteristics models for flow simulation", *Journal of Hydraulic Engineering*, 1988, **114**, 1074-1097.

65. Glass, J. and Rodi, W., "A higher order numerical scheme for scalar transport", *Computer methods in applied mechanics and engineering*, 1982, **31**, 337-358.

Chapter 3

One-Dimensional Finite Difference Methods

3.1 Introduction 36

3.1.1 Definitions and terms used in finite difference methods. 36

3.1.2 First order upwinding 46

3.1.3 Second order central differencing 50

3.1.4 Quadratic Upstream Interpolation for Convective Kinematics (QUICK) 53

3.1.5 Quadratic Upstream Interpolation for Convective Kinematics with Estimated Streaming Terms (QUICKEST) 58

3.2 Testing of finite difference schemes using one-dimensional idealised testcases 62

3.2.1 Results for the point release of pollution 64

3.2.2 Results using the linear distribution of pollution 69

3.2.3 Results using the Gaussian distribution of pollution 73

3.3 Conclusions 76

3.4 References 81

3.1 Introduction

The finite difference method is the oldest numerical scheme which is applied to the solution of differential equations; Hirsch[1] sites Euler as being the first to apply it in 1768. It is a simple approach, based on the properties of Taylor series expansions and of, the subsequent application of the definition of its derivatives.[1-3] There are several options for the solution of such a scheme, some of which are described in detail in the literature.[1-9]

3.1.1 Definitions and terms used in finite difference methods.

The finite difference method involves the substitution of partial differential equations with finite difference equations, in terms of spatial and temporal grid co-ordinates. By this replacement, the method translates the partial differential equations written as a continuum function to an arithmetic representation, which allows the equation to be solved more easily.[1-3] The finite difference equations link the values of dependant variables at a set of points such that, a grid of points is used to represent the continuous physical domain. The resulting numerical scheme is therefore based upon values defined at predetermined grid points.

This scheme requires use of a regular grid and to facilitate explanation of the approach, it will be considered that it is uniform, although in reality this is not essential. Critically the grid must be constructed such that the nodal points are located at the intersection of either rectilinear or curved lines. These lines appear as a set of numerical co-ordinates, which is illustrated in one-dimension by Figure (3.1). The spatial axis is plotted in the x-direction, where the co-ordinates are defined in terms of i, the increment being Δx (if this were two-dimensional the increment in the y-direction would similarly be Δy). Time has the increment Δt and is plotted in the y-direction, denoted by the letter n. It is constructed with a series of parallel lines in the x-direction which are intersected by perpendicular lines in the y-direction. The points at which the lines cross denote the co-ordinate location of the nodal points.

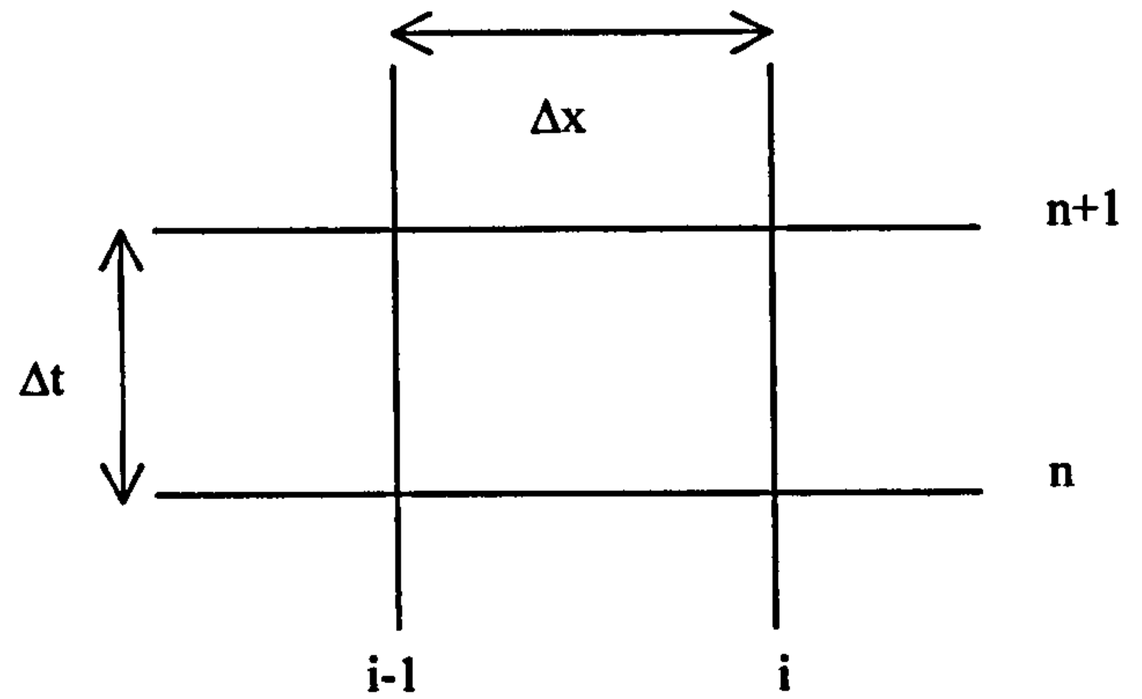

Figure (3.1) Location of node points on a finite difference mesh

Finite difference derivatives

The finite difference method is based on the estimation of a partial derivative using Taylor series expansions. This can be illustrated by considering how a derivative of a function is derived and expressed mathematically. Consider the truncated Taylor expansion used to express a function $\phi(x)$ at the location $\phi(x+\Delta x)$, represented as equation (3.1):

$$\phi(x+\Delta x)=\phi(x)+\phi_x(x)\frac{\Delta x}{1!}+\phi_{xx}(x)\frac{\Delta x^2}{2!}+\phi_{xxx}(x)\frac{\Delta x^3}{3!}=\sum_{n=0}^{\infty}f^{(n)}(x)\frac{\Delta x^n}{n!} \qquad (3.1)$$

The second and third order terms in equation (3.1) are neglected for the purposes of this derivation. This can now easily be manipulated and rewritten in terms of the first derivative, $\phi(x)$:

$$\phi_x=\frac{\partial\phi}{\partial x}=\lim_{\Delta x\to 0}\frac{\phi(x+\Delta x)-\phi(x)}{(x+\Delta x)-(x)}$$

which simplifies to:

$$\phi_x = \frac{\partial \phi}{\partial x} = \lim_{\Delta x \to 0} \frac{\phi(x+\Delta x) - \phi(x)}{\Delta x} \tag{3.2}$$

If Δx is finite and also small, the right hand side of equation (3.2) is an approximate representation of the exact value of the left hand side. This could be made more accurate by further reducing the value of Δx. For any numerical scheme it would be impractical to solve for an infinite number of terms in an expansion so the expansion is truncated to a suitable degree of accuracy. In this case the derivative is first order accurate as the second and higher order terms have been neglected. The first order approximation of $\phi_x(x)$ is thus written as shown in equation (3.3):

$$\frac{\phi(x+\Delta x) - \phi(x)}{\Delta x} = \phi_x(x) + 0(\Delta x) \tag{3.3}$$

where the truncation error, $0(\Delta x)$ tends to zero as $\Delta x \to 0$. Correspondingly higher order approximations can be derived.

Requirements of a numerical scheme

There are three main requirements of a numerical scheme namely, consistency, stability and convergence. These describe the different relationships between, the finite difference form of a partial differential equation, the calculated solution using a numerical scheme and the ideal solution.[1, 3, 10]

Consistency

The definition of consistency is that, the finite difference equation should tend to the partial differential equation, as Δt and Δx tend towards zero. It is possible to analyse consistency by developing the functions in a finite difference equation, using Taylor series expansions.[1, 3] This statement can be illustrated by way of numerical example.

Consider the advection equation, (3.4), and its corresponding finite difference form, equation (3.1): forward and upwinding discretisation techniques for the temporal and spatial terms respectively. This derivation will be described fully in Section 3.1.2.

$$\frac{\partial C}{\partial t}+u\frac{\partial C}{\partial x}=0 \tag{3.4}$$

$$\frac{C_i^{n+1}-C_i^n}{\Delta t}+u\left(\frac{C_i^n-C_{i-1}^n}{\Delta x}\right)=0 \tag{3.5}$$

Expanding the terms, C_i^{n+1} and C_{i-1}^n about C_i^{n+1} using Taylor expansions gives the backward spatial derivative:

$$C_{i-1}^n=C_i^n-\left(\frac{\partial C}{\partial x}\right)_i^n\frac{\Delta x}{1!}+\left(\frac{\partial^2 C}{\partial x^2}\right)_i^n\frac{\Delta x^2}{2!}-\left(\frac{\partial^3 C}{\partial x^3}\right)_i^n\frac{\Delta x^3}{3!}+H.O.T \tag{3.6}$$

Where H.O.T refers to higher order terms and the forward temporal derivatives can be obtained from:

$$C_i^{n+1}=C_i^n+\left(\frac{\partial C}{\partial t}\right)_i^n\frac{\Delta t}{1!}+\left(\frac{\partial^2 C}{\partial t^2}\right)_i^n\frac{\Delta t^2}{2!}+\left(\frac{\partial^3 C}{\partial t^3}\right)_i^n\frac{\Delta t^3}{3!}+H.O.T \tag{3.7}$$

Substitution of equations (3.6) and (3.7) into (3.5) gives:

$$\left[C_i^n+\left(\frac{\partial C}{\partial t}\right)_i^n\frac{\Delta t}{1!}+\left(\frac{\partial^2 C}{\partial t^2}\right)_i^n\frac{\Delta t^2}{2!}+\left(\frac{\partial^3 C}{\partial t^3}\right)_i^n\frac{\Delta t^3}{3!}+H.O.T-C_i^n\right]\frac{1}{\Delta t}+ \tag{3.8}$$

$$\frac{u}{\Delta x}\left[C_i^n-C_i^n+\left(\frac{\partial C}{\partial x}\right)_i^n\frac{\Delta x}{1!}-\left(\frac{\partial^2 C}{\partial x^2}\right)_i^n\frac{\Delta x^2}{2!}+\left(\frac{\partial^3 C}{\partial x^3}\right)_i^n\frac{\Delta x^3}{3!}+H.O.T\right]=0$$

Simplifying equation (3.8) by cancelling terms produces:

$$\left[\left(\frac{\partial C}{\partial t}\right)_i^n + \left(\frac{\partial^2 C}{\partial t^2}\right)_i^n \frac{\Delta t}{2!} + \left(\frac{\partial^3 C}{\partial t^3}\right)_i^n \frac{\Delta t^2}{3!} + H.O.T\right] + \tag{3.9}$$
$$u\left[+\left(\frac{\partial C}{\partial x}\right)_i^n - \left(\frac{\partial^2 C}{\partial x^2}\right)_i^n \frac{\Delta x}{2!} + \left(\frac{\partial^3 C}{\partial x^3}\right)_i^n \frac{\Delta x^2}{3!} + H.O.T\right] = 0$$

which can be manipulated to give:

$$\left[\left(\frac{\partial C}{\partial t}\right)_i^n + u\left(\frac{\partial C}{\partial x}\right)_i^n\right] + \tag{3.10}$$
$$\left[\left(\frac{\partial^2 C}{\partial t^2}\right)_i^n \frac{\Delta t}{2!} + \left(\frac{\partial^3 C}{\partial t^3}\right)_i^n \frac{\Delta t^2}{3!} - u\left(\frac{\partial^2 C}{\partial x^2}\right)_i^n \frac{\Delta x}{2!} + u\left(\frac{\partial^3 C}{\partial x^3}\right)_i^n \frac{\Delta x^2}{3!} + H.O.T\right] = 0$$

If Δt and Δx tend to zero then equation (3.10) reduces to the original form of the advection equation. It is clear that the original partial differential equation has been recovered, so the finite difference equation is defined as being consistent with the partial differential equation under these circumstances.

Stability and the Courant-Freidrich-Lewy Condition

The solution of a finite difference equation will not always exactly match the solution of the corresponding difference equation. This is primarily due to rounding errors throughout the calculation. The more interpolations which take place, then the more likely numerical errors are to develop.[9] In this work, the von Neuman stability analysis will be used to analyse the stability of the finite difference schemes; a detailed explanation is described in the literature.[3, 4, 6, 11, 12]

The von Neuman analysis is based on Fourier series and the corresponding amplification factor which indicates the behaviour of rounding errors as the calculation progresses. The criteria for numerical stability of a scheme is that the amplification factor G, must be less than or equal to 1 over a complete time step.[1, 11] This requirement ensures that any errors do not significantly increase as the calculation

progresses. For illustrative purposes consider again the upwinding discretised form of the advection equation, equation (3.5).

The finite difference scheme can be written using Fourier series of the form:

$$C_j^n = \sum_{k=1}^{N} V_k^n e^{ikaj} \tag{3.11}$$

in which V_k^n is the Fourier co-efficient for wave number k and time n. The term α is the dimensionless wave number, N is the number of terms in the Fourier series.[1, 3, 11]

$$C_j^n = V^n e^{i\alpha j} \tag{3.12}$$

$$C_j^{n+1} = V^{n+1} e^{i\alpha j}$$

$$C_{j-1}^n = V^n e^{i\alpha(j-1)}$$

The definitions set out as equation (3.12) are substituted into equation (3.5), which is rewritten as:

$$V^{n+1} e^{i\alpha j} = \left(1 - \frac{u\Delta t}{\Delta x}\right) V^n e^{i\alpha j} + \left(\frac{u\Delta t}{\Delta x}\right) V^n e^{i\alpha(j-1)} \tag{3.13}$$

Dividing throughout by $e^{i\alpha j}$ and simplifying gives:

$$V^{n+1} = \left[\left(1 - \frac{u\Delta t}{\Delta x}\right) + \left(\frac{u\Delta t}{\Delta x}\right) e^{-i\alpha}\right] V^n$$

The amplification factor, G, is thus derived:

$$G = \frac{V^{n+1}}{V^n} \tag{3.14}$$

$$G = \left[\left(1 - \frac{u\Delta t}{\Delta x}\right) + \left(\frac{u\Delta t}{\Delta x}\right)e^{-i\alpha}\right]$$

where G must be less than or equal to one for stability.[1, 3] This criterion is also known as the Courant-Freidrich-Lewy condition. This leads to the definition of the Courant number in equation (3.15) below, in which u is the local velocity:

$$Cr = \frac{u\Delta t}{\Delta x} \tag{3.15}$$

In practice the limiting factor for explicit finite difference schemes is the time step. The CFL condition states that for any explicit scheme to be numerically stable, the ratio of the distance travelled in one time step to the spatial increment must be less than or equal to one. This is in agreement with the mathematical representation of the von Neuman stability criteria.

To complete the stability analysis, the graph of equation (3.14) can be drawn as in Figure (3.2).[3] The equation is recognisable as the equation of a circle of radius Cr centred at the point (1-Cr).

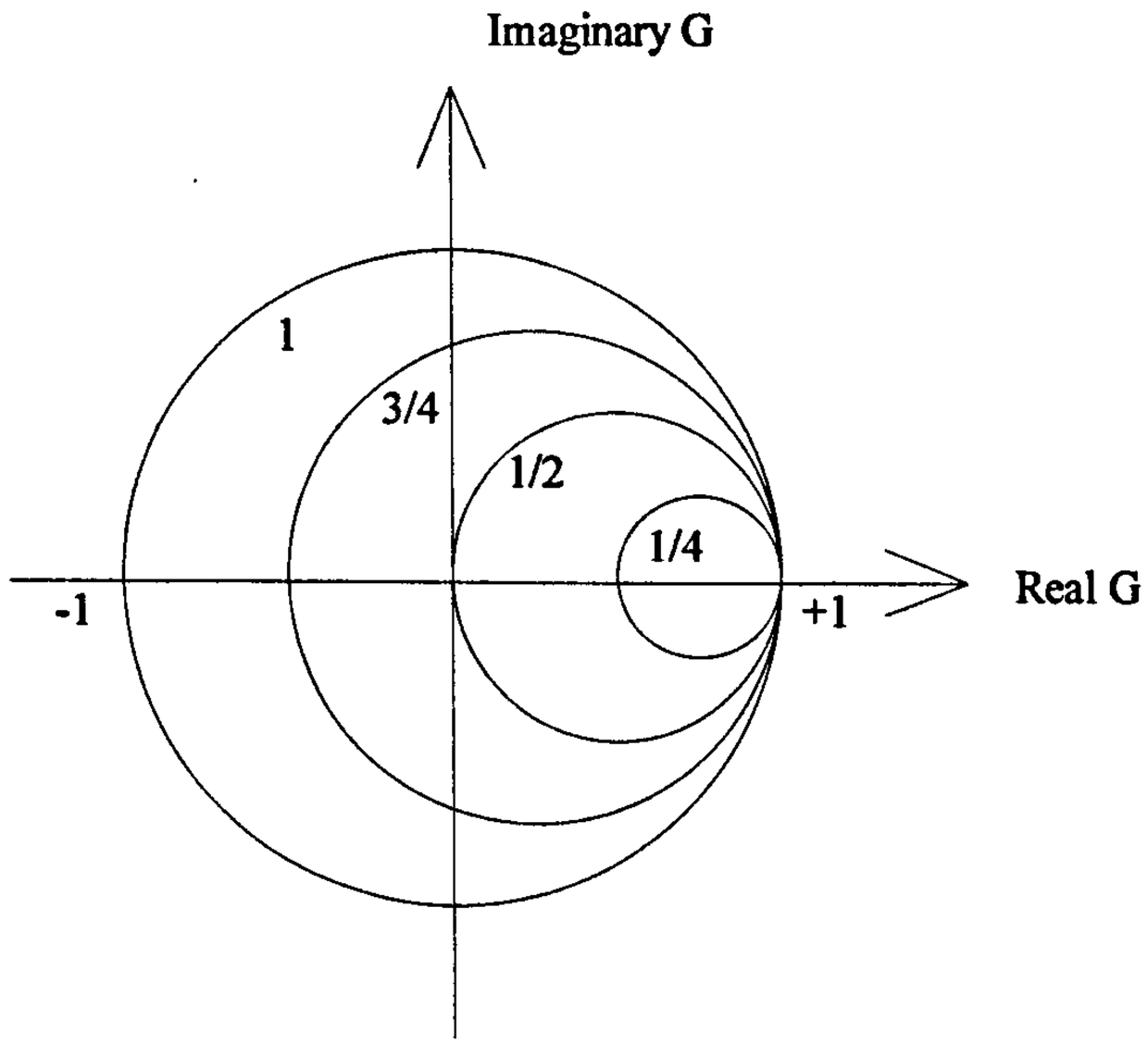

Figure (3.2) Complex G plane diagram of the upwind scheme after Abbott and Basco[3]

From the diagram it can be seen that for all Courant numbers less than one, the amplitude, G is also less than one, hence the scheme is stable under these conditions. This is confirmed in the literature and similar analysis can be carried out for other finite difference schemes.[1, 3, 6, 11]

Convergence

For a finite difference scheme to be convergent, the calculated numerical solution of the equation must approach the exact ideal solution at any point in time and space, when Δt and Δx tend towards zero.[1] The conditions of consistency, stability and convergence are interlinked by the Lax Equivalence Theorem, which greatly simplifies the determination of convergence. The theorem states that, if a discretised equation is consistent, then provided the stability criterion is also met, it is also convergent.[1, 12-14]

Accuracy

The accuracy of a finite difference scheme is largely dependant on the magnitude of the truncation error. Even if the finite difference equation is consistent and stable, the collective truncation error can cause inaccuracies in the numerical solution. The truncation error terms from the Taylor series expansion, give some indication of the order of accuracy of the scheme, as previously stated.[15]

Numerical inaccuracy can be defined in terms of amplitude and by phase errors.[1, 16] In the advection equation if $G<1$ there is numerical diffusion and the solution is smoothed.

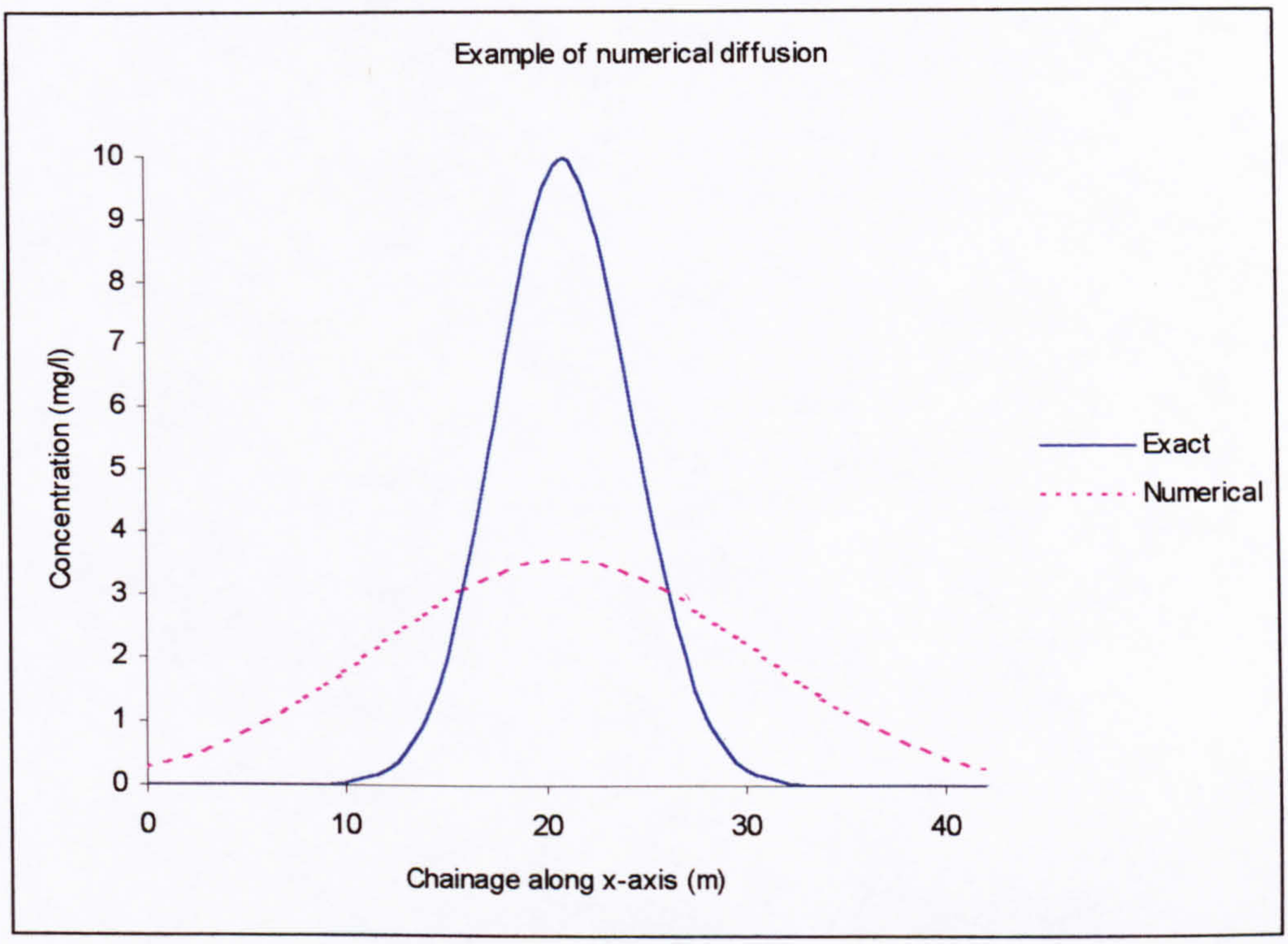

Figure (3.3) Plot showing the exact and numerical solutions for the case of G<1

This is easily described by Figure (3.3), in which the distribution is reduced and spread out over a larger distance. If G>1, then the result is amplification of the solution, which leads to instability.

Phases errors, or numerical dispersion is due to the discrete approximations of the spatial derivatives in the finite difference equation and the celerity ratio of the physical and numerical Fourier terms. They are manifested as spurious ripples which range from extreme positive to negative values, as shown in Figure (3.4).

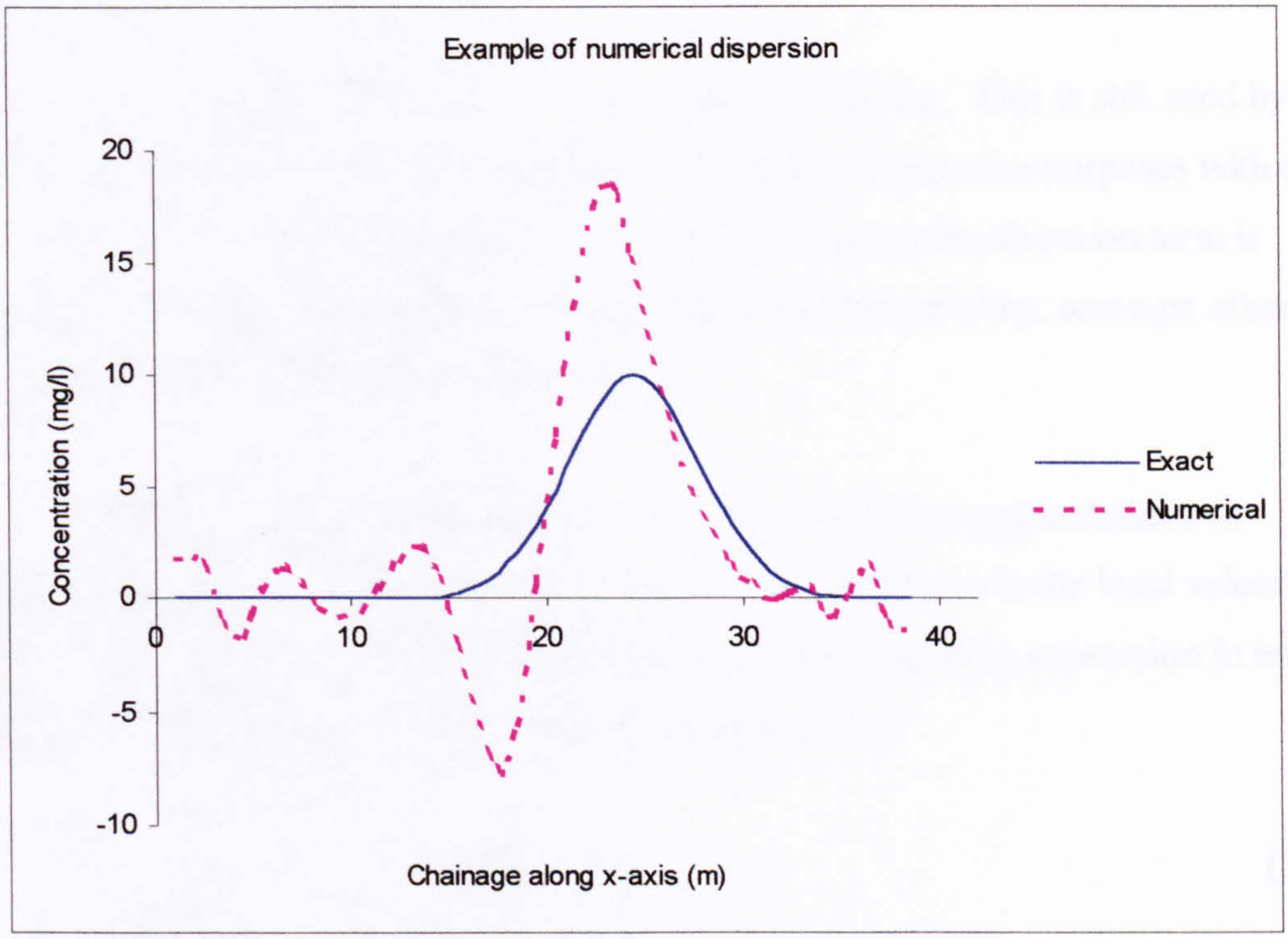

Figure (3.4) Plot showing numerical dispersion

The accuracy of the schemes examined in this work will also be described by comparing the ideal and numerical solution at each nodal point. The root mean square method is used to calculate the average error at each point.[12, 17-19] The RMS error is given by equation (3.16):

$$RMS = \frac{\sqrt{\left[\sum_{i=0}^{N}\left(C_{i,j} - C_{i,j}^{*}\right)^2\right]}}{N+1} \tag{3.16}$$

in which $C_{i,j}$ is the solution calculated by the numerical scheme, $C_{i,j}^{*}$ is the exact ideal solution and N is the number of internal and boundary nodes.[18]

3.1.2 First Order Upwinding

The simplest finite difference scheme is first order upwinding. This is still used by industry and is often considered as a benchmark or for comparative purposes with other schemes.[20-26] The derivation of this numerical solution for the advection term is straightforward, and the approach used here is also implemented by, amongst others, van Eijkeren *et al*[27] and Abbott and Basco[3].

The pure advection equation assumes that there is no diffusion and is defined as equation (3.17), in which C represents concentration, t is time, u is the local velocity and x is the spatial increment. This can be manipulated to give an expression in terms of the local rate of change of concentration, C, as in (3.18):

$$\frac{\partial C}{\partial t} + u\frac{\partial C}{\partial x} = 0 \tag{3.17}$$

$$\frac{\partial C}{\partial t} = -u\frac{\partial C}{\partial x} \tag{3.18}$$

The Taylor series expansion of $f(x-\Delta x)$ about x, has the general form shown in equation (3.19):[3]

$$f(x-\Delta x) = f(x) - f'(x)\frac{\Delta x}{1!} + f''(x)\frac{\Delta x^2}{2!} - f'''(x)\frac{\Delta x^3}{3!} = \sum_{n=0}^{\infty} f^{(n)}(x)\frac{\Delta x^n}{n!} \tag{3.19}$$

This is best explained with reference to Figure (3.5). The x-axis represents the spatial axis and the y-axis is the temporal axis, n being the current time and n+1 representing the next time step. The expansion defined by equation (3.19), is located at the point i on the finite difference grid which corresponds to the location, x.

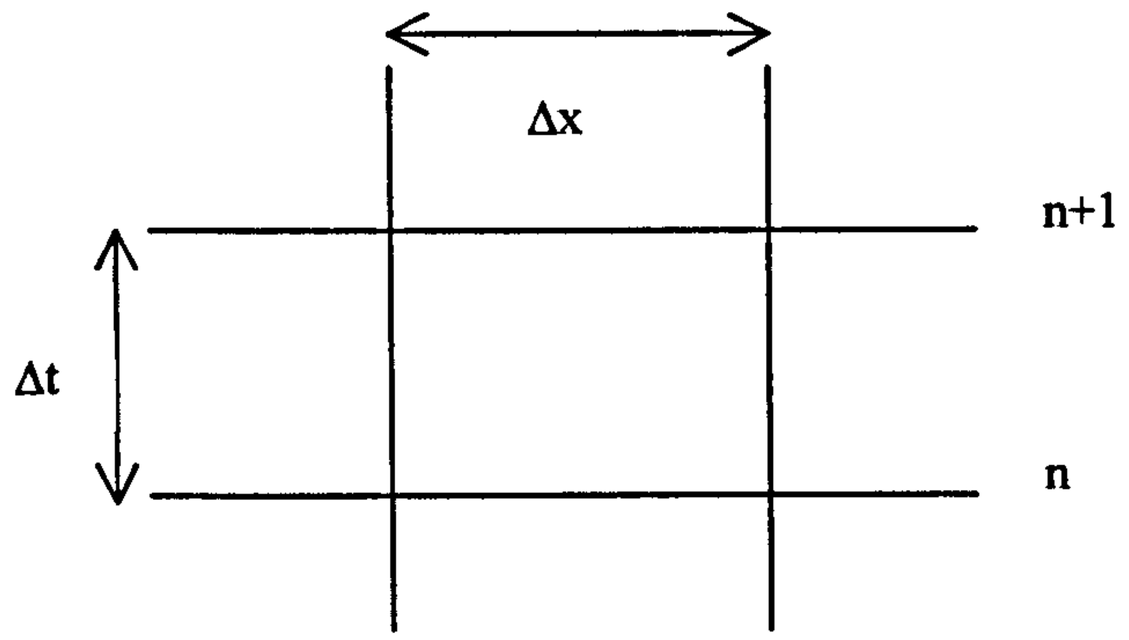

Figure (3.5) Finite difference grid used to derive the upwind scheme

In terms of the expansion from i to i-1, the variables used in equation (3.19) are defined as:

$$f(x-\Delta x)=C_{i-1}^{n} \tag{3.20}$$

$$f(x)=C_{i}^{n}$$

$$f'(x)=\left(\frac{\partial C}{\partial x}\right)_{i}^{n}$$

$$f''(x)=\left(\frac{\partial^2 C}{\partial x^2}\right)_{i}^{n}$$

$$f'''(x)=\left(\frac{\partial^3 C}{\partial x^3}\right)_{i}^{n}$$

Substitution of equation (3.20) into (3.19) gives:

$$C_{i-1}^{n}=C_{i}^{n}-\left(\frac{\partial C}{\partial x}\right)_{i}^{n}\frac{\Delta x}{1!}+\left(\frac{\partial^2 C}{\partial x^2}\right)_{i}^{n}\frac{\Delta x^2}{2!}-\left(\frac{\partial^3 C}{\partial x^3}\right)_{i}^{n}\frac{\Delta x^3}{3!}+H.O.T \tag{3.21}$$

Rearranging this equation and dividing by a factor of Δx produces:

$$\left(\frac{\partial C}{\partial x}\right)_i^n = \frac{C_i^n - C_{i-1}^n}{\Delta x} + \left(\frac{\partial^2 C}{\partial x^2}\right)_i^n \frac{\Delta x}{2!} - \left(\frac{\partial^3 C}{\partial x^3}\right)_i^n \frac{\Delta x^2}{3!} + H.O.T \tag{3.22}$$

By neglecting all terms greater than and equal to second order, *i.e.* truncating the equation to first order accuracy, the partial differential approximation is defined as equation (3.23) below:

$$\left(\frac{\partial C}{\partial x}\right)_i^n = \frac{C_i^n - C_{i-1}^n}{\Delta x} + (0)\Delta x \tag{3.23}$$

Substituting this equation back into equation (3.18) gives:

$$\left(\frac{\partial C}{\partial t}\right) = -u\left(\frac{C_i^n - C_{i-1}^n}{\Delta x}\right) \tag{3.24}$$

and simple forward discretisation of the local rate of change develops the equation to:

$$\frac{C_i^{n+1} - C_i^n}{\Delta t} = -u\left(\frac{C_i^n - C_{i-1}^n}{\Delta x}\right) \tag{3.25}$$

This is easily rearranged to provide an estimate of the concentration at the next time step.

$$C_i^{n+1} = C_i^n - \frac{u\Delta t}{\Delta x}\left(C_i^n - C_{i-1}^n\right) \tag{3.26}$$

The advantage of the upwinding scheme is that it is a very simple first order equation where the choice of direction depends upon the local velocity, *i.e.* a positive velocity uses i-1 and i, a negative velocity uses i+1 and i, in the opposite direction.

Leonard[6] includes as part of his analysis of upwinding, a graph showing the results of a von Neuman stability analysis of the scheme. He takes account of both advection and

diffusion in this analysis. For the case of pure advection the stability zone relating to zero diffusivity is considered. The diagram is included here as Figure (3.6), the limiting conditions being that:

$$\alpha \leq 0.5$$

$$-2\alpha + 1 \leq Cr$$

where α is the diffusivity term defined as:

$$\alpha = \frac{D\Delta t}{\Delta x^2}$$

where D is the co-efficient of diffusion. This complicated analysis is explained more fully by Roache[28] and Vreugdenhil[11].

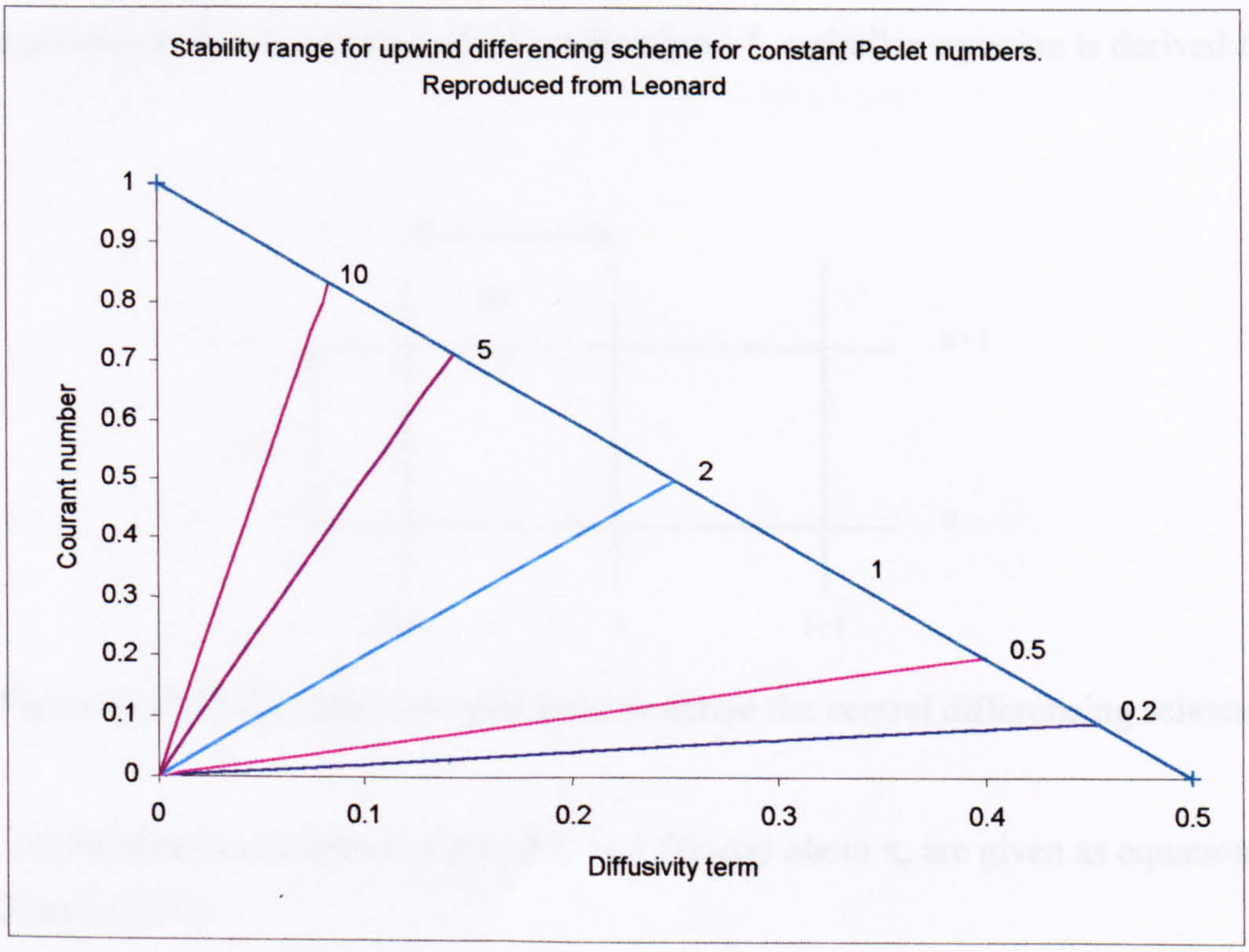

Figure (3.6) von Neuman stability analysis of the Upwinding scheme[6]

For the advection only situation the upwinding scheme is shown to be stable for all Courant numbers from zero to one.[1, 3, 11] (This stability range has been confirmed using the Fourier series analysis in Section 3.1.1) However it is noticeable that as diffusion increases, the stability range of the scheme reduces.

Van Eijkeren *et al*[27] also state that the upwinding scheme conserves mass well and that it gives an exact solution for Courant numbers equal to one.

3.1.3 Second Order Central Differencing

Second order central differencing, such as Lax-Wendroff and the Leap Frog scheme, is another option for solving the advection equation. It is derived, as described by Koutitas[7], in the same way as upwinding, but is of higher order accuracy. Where upwinding considers expansions about i to i-1, central differencing uses i-1 to i+1; the location i being at the centre of these two points, as shown in Figure (3.7). Using the same process to derive equation (3.21) at location i-1, a similar equation is derived for i+1.

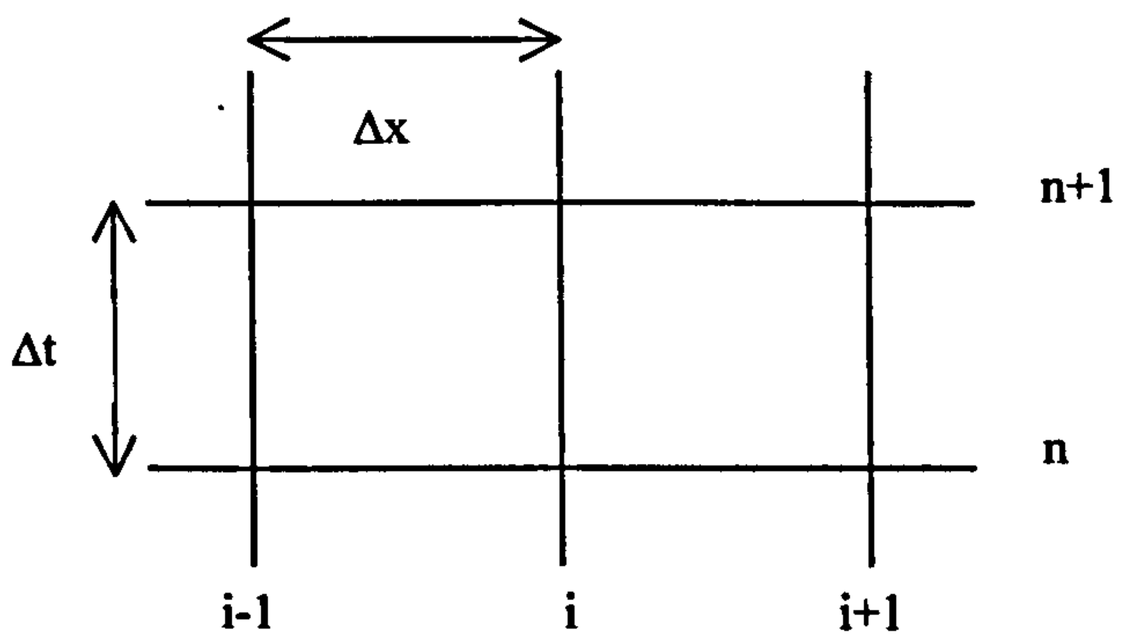

Figure (3.7) Finite difference grid used to derive the central differencing scheme

The Taylor series expansions of $f(x+\Delta x)$ and $f(x-\Delta x)$ about x, are given as equations (3.27) and (3.28):

$$C_{i-1}^n = C_i^n - \left(\frac{\partial C}{\partial x}\right)_i^n \frac{\Delta x}{1!} + \left(\frac{\partial^2 C}{\partial x^2}\right)_i^n \frac{\Delta x^2}{2!} - \left(\frac{\partial^3 C}{\partial x^3}\right)_i^n \frac{\Delta x^3}{3!} + H.O.T \tag{3.27}$$

$$C_{i+1}^n = C_i^n + \left(\frac{\partial C}{\partial x}\right)_i^n \frac{\Delta x}{1!} + \left(\frac{\partial^2 C}{\partial x^2}\right)_i^n \frac{\Delta x^2}{2!} + \left(\frac{\partial^3 C}{\partial x^3}\right)_i^n \frac{\Delta x^3}{3!} + H.O.T \tag{3.28}$$

Addition of (3.27) and (3.28) produces equation (3.29):

$$C_{i-1}^n + C_{i+1}^n = 2C_i^n + 2\left(\frac{\partial^2 C}{\partial x^2}\right)_i^n \frac{\Delta x^2}{2!} + H.O.T \tag{3.29}$$

which is easily simplified and rearranged to form:

$$\left(\frac{\partial^2 C}{\partial x^2}\right)_i^n = \frac{C_{i-1}^n + C_{i+1}^n - 2C_i^n}{\Delta x^2} \tag{3.30}$$

Substitution of (3.30) into (3.19), and neglecting all terms higher than second order results in:

$$C_{i-1}^n = C_i^n - \left(\frac{\partial C}{\partial x}\right)_i^n \frac{\Delta x}{1!} + \left(\frac{C_{i-1}^n + C_{i+1}^n - 2C_i^n}{\Delta x^2}\right)_i^n \frac{\Delta x^2}{2!} \tag{3.31}$$

Simplifying and rewriting in terms of the first order partial derivative:

$$\left(\frac{\partial C}{\partial x}\right)_i^n = C_i^n - C_{i-1}^n + \left(\frac{C_{i-1}^n + C_{i+1}^n - 2C_i^n}{2}\right)_i^n \tag{3.32}$$

$$\left(\frac{\partial C}{\partial x}\right)_i^n = \frac{C_{i+1}^n - C_{i-1}^n}{2\Delta x} \tag{3.33}$$

Subtracting equation (3.28) from (3.27) gives the second order central differencing equation:

$$C_i^{n+1} = C_i^n - \frac{u\Delta t}{2\Delta x}\left(C_{i+1}^n - C_{i-1}^n\right) \tag{3.34}$$

Like upwinding, the central differencing equation is very easy to derive. However inspection of the equation reveals it is based on conditions at points i-1 and i+1, which does not take proper account of conditions at location i. This leads to problems with convective stability, which can be observed as grid scale oscillations or wiggles.[29, 6] Rassmussen[5] and Manson and Wallis[9] , discuss how central differencing schemes are not inherently stable, and wiggles are very likely to occur for Péclet numbers greater than 3. In general wiggles can be reduced by decreasing the spatial increment, thus increasing spatial resolution.

As for the upwinding scheme, the literature gives details of the stability range of the central differencing scheme related to the value of the Courant number, using a von Neuman stability analysis.[6, 11, 28] The stability criteria for the central differencing scheme are that:

$$\alpha \leq 0.5$$

$$Cr^2 \leq 2\alpha$$

This indicates that when the diffusivity term is less than or equal to 0.5, the scheme is stable at Courant numbers less than 1. However examination of the plot of the von Neuman stability analysis, included as Figure (3.8), shows that when diffusivity is zero, the central differencing scheme is unstable for all Courant numbers. This point will be taken into consideration during the testing of this scheme.

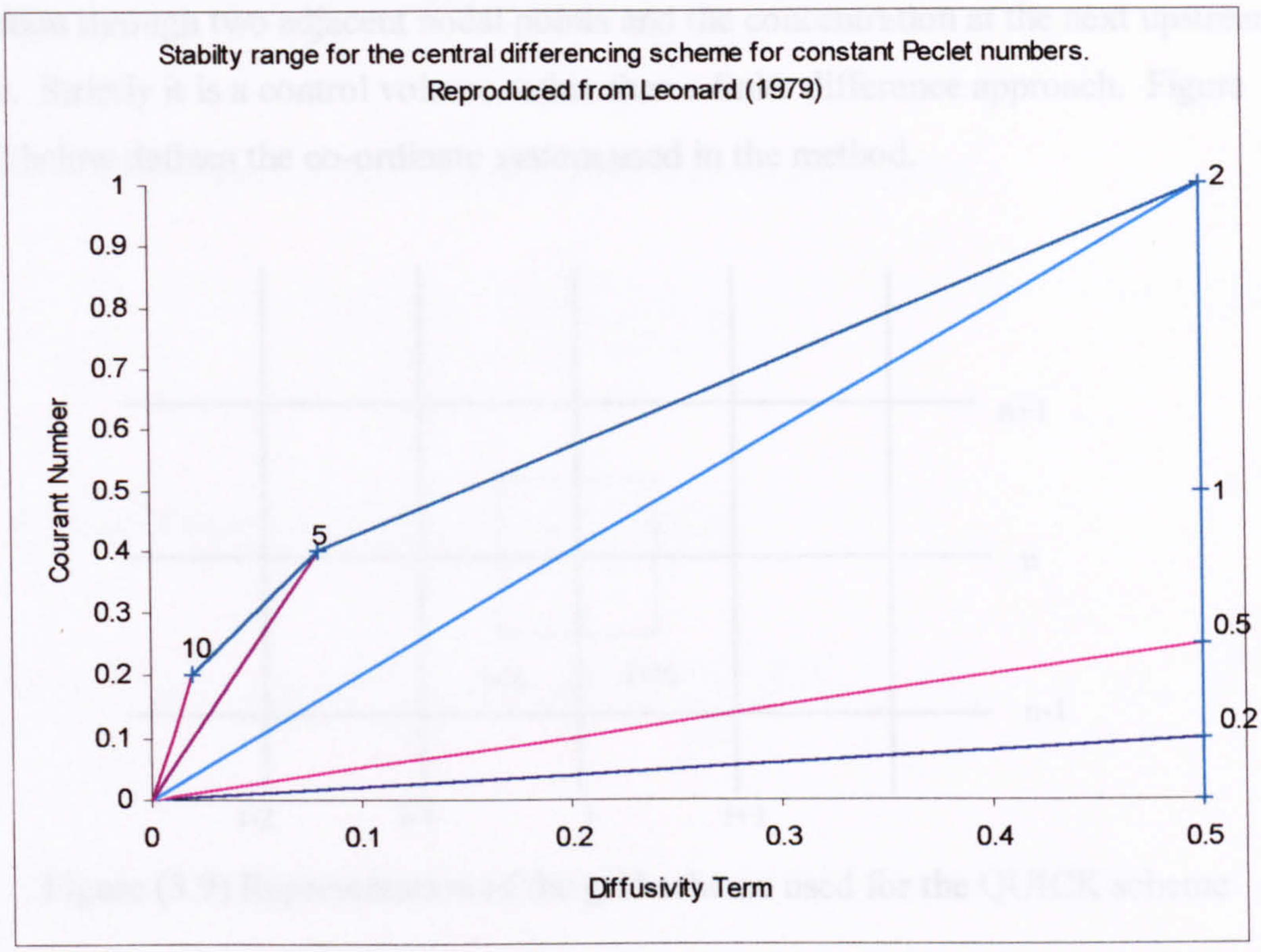

Figure (3.8) von Neuman stability analysis of the central differencing scheme[6]

3.1.4 Quadratic Upstream Interpolation for Convective Kinematics (QUICK)

The limitations of upwinding and central finite difference schemes are widely reported in the literature.[5, 6, 9] The difficulty arises when trying to develop a scheme that will give a stable and accurate solution that is also conservative. A quadratic interpolation scheme centred about a location i would be accurate, but it would suffer from the same conservation difficulties experienced with central differencing.[6] Leonard[29] also concludes that the conservativity of symmetrically centred schemes is highly dependent upon the velocity field and favours the development of an asymmetrical approach. The method he developed is a three point upstream quadratic interpolation scheme for convective kinematics for steady transport given the name QUICK.[6, 8, 30]

QUICK is a third order accurate in space scheme based upon the solution of a quadratic equation through two adjacent nodal points and the concentration at the next upstream node. Strictly it is a control volume rather than a finite difference approach. Figure (3.9) below defines the co-ordinate system used in the method.

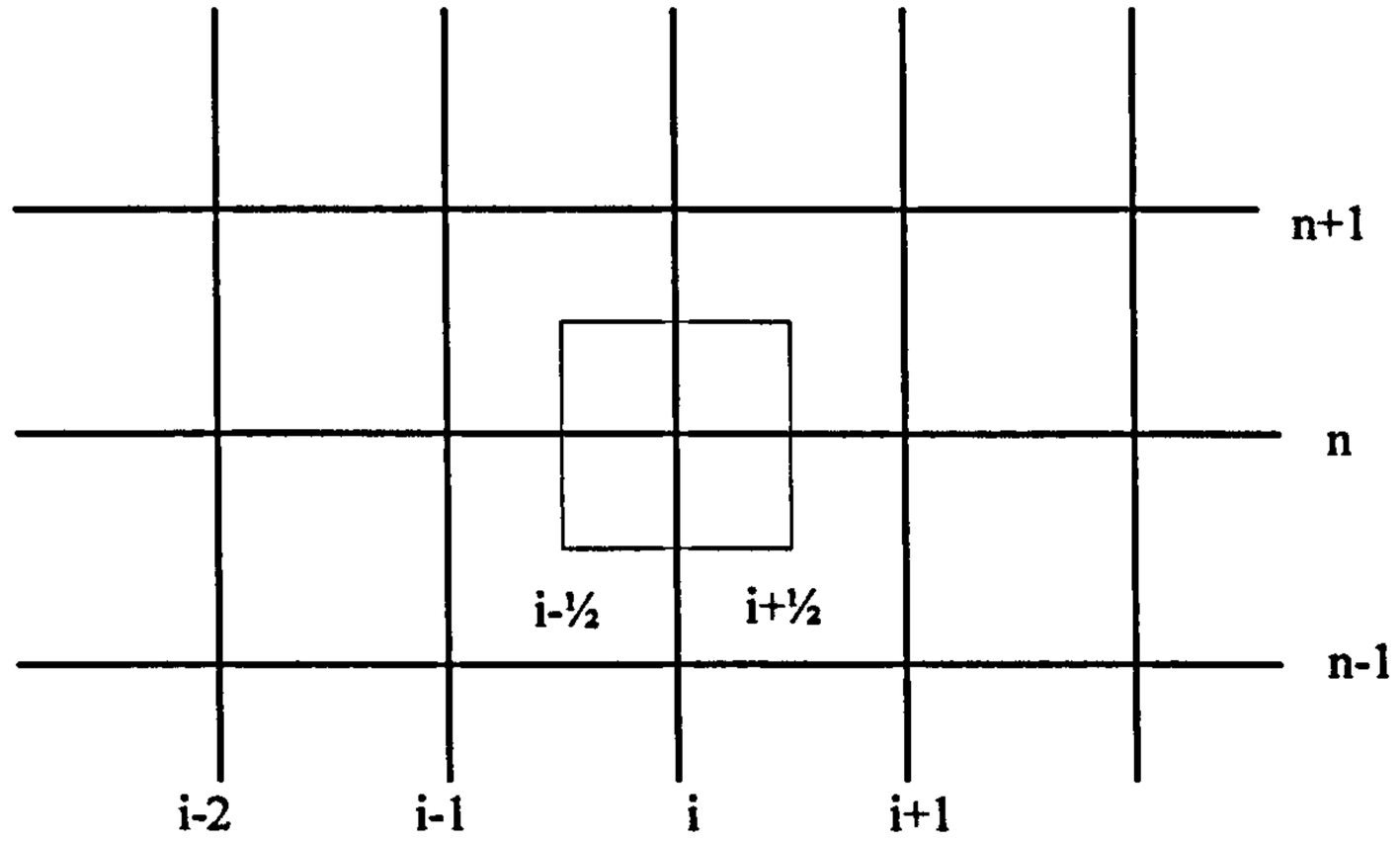

Figure (3.9) Representation of the grid scheme used for the QUICK scheme

In essence, two sets of concentrations are derived. That which is calculated using values at i-1, i and i+1, known as the forward component and the backward is derived from concentrations at i-2, i-1 and i, assuming the velocity is positive. This results in the calculation of the concentration gradient across the points at i±½, as indicated in Figure (3.9). The QUICK scheme can then be applied to calculate the concentration at the next time step. It is assumed for simplicity, that the grid spacing is constant.

The derivation of the backward component uses Taylor series expansions centred about i-1, which have the same format as equations (3.27) and (3.28):

$$C_{i-2}^{n} = C_{i-1}^{n} - \left(\frac{\partial C}{\partial x}\right)_{i-1}^{n} \frac{\Delta x}{1!} + \left(\frac{\partial^2 C}{\partial x^2}\right)_{i-1}^{n} \frac{\Delta x^2}{2!} - \left(\frac{\partial^3 C}{\partial x^3}\right)_{i-1}^{n} \frac{\Delta x^3}{3!} + H.O.T \tag{3.35}$$

$$C_{i}^{n} = C_{i-1}^{n} + \left(\frac{\partial C}{\partial x}\right)_{i-1}^{n} \frac{\Delta x}{1!} + \left(\frac{\partial^2 C}{\partial x^2}\right)_{i-1}^{n} \frac{\Delta x^2}{2!} + \left(\frac{\partial^3 C}{\partial x^3}\right)_{i-1}^{n} \frac{\Delta x^3}{3!} + H.O.T \tag{3.36}$$

Addition of equations (3.35) and (3.36) gives:

$$C_{i-2}^n + C_i^n = 2C_{i-1}^n + 2\left(\frac{\partial^2 C}{\partial x^2}\right)_{i-1}^n \frac{\Delta x^2}{2!} + H.O.T \tag{3.37}$$

Neglecting terms greater than second order and rearranging gives:

$$\left(\frac{\partial^2 C}{\partial x^2}\right)_{i-1}^n = \frac{C_{i-2}^n + C_i^n - 2C_{i-1}^n}{\Delta x^2} \tag{3.38}$$

Substitution of equation (3.38) into (3.35) leads to:

$$C_{i-2}^n = C_{i-1}^n - \left(\frac{\partial C}{\partial x}\right)_{i-1}^n \frac{\Delta x}{1!} + \left(\frac{C_{i-2}^n + C_i^n - 2C_{i-1}^n}{\Delta x^2}\right)_{i-1}^n \frac{\Delta x^2}{2!} \tag{3.39}$$

Simplifying and rewriting in terms of the first order partial derivative gives:

$$\left(\frac{\partial C}{\partial x}\right)_{i-1}^n = C_{i-1}^n - C_{i-2}^n + \left(\frac{C_{i-2}^n + C_i^n - 2C_{i-1}^n}{2}\right)_{i-1}^n \tag{3.40}$$

$$\left(\frac{\partial C}{\partial x}\right)_{i-1}^n = \frac{C_i^n - C_{i-2}^n}{2\Delta x} \tag{3.41}$$

Use of $\Delta x/2$ instead of Δx gives an equation with the same format as equation (3.35) at the i-½ location:

$$C_{i-½}^n = C_{i-1}^n + \left(\frac{\partial C}{\partial x}\right)_{i-1}^n \left(\frac{\Delta x}{2}\right) + \left(\frac{\partial^2 C}{\partial x^2}\right)_{i-1}^n \left(\frac{\Delta x}{2}\right)^2 \left(\frac{1}{2!}\right) + H.O.T \tag{3.42}$$

Substitution of (3.38) and (3.41) into equation (3.42) gives:

$$C_{i-½}^n = C_{i-1}^n + \left(\frac{C_i^n - C_{i-2}^n}{\Delta x}\right)_{i-1}^n \left(\frac{\Delta x}{2}\right) + \left(\frac{C_{i-2}^n + C_i^n - 2C_{i-1}^n}{\Delta x^2}\right)_{i-1}^n \left(\frac{\Delta x}{2}\right)^2 \left(\frac{1}{2!}\right) \tag{3.43}$$

which simplifies to:

$$C_{i-\frac{1}{2}}^{n} = \frac{3C_i^n}{8} + \frac{6C_{i-1}^n}{8} - \frac{C_{i-2}^n}{8} \tag{3.44}$$

This can also be rearranged and written in the more usual form of the equation specified by Leonard[6] as:

$$C_{i-\frac{1}{2}}^{n} = \frac{1}{2}\left(C_{i-1}^n + C_i^n\right) - \frac{1}{8}\left(C_{i-2}^n + C_i^n - 2C_{i-1}^n\right) \tag{3.45}$$

A similar derivation can be carried out for the forward component at i+½, using Taylor expansions about i:

$$C_{i+\frac{1}{2}}^{n} = \frac{1}{2}\left(C_i^n + C_{i+1}^n\right) - \frac{1}{8}\left(C_{i-1}^n + C_{i+1}^n - 2C_i^n\right) \tag{3.46}$$

Leonard[6] describes this equation in term in the equation as wall gradient (GRAD) and the second as curvature (CURV).

$$GRAD = \frac{\left(C_i^n + C_{i+1}^n\right)}{\Delta x}$$

$$CURV = \frac{\left(C_{i-1}^n + C_{i+1}^n - 2C_i^n\right)}{\Delta x^2}$$

$$C_{i+\frac{1}{2}}^{n} = \frac{\Delta x}{2} GRAD - \frac{\Delta x^2}{8} CURV$$

This is identical to equation (3.46). In terms of the solution of the advection equation in one-dimension, the spatial derivative is replaced by:

$$C^n_{i+½} - C^n_{i-½} \tag{3.47}$$

Hence:

$$\frac{\partial C}{\partial t} = -\frac{u}{\Delta x}\left(C^n_{i+½} - C^n_{i-½}\right) \tag{3.48}$$

Using a forward explicit method to discretise the temporal rate of change and then expanding the brackets, gives the one-dimensional QUICK equation:

$$C_i^{n+1} = C_i^n - \frac{u\Delta t}{\Delta x}\left\{\left(\frac{C_i^n + C_{i+1}^n}{2} - \frac{C_{i-1}^n + C_{i+1}^n - 2C_i^n}{8}\right) - \left(\frac{C_{i-1}^n + C_i^n}{2} - \frac{C_{i-2}^n + C_i^n - 2C_{i-1}^n}{8}\right)\right\} \tag{3.49}$$

The drawback with QUICK is that it is only applicable to steady transport situations which makes it impractical when considering real flows. Leonard also shows that the von Neuman stability conditions for QUICK are very restrictive as illustrated in Figure (3.10).[6, 31, 32]

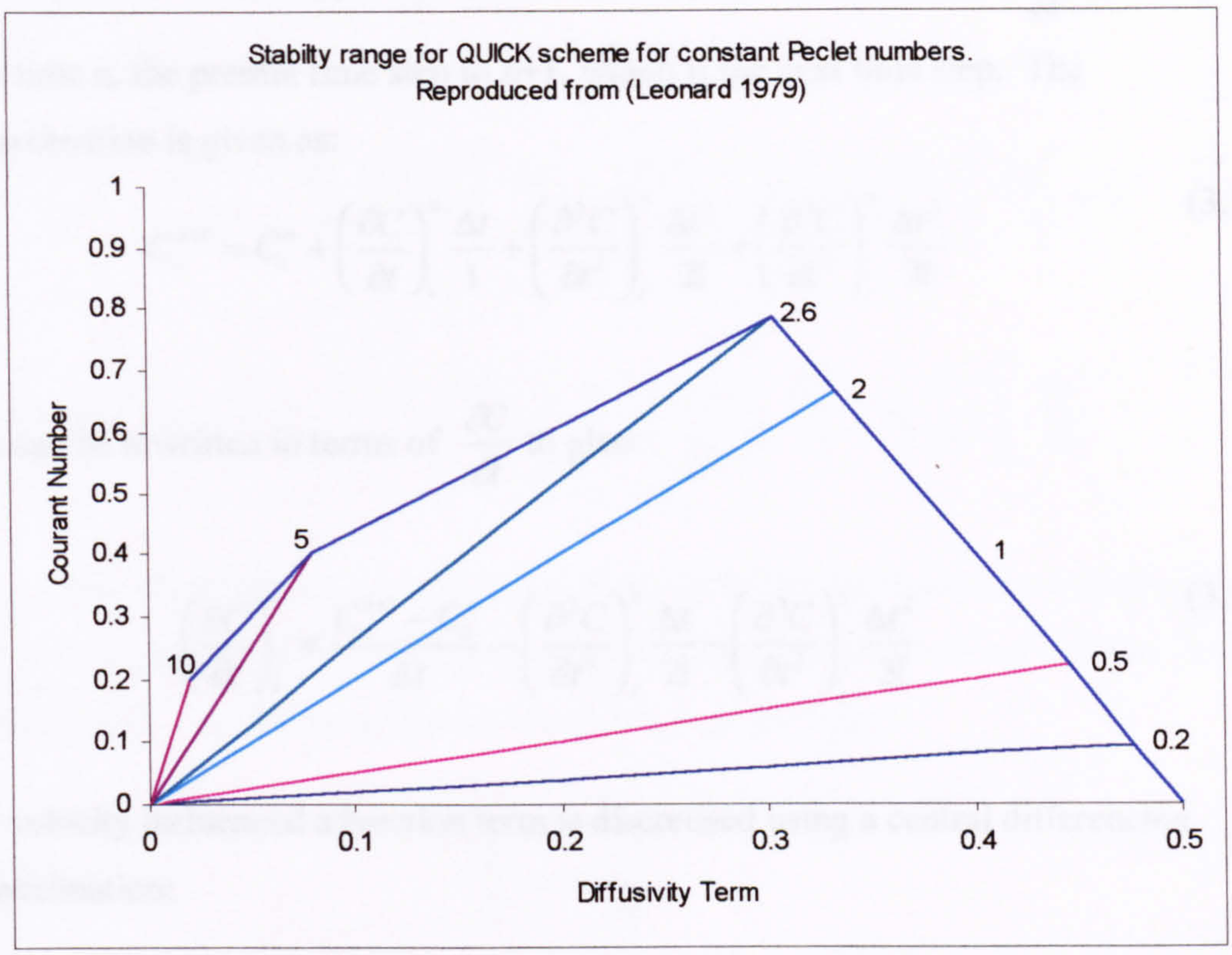

Figure (3.10) Stability range for the QUICK scheme, Leonard[6]

3.1.5 Quadratic Upstream Interpolation for Convective Kinematics with Estimated Streaming Terms (QUICKEST)

The QUICK scheme was further developed so that it could be applied to unsteady transport conditions, creating QUICKEST.[6] QUICKEST is defined as QUICK with estimated streaming terms.

The derivation follows the same general procedure used for QUICK but is more complicated. The original form of the pure advection equation in one-dimension is as set out in equation (3.17).

The forward difference approximation of the temporal rate of change, $\frac{\partial C}{\partial t}$, is derived from time n, the present time step to n+1, which is the next time step. The approximation is given as:

$$C_i^{n+1} = C_i^n + \left(\frac{\partial C}{\partial t}\right)_i^n \frac{\Delta t}{1} + \left(\frac{\partial^2 C}{\partial t^2}\right)_i^n \frac{\Delta t^2}{2!} + \left(\frac{\partial^3 C}{\partial t^3}\right)_i^n \frac{\Delta t^3}{3!} \tag{3.50}$$

This can be rewritten in terms of $\frac{\partial C}{\partial t}$ to give:

$$\left(\frac{\partial C}{\partial t}\right)_i^n = \frac{C_i^{n+1} - C_i^n}{\Delta t} - \left(\frac{\partial^2 C}{\partial t^2}\right)_i^n \frac{\Delta t}{2!} - \left(\frac{\partial^3 C}{\partial t^3}\right)_i^n \frac{\Delta t^2}{3!} \tag{3.51}$$

The velocity influenced advection term is discretised using a central differencing approximation:

$$uC_{i-1}^n = uC_i^n - u\left(\frac{\partial C}{\partial x}\right)_i^n \frac{\Delta x}{1!} + u\left(\frac{\partial^2 C}{\partial x^2}\right)_i^n \frac{\Delta x^2}{2!} - u\left(\frac{\partial^3 C}{\partial x^3}\right)_i^n \frac{\Delta x^3}{3!} + H.O.T \tag{3.52}$$

$$uC_{i+1}^n = uC_i^n + u\left(\frac{\partial C}{\partial x}\right)_i^n \frac{\Delta x}{1!} + u\left(\frac{\partial^2 C}{\partial x^2}\right)_i^n \frac{\Delta x^2}{2!} + u\left(\frac{\partial^3 C}{\partial x^3}\right)_i^n \frac{\Delta x^3}{3!} + H.O.T \tag{3.53}$$

Subtraction of equation (3.52) from (3.53) gives:

$$u\left(C_{i+1}^n - C_{i-1}^n\right) = 2u\left(\frac{\partial C}{\partial x}\right)_i^n \frac{\Delta x}{1} + 2u\left(\frac{\partial^3 C}{\partial x^3}\right)_i^n \frac{\Delta x^3}{3!} \tag{3.54}$$

Rewriting in terms of the first spatial derivative:

$$u\left(\frac{\partial C}{\partial x}\right)_i^n = u\frac{\left(C_{i+1}^n - C_{i-1}^n\right)}{2\Delta x} - u\left(\frac{\partial^3 C}{\partial x^3}\right)_i^n \frac{\Delta x^2}{3!} \tag{3.55}$$

Substitution of (3.51) and (3.55) into equation (3.17) gives the one-dimensional equation:

$$\frac{C_i^{n+1}-C_i^n}{\Delta t}-\left(\frac{\partial^2 C}{\partial t^2}\right)_i^n\frac{\Delta t}{2!}-\left(\frac{\partial^3 C}{\partial t^3}\right)_i^n\frac{\Delta t^2}{3!}+u\frac{\left(C_{i+1}^n-C_{i-1}^n\right)}{2\Delta x}-u\left(\frac{\partial^3 C}{\partial x^3}\right)_i^n\frac{\Delta x^2}{3!}=0 \tag{3.56}$$

$$\frac{C_i^{n+1}-C_i^n}{\Delta t}+u\frac{\left(C_{i+1}^n-C_{i-1}^n\right)}{2\Delta x}=\left(\frac{\partial^2 C}{\partial t^2}\right)_i^n\frac{\Delta t}{2!}+\left(\frac{\partial^3 C}{\partial t^3}\right)_i^n\frac{\Delta t^2}{3!}+u\left(\frac{\partial^3 C}{\partial x^3}\right)_i^n\frac{\Delta x^2}{3!} \tag{3.57}$$

The equation is simplified by conversion of the temporal derivatives to spatial ones. This requires returning to the original one-dimensional pure advection equation defined as equation (3.17). Rearranging this equation gives the form:

$$\frac{\partial C}{\partial t}=-u\frac{\partial C}{\partial x} \tag{3.58}$$

Development of this equation to give spatial equivalents of higher order temporal derivatives is straightforward.

$$\frac{\partial^2 C}{\partial t^2}=-u\frac{\partial C}{\partial x}\times\frac{\partial C}{\partial t}=-u\frac{\partial C}{\partial x}\times-u\frac{\partial C}{\partial x} \tag{3.59}$$

$$\frac{\partial^2 C}{\partial t^2}=u^2\frac{\partial^2 C}{\partial x^2} \tag{3.60}$$

$$\frac{\partial^3 C}{\partial t^3}=-u^3\frac{\partial^3 C}{\partial x^3} \tag{3.61}$$

Replacing these new terms in equation (3.57):

$$\frac{C_i^{n+1}-C_i^n}{\Delta t}+u\frac{\left(C_{i+1}^n-C_{i-1}^n\right)}{2\Delta x}=u^2\left(\frac{\partial^2 C}{\partial x^2}\right)_i^n\frac{\Delta t}{2!}-u^3\left(\frac{\partial^3 C}{\partial x^3}\right)_i^n\frac{\Delta t^2}{3!}+u\left(\frac{\partial^3 C}{\partial x^3}\right)_i^n\frac{\Delta x^2}{3!} \tag{3.62}$$

Discretised forms of the spatial derivatives are:

$$\frac{\partial^2 C}{\partial x^2} = \frac{C_{i-1}^n + C_{i+1}^n - 2C_i^n}{\Delta x^2} \tag{3.63}$$

$$\frac{\partial^3 C}{\partial x^3} = \frac{C_{i+1}^n - 3C_i^n + 3C_{i-1}^n - C_{i-2}^n}{\Delta x^3} \tag{3.64}$$

Substituting (3.63) and (3.64) in equation (3.62):

$$\frac{C_i^{n+1} - C_i^n}{\Delta t} + u\frac{\left(C_{i+1}^n - C_{i-1}^n\right)}{2\Delta x} = u^2\left(\frac{C_{i-1}^n + C_{i+1}^n - 2C_i^n}{\Delta x^2}\right)_i^n \frac{\Delta t}{2!} + \left(\frac{C_{i+1}^n - 3C_i^n + 3C_{i-1}^n - C_{i-2}^n}{\Delta x^3}\right)_i^n \left(-u^3\frac{\Delta t^2}{3!} + u\frac{\Delta x^2}{3!}\right) \tag{3.65}$$

In terms of the concentration at the next time step:

$$C_i^{n+1} = \frac{-u\Delta t}{2\Delta x}\left(C_{i+1}^n - C_{i-1}^n\right) + \frac{u^2\Delta t^2}{2\Delta x^2}\left(C_{i-1}^n + C_{i+1}^n - 2C_i^n\right) + \left(\frac{u\Delta t}{6\Delta x} - \frac{u^2\Delta t^3}{6\Delta x^3}\right)\left(C_{i+1}^n - 3C_i^n + 3C_{i-1}^n - C_{i-2}^n\right)_i^n \tag{3.66}$$

Equation (3.66) represents the generalised form of the one-dimensional QUICKEST equation. Leonard[6] uses a different form of the equation, but it is numerically identical. It is included as equation (3.67):

$$C_i^{n+1} = C_i^n - Cr\left\{\begin{array}{l}\left[\frac{1}{2}\left(C_i^n + C_{i+1}^n\right) - \frac{\Delta x}{2}Cr * GRAD_R - \frac{\Delta x^2}{6}\left(1 - Cr^2\right) * CURV_R\right] - \\ \left[\frac{1}{2}\left(C_{i-1}^n + C_i^n\right) - \frac{\Delta x}{2}Cr * GRAD_L - \frac{\Delta x^2}{6}\left(1 - Cr^2\right) * CURV_L\right]\end{array}\right\} \tag{3.67}$$

The GRAD and CURV terms are as defined by Leonard.[6]

3.2 Testing of finite difference schemes using one-dimensional idealised testcases

Although the literature indicates the shortcomings and advantages of these finite difference schemes, it is beneficial with regard to the development of the ideas presented here to discuss it further.[6, 10, 33, 34]

A simple one-dimensional test case is used to demonstrate the stability and accuracy of the four schemes, upwinding, central differencing, QUICK and QUICKEST. A straight channel with a constant velocity, u, of 1m/s is used. The finite difference grid is regular with spatial increments in the x-direction of 100m and various time increments are applied. Three different representations of pollutant are introduced at the upstream end. The tests consider a point release, a linear distribution and a Gaussian distribution of pollution. Plots of these initial conditions are included as Figure (3.11) to (3.14).

These simulations give some insight into how each finite difference scheme behaves, depending on the shape and degree to which the distribution is defined and also the effect of the Courant number. The tests give results in terms of the difference between the solution calculated by each numerical scheme and the ideal solution, and the percentage of the peak value maintained.

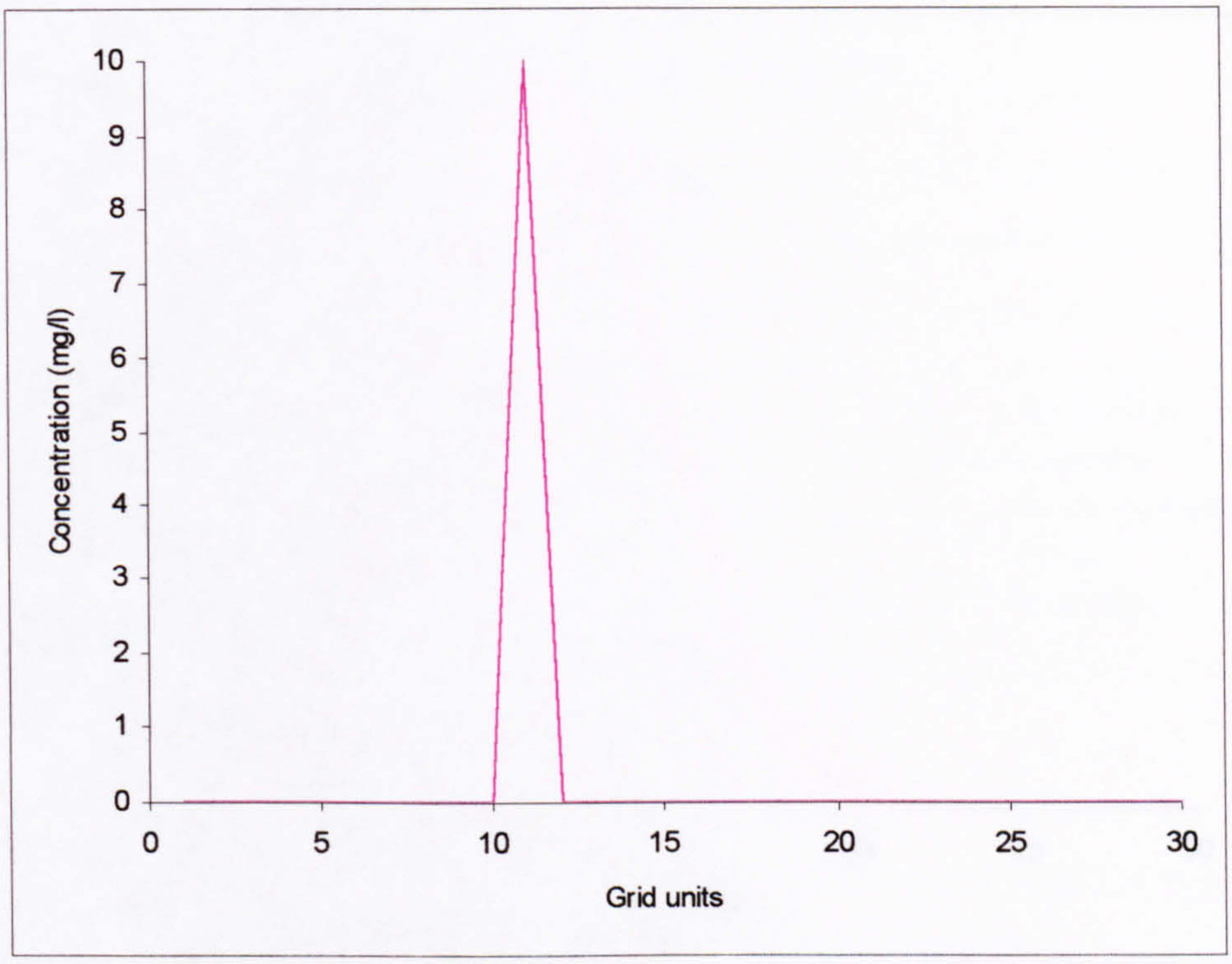

Figure (3.11) Plot of the initial point release of pollution

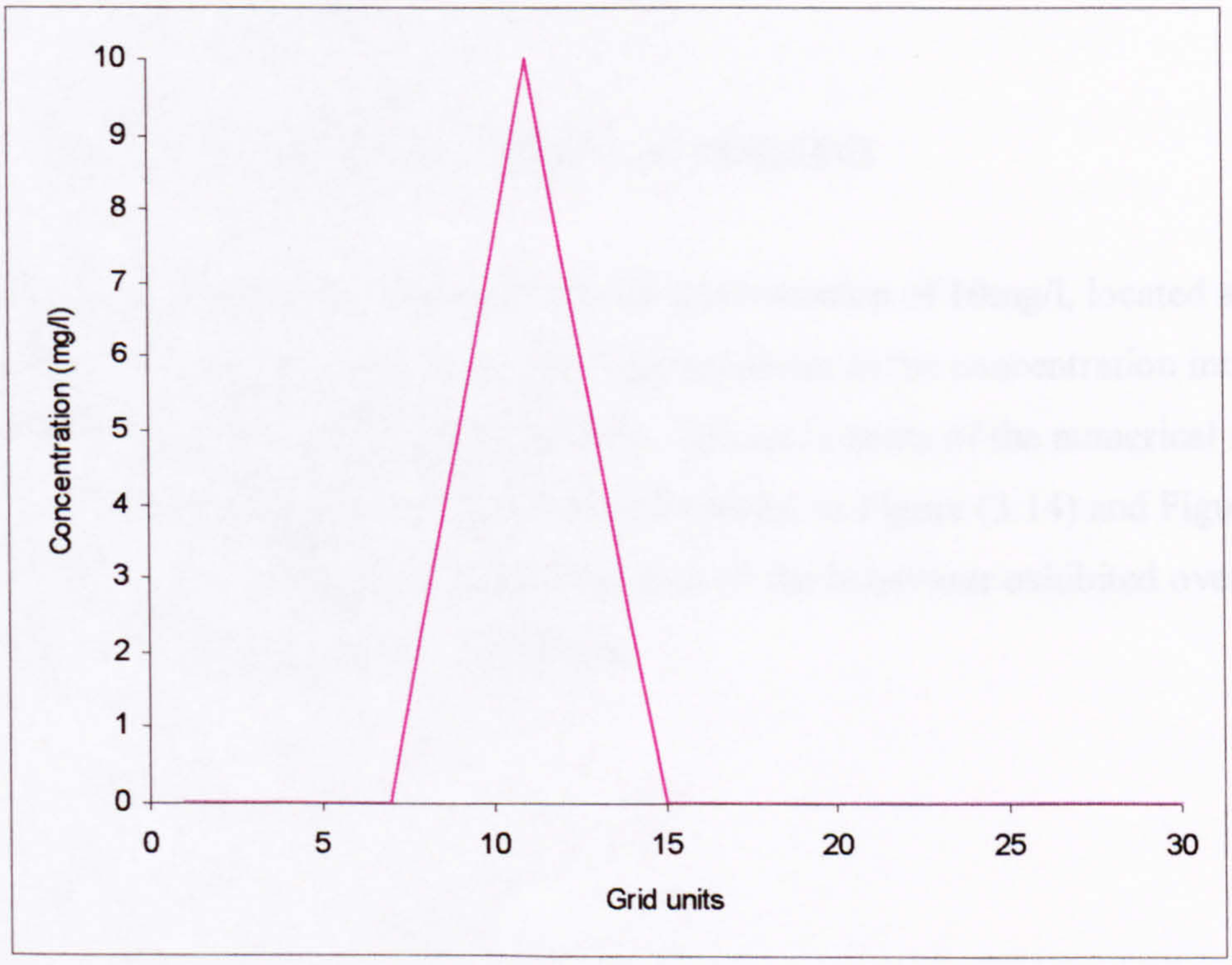

Figure (3.12) Plot of the initial linear distribution of pollution

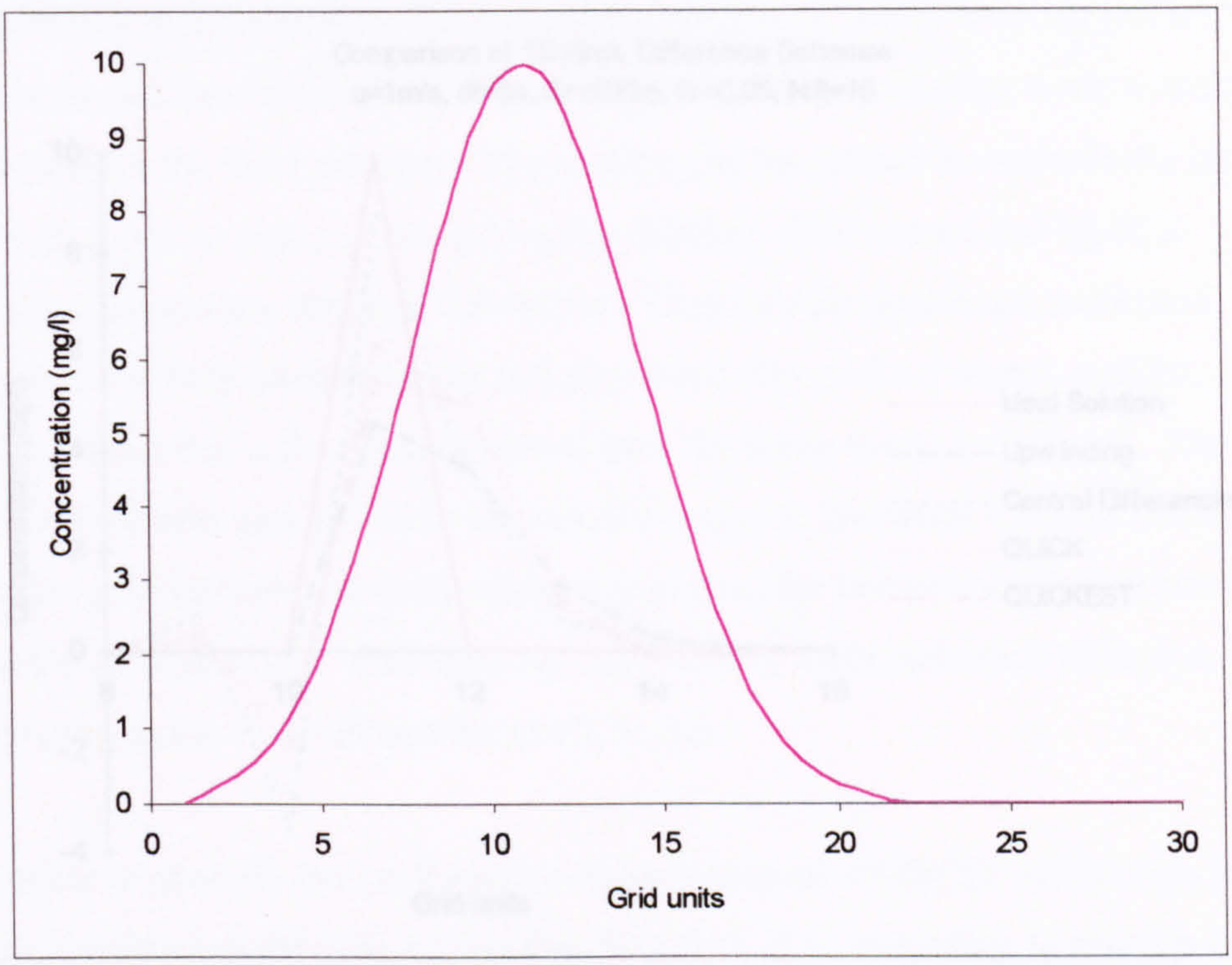

Figure (3.13) Plot of the initial Gaussian distribution of pollution

3.2.1 Results for the point release of pollution

The point release consists of a single value of concentration of 10mg/l, located at i=11, Figure (3.11). This distribution has very steep gradients as the concentration increases from zero to ten in a single spatial increment. Selected results of the numerical solution at Courant numbers equal to 0.05 and 0.8 are included as Figure (3.14) and Figure (3.15) respectively. These graphs are indicative of the behaviour exhibited over the 0.05-1 range of Courant number considered.

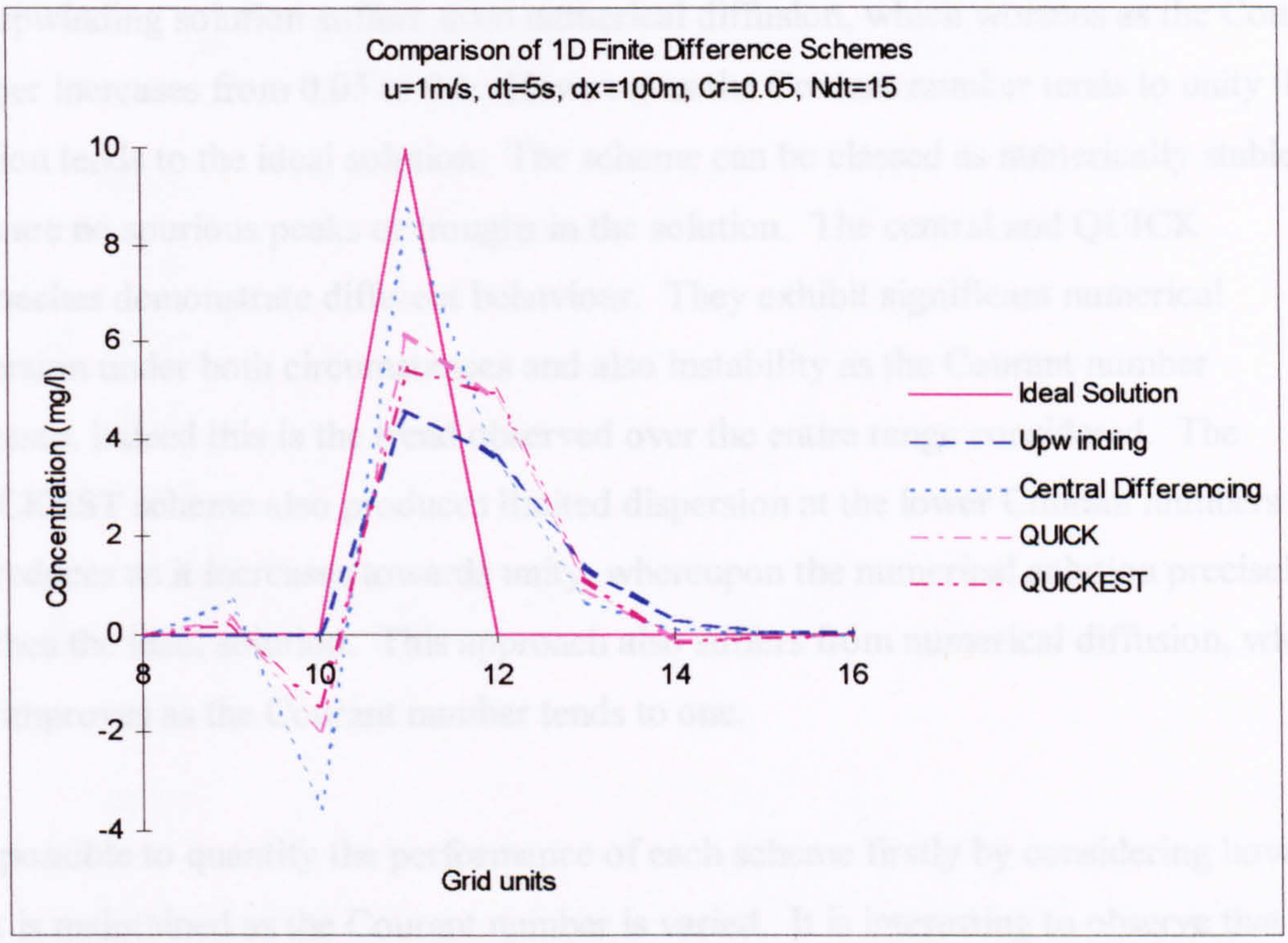

Figure (3.14) Comparison of 1D FDS, using a point release at Cr=0.05

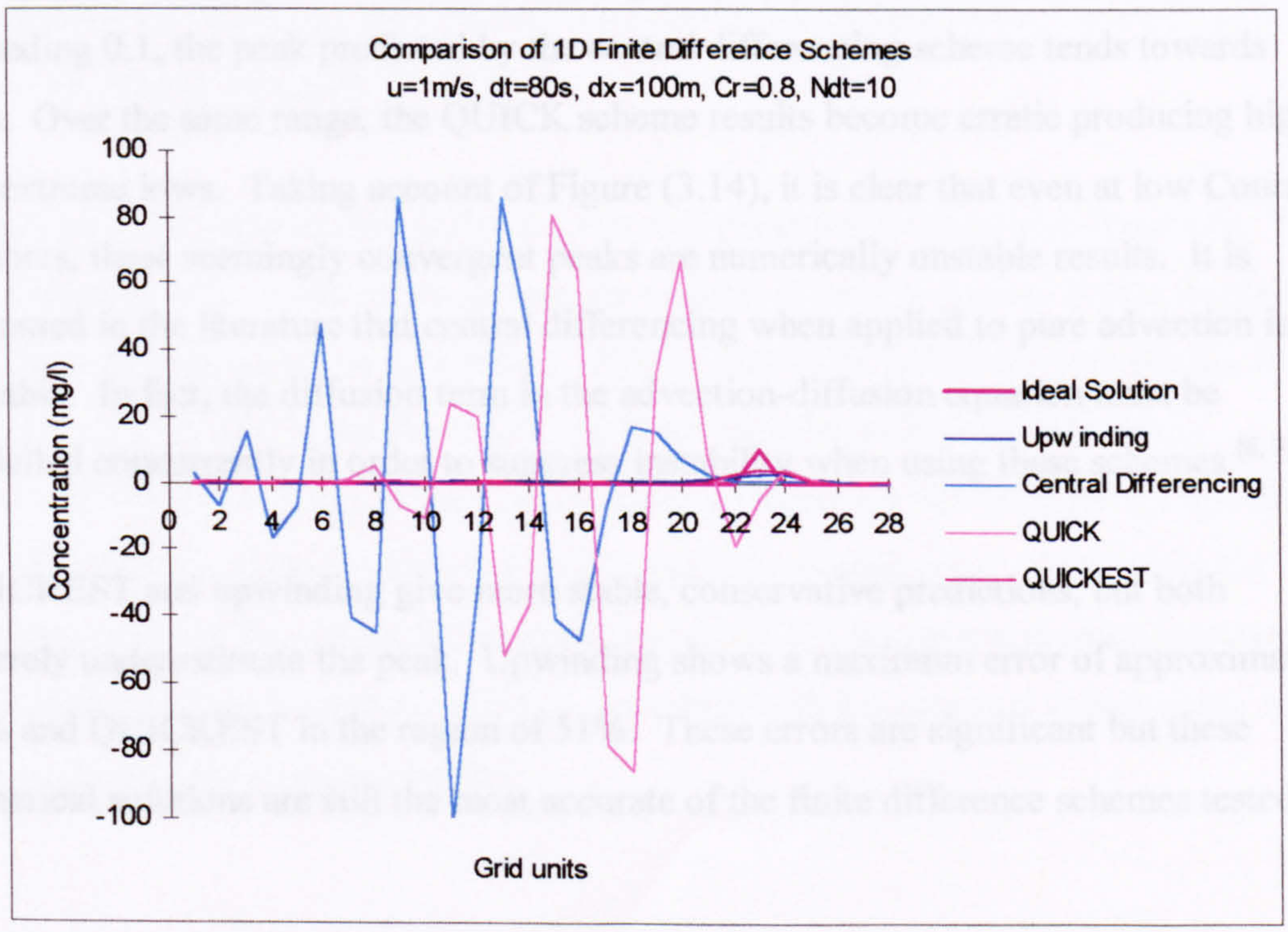

Figure (3.15) Comparison of 1D FDS, using a point release at Cr=0.8

Observations regarding numerical diffusion, instability and dispersion can be made. The upwinding solution suffers from numerical diffusion, which worsens as the Courant number increases from 0.05 to 0.8. However as the Courant number tends to unity the solution tends to the ideal solution. The scheme can be classed as numerically stable, as there are no spurious peaks or troughs in the solution. The central and QUICK approaches demonstrate different behaviour. They exhibit significant numerical dispersion under both circumstances and also instability as the Courant number increases, indeed this is the trend observed over the entire range considered. The QUICKEST scheme also produces limited dispersion at the lower Courant numbers but this reduces as it increases towards unity, whereupon the numerical solution precisely matches the ideal solution. This approach also suffers from numerical diffusion, which also improves as the Courant number tends to one.

It is possible to quantify the performance of each scheme firstly by considering how the peak is maintained as the Courant number is varied. It is interesting to observe that for Courant numbers less than 0.1, the QUICK and central differencing scheme maintain the highest percentage of the peak value, Figure (3.16). However at Courant numbers exceeding 0.1, the peak predicted by the central differencing scheme tends towards zero. Over the same range, the QUICK scheme results become erratic producing highs and extreme lows. Taking account of Figure (3.14), it is clear that even at low Courant numbers, these seemingly convergent peaks are numerically unstable results. It is discussed in the literature that central differencing when applied to pure advection is unstable. In fact, the diffusion term in the advection-diffusion equation must be modelled concurrently in order to suppress instability when using these schemes.[6, 7]

QUICKEST and upwinding give more stable, conservative predictions, but both severely underestimate the peak. Upwinding shows a maximum error of approximately 62% and QUICKEST in the region of 51%. These errors are significant but these numerical solutions are still the most accurate of the finite difference schemes tested.

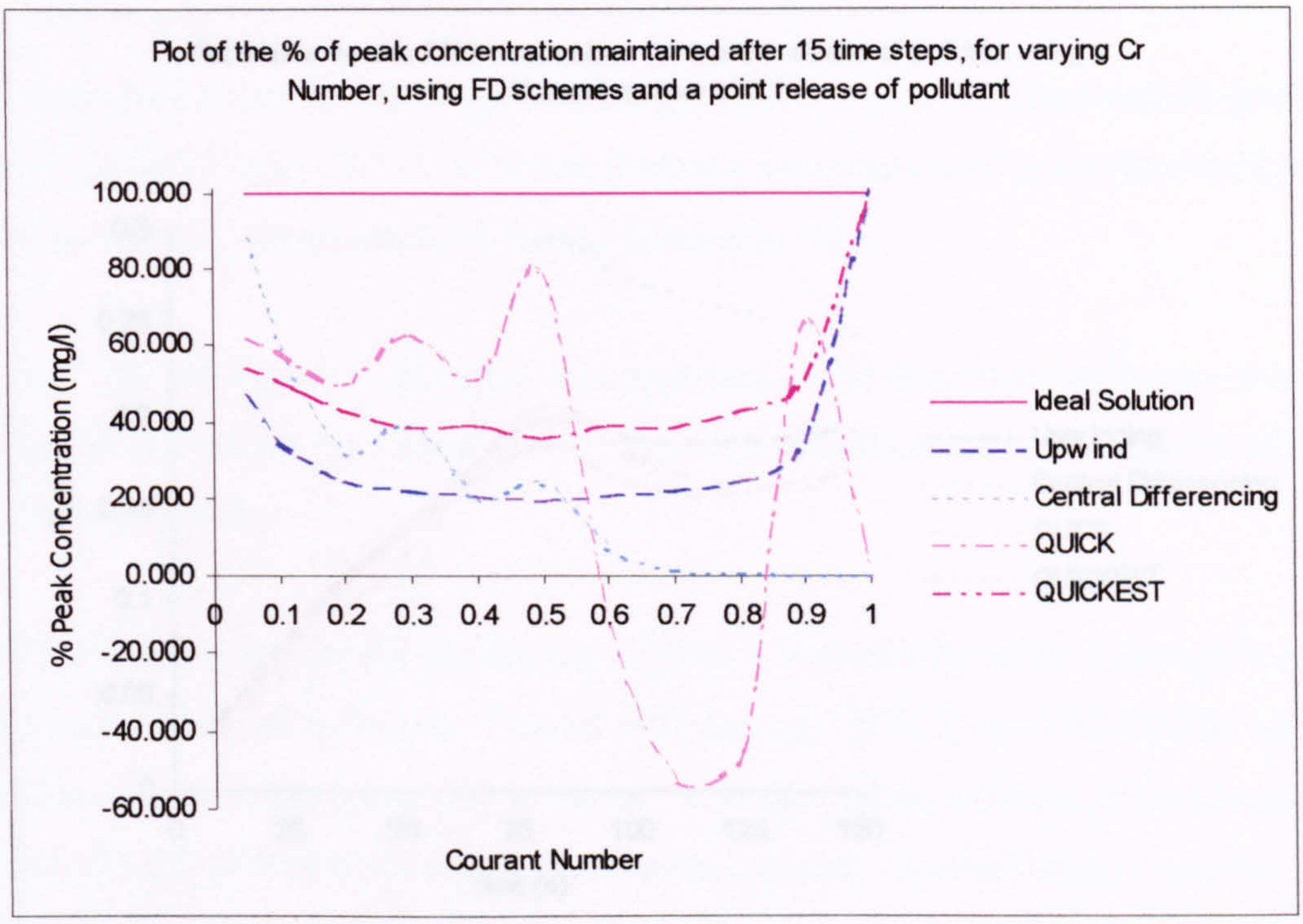

Figure (3.16) Plot of the % point release peak maintained after 15 time steps

Considering the global errors in terms of the root mean square value, Figure (3.17) and Figure (3.18) are produced.[12, 17-19]

The graph shows that as time increases, the root mean square error also increases. This indicates that as the solution progresses the numerical error is grows. It also illustrates that the overall accuracy of upwinding, QUICK and QUICKEST are very similar for a Courant number of 0.1, but the central differencing scheme is more inaccurate. Referring to Figure (3.16), as the Courant number increases, the error for the upwinding and QUICKEST schemes reduce: at Cr=1 there is no visible error. Conversely the solutions obtained by central differencing and QUICK become much more inaccurate as the Courant number increases, which is consistent with the previous observations made regarding their numerical instability.

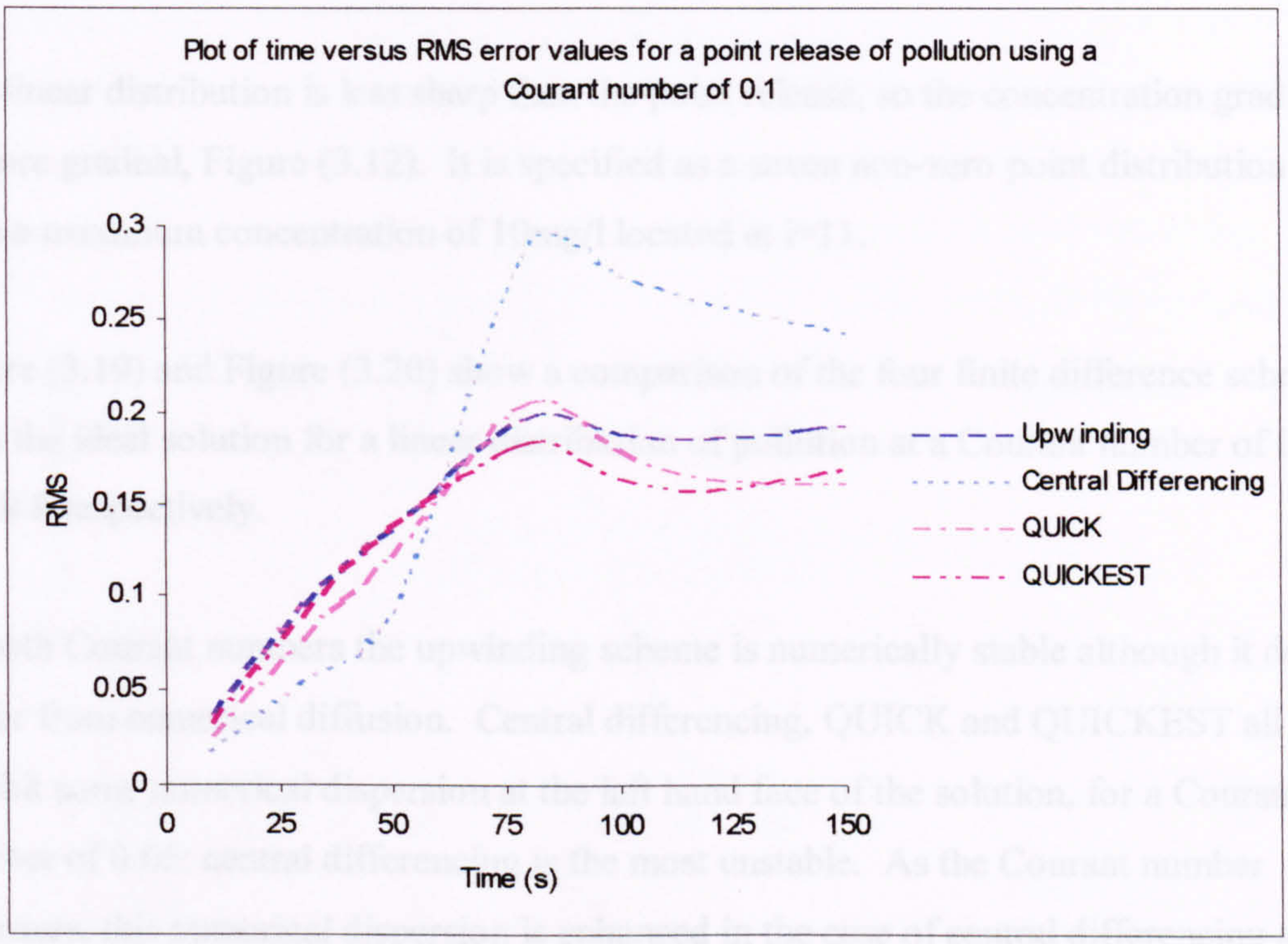

Figure (3.17) Plot of the RMS error values for a point release at Cr=0.1

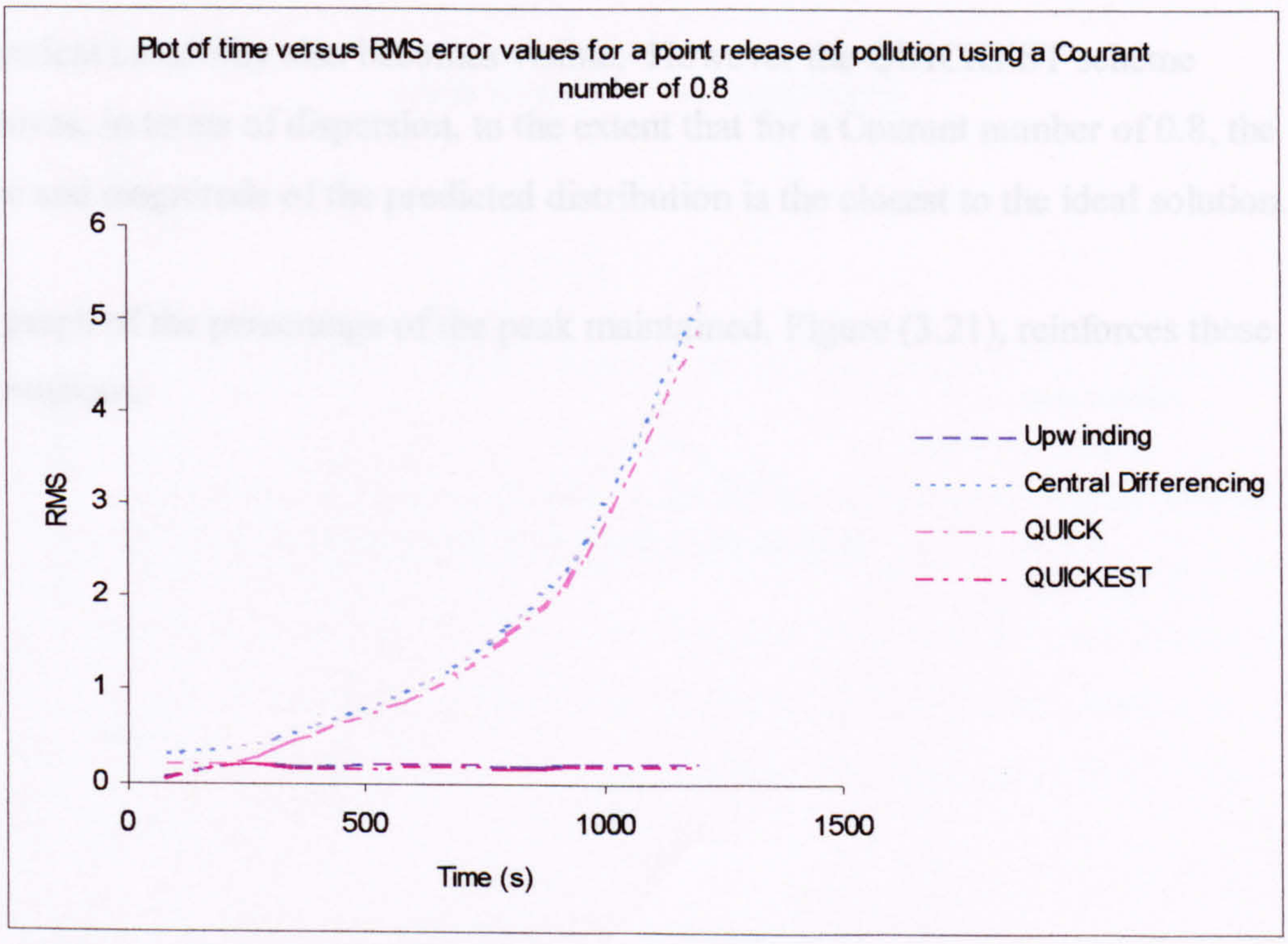

Figure (3.18) Plot of the RMS error values for a point release at Cr=0.8

3.2.2 Results using the linear distribution of pollution

The linear distribution is less sharp than the point release, so the concentration gradient is more gradual, Figure (3.12). It is specified as a seven non-zero point distribution with a maximum concentration of 10mg/l located at i=11.

Figure (3.19) and Figure (3.20) show a comparison of the four finite difference schemes with the ideal solution for a linear distribution of pollution at a Courant number of 0.05 and 0.8 respectively.

At both Courant numbers the upwinding scheme is numerically stable although it does suffer from numerical diffusion. Central differencing, QUICK and QUICKEST all exhibit some numerical dispersion at the left hand face of the solution, for a Courant number of 0.05: central differencing is the most unstable. As the Courant number increases, this numerical dispersion is enhanced in the case of central differencing and QUICK as indicated in Figure (3.20).

Numerical instability also becomes visible. However the QUICKEST scheme improves, in terms of dispersion, to the extent that for a Courant number of 0.8, the shape and magnitude of the predicted distribution is the closest to the ideal solution.

The graph of the percentage of the peak maintained, Figure (3.21), reinforces these observations.

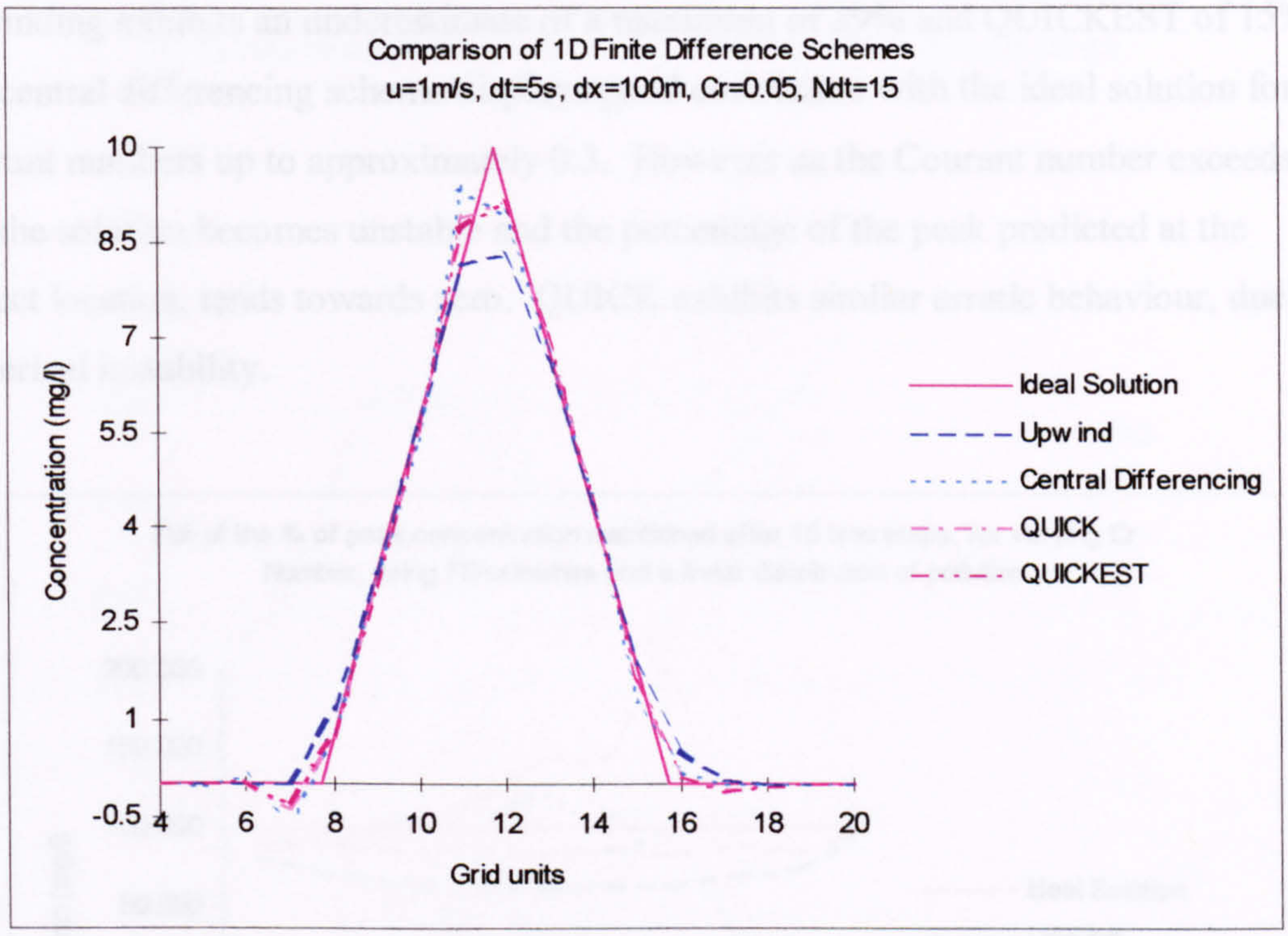

Figure (3.19) Comparison of 1D FDS, using a linear distribution at Cr=0.05

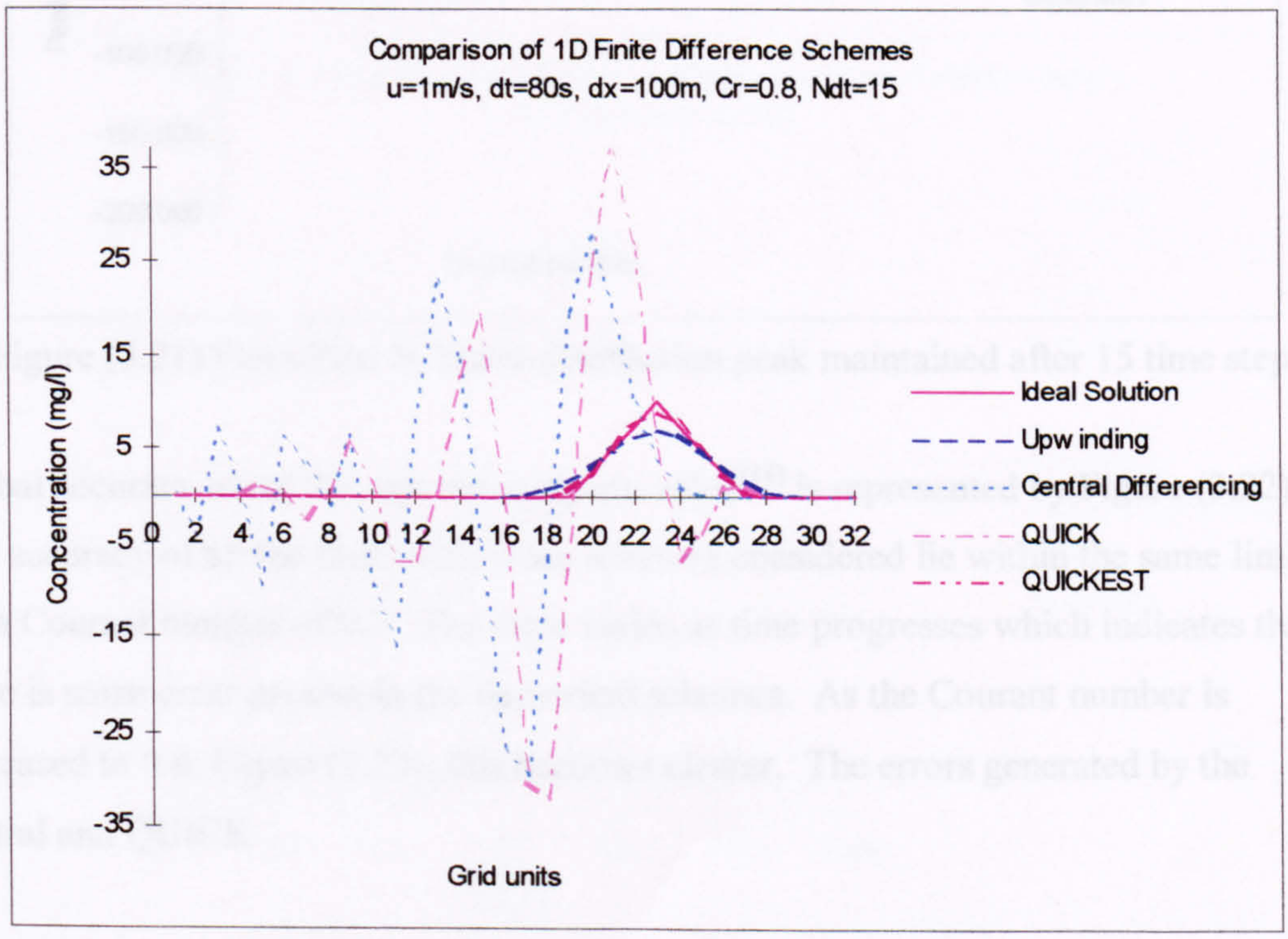

Figure (3.20) Comparison of 1D FDS, using a linear distribution at Cr=0.8

The upwinding and QUICKEST schemes predict the most accurate values of the peak. Upwinding exhibits an underestimate of a maximum of 39% and QUICKEST of 15%. The central differencing scheme displays good correlation with the ideal solution for Courant numbers up to approximately 0.3. However as the Courant number exceeds 0.3, the solution becomes unstable and the percentage of the peak predicted at the correct location, tends towards zero. QUICK exhibits similar erratic behaviour, due to numerical instability.

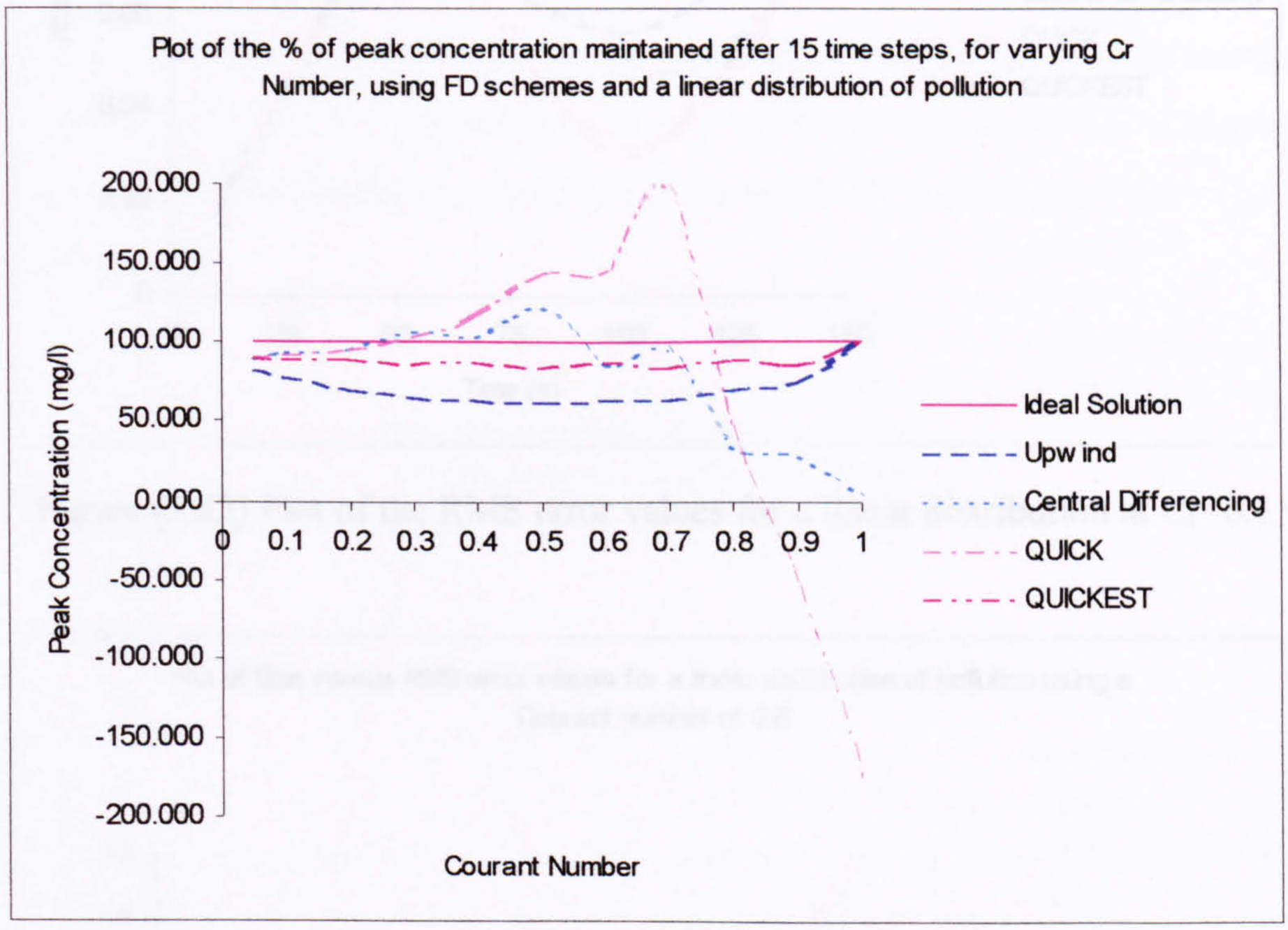

Figure (3.21) Plot of the % linear distribution peak maintained after 15 time steps

Global accuracy using the root mean square value[18] is represented by Figure (3.22). The accuracy of all the finite difference schemes considered lie within the same limits for a Courant number of 0.1. The error varies as time progresses which indicates that there is some error present in the numerical schemes. As the Courant number is increased to 0.8, Figure (3.23), this becomes clearer. The errors generated by the central and QUICK

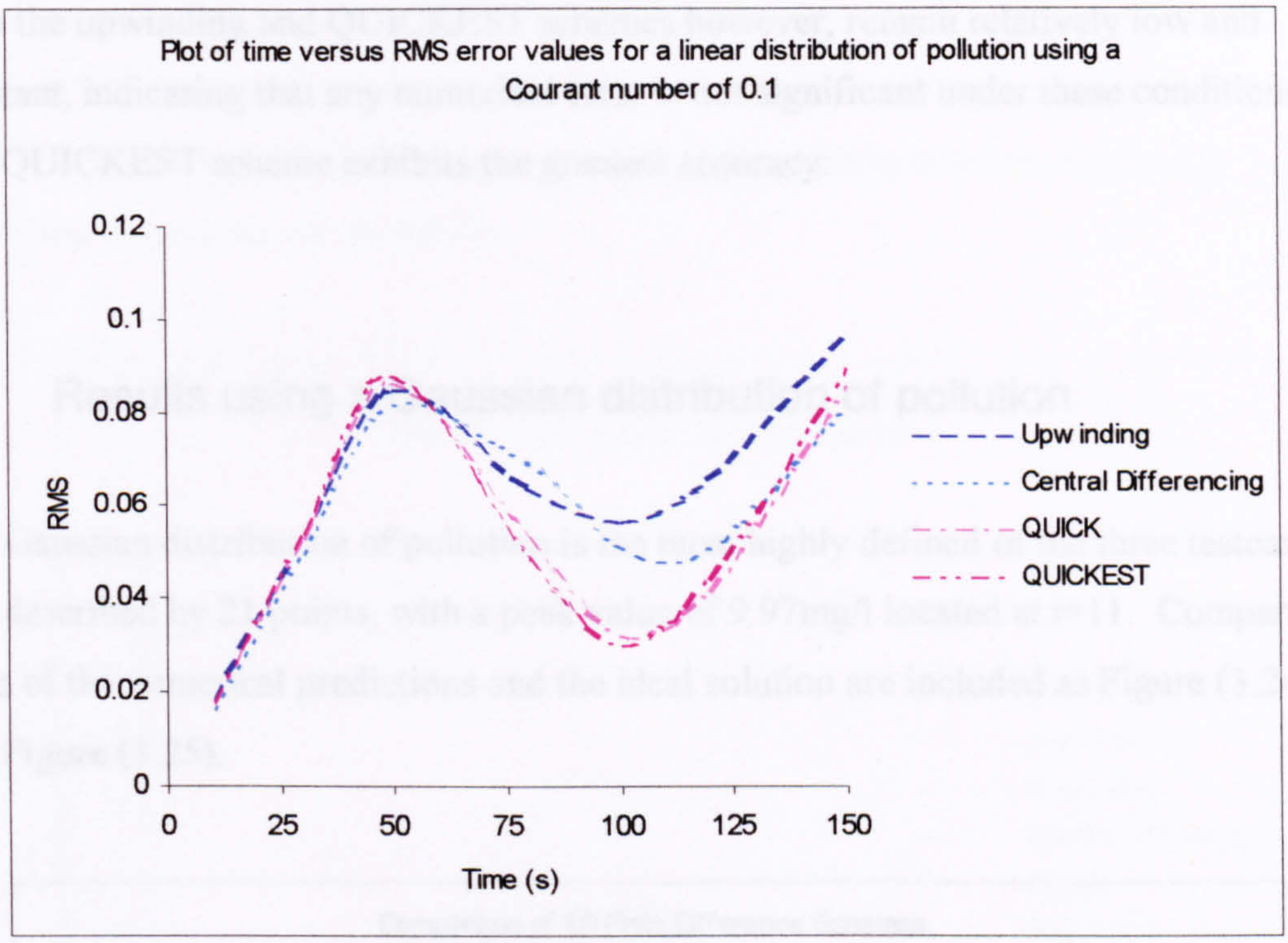

Figure (3.22) Plot of the RMS error values for a linear distribution at Cr=0.1

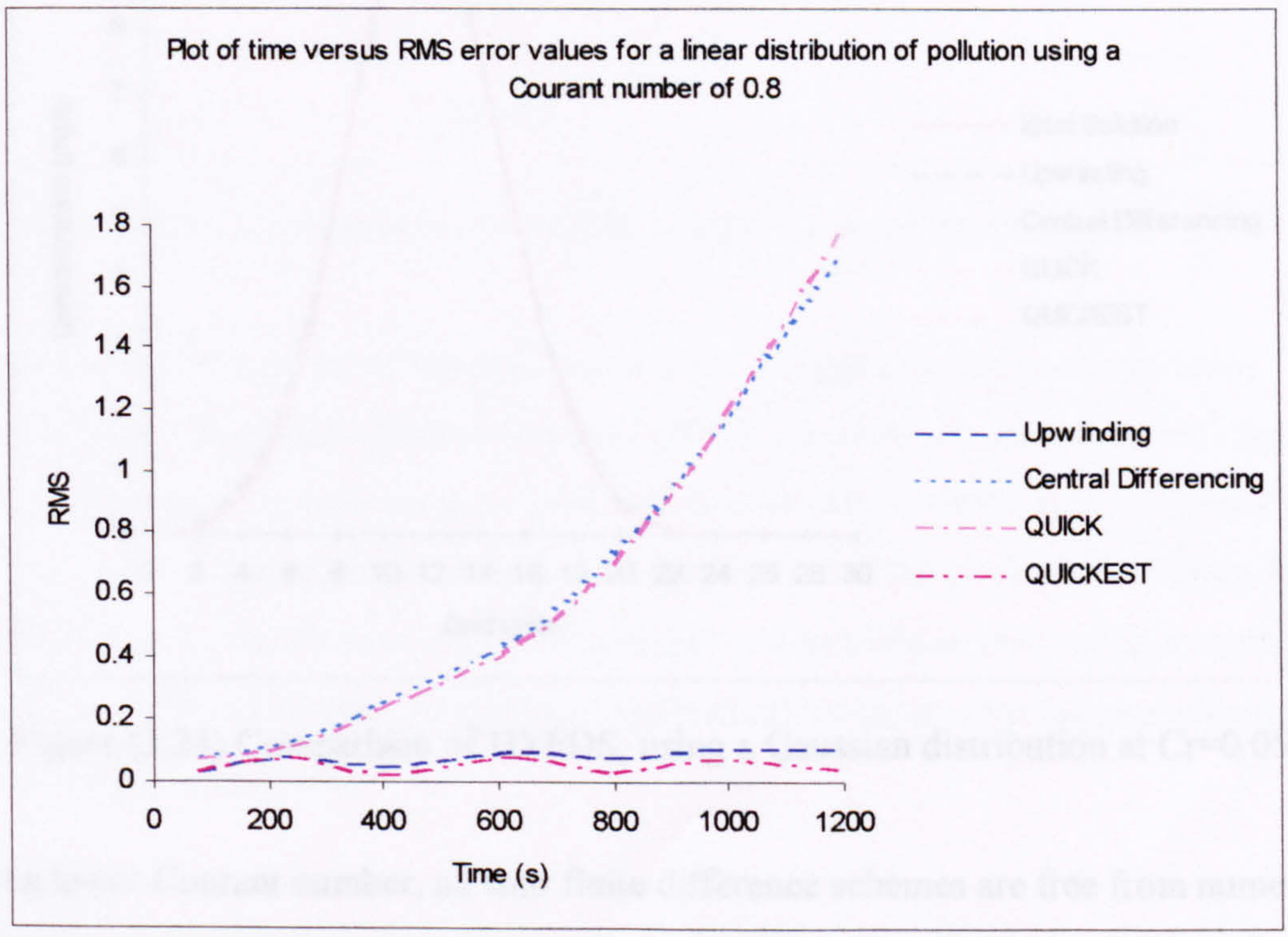

Figure (3.23) Plot of the RMS error values for a linear distribution at Cr=0.8

schemes increase dramatically over time, confirming numerical instability. The error from the upwinding and QUICKEST schemes however, remain relatively low and constant, indicating that any numerical error is not significant under these conditions. The QUICKEST scheme exhibits the greatest accuracy.

3.2.3 Results using a Gaussian distribution of pollution

The Gaussian distribution of pollution is the most highly defined of the three testcases. It is described by 21 points, with a peak value of 9.97mg/l located at i=11. Comparative plots of the numerical predictions and the ideal solution are included as Figure (3.24) and Figure (3.25).

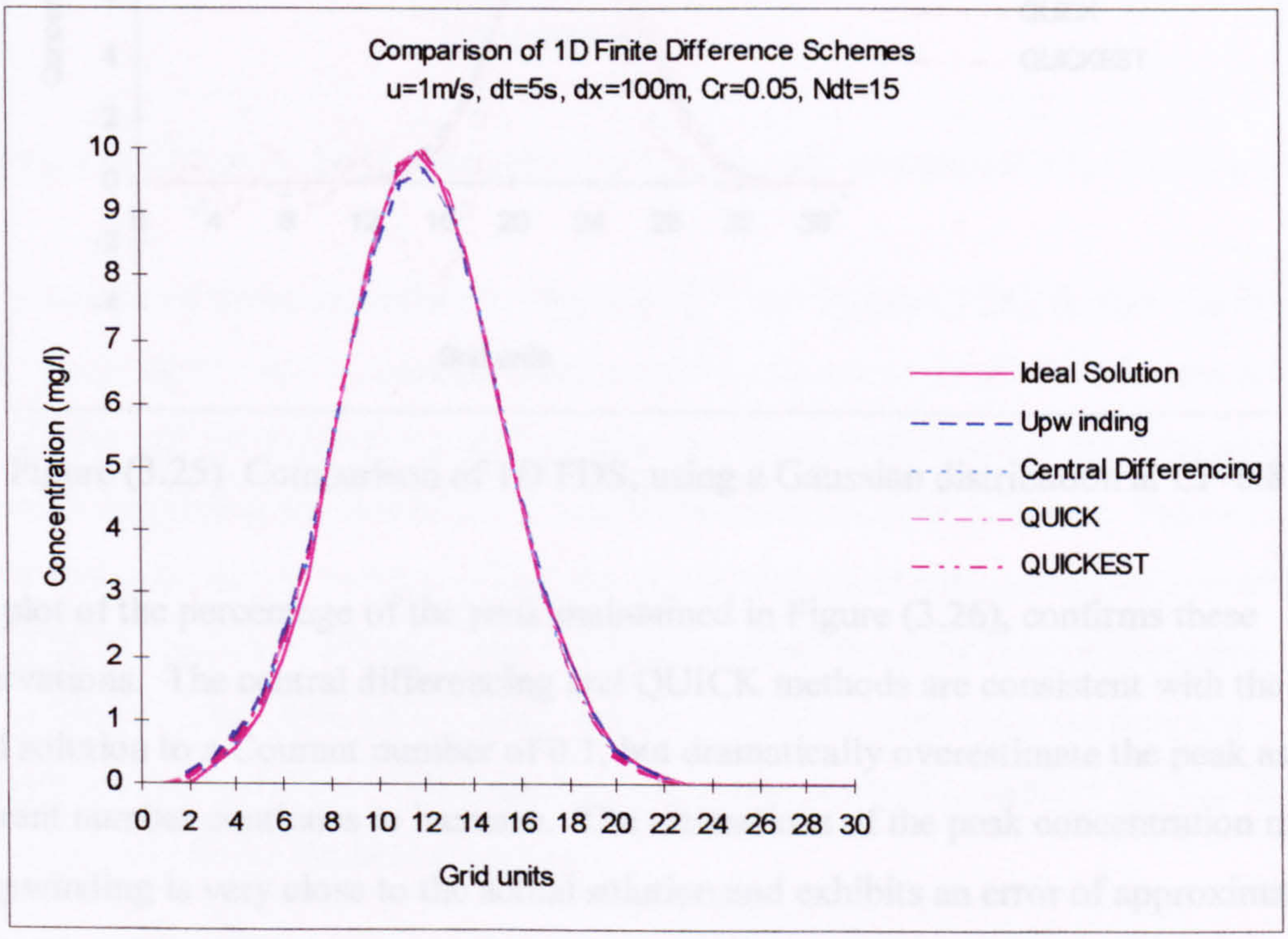

Figure (3.24) Comparison of 1D FDS, using a Gaussian distribution at Cr=0.05

At the lower Courant number, all four finite difference schemes are free from numerical dispersion and instability. Indeed they all accurately predict the ideal solution. The only minor exception is the upwinding scheme which displays a degree of numerical diffusion.

Figure (3.25) illustrates behaviour at the higher Courant number of 0.8. Under these circumstances, the QUICKEST and upwinding schemes remain stable and accurate. The upwinding scheme continues to suffer from numerical diffusion. However the central differencing and QUICK approaches overpredict the solution, exhibiting numerical dispersion and instability.

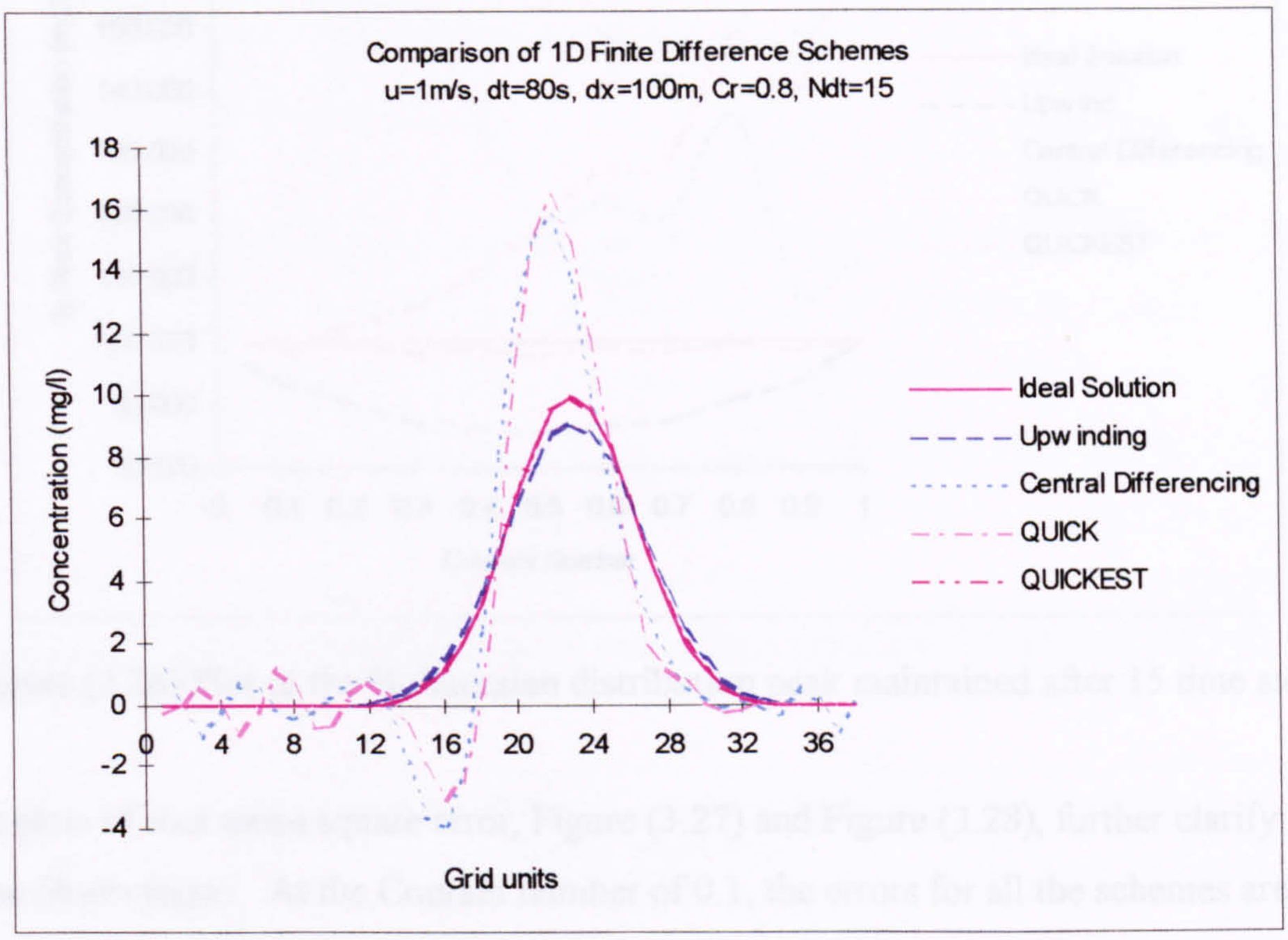

Figure (3.25) Comparison of 1D FDS, using a Gaussian distribution at Cr=0.8

The plot of the percentage of the peak maintained in Figure (3.26), confirms these observations. The central differencing and QUICK methods are consistent with the ideal solution to a Courant number of 0.1, but dramatically overestimate the peak as the Courant number continues to increase. The estimations of the peak concentration made by upwinding is very close to the actual solution and exhibits an error of approximately 15%. The QUICKEST approach is more accurate, showing an error of approximately 2%, which is insignificant.

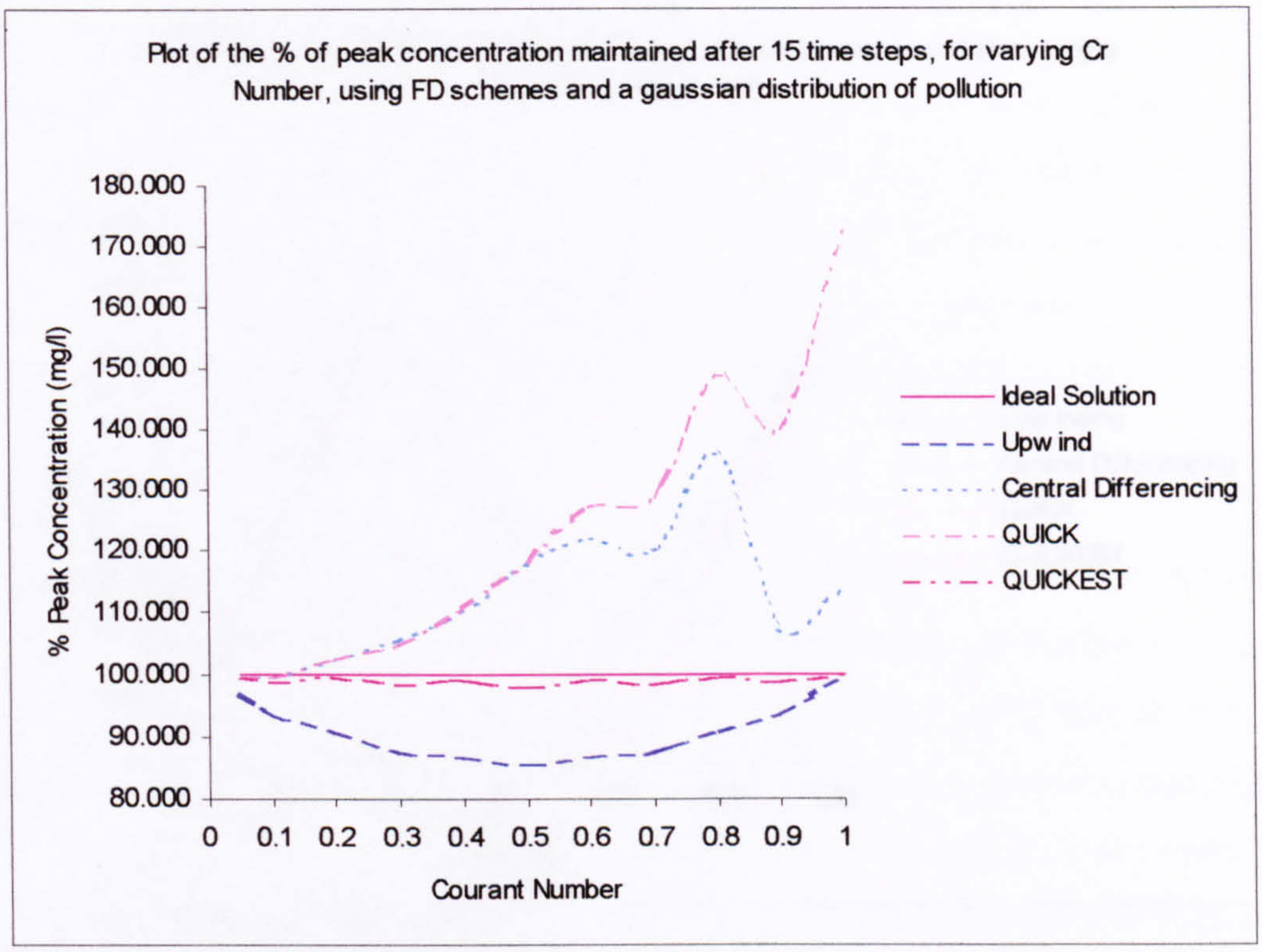

Figure (3.26) Plot of the % Gaussian distribution peak maintained after 15 time steps

The plots of root mean square error, Figure (3.27) and Figure (3.28), further clarify these observations. At the Courant number of 0.1, the errors for all the schemes are very similar and lie within the same boundaries. There is variation in the error as time increases, suggesting some numerical instability in the solution methods. Figure (3.28) shows that at a Courant number of 0.8, the errors associated with central differencing and QUICK escalate, confirming the conclusions made from the comparative plots. The upwinding and QUICKEST errors remain within the same limits as time and Courant number increases. There appears to be some form of instability but this does not accumulate as the solution progresses.

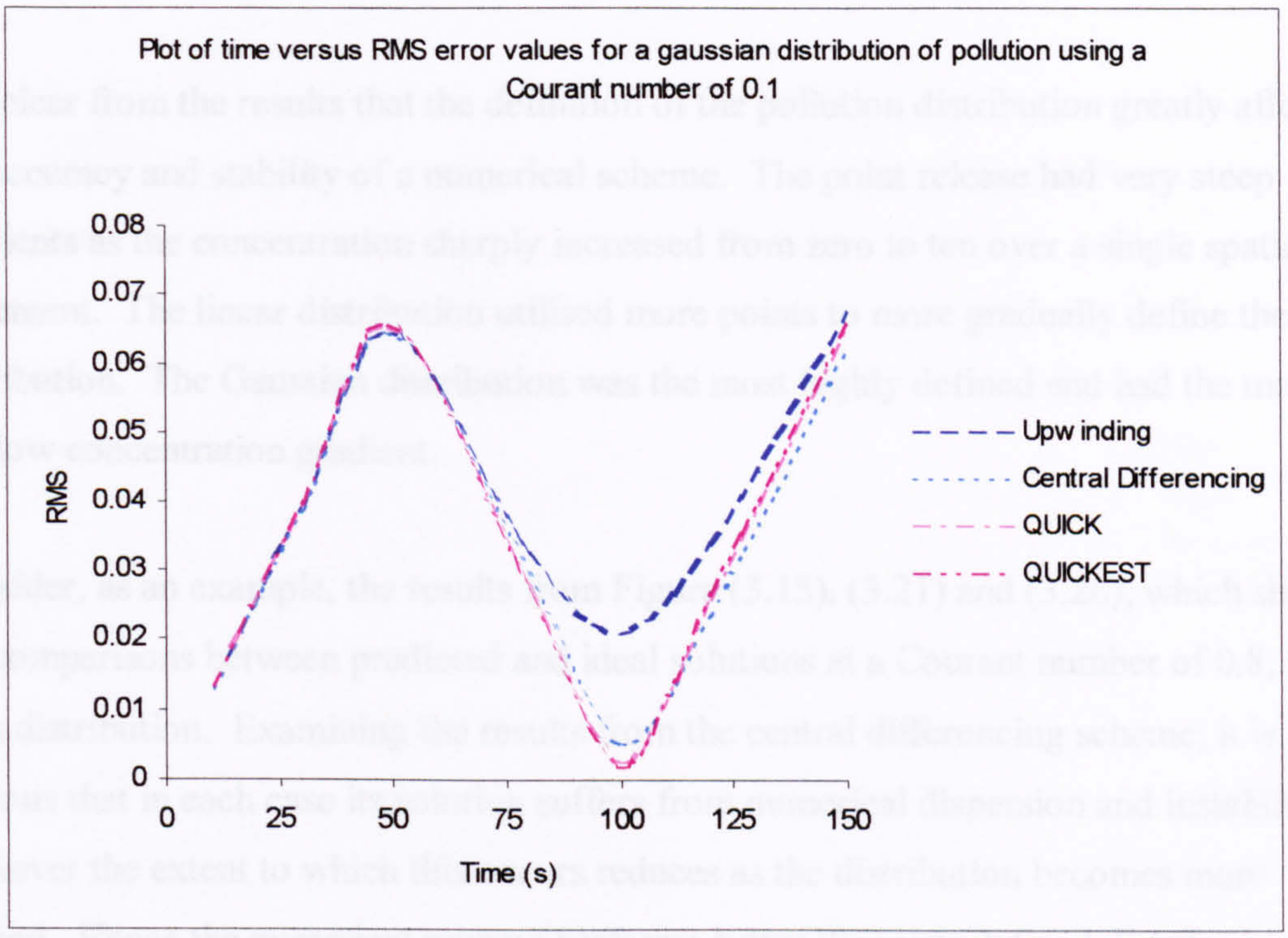

Figure (3.27) Plot of the RMS error values for a Gaussian distribution at Cr=0.1

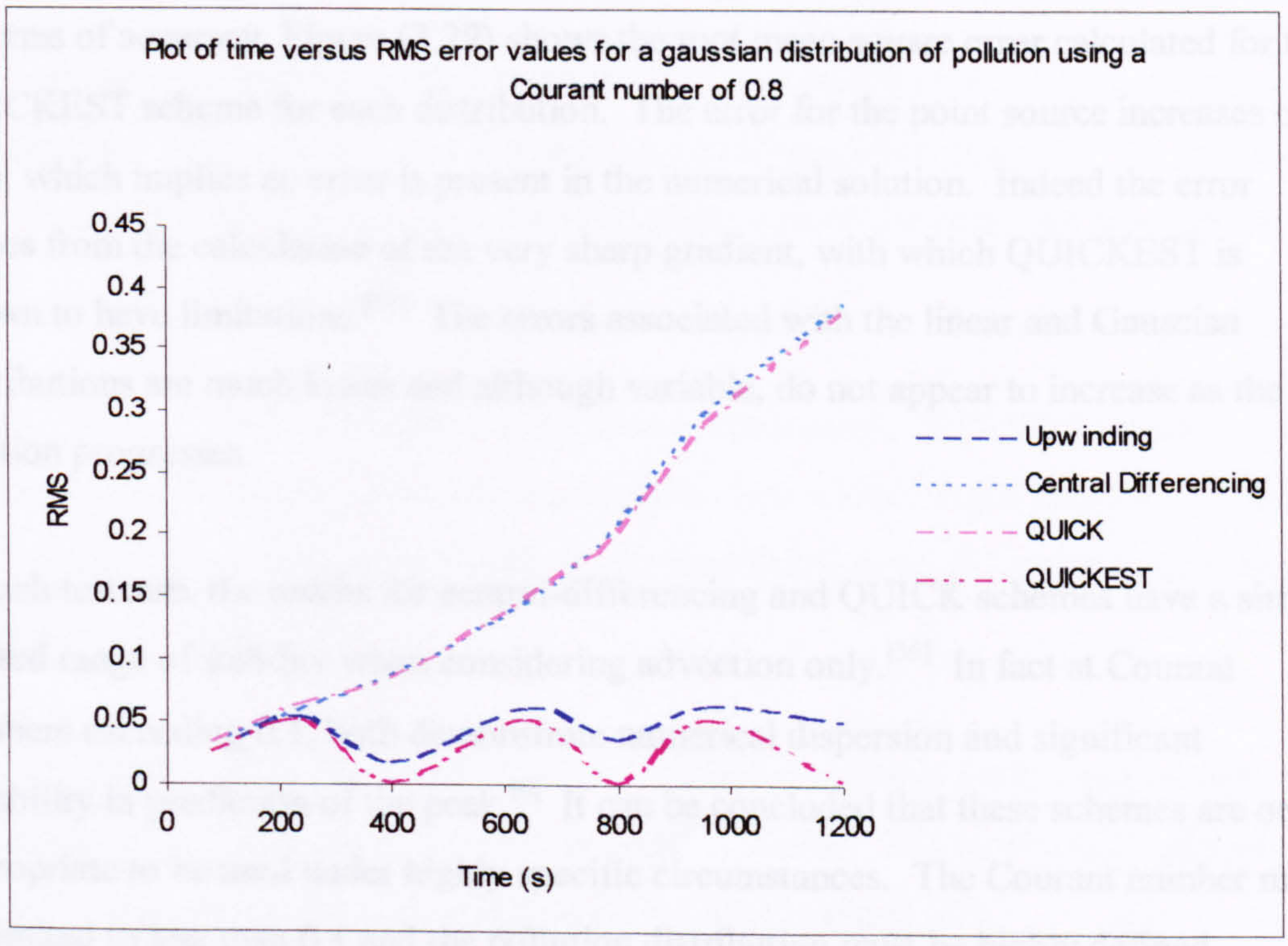

Figure (3.28) Plot of the RMS error values for a Gaussian distribution at Cr=0.8

3.3 Conclusions

It is clear from the results that the definition of the pollution distribution greatly affects the accuracy and stability of a numerical scheme. The point release had very steep gradients as the concentration sharply increased from zero to ten over a single spatial increment. The linear distribution utilised more points to more gradually define the distribution. The Gaussian distribution was the most highly defined and had the most shallow concentration gradient.

Consider, as an example, the results from Figure (3.15), (3.21) and (3.26), which show the comparisons between predicted and ideal solutions at a Courant number of 0.8, for each distribution. Examining the results from the central differencing scheme, it is obvious that in each case its solution suffers from numerical dispersion and instability. However the extent to which this occurs reduces as the distribution becomes more refined. Hence the numerical scheme performs better if a more defined distribution of pollution is used. This also applies to the other schemes.

In terms of accuracy, Figure (3.29) shows the root mean square error calculated for the QUICKEST scheme for each distribution. The error for the point source increases over time, which implies an error is present in the numerical solution. Indeed the error comes from the calculation of the very sharp gradient, with which QUICKEST is known to have limitations.[35] The errors associated with the linear and Gaussian distributions are much lower and although variable, do not appear to increase as the solution progresses.

In each testcase, the results for central-differencing and QUICK schemes have a similar limited range of stability when considering advection only.[36] In fact at Courant numbers exceeding 0.1, both demonstrate numerical dispersion and significant instability in prediction of the peak.[6] It can be concluded that these schemes are only appropriate to be used under highly specific circumstances. The Courant number must be limited to less than 0.1 and the pollution distribution must be highly defined.

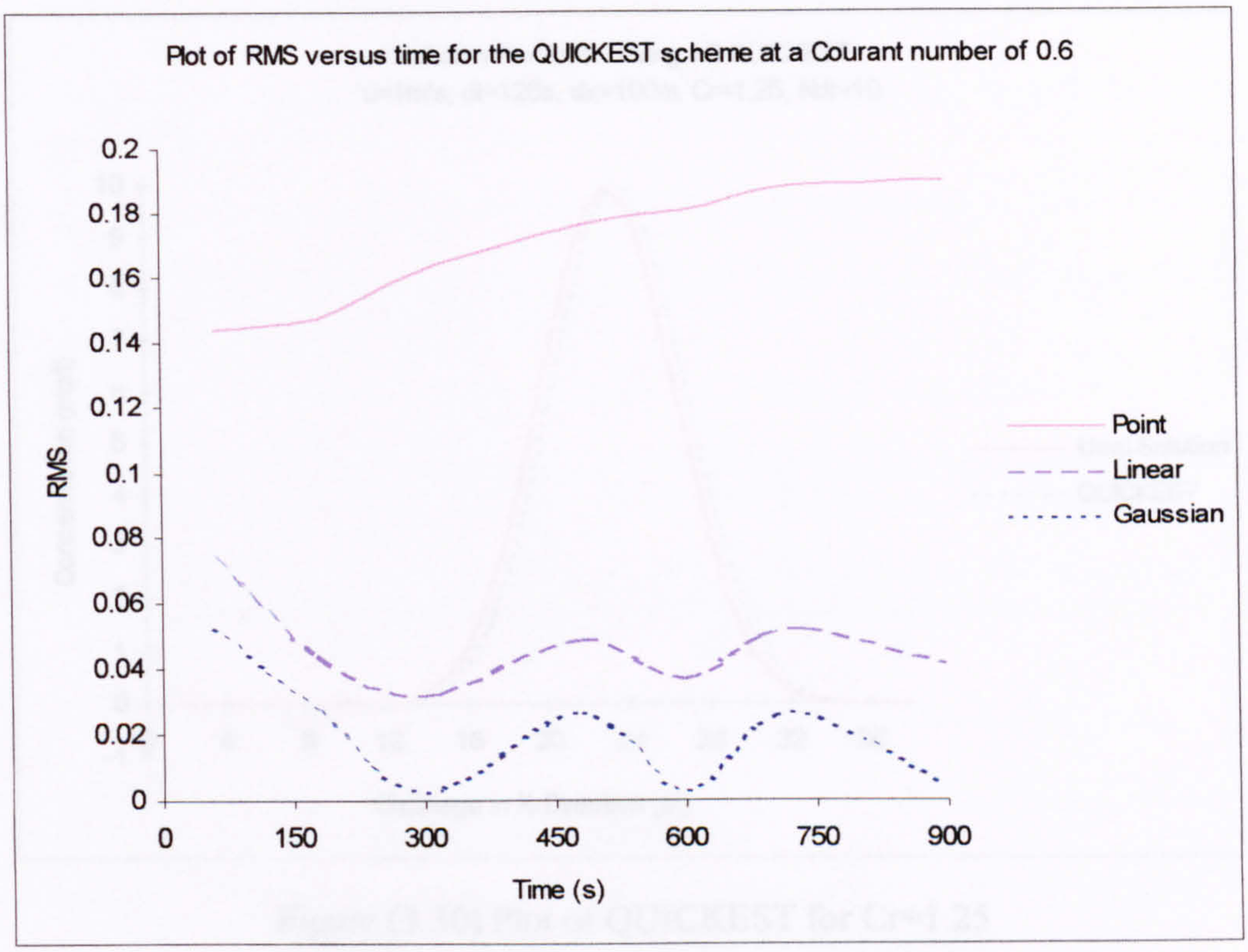

Figure (3.29) Comparison of RMS error for QUICKEST scheme

The first order upwinding method performs far better which explains why, although it is a limited low-order scheme, it is still used as a benchmark test scheme.[20-25] It exhibits numerical diffusion, which is obvious by the reduction of the peak, but is numerically stable.

For the range of Courant numbers and testcases considered, QUICKEST gives by far the most accurate results. This scheme performs best when using a linear or Gaussian distribution, and predicts most closely to the ideal solution using a point source than the other schemes considered.

Further, tests revealed that the QUICKEST method is unstable for Courant numbers greater than one, when advection only is being modelled. The results of these one-dimensional tests are included as Figure (3.30), (3.32) and (3.33).

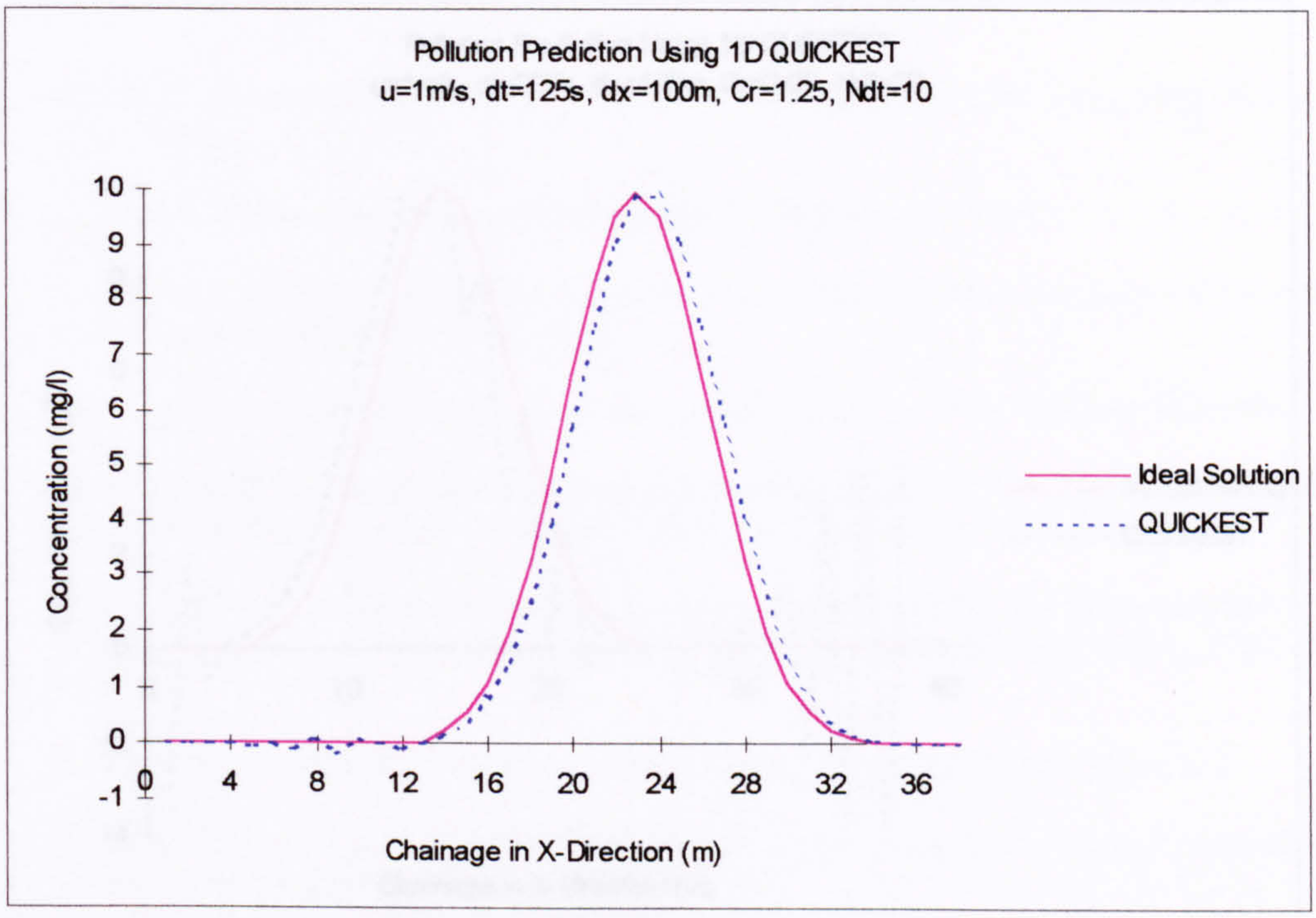

Figure (3.30) Plot of QUICKEST for Cr=1.25

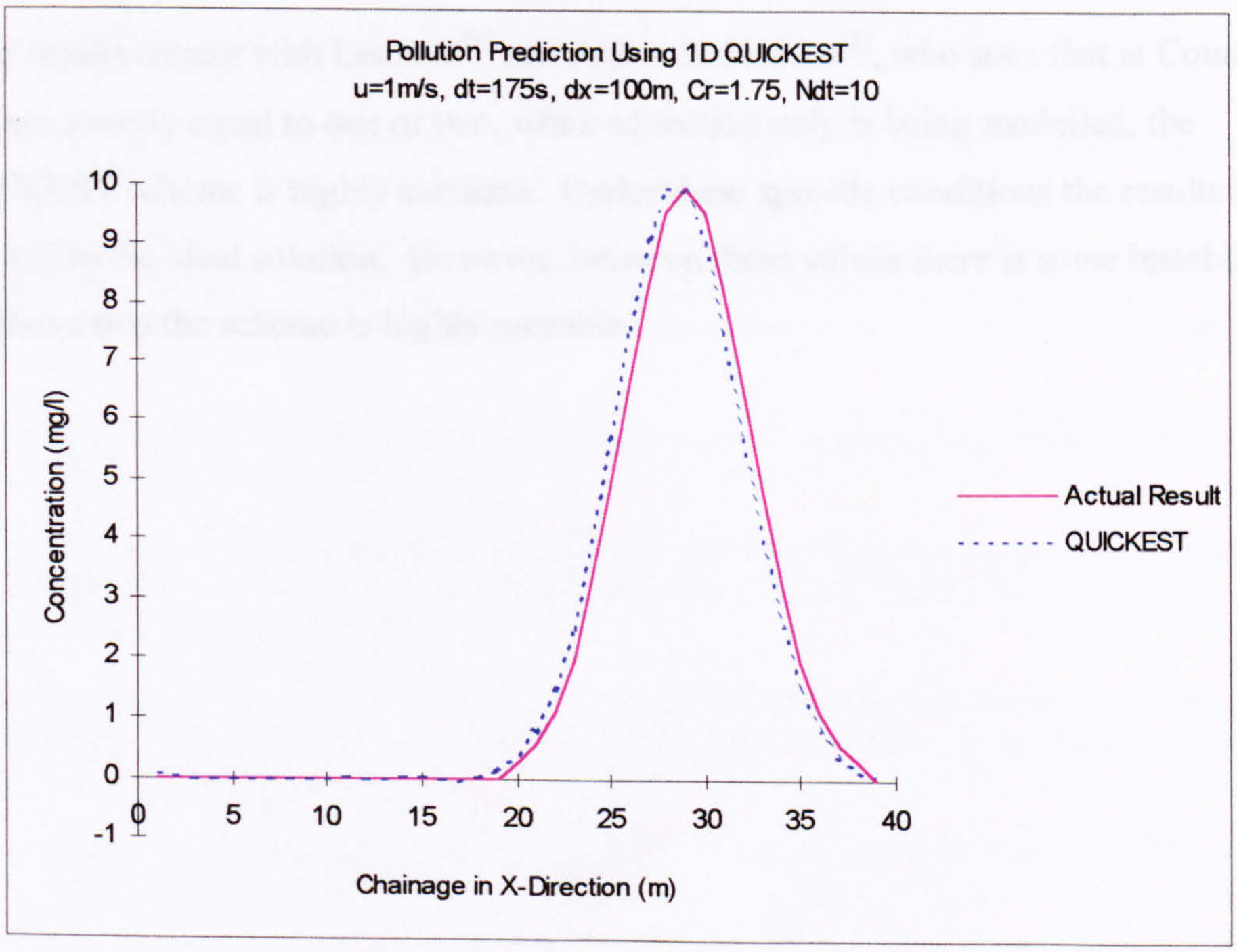

Figure (3.31) Plot of QUICKEST for Cr=1.75

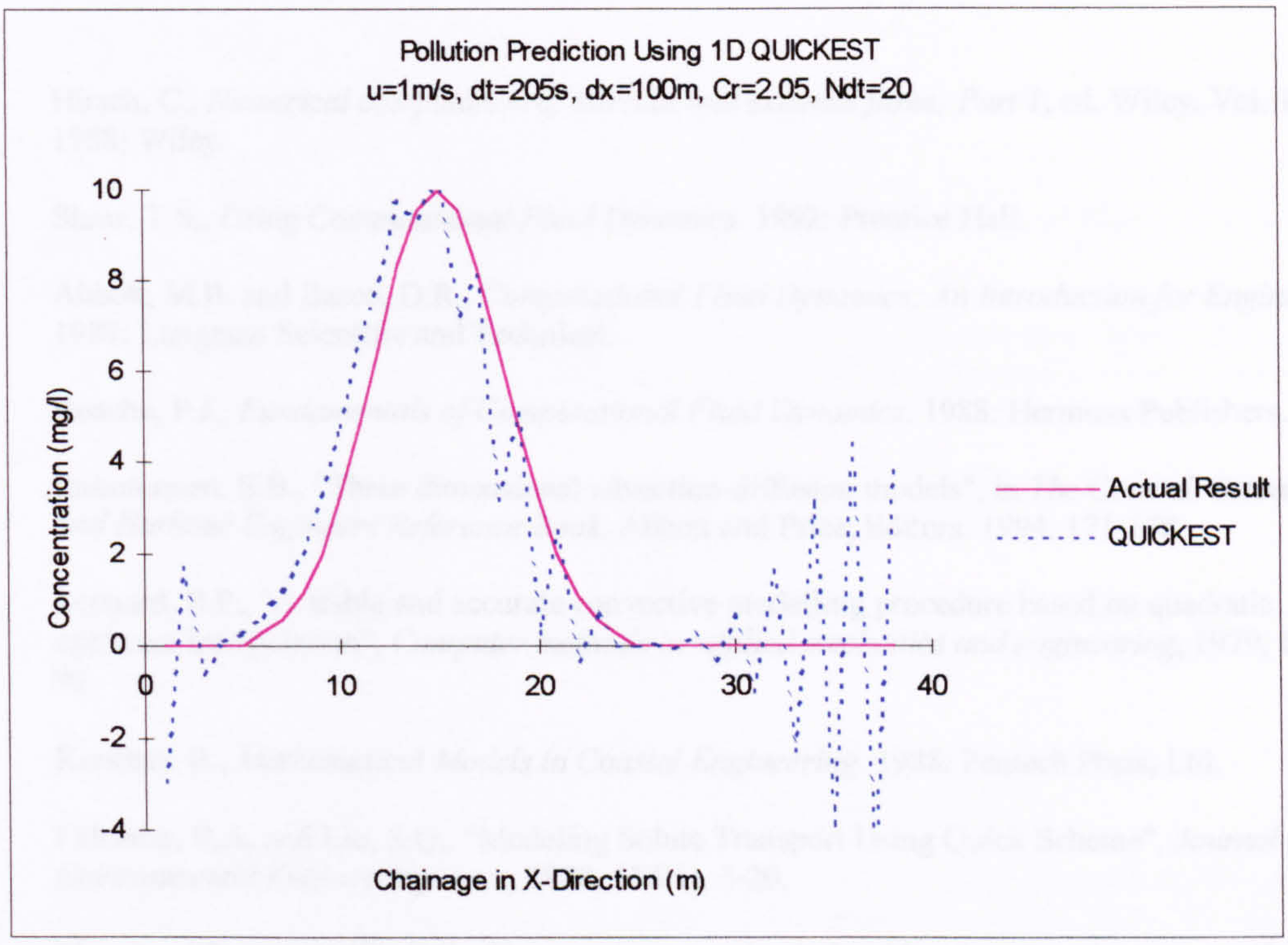

Figure (3.32) Plot of QUICKEST for Cr=2.05

These results concur with Leonard[6] and Abbot and Basco[3], who state that at Courant numbers exactly equal to one or two, when advection only is being modelled, the QUICKEST scheme is highly accurate. Under these specific conditions the results are identical to the ideal solution. However, between these values there is some instability and above two the scheme is highly unstable.

3.4 References

1. Hirsch, C., *Numerical computation of internal and external flows; Part 1*, ed. Wiley. Vol. 1. 1988: Wiley.

2. Shaw, T.S., *Using Computational Fluid Dynamics*. 1992: Prentice Hall.

3. Abbott, M.B. and Basco, D.R., *Computational Fluid Dynamics; An Introduction for Engineers*. 1989: Longman Scientific and Technical.

4. Roache, P.J., *Fundamentals of Computational Fluid Dynamics*. 1988: Hermosa Publishers.

5. Rassmussen, E.B., "Three dimensional advection-diffusion models", in *The Coastal, Estuarial and Harbour Engineers Reference Book*, Abbott and Price, Editors. 1994. 171-178.

6. Leonard, B.P., "A stable and accurate convective modelling procedure based on quadratic upstream interpolation", *Computer methods in applied mechanics and engineering*, 1979, **19**, 59-98.

7. Koutitas, B., *Mathematical Models in Coastal Engineering*. 1988: Pentech Press, Ltd.

8. Falconer, R.A. and Liu, S.Q., "Modeling Solute Transport Using Quick Scheme", *Journal of Environmental Engineering-Asce*, 1988, **114**(1), 3-20.

9. Manson, J.R. and Wallis, S.G., "An accurate numerical algorithm for advective transport", *Communications in Numerical Methods in Engineering*, 1995, **11**(12), 1039-1045.

10. Runchal, A.K., "Convergence and accuracy of three finite difference schemes for a two-dimensional conduction and convection problem", *International Journal of Numerical Methods in Engineering*, 1972, **4**, 541-550.

11. Vreugdenhil, C.B. and Koren, B., *Notes on Numerical Fluid Mechanics; Numerical methods for advection-diffusion problems*. 1993: Vieweg.

12. Hogarth, W.L., Noye, B.J., Stagnitti, J., Parlange, J.Y., and Bolt, G., "A Comparative-Study of Finite-Difference Methods For Solving the One-Dimensional Transport-Equation With an Initial Boundary-Value Discontinuity", *Computers & Mathematics With Applications*, 1990, **20**(11), 67-82.

13. Richtmyer, R.D. and Morton, K.W., *Difference methods for initial-value problems*. 1967, New York: Interscience Publishers Inc.

14. Brebbia, C.A. and Connor, J.J. *Numerical Methods in fluid Dynamics*. in *Proceedings of the International Conference on Numerical methods in Fluid Dynamics*. 1973. University of Southampton: Pentch Press.

15. Bradley, D., Missaghi, M., and Chin, S.B., "A Taylor-series approach to numerical accuracy and a third order scheme for strong onvective flows", *Computer methods in Applied Mechanical Engineering*, 1988, **69**, 133-151.

16. Oran, E.S. and Boris, J.P., *Numerical simulation of reactive flow*. 1987, New York: Elsevier Science Publishing Co. Inc.

17. Roberts, D.L. and Selim, M.S., "Comparative-Study of 6 Explicit and 2 Implicit Finite-Difference Schemes For Solving One-Dimensional Parabolic Partial-Differential Equations", *International Journal For Numerical Methods in Engineering*, 1984, **20**(5), 817-844.

18. Towler, B.F. and Yang, R.Y.K., "On comparing the accuracy of some finite difference methods for parabolic partial differential equations", *International Journal for Numerical Methods in Engineering*, 1979, **14**, 1021-1035.

19. Wornom, S.F., "Application of 2-Point Implicit Central-Difference Methods to Hyperbolic Systems", *Computers & Fluids*, 1991, **20**(3), 321-331.

20. Falconer, R.A., "Flow and Water-Quality Modeling in Coastal and Inland Water", *Journal of Hydraulic Research*, 1992, **30**(4), 437-452.

21. Karpik, S.R. and Crockett, S.R., "Semi-Lagrangian algorithm for two-dimensional advection-diffusion equation on curvilinear coordinate meshes", *Journal of Hydraulic Engineering-Asce*, 1997, **123**(5), 389-401.

22. Leonard, B.P. and Niknafs, H.S., "Sharp Monotonic Resolution of Discontinuities Without Clipping of Narrow Extrema", *Computers & Fluids*, 1991, **19**(1), 141-154.

23. Komatsu, T., Ohgushi, K., Asai, K., and Holly Jr., F.M., "Accurate numerical simulation of scalar advective transport", *Journal of Hydroscience and hydraulic Engineering*, 1989, **7**(1), 63-73.

24. Vested, H.J., Justesen, P., and Ekebjaerg, L., "Advection-Dispersion Modeling in 3 Dimensions", *Applied Mathematical Modelling*, 1992, **16**(10), 506-519.

25. Zoppou, C. and Roberts, S., "Refined numerical scheme for advective transport in diffusion simulation - Discussion", *Journal of Hydraulic Engineering-Asce*, 1998, **124**(7), 765-767.

26. Noye, B.J. and Tan, H.H., "Finite-Difference Methods For Solving the Two-Dimensional Advection Diffusion Equation", *International Journal For Numerical Methods in Fluids*, 1989, 9(1), 75-98.

27. van Eijkeren, J.C.H., de Haan, B.J., Stelling, G.S., and van Stijn, T.L., "Linear Upwind Biased Methods", in *Numerical Methods for Advection-Diffusion Problems*, C.B. Vreugdenhil and B. Koren, Editors. 1993. 55-88.

28. Roache, P.J., *Computational Fluid Dynamics*. 1976: Hermosa.

29. Hill, D.L. and Baskarone, E.A., "A monotone streamline upwind method for quadratic finite elements", *International Journal of Numerical Methods in Fluids*, 1993, **17**, 463-475.

30. Lui, S.-Q. and Falconer, R.A. *Application of the QUICK difference scheme for two-dimensional water quality modelling*. in *Hydraulic and Environmental Modelling of Coastal, Estuarine and River Waters, Proceedings of the International Conference*. 1989. Bradford.

31. Hervouet, J.M., "Application of the method of characteristics in their weak formulation to solving two-dimensional advection equations on mesh grids", in *Computational Techniques for Fluid Flow, Vol 5: Recent advances in Numerical Methods in Fluids*, C. Taylor, J.A. Johnson, and W.R. Smith, Editors. 1986, Pineridge Press: Swansea. 149-185.

32. Chen, Y.P. and Falconer, R.A., "Advection Diffusion Modeling Using the Modified Quick Scheme", *International Journal For Numerical Methods in Fluids*, 1992, **15**(10), 1171-1196.

33. Spalding, D.B., "A novel finite difference formualtion for differential expressions involving both first and second derivatives", *International Journal of Numerical Methods in Engineering*, 1972, **4**, 551-559.

34. Chen, Y.P. and Falconer, R.A., "Modified Forms of the 3rd-Order Convection, 2nd-Order Diffusion Scheme For the Advection-Diffusion Equation", *Advances in Water Resources*, 1994, **17**(3), 147-170.

35. Leonard, B.P., "The Ultimate Conservative Difference Scheme Applied to Unsteady One-Dimensional Advection", *Computer Methods in Applied Mechanics and Engineering*, 1991, 88(1), 17-74.

36. Leonard, B.P., "Simple High-Accuracy Resolution Program For Convective Modeling of Discontinuities", *International Journal For Numerical Methods in Fluids*, 1988, 8(10), 1291-1318.

Chapter 4

One-Dimensional Methods of Characteristics

4.1 Introduction 85

4.1.1 Basis of the method of characteristics 85

4.1.2 Linear method of characteristics 88

4.1.3 Cubic interpolation methods 89

4.1.4 Eight point method of characteristics 93

4.1.5 Six point method of characteristics 99

4.2 Testing of the method of characteristic schemes using one-dimensional idealised testcases 102

4.2.1 Results for the point release of pollution 102

4.2.2 Results for the linear distribution of pollution 107

4.2.3 Results for the Gaussian distribution of pollution 111

4.3 Conclusions 115

4.4 References 117

4.1 Introduction

There are several alternative approaches to finite difference schemes, which can be used to solve partial differential equations.[1-6] One such approach is the method of characteristics.[7-13]

4.1.1 Basis of the method of characteristics

In basic terms a characteristic is defined as, a path, or trajectory, which is followed by some quantity as it is propagated in space and time.[7] In this work, concentration is propagated from a location at the current time, to a new location at the next time step. The method of characteristics differs from the finite difference scheme in the way that it calculates the value of the advected concentration. It is derived using interpolating polynomials to predict concentration at the foot of the characteristic at a specific node.[14] If all of the values of concentration at the original time level are known then, the concentration at any location at any time step can be calculated.

The mathematical concept of the method of characteristics is most easily explained in terms of one-dimension. Consider the definition of the total differential, dC, for C(x,t):[3, 11, 12, 15, 16]

$$dC = \frac{\partial C}{\partial t}dt + \frac{\partial C}{\partial x}dx \tag{4.1}$$

Dividing throughout by dt:

$$\frac{dC}{dt} = \frac{\partial C}{\partial t} + \frac{\partial C}{\partial x}\left(\frac{dx}{dt}\right) \tag{4.2}$$

Using the relationship between speed, distance and time and considering that the concentration, C, is constant, equation (4.2) is seen to be similar to the pure advection equation defined as equation (3.17):

$$\frac{dC}{dt} = \frac{\partial C}{\partial t} + \frac{\partial C}{\partial x} u = 0 \tag{4.3}$$

Equation (4.3) can be written in terms of the ordinary differentials; $\frac{dC}{dt} = 0$ along $\frac{dx}{dt} = u$ which states that, the concentration remains constant along its space-time trajectory given by the ordinary differential equation $\frac{dx}{dt} = u(x,t)$.[11, 12, 15] This defines the slope of the characteristic lines along which the concentration travels. If the velocity is positive then the slope is positive and the characteristic is a forward characteristic, often referred to as C_+. If the velocity is negative then the characteristic is backwards and referred to as C_-. It is important that these terms are not confused with the C term used to define concentration.

Consider the solution of these ordinary differential equations using a one-dimensional grid.

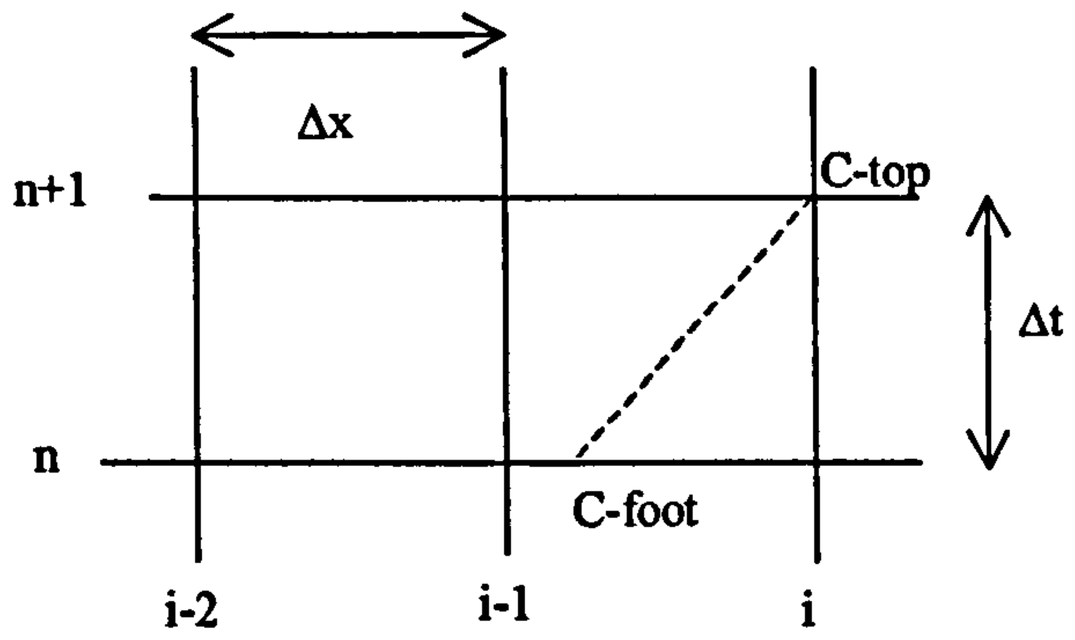

Figure (4.1) One-dimensional grid

In Figure (4.1), C-top is the concentration at location x=i at the next time step, n+1. C-foot is the concentration at some location on the x-axis at the current time step. The

concentrations at the current time step at each nodal point are all known values in this case hence, the scheme is explicit.

The relationship between the present and future concentrations can be defined using the advection equation, which is written in a slightly different format as equation (4.4), which is identical to equation (3.17):

$$\frac{\partial C(x,t)}{\partial t}+\frac{\partial C(x,t)}{\partial x}u(x,t)=0 \tag{4.4}$$

If velocity, u, is constant then the formal solution to equation (4.4) can be written as:[10, 11]

$$C(x,t+\Delta t)=C(x-u\Delta t,t) \tag{4.5}$$

This confirms equation (4.3), which states that the concentration travels along the trajectory without changing, therefore the concentration at the top of the trajectory is equal to the value of at the foot. Essentially the concentration at the next time step is equal to the concentration at the previous time step at a specific location on the x-axis.

An interpolating scheme can then be applied to calculate the concentration at the foot of the trajectory.

The method of characteristics has proved to be a popular alternative for solving the advection equation. It is relatively easy to implement and handles advection dominated flows effectively.[9, 17-19] There are however, some drawbacks to the process. The most significant problem, with respect to this work, is that the time step is severely restricted by the Courant stability criterion, which is prohibitive in numerical modelling.[9] However this problem can be tackled by adopting a spatial reachout scheme, which will be discussed later.[15, 20-22]

4.1.2 Linear method of characteristics

The simplest form of the method of characteristics uses linear interpolation.[7, 10, 11] The scheme is easy to derive in one and two dimensions if required.[23] Consider the one-dimensional linear equation, (4.6):

$$Y(\alpha) = A\alpha + B \tag{4.6}$$

Equation (4.6) is the simple equation of a straight line written in terms of the variable α. Alpha is defined as being the ratio of, the distance from the node of reference, located at x=i, to the point of intersection with the interpolating polynomial, to the distance between adjacent node points. This is illustrated using Figure (4.2) and with reference to equation (4.7). This is also equivalent to the Courant number.

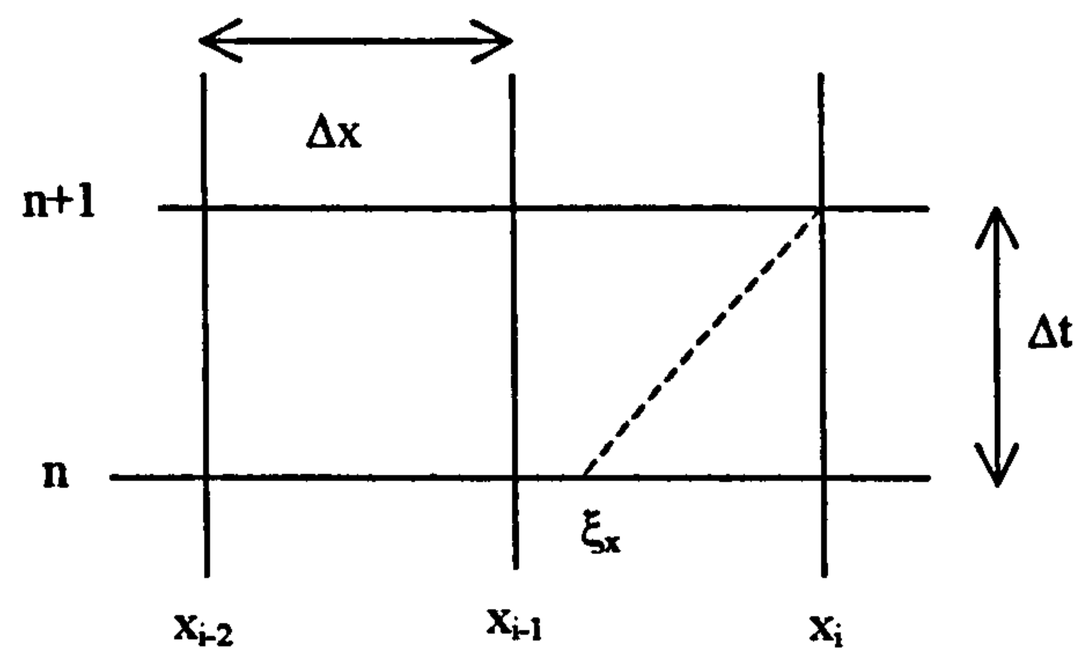

Figure (4.2) One-dimensional grid depicting the values used to derive alpha

$$\alpha = \frac{x_i - \xi_x}{x_i - x_{i-1}} \tag{4.7}$$

The linear equation is solved easily, using the specified initial conditions:

$$Y(0) = C_i^n \tag{4.8}$$

$$Y(1) = C_{i-1}^n \tag{4.9}$$

Substituting the first boundary condition, represented by equation (4.8), into equation (4.6) gives a value for the parameter B:

$$Y(0) = A(0) + B = C_i^n \tag{4.10}$$

This result is used to calculate the value of the parameter A, using the second boundary condition:

$$Y(1) = A(1) + B = C_{i-1}^n \tag{4.11}$$

$$A = C_{i-1}^n - C_i^n \tag{4.12}$$

Replacing these values of concentration, (4.10) and (4.12) in equation (4.6) gives:

$$Y(\alpha) = (C_{i-1}^n - C_i^n)\alpha + C_i^n \tag{4.13}$$

The linear interpolation technique is simple to both derive and apply. However it is unstable when alpha exceeds one (alpha is equal to the Courant number specified in Chapter 3); which occurs if the polynomial crosses the spatial axis at a point outwith the region between two adjacent nodal points.[23]

4.1.3 Cubic interpolation methods

The same basic method used in the derivation of the linear equations is implemented to derive a cubic interpolation scheme. This requires more work in both derivation and application than the linear approach.[20, 24]

Consider the cubic polynomial, equation (4.14), written in terms of alpha:

$$Y(\alpha) = A\alpha^3 + B\alpha^2 + D\alpha + E \tag{4.14}$$

There are four unknowns and in order to solve the equation. For simplicity, it can be rewritten in terms of x, where α=-x:

$$Y(x) = -Ax^3 + Bx^2 - Dx + E \tag{4.15}$$

The first derivative of this equation is calculated:

$$Y'(x) = -3Ax^2 + 2Bx - D \tag{4.16}$$

and rewritten in terms of alpha:

$$Y'(\alpha) = -3A\alpha^2 - 2B\alpha - D \tag{4.17}$$

Holly and Preissmann[10], describe a scheme which uses this cubic polynomial and its derivatives, to solve the advection equation in one dimension. They derived two third degree interpolating polynomials, between the points i-1 and i, using the boundary conditions:

$$Y(0) = C_i^n \tag{4.18}$$

$$Y(1) = C_{i-1}^n \tag{4.19}$$

$$Y'(0) = CX_i^n \tag{4.20}$$

$$Y'(1) = CX_{i-1}^n \tag{4.21}$$

Where C refers to the concentration and CX is the spatial derivative.

Using these boundary conditions and solving for alpha equals zero equation (4.14) becomes:

$$Y(0) = A(0)^3 + B(0)^2 + D(0) + E = C_i^n \tag{4.22}$$

$$E = C_i^n \tag{4.23}$$

Similarly setting alpha to zero in the first derivative gives:

$$Y'(0) = -3A(0)^2 - 2B(0) - D = CX_i^n \tag{4.24}$$

$$D = -CX_i^n \tag{4.25}$$

Substituting (4.23) and (4.25) into equations (4.14) and (4.17) gives a pair of equations which can be solved simultaneously:

$$Y(1) = A(1)^3 + B(1)^2 - CX_i^n(1) + C_i^n = C_{i-1}^n \tag{4.26}$$

$$Y'(1) = -3A(1)^2 - 2B(1) + CX_i^n = CX_{i-1}^n \tag{4.27}$$

Rearranging and writing in terms of the unknowns:

$$A + B = CX_i^n - C_i^n + C_{i-1}^n \tag{4.28}$$

$$-3A - 2B = -CX_i^n + CX_{i-1}^n \tag{4.29}$$

which are solved to give expressions for A and B:

$$A = -2C_{i-1}^n + 2C_i^n - CX_{i-1}^n - CX_i^n \tag{4.30}$$

$$B = 3C_{i-1}^n - 3C_i^n + CX_{i-1}^n + 2CX_i^n \tag{4.31}$$

Replacing these new values for A, B, D and E in equation (4.14) gives the more complex form of the original cubic equation:

$$Y(\alpha) = (-2C_{i-1}^n + 2C_i^n - CX_{i-1}^n - CX_i^n)\alpha^3 + (3C_{i-1}^n - 3C_i^n + CX_{i-1}^n + 2CX_i^n)\alpha^2 + (-CX_i^n)\alpha + C_i^n \quad (4.32)$$

Grouping the terms allows this equation to be written in a more manageable format:

$$Y(\alpha) = \alpha^2(3-2\alpha)C_{i-1}^n + (1-\alpha^2(3-2\alpha))C_i^n + \alpha^2(1-\alpha)(x_i - x_{i-1})CX_{i-1}^n + (\alpha^2(1-\alpha)-1)(x_i - x_{i-1})CX_i^n \quad (4.33)$$

where Y(α) is the concentration at location i, at the next time step:

$$Y(\alpha) = C_i^{n+1} \quad (4.34)$$

The concentration derivatives, however, must also be calculated by substituting the calculated values of A, B and D into equation (4.17). Y'(α) is the concentration derivative at location i, at the next time step.

$$Y'(\alpha) = 6(\alpha^2 - \alpha)(x_i - x_{i-1})C_{i-1}^n - 6(\alpha^2 - \alpha)(x_i - x_{i-1})C_i^n + (3\alpha^2 - 2\alpha)CX_{i-1}^n + (3\alpha^2 - 4\alpha + 1)CX_i^n \quad (4.35)$$

$$Y'(\alpha) = CX_i^{n+1} \quad (4.36)$$

This approach is simple to derive but somewhat more difficult to apply as the concentration derivatives must be advected along with the concentrations. In one-dimension this is manageable, however it becomes a complicated process in two-dimensions.[12, 19, 25]

4.1.4 Eight point method of characteristics

It has been suggested that numerical schemes employing more than two grid points should be used to improve accuracy and reduce numerical dispersion.[23] To this end schemes requiring the use of a greater number of points have been developed.[12, 23, 25, 26]

Holly Jr. and Komatsu[25] developed an eight point method of characteristic scheme. In this case, third order Taylor series expansions, around locations i-1 and i, are used to generate cubic polynomials at the points i-4 to i+3. These are averaged using a weighting factor to obtain cubic expressions for each point. Based on "intuitive reasoning" they also employ the concentration at grid point i-½. The physical basis for this step is not clear and therefore a variation of the scheme excluding, the i-½ term has been used in this work.

The one-dimensional cubic polynomial to be solved is as specified in equation (4.33). However, this scheme adopts a different approach from Holly-Preissmann to calculate the spatial derivatives. Taylor expansions are taken about i-1 and i on a one-dimensional grid, taking account of the points, i-4 to i+3.

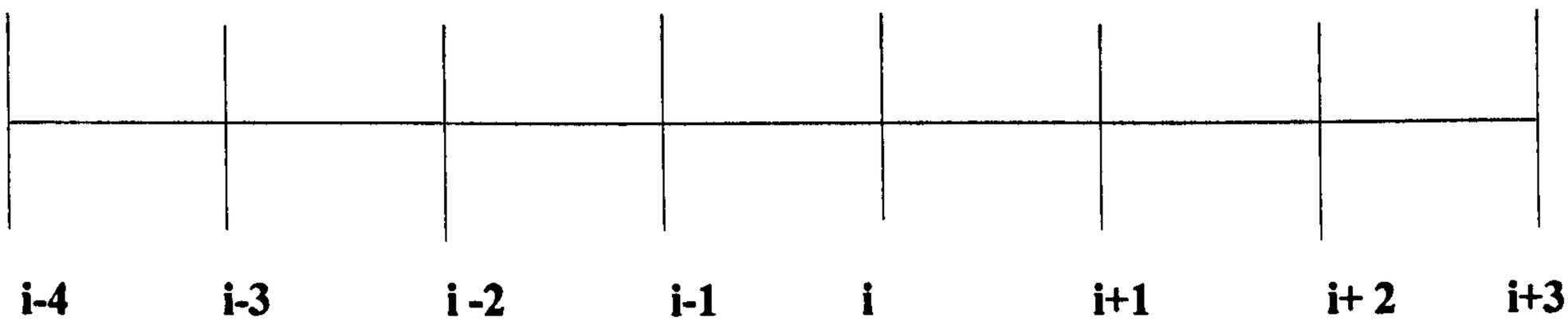

Figure (4.3) One-Dimensional Grid used for the derivation of the 8 Point Method of Characteristics

Consider the Taylor expansions about point, i-1:

$$C_{i-4}^{n} = C_{i-1}^{n} - CX_{i-1}^{n}(3\Delta x) + \frac{1}{2!}CXX_{i-1}^{n}(3\Delta x)^2 - \frac{1}{3!}CXXX_{i-1}^{n}(3\Delta x)^3 \qquad (4.37)$$

$$C_{i-3}^n = C_{i-1}^n - CX_{i-1}^n(2\Delta x) + \frac{1}{2!}CXX_{i-1}^n(2\Delta x)^2 - \frac{1}{3!}CXXX_{i-1}^n(2\Delta x)^3 \tag{4.38}$$

$$C_{i-2}^n = C_{i-1}^n - CX_{i-1}^n(\Delta x) + \frac{1}{2!}CXX_{i-1}^n(\Delta x)^2 - \frac{1}{3!}CXXX_{i-1}^n(\Delta x)^3 \tag{4.39}$$

$$C_i^n = C_{i-1}^n + CX_{i-1}^n(\Delta x) + \frac{1}{2!}CXX_{i-1}^n(\Delta x)^2 + \frac{1}{3!}CXXX_{i-1}^n(\Delta x)^3 \tag{4.40}$$

$$C_{i+1}^n = C_{i-1}^n + CX_{i-1}^n(2\Delta x) + \frac{1}{2!}CXX_{i-1}^n(2\Delta x)^2 + \frac{1}{3!}CXXX_{i-1}^n(2\Delta x)^3 \tag{4.41}$$

$$C_{i+2}^n = C_{i-1}^n + CX_{i-1}^n(3\Delta x) + \frac{1}{2!}CXX_{i-1}^n(3\Delta x)^2 + \frac{1}{3!}CXXX_{i-1}^n(3\Delta x)^3 \tag{4.42}$$

Expansions about the grid point i, are generated in the same way:

$$C_{i-3}^n = C_i^n - CX_i^n(3\Delta x) + \frac{1}{2!}CXX_i^n(3\Delta x)^2 - \frac{1}{3!}CXXX_i^n(3\Delta x)^3 \tag{4.43}$$

$$C_{i-2}^n = C_i^n - CX_i^n(2\Delta x) + \frac{1}{2!}CXX_i^n(2\Delta x)^2 - \frac{1}{3!}CXXX_i^n(2\Delta x)^3 \tag{4.44}$$

$$C_{i-1}^n = C_i^n - CX_i^n(\Delta x) + \frac{1}{2!}CXX_i^n(\Delta x)^2 - \frac{1}{3!}CXXX_i^n(\Delta x)^3 \tag{4.45}$$

$$C_{i+1}^n = C_i^n + CX_i^n(\Delta x) + \frac{1}{2!}CXX_i^n(\Delta x)^2 + \frac{1}{3!}CXXX_i^n(\Delta x)^3 \tag{4.46}$$

$$C_{i+2}^n = C_i^n + CX_i^n(2\Delta x) + \frac{1}{2!}CXX_i^n(2\Delta x)^2 + \frac{1}{3!}CXXX_i^n(2\Delta x)^3 \tag{4.47}$$

$$C_{i+3}^n = C_i^n + CX_i^n(3\Delta x) + \frac{1}{2!}CXX_i^n(3\Delta x)^2 + \frac{1}{3!}CXXX_i^n(3\Delta x)^3 \tag{4.48}$$

The spatial derivatives, CX_i and CX_{i-1}, are solved using sets of simultaneous equations. In each case, four combinations of the Taylor series are developed using a sequence of four consecutive points:

$$CX_{i-1}^{1} = f\left(C_{i-4}^{n}, C_{i-3}^{n}, C_{i-2}^{n}, C_{i-1}^{n}\right) \tag{4.49}$$

$$CX_{i-1}^{2} = f\left(C_{i-3}^{n}, C_{i-2}^{n}, C_{i-1}^{n}, C_{i}^{n}\right) \tag{4.50}$$

$$CX_{i-1}^{3} = f\left(C_{i-2}^{n}, C_{i-1}^{n}, C_{i}^{n}, C_{i+1}^{n}\right) \tag{4.51}$$

$$CX_{i-1}^{4} = f\left(C_{i-1}^{n}, C_{i}^{n}, C_{i+1}^{n}, C_{i+2}^{n}\right) \tag{4.52}$$

$$CX_{i}^{2} = f\left(C_{i-3}^{n}, C_{i-2}^{n}, C_{i-1}^{n}, C_{i}^{n}\right) \tag{4.53}$$

$$CX_{i}^{3} = f\left(C_{i-2}^{n}, C_{i-1}^{n}, C_{i}^{n}, C_{i+1}^{n}\right) \tag{4.54}$$

$$CX_{i}^{4} = f\left(C_{i-1}^{n}, C_{i}^{n}, C_{i+1}^{n}, C_{i+2}^{n}\right) \tag{4.55}$$

$$CX_{i}^{5} = f\left(C_{i}^{n}, C_{i+1}^{n}, C_{i+2}^{n}, C_{i+3}^{n}\right) \tag{4.56}$$

Manipulation of the appropriate values in equations (4.49) to (4.56) gives the corresponding spatial derivatives. By way of example the spatial derivative about i-1, at i-4, equation (4.49), is calculated here.

Rewriting equations (4.37) to (4.39) in terms of the spatial derivative at i-1:

$$CX_{i-1}^{n} = \frac{C_{i-1}^{n}}{3\Delta x} - \frac{C_{i-4}^{n}}{3\Delta x} + \frac{1}{2!}\frac{CXX_{i-1}^{n}}{3\Delta x}(3\Delta x)^2 - \frac{1}{3!}\frac{CXXX_{i-1}^{n}}{3\Delta x}(3\Delta x)^3$$

$$CX_{i-1}^{n} = \frac{C_{i-1}^{n}}{2\Delta x} - \frac{C_{i-3}^{n}}{2\Delta x} + \frac{1}{2!}\frac{CXX_{i-1}^{n}}{2\Delta x}(2\Delta x)^2 - \frac{1}{3!}\frac{CXXX_{i-1}^{n}}{2\Delta x}(2\Delta x)^3$$

$$CX_{i-1}^{n} = \frac{C_{i-1}^{n}}{\Delta x} - \frac{C_{i-2}^{n}}{\Delta x} + \frac{1}{2!}\frac{CXX_{i-1}^{n}}{\Delta x}(\Delta x)^2 - \frac{1}{3!}\frac{CXXX_{i-1}^{n}}{\Delta x}(\Delta x)^3$$

Simplifying these equations gives the more manageable format:

$$CX_{i-1}^{n} = \frac{C_{i-1}^{n}}{3\Delta x} - \frac{C_{i-4}^{n}}{3\Delta x} + \frac{3\Delta x}{2}CXX_{i-1}^{n} - \frac{3\Delta x^2}{2}CXXX_{i-1}^{n}$$

$$CX_{i-1}^{n} = \frac{C_{i-1}^{n}}{2\Delta x} - \frac{C_{i-3}^{n}}{2\Delta x} + \frac{\Delta x}{1}CXX_{i-1}^{n} - \frac{2\Delta x^2}{3}CXXX_{i-1}^{n}$$

$$CX_{i-1}^{n} = \frac{C_{i-1}^{n}}{\Delta x} - \frac{C_{i-2}^{n}}{\Delta x} + \frac{\Delta x}{2}CXX_{i-1}^{n} - \frac{\Delta x^2}{6}CXXX_{i-1}^{n}$$

These equations are solved simultaneously to give an expression for the first spatial concentration:

$$CX_{i-1}^{1} = \frac{11C_{i-1}^{n}}{6\Delta x} - \frac{3C_{i-2}^{n}}{\Delta x} + \frac{3C_{i-3}^{n}}{2\Delta x} - \frac{C_{i-4}^{n}}{3\Delta x} \tag{4.57}$$

Similar calculations are used for the development of the remaining spatial concentrations about i and i-1:

$$CX_{i-1}^{2} = \frac{C_{i}^{n}}{3\Delta x} + \frac{C_{i-1}^{n}}{2\Delta x} - \frac{C_{i-2}^{n}}{\Delta x} + \frac{C_{i-3}^{n}}{6\Delta x} \tag{4.58}$$

$$CX_{i-1}^{3} = -\frac{C_{i+1}^{n}}{6\Delta x} + \frac{C_{i}^{n}}{\Delta x} - \frac{C_{i-1}^{n}}{2\Delta x} - \frac{C_{i-2}^{n}}{3\Delta x} \tag{4.59}$$

$$CX_{i-1}^{4} = \frac{C_{i+2}^{n}}{3\Delta x} - \frac{3C_{i+1}^{n}}{2\Delta x} + \frac{3C_{i}^{n}}{\Delta x} - \frac{11C_{i-1}^{n}}{6\Delta x} \tag{4.60}$$

$$CX_{i}^{2} = \frac{11C_{i}^{n}}{6\Delta x} - \frac{3C_{i-1}^{n}}{\Delta x} + \frac{3C_{i-2}^{n}}{2\Delta x} - \frac{C_{i-3}^{n}}{3\Delta x} \tag{4.61}$$

$$CX_i^3 = \frac{C_{i+1}^n}{3\Delta x} + \frac{C_i^n}{2\Delta x} - \frac{C_{i-1}^n}{\Delta x} + \frac{C_{i-2}^n}{6\Delta x} \tag{4.62}$$

$$CX_i^4 = -\frac{C_{i+2}^n}{6\Delta x} + \frac{C_{i+1}^n}{\Delta x} - \frac{C_i^n}{2\Delta x} - \frac{C_{i-1}^n}{3\Delta x} \tag{4.63}$$

$$CX_i^5 = \frac{C_{i+3}^n}{3\Delta x} - \frac{3C_{i+2}^n}{2\Delta x} + \frac{3C_{i+1}^n}{\Delta x} - \frac{11C_i^n}{6\Delta x} \tag{4.64}$$

These values are averaged, using weighting factors, to give final estimates of the spatial derivatives by substitution of (4.57) to (4.64), in equations (4.65) and (4.66). The weighting factor used here is as recommended by Komatsu *et al*[26] and equal to 9.55.

$$CX_{i-1}^n = \frac{1}{2(\ell+1)}\left(CX_{i-1}^1 + \ell CX_{i-1}^2 + \ell CX_{i-1}^3 + CX_{i-1}^4\right) \tag{4.65}$$

$$CX_i^n = \frac{1}{2(\ell+1)}\left(CX_i^2 + \ell CX_i^3 + \ell CX_i^4 + CX_i^5\right) \tag{4.66}$$

Therefore:

$$CX_{i-1}^n = \frac{1}{2(9.5+1)}\left\{\begin{array}{l}\left(\frac{11C_{i-1}^n}{6\Delta x} - \frac{3C_{i-2}^n}{\Delta x} + \frac{3C_{i-3}^n}{2\Delta x} - \frac{C_{i-4}^n}{3\Delta x}\right) \\ +9.5\left(\frac{C_i^n}{3\Delta x} + \frac{C_{i-1}^n}{2\Delta x} - \frac{C_{i-2}^n}{\Delta x} + \frac{C_{i-3}^n}{6\Delta x}\right) \\ +9.5\left(-\frac{C_{i+1}^n}{6\Delta x} + \frac{C_i^n}{\Delta x} - \frac{C_{i-1}^n}{2\Delta x} - \frac{C_{i-2}^n}{3\Delta x}\right) \\ +\left(\frac{C_{i+2}^n}{3\Delta x} - \frac{3C_{i+1}^n}{2\Delta x} + \frac{3C_i^n}{\Delta x} - \frac{11C_{i-1}^n}{6\Delta x}\right)\end{array}\right\} \tag{4.67}$$

$$CX_i^n = \frac{1}{2(9.5+1)}\left\{\begin{array}{l}\left(\frac{11C_i^n}{6\Delta x}-\frac{3C_{i-1}^n}{\Delta x}+\frac{3C_{i-2}^n}{2\Delta x}-\frac{C_{i-3}^n}{3\Delta x}\right)\\ +9.5\left(\frac{C_{i+1}^n}{3\Delta x}+\frac{C_i^n}{2\Delta x}-\frac{C_{i-1}^n}{\Delta x}+\frac{C_{i-2}^n}{6\Delta x}\right)\\ +9.5\left(-\frac{C_{i+2}^n}{6\Delta x}+\frac{C_{i+1}^n}{\Delta x}-\frac{C_i^n}{2\Delta x}-\frac{C_{i-1}^n}{3\Delta x}\right)\\ +\left(\frac{C_{i+3}^n}{3\Delta x}-\frac{3C_{i+2}^n}{2\Delta x}+\frac{3C_{i+1}^n}{\Delta x}-\frac{11C_i^n}{6\Delta x}\right)\end{array}\right\} \tag{4.68}$$

Which simplify to:

$$CX_{i-1}^n = -\frac{C_{i-4}^n}{63.3\Delta x}+\frac{3.1C_{i-3}^n}{21.1\Delta x}-\frac{15.73C_{i-2}^n}{21.1\Delta x}+\frac{15.73C_i^n}{21.1\Delta x}-\frac{3.1C_{i+1}^n}{21.1\Delta x}+\frac{C_{i+2}^n}{63.3\Delta x} \tag{4.69}$$

$$CX_i^n = -\frac{C_{i-3}^n}{63.3\Delta x}+\frac{3.1C_{i-2}^n}{21.1\Delta x}-\frac{15.73C_{i-1}^n}{21.1\Delta x}+\frac{15.73C_{i+1}^n}{21.1\Delta x}-\frac{3.1C_{i+2}^n}{21.1\Delta x}+\frac{C_{i+3}^n}{63.3\Delta x} \tag{4.70}$$

These estimated values for the spatial derivatives are substituted into equation (4.33):

$$Y(\alpha) = \alpha^2(3-2\alpha)C_{i-1}^n + (1-\alpha^2(3-2\alpha))C_i^n \tag{4.71}$$

$$+\alpha^2(1-\alpha)\Delta x\left(\begin{array}{l}-\frac{C_{i-4}^n}{63.3\Delta x}+\frac{3.1C_{i-3}^n}{21.1\Delta x}-\frac{15.73C_{i-2}^n}{21.1\Delta x}\\ +\frac{15.73C_i^n}{21.1\Delta x}-\frac{3.1C_{i+1}^n}{21.1\Delta x}+\frac{C_{i+2}^n}{63.3\Delta x}\end{array}\right)$$

$$+(\alpha^2(1-\alpha)-1)\Delta x\left(\begin{array}{l}-\frac{C_{i-3}^n}{63.3\Delta x}+\frac{3.1C_{i-2}^n}{21.1\Delta x}-\frac{15.73C_{i-1}^n}{21.1\Delta x}\\ +\frac{15.73C_{i+1}^n}{21.1\Delta x}-\frac{3.1C_{i+2}^n}{21.1\Delta x}+\frac{C_{i+3}^n}{63.3\Delta x}\end{array}\right)$$

Using the definition of the variable alpha given as equation (4.7), the expansion of equation (4.71) becomes:

$$
\begin{aligned}
Y(\alpha) = {} & C_{i-4}^{n}\frac{\left(\alpha^3-\alpha^2\right)}{63.3} \\
& + C_{i-3}^{n}\frac{\left(-8.3\alpha^3+7.3\alpha^2+\alpha\right)}{63.3} \\
& + C_{i-2}^{n}\frac{\left(12.63\alpha^3-9.53\alpha^2-3.1\alpha\right)}{21.1} \\
& + C_{i-1}^{n}\frac{\left(-26.47\alpha^3+31.48\alpha^2+15.73\alpha\right)}{21.1} \\
& + C_{i}^{n}\left(\frac{26.47\alpha^3-47.57\alpha^2+21.1}{21.1}\right) \\
& + C_{i+1}^{n}\left(\frac{-12.63\alpha^3+28.36\alpha^2-15.73\alpha}{21.1}\right) \\
& + C_{i+2}^{n}\left(\frac{8.3\alpha^3-17.6\alpha^2+9.3\alpha}{63.3}\right) \\
& + C_{i+3}^{n}\left(\frac{-\alpha^3+2\alpha^2-\alpha}{63.3}\right)
\end{aligned}
\tag{4.72}
$$

This can be written more conveniently as:

$$
\begin{aligned}
C_{i,j}^{n+1} = {} & b1C_{i-4}+b2C_{i-3}+b3C_{i-2} \\
& +b4C_{i-1}+b5C_{i}+b6C_{i+1}+b7C_{i+2}+b8C_{i+3}
\end{aligned}
\tag{4.73}
$$

4.1.5 Six point method of characteristics

The eight point method of characteristics although accurate is also unwieldy. However this would not be considered an obstacle if the solution was highly accurate. Regardless it is viable to consider a more compact solution scheme based on the same approach. Komatsu *et al*[26] came to the same conclusion about the scheme and they derived a six point method of characteristics from their original eight point approach. The same idea has been put into practice here.

At first sight, it may be considered logical to simply truncate the eight point scheme at the extremities and to develop a new six point scheme based on this. However this

would require the removal of terms i-4 and i+3 which are included in CX_{i-1}^{1} and CX_{i}^{5}. Inspection of equations (4.67) and (4.68) reveal that these spatial derivatives cancel out other terms in the derivation of equations (4.69) and (4.70). Therefore these values cannot simply be truncated. Instead the concentrations at i-4 and i+3 are estimated in terms of the values at neighbouring points. Linear extrapolation gives:

$$C_{i-4}^{est} = 2C_{i-3}^{n} - C_{i-2}^{n} \tag{4.74}$$

$$C_{i+3}^{est} = 2C_{i+2}^{n} - C_{i+1}^{n} \tag{4.75}$$

Substitution of these estimated terms in equations (4.67) and (4.68) gives:

$$CX_{i-1}^{n} = \frac{1}{2(9.5+1)}\left\{\begin{array}{l}\left(\dfrac{11C_{i-1}^{n}}{6\Delta x} - \dfrac{3C_{i-2}^{n}}{\Delta x} + \dfrac{3C_{i-3}^{n}}{2\Delta x} - \dfrac{\left(2C_{i-3}^{n} - C_{i-2}^{n}\right)}{3\Delta x}\right) \\ +9.5\left(\dfrac{C_{i}^{n}}{3\Delta x} + \dfrac{C_{i-1}^{n}}{2\Delta x} - \dfrac{C_{i-2}^{n}}{\Delta x} + \dfrac{C_{i-3}^{n}}{6\Delta x}\right) \\ +9.5\left(-\dfrac{C_{i+1}^{n}}{6\Delta x} + \dfrac{C_{i}^{n}}{\Delta x} - \dfrac{C_{i-1}^{n}}{2\Delta x} - \dfrac{C_{i-2}^{n}}{3\Delta x}\right) \\ +\left(\dfrac{C_{i+2}^{n}}{3\Delta x} - \dfrac{3C_{i+1}^{n}}{2\Delta x} + \dfrac{3C_{i}^{n}}{\Delta x} - \dfrac{11C_{i-1}^{n}}{6\Delta x}\right)\end{array}\right\} \tag{4.76}$$

$$CX_{i}^{n} = \frac{1}{2(9.5+1)}\left\{\begin{array}{l}\left(\dfrac{11C_{i}^{n}}{6\Delta x} - \dfrac{3C_{i-1}^{n}}{\Delta x} + \dfrac{3C_{i-2}^{n}}{2\Delta x} - \dfrac{C_{i-3}^{n}}{3\Delta x}\right) \\ +9.5\left(\dfrac{C_{i+1}^{n}}{3\Delta x} + \dfrac{C_{i}^{n}}{2\Delta x} - \dfrac{C_{i-1}^{n}}{\Delta x} + \dfrac{C_{i-2}^{n}}{6\Delta x}\right) \\ +9.5\left(-\dfrac{C_{i+2}^{n}}{6\Delta x} + \dfrac{C_{i+1}^{n}}{\Delta x} - \dfrac{C_{i}^{n}}{2\Delta x} - \dfrac{C_{i-1}^{n}}{3\Delta x}\right) \\ +\left(\dfrac{\left(2C_{i+2}^{n} - C_{i+1}^{n}\right)}{3\Delta x} - \dfrac{3C_{i+2}^{n}}{2\Delta x} + \dfrac{3C_{i+1}^{n}}{\Delta x} - \dfrac{11C_{i}^{n}}{6\Delta x}\right)\end{array}\right\} \tag{4.77}$$

Solution of these equations gives:

$$CX_{i-1}^{n} = \frac{14.55C_{i-3}^{n}}{126.6\Delta x} - \frac{15.4C_{i-2}^{n}}{21.1\Delta x} + \frac{15.73C_{i}^{n}}{21.1\Delta x} - \frac{3.1C_{i+1}^{n}}{21.1\Delta x} + \frac{C_{i+2}^{n}}{63.3\Delta x} \tag{4.78}$$

$$CX_{i}^{n} = -\frac{C_{i-3}^{n}}{63.3\Delta x} + \frac{3.1C_{i-2}^{n}}{21.1\Delta x} - \frac{15.73C_{i-1}^{n}}{21.1\Delta x} + \frac{15.73C_{i+1}^{n}}{21.1\Delta x} - \frac{14.55C_{i+2}^{n}}{126.6\Delta x} \tag{4.79}$$

Substitution of these expressions into equation (4.33):

$$Y(\alpha) = \alpha^2(3-2\alpha)C_{i-1}^{n} + (1-\alpha^2(3-2\alpha))C_{i}^{n} \tag{4.80}$$

$$+\alpha^2(1-\alpha)\Delta x\left(\frac{14.55C_{i-3}^{n}}{126.6\Delta x} - \frac{15.73C_{i-2}^{n}}{21.1\Delta x} + \frac{15.73C_{i}^{n}}{21.1\Delta x} - \frac{3.1C_{i+1}^{n}}{21.1\Delta x} + \frac{C_{i+2}^{n}}{63.3\Delta x}\right)$$

$$+(\alpha^2(1-\alpha)-1)\Delta x\left(-\frac{C_{i-3}^{n}}{63.3\Delta x} + \frac{3.1C_{i-2}^{n}}{21.1\Delta x} - \frac{15.73C_{i-1}^{n}}{21.1\Delta x} + \frac{15.73C_{i+1}^{n}}{21.1\Delta x} - \frac{14.55C_{i+2}^{n}}{126.6\Delta x}\right)$$

Expansion of the one-dimensional cubic written in this form gives the equation:

$$\begin{aligned} Y(\alpha) = {} & C_{i-3}^{n}\frac{\left(-12.55\alpha^3 + 10.5\alpha^2 + 2\alpha\right)}{126.6} \\ & + C_{i-2}^{n}\frac{\left(12.308\alpha^3 - 9.216\alpha^2 - 3.1\alpha\right)}{21.1} \\ & + C_{i-1}^{n}\frac{\left(-26.47\alpha^3 + 31.48\alpha^2 + 15.73\alpha\right)}{21.1} \\ & + C_{i}^{n}\left(\frac{26.47\alpha^3 - 47.57\alpha^2 + 21.1}{21.1}\right) \\ & + C_{i+1}^{n}\left(\frac{-12.308\alpha^3 + 27.708\alpha^2 - 15.4\alpha}{21.1}\right) \\ & + C_{i+2}^{n}\left(\frac{12.55\alpha^3 - 27.1\alpha^2 + 14.55\alpha}{63.3}\right) \end{aligned} \tag{4.81}$$

This is more expressed more compactly as:

$$C_{i,j}^{n+1} = b1C_{i-3}^{n} + b2C_{i-2}^{n} + b3C_{i-1}^{n} + b4C_{i}^{n} + b5C_{i+1}^{n} + b6C_{i+2}^{n} \qquad (4.82)$$

4.2 Testing of the method of characteristic schemes using one-dimensional idealised testcases

The stability and accuracy of the various methods of characteristics is widely discussed in the literature.[10, 11, 27, 28] These attributes will be examined here for a linear approach, Holly-Preissmann[10], an eight and six point scheme and the corresponding eight and six point schemes derived by Holly Jr.[25] and Komatsu *et al*[11, 26].

Straight channel testcases, identical to those used for the testing of the one-dimensional finite difference schemes, are used to test the one-dimensional method of characteristics. As before the initial conditions are that the velocity in the x-direction is 1m/s, the spatial increment in the x-direction on the grid is 100m and the time increment is increased from 5 to 100 seconds. The results of the advection of a point release, linear distribution and Gaussian distribution of pollution are compared with the ideal solution.

The results of the simulations are quantified in terms of the root mean square errors[29-32], the percentage of the peak which is maintained and the shape and of the predicted distribution. The effect of the Courant number and refinement of the initial conditions is considered when analysing the data. For comparative purposes, the results is considered at the same time increments and Courant numbers used previously in the analysis of the finite difference schemes in Section 3.2

4.2.1 Results for the point release of pollution

The point source distribution has a single peak concentration of 10mg/l, located at i=11, as shown in Figure (3.12). It is the least refined of the distributions and has very sharp slopes as the concentration increases from zero to ten in a single spatial increment. The

predicted numerical solutions at Courant numbers of 0.05 and 0.8 are included here as Figure (4.4) and Figure (4.5) respectively.

The solution predicted by the linear characteristics equation, exhibits numerical diffusion which becomes more severe as the Courant number increases from 0.05 to 0.8. As the Courant number tends towards one, however, the prediction tends towards the exact solution. For the range of time increments considered, the linear approach remains numerically stable and does not manifest irregularities in the solution.

The Holly-Preissmann approach suffers less from numerical diffusion, but does exhibit some dispersion. In fact all of the methods of characteristics, with the exception of the linear approach, demonstrate numerical dispersion. It is difficult, using these figures alone to distinguish these results as they are all very similar. All indicate some diffusion and also inaccuracy at the extremes of the pollution distribution.

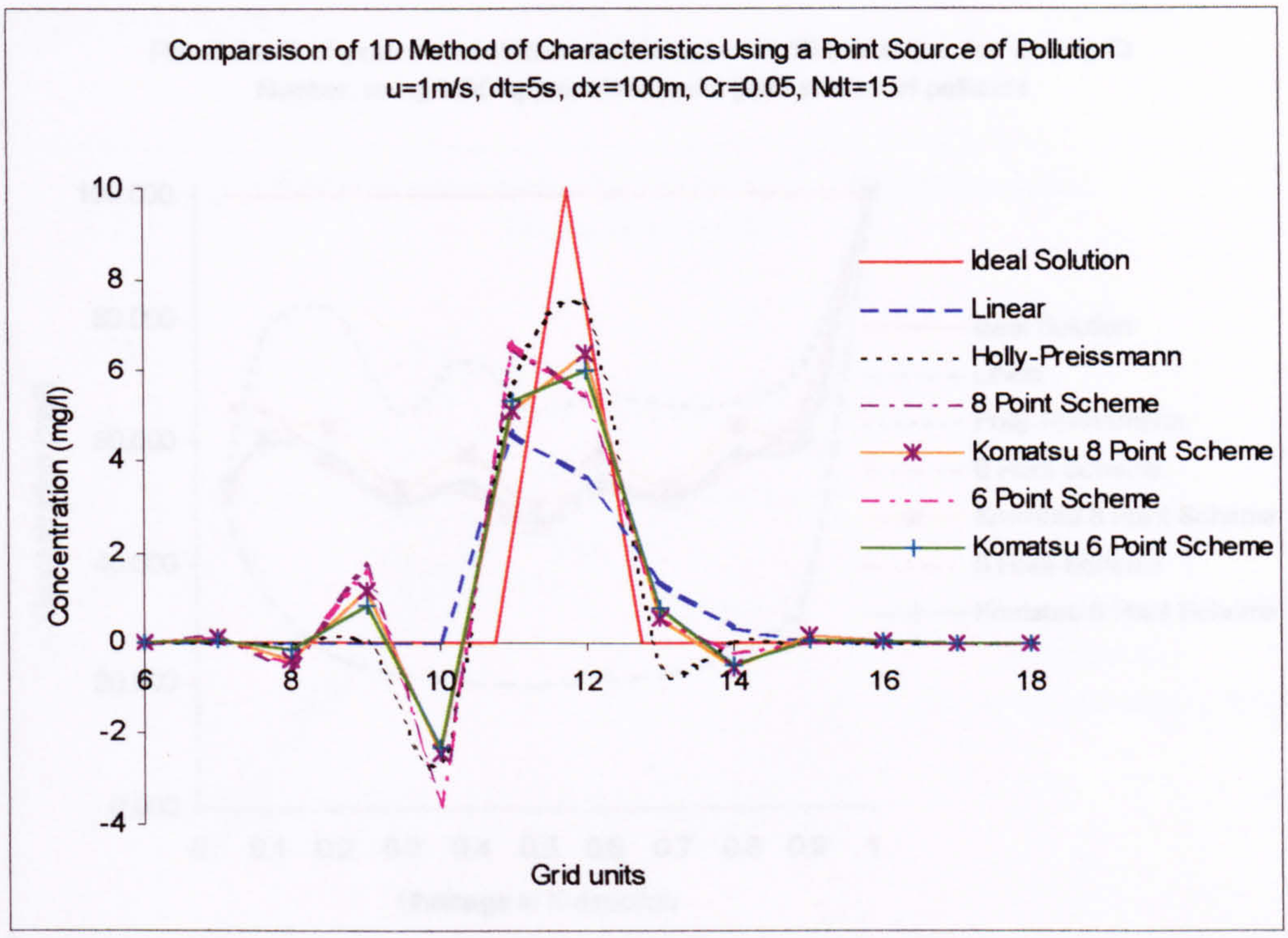

Figure (4.4) Comparison of 1D MOC, using a point source of pollution at Cr=0.05

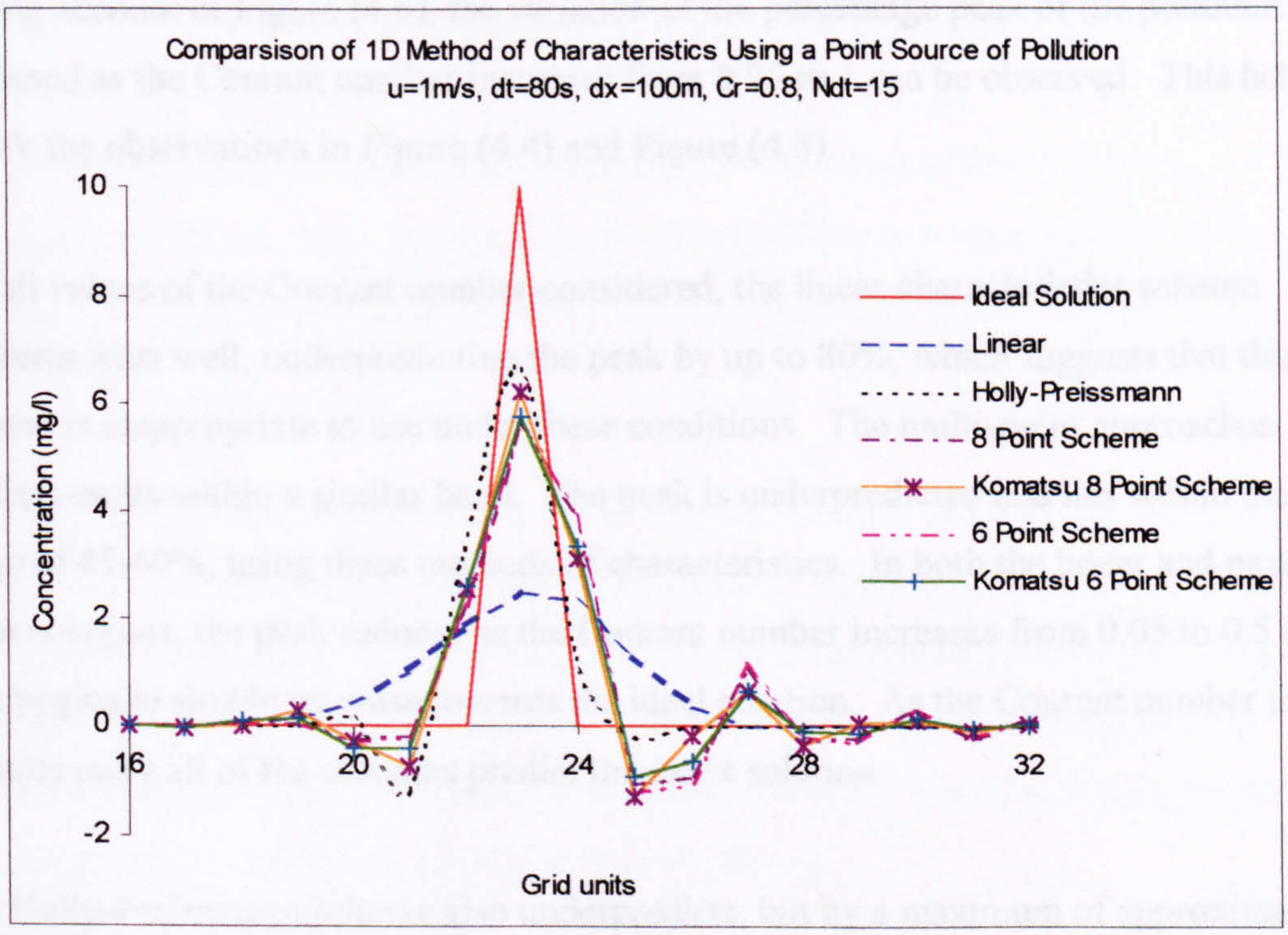

Figure (4.5) Comparison of 1D MOC, using a point source of pollution at Cr=0.8

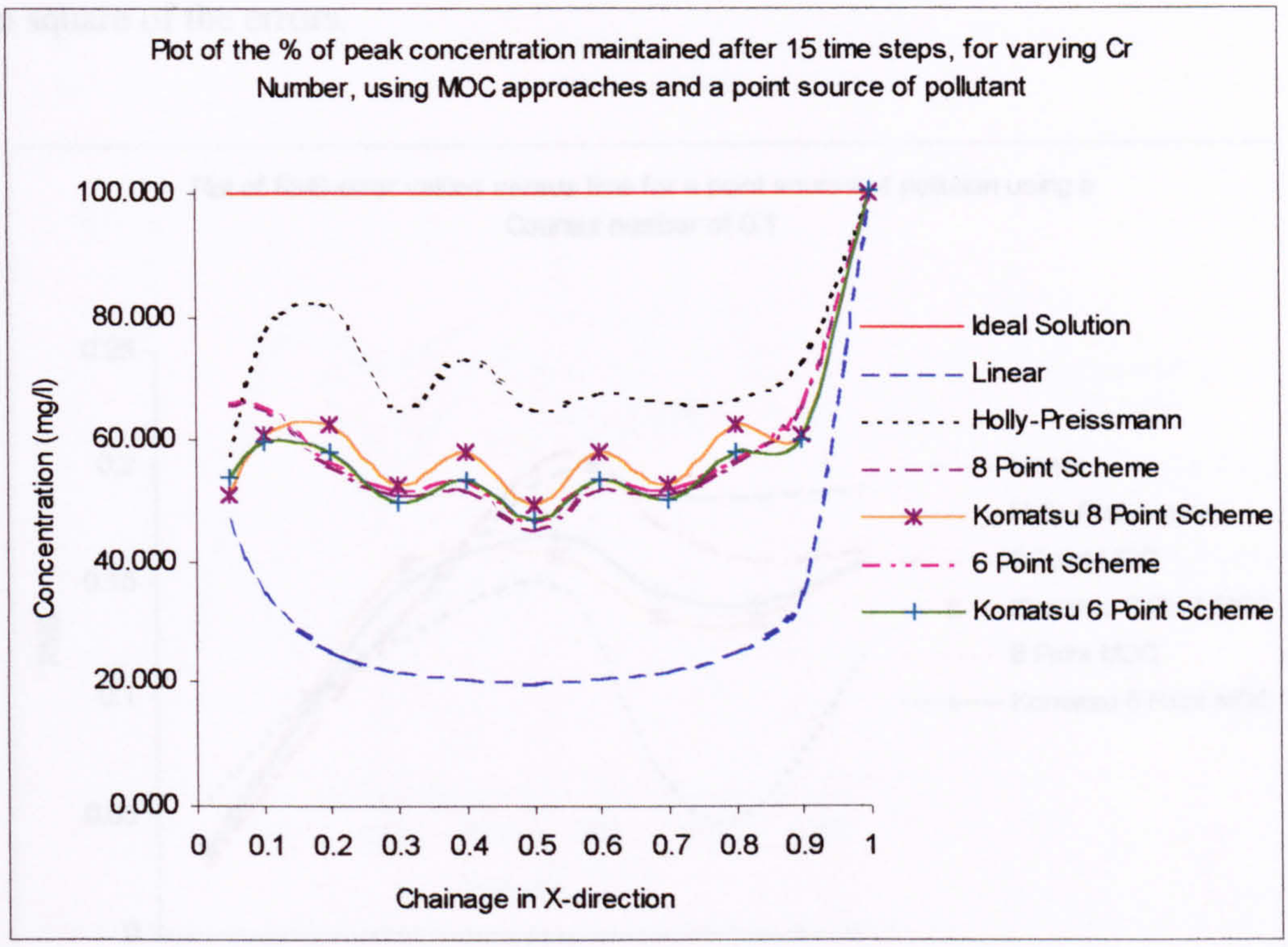

Figure (4.6) Plot of the % point source peak maintained after 15 time steps

Taking account of Figure (4.6), the variation of the percentage peak of the pollutant predicted as the Courant number increases from 0.05 to 1 can be observed. This helps clarify the observations in Figure (4.4) and Figure (4.5).

For all values of the Courant number considered, the linear characteristics scheme performs least well, underpredicting the peak by up to 80%, which suggests that this scheme is inappropriate to use under these conditions. The multi-point approaches predict results within a similar band. The peak is underpredicted and lies within the range of 45-60%, using these methods of characteristics. In both the linear and multi-point solutions, the peak reduces as the Courant number increases from 0.05 to 0.5 and then begins to slowly increase towards the ideal solution. As the Courant number tends towards unity all of the schemes predict the exact solution.

The Holly-Preissmann scheme also underpredicts, but by a maximum of approximately 35%, which is closer to the exact solution than the other schemes.

In terms of the global errors introduced in the solution, Figure (4.7) illustrates the root mean square of the errors.

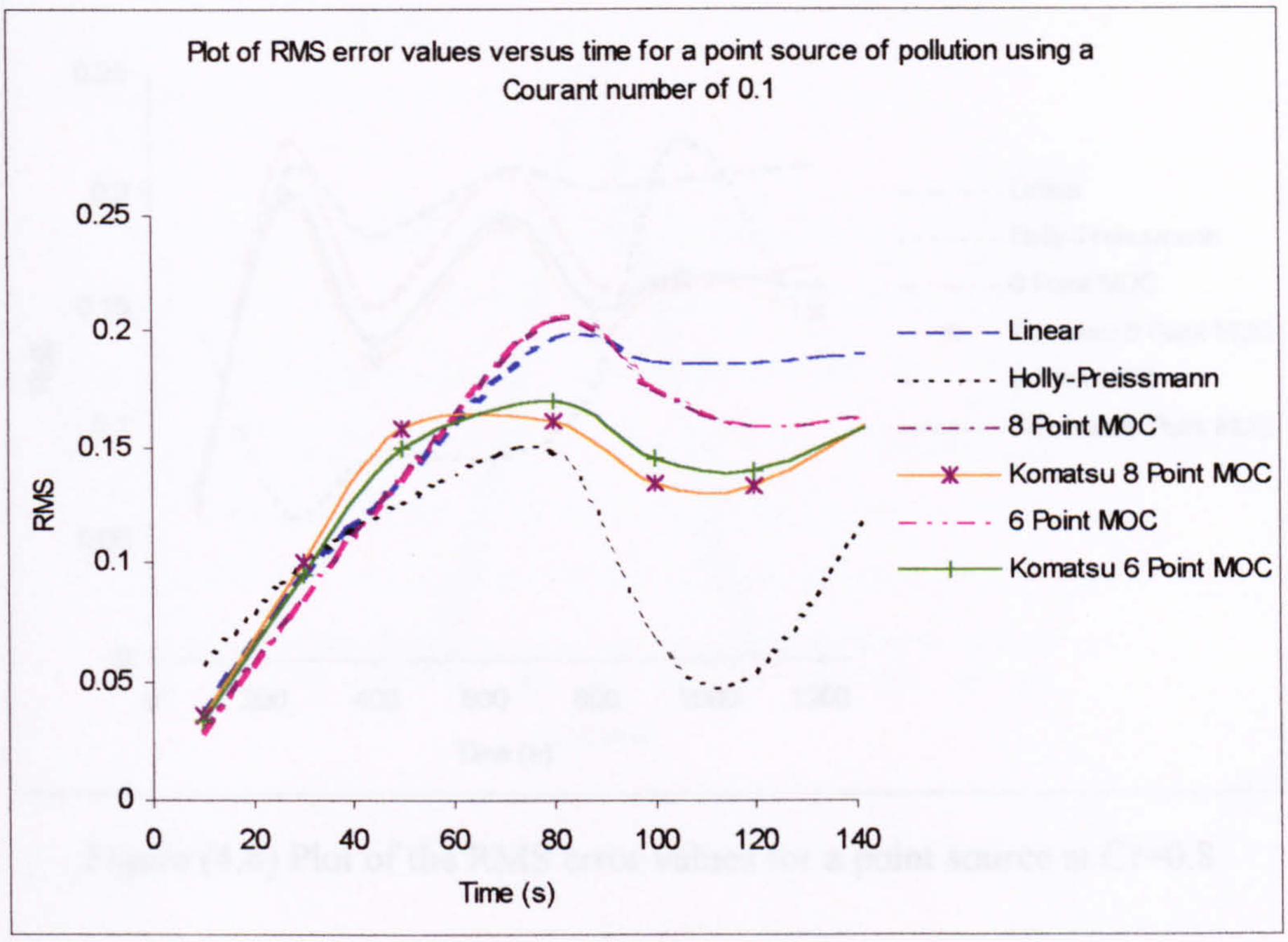

Figure (4.7) Plot of the RMS error values for a point source at Cr=0.1

The root mean square values increase sharply over the range of time from 0 to approximately 75 seconds. From this point the values become more consistent in all cases except for Holly-Preissmann which is observed to vary quite dramatically in comparison.

At the higher Courant number of 0.8 the results are similar, Figure (4.8). There is an initial severe increase in the root mean square values, which then assumes an oscillating trend as time progresses. However the range of the error remains consistent. This implies that although some inaccuracy is present in the numerical scheme it is not amplified as the solution progresses. The values associated with the Holly-Preissmann scheme are again clearly more variable than the others.

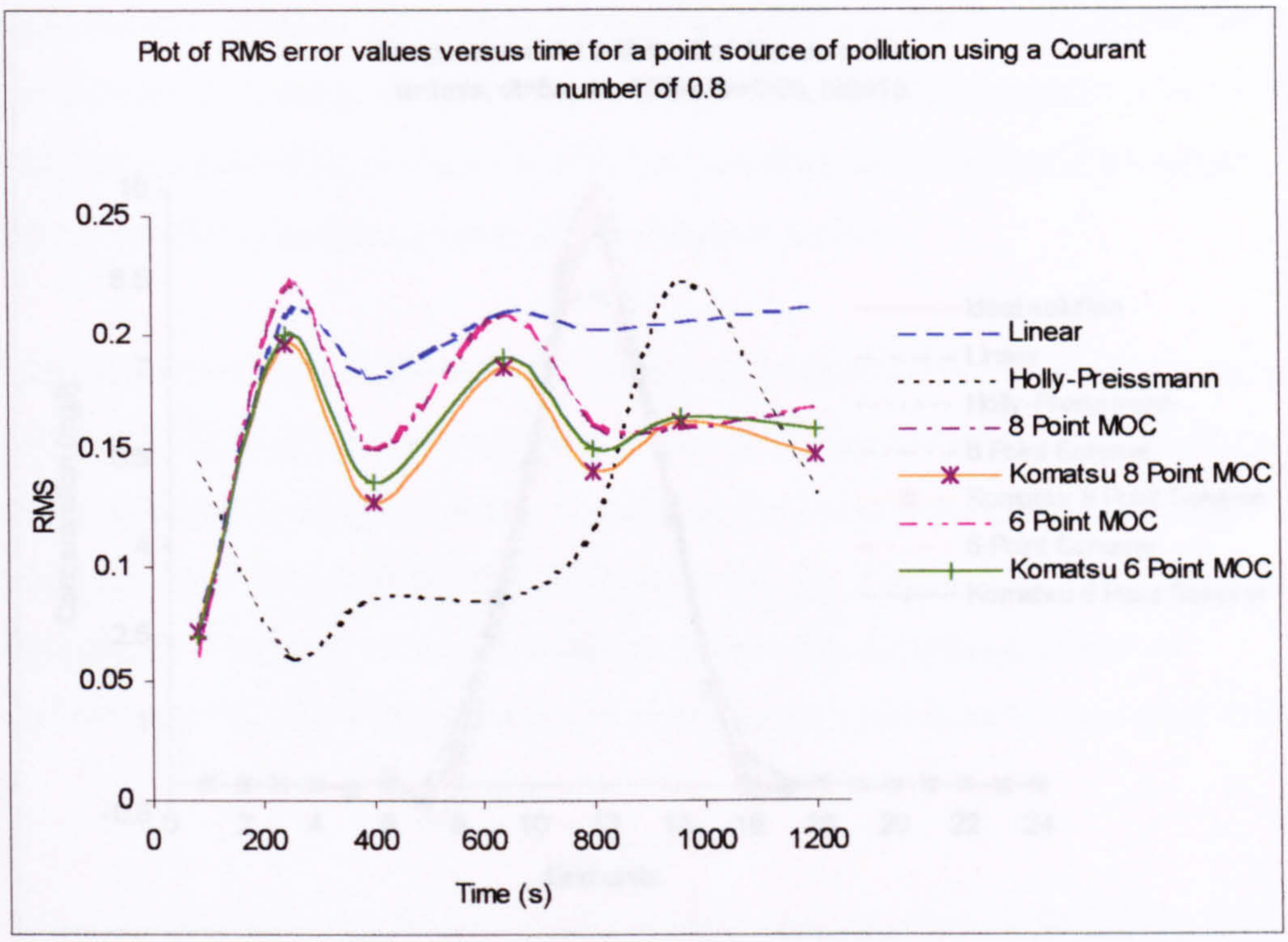

Figure (4.8) Plot of the RMS error values for a point source at Cr=0.8

4.2.2 Results for the linear distribution of pollution

Consider the less severe linear distribution test case, as shown in Figure (3.13). Where the point source had only one location where pollutant was released, this case uses seven. The gradient is still sharp, as the concentration increments are 2.5mg/l over each spatial increment.

Observations regarding the overall shape and dimensions of the predicted distribution can be made using Figure (4.9) and Figure (4.10). These depict the numerical solutions at Courant numbers of 0.05 and 0.8 respectively. In both cases the results are highly similar. The linear characteristics scheme, demonstrates numerical diffusion, which becomes more pronounced at the higher Courant number. The solution also remains numerically stable and shows no signs of dispersion.

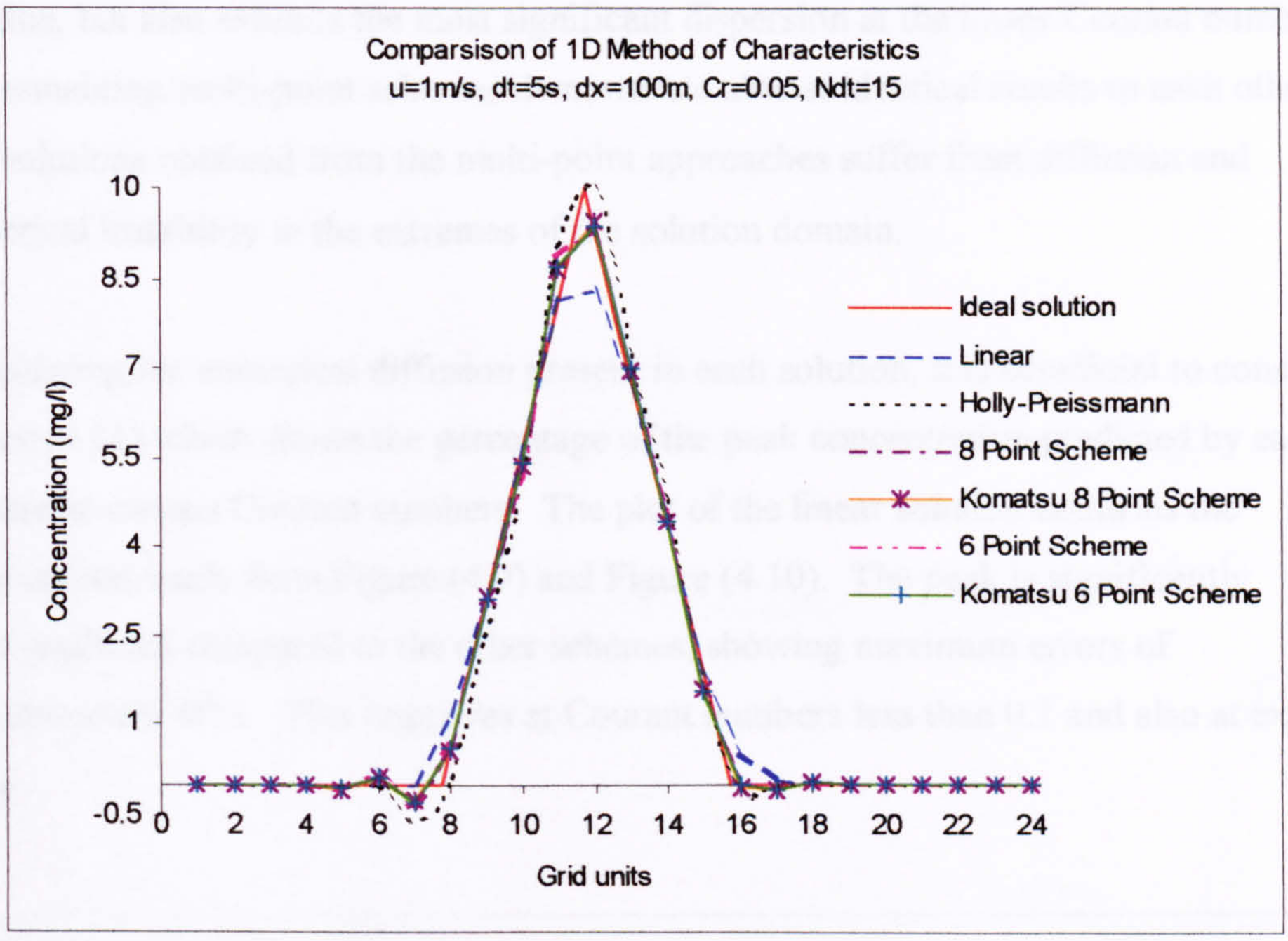

Figure (4.9) Comparison of 1D MOC, using a linear distribution of pollution at Cr=0.1

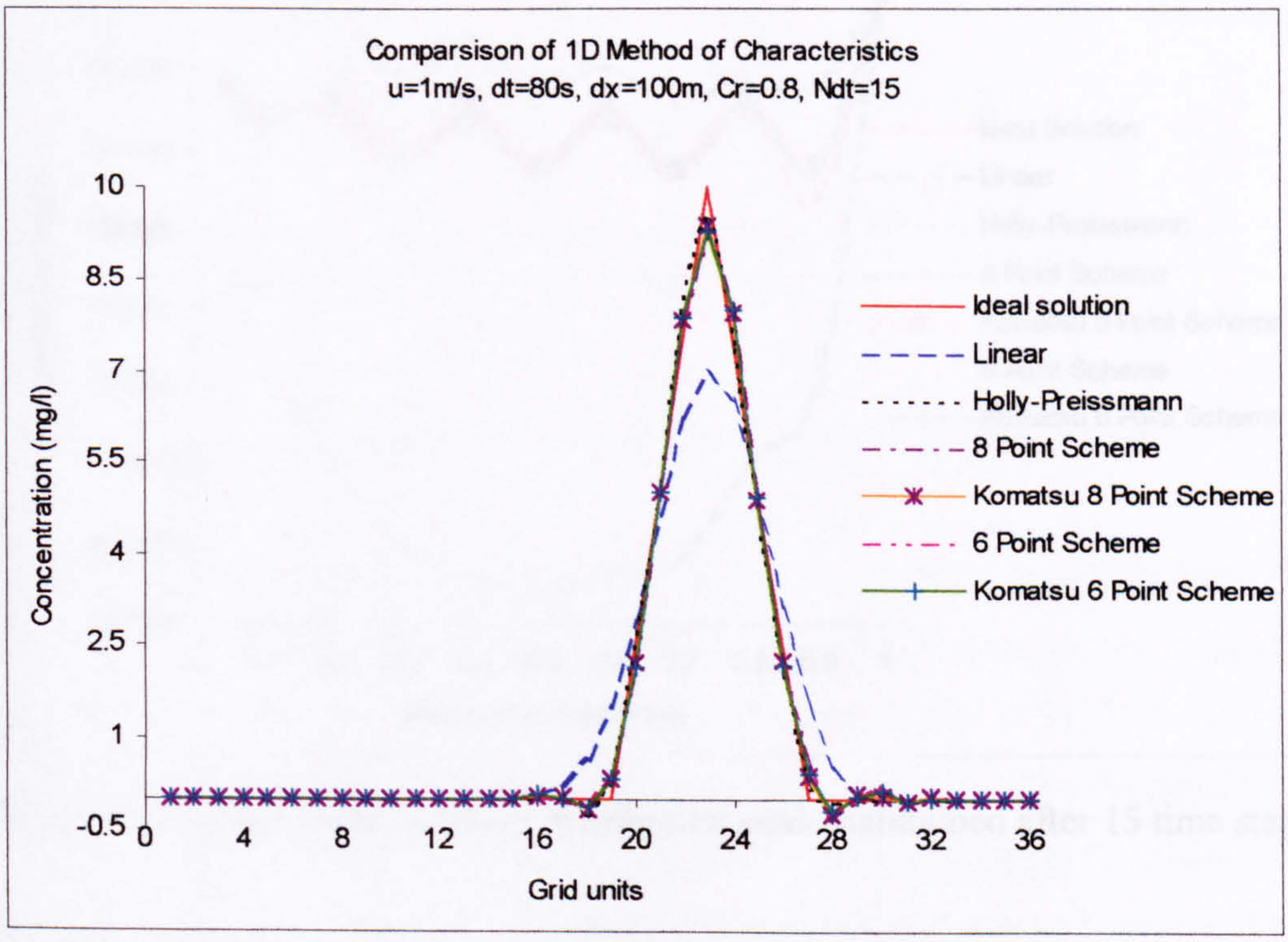

Figure (4.10) Comparison of 1D MOC, using a linear distribution of pollution at Cr=0.8

The Holly-Preissmann scheme gives a numerical solution which is similar to the ideal solution, but also exhibits the most significant dispersion at the lower Courant number. The remaining multi-point schemes demonstrate almost identical results to each other. The solutions obtained from the multi-point approaches suffer from diffusion and numerical instability at the extremes of the solution domain.

Considering the numerical diffusion present in each solution, it is beneficial to consider Figure (4.11) which shows the percentage of the peak concentration predicted by each scheme at various Courant numbers. The plot of the linear solution confirms the observations made from Figure (4.9) and Figure (4.10). The peak is significantly underpredicted compared to the other schemes, showing maximum errors of approximately 40%. This improves at Courant numbers less than 0.1 and also at exactly unity.

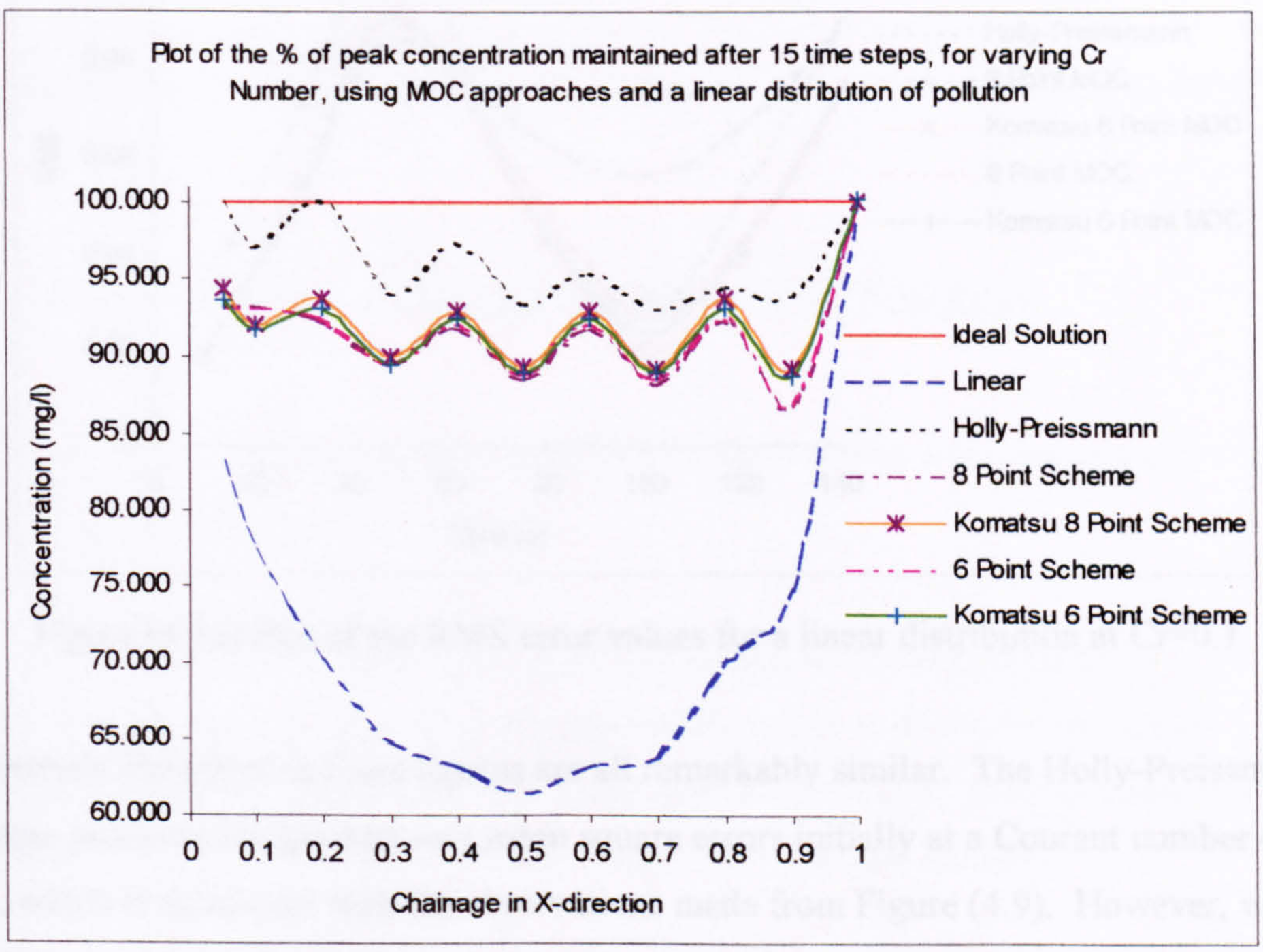

Figure (4.11) Plot of the % linear distribution peak maintained after 15 time steps

The multi-point methods, demonstrate far better prediction of the peak, with maximum error being in the region of 13%. The schemes follow the same trend very closely. The

Holly-Preissmann approach indicates the greatest accuracy in maintaining the peak, although it does indicate very slight instability at a Courant number of 0.2. In all of these cases as the Courant number increases, the numerical solutions move further from the ideal solutions: with the exception of the case where the Courant number is equal to one.

It is also useful to consider the root mean square errors, to try to establish any significant variations between the schemes, Figure (4.12) and Figure (4.13).

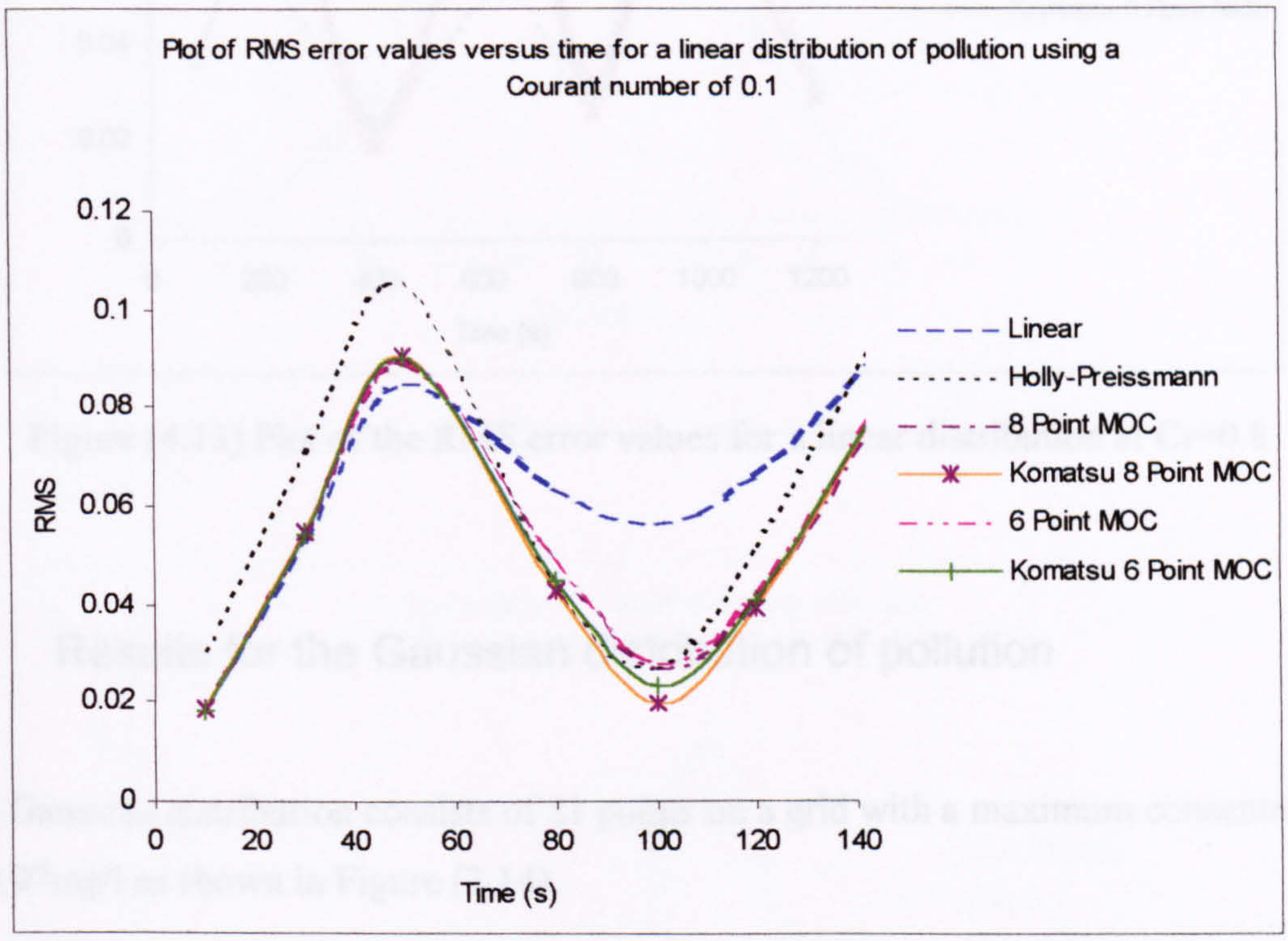

Figure (4.12) Plot of the RMS error values for a linear distribution at Cr=0.1

The trends illustrated in these figures are all remarkably similar. The Holly-Preissmann scheme produces the greatest root mean square errors initially at a Courant number of one, which is consistent with the observations made from Figure (4.9). However, when the Courant number is increased to 0.8, the predicted solution exhibits the smallest errors. As the solution progresses the root mean square values appear to oscillate within the same range in all cases except the linear approach, which tends to increase. This suggests that some inherent error exists in the linear scheme.

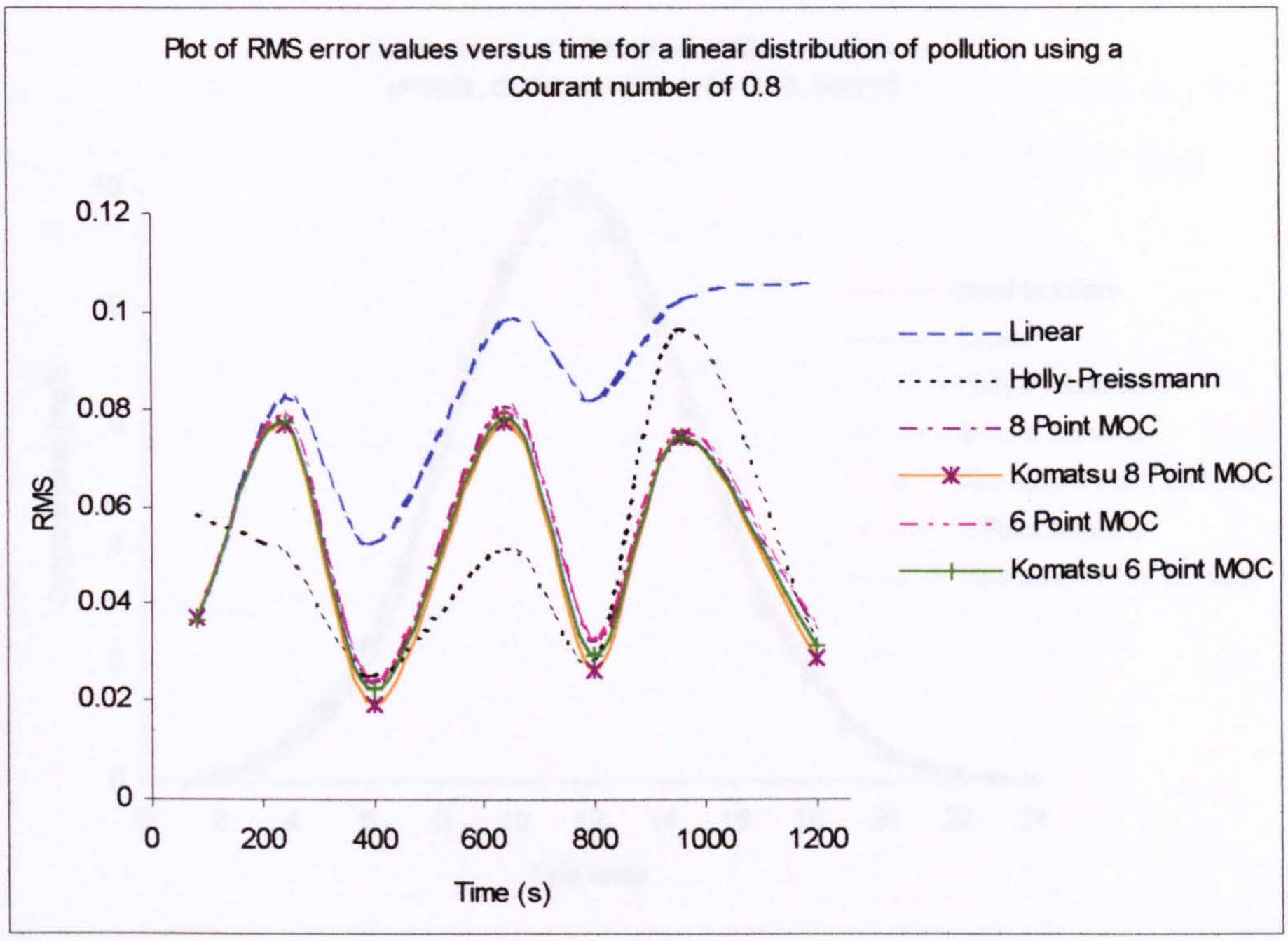

Figure (4.13) Plot of the RMS error values for a linear distribution at Cr=0.8

4.2.3 Results for the Gaussian distribution of pollution

The Gaussian distribution consists of 21 points on a grid with a maximum concentration of 9.97mg/l as shown in Figure (3.14).

Analysis of Figure (4.14) and Figure (4.15) show that all of the method of characteristics predict a numerical solution which closely matches the shape and dimensions of the exact solution. The linear approach however, exhibits numerical diffusion which becomes more obvious at the higher Courant number.

The percentage of the peak concentrations are also evaluated by considering Figure (4.16). The figure shows first of all, that indeed the linear characteristic method significantly

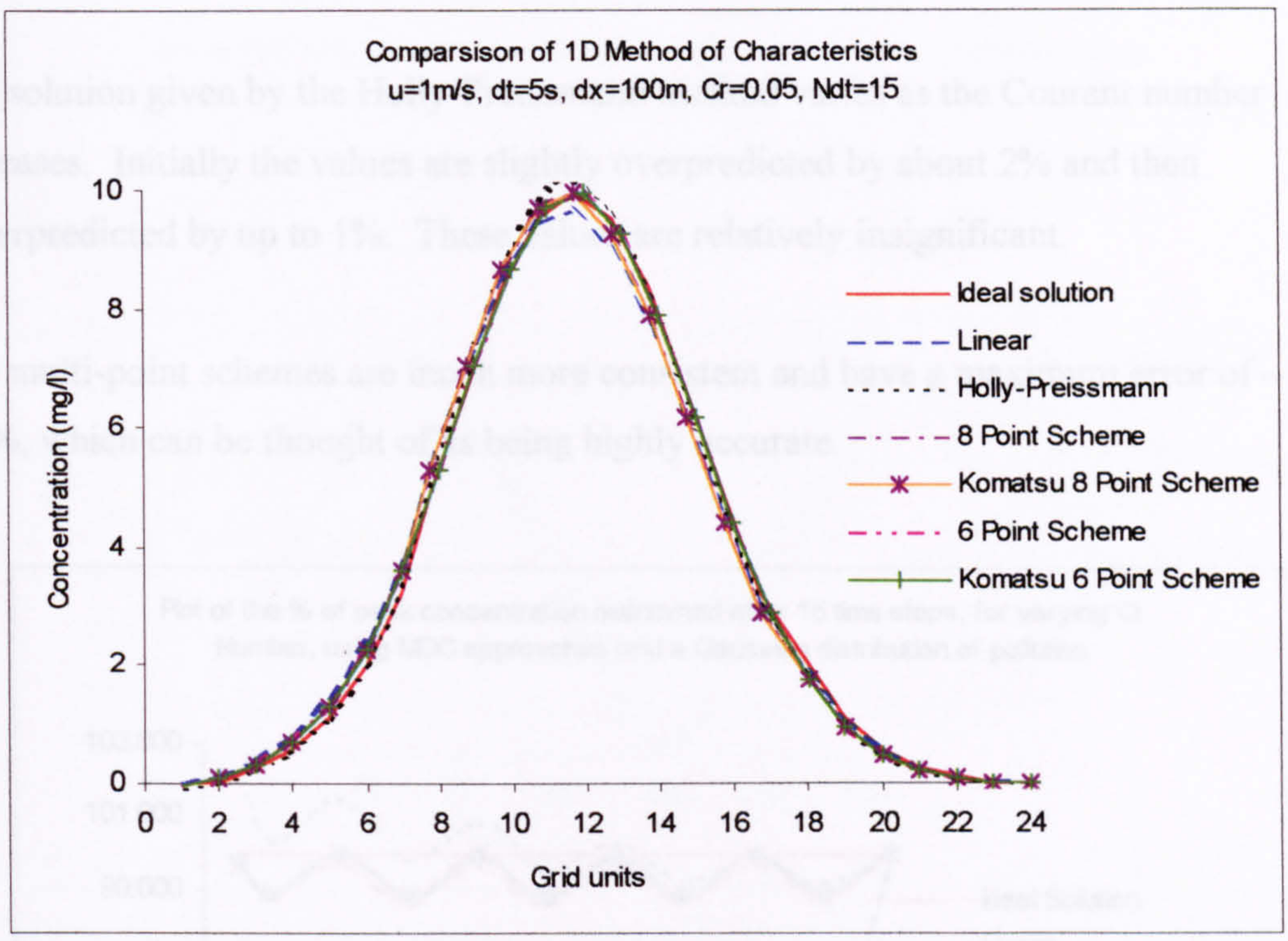

Figure (4.14) Comparison of 1D MOC, using a Gaussian distribution at Cr=0.1

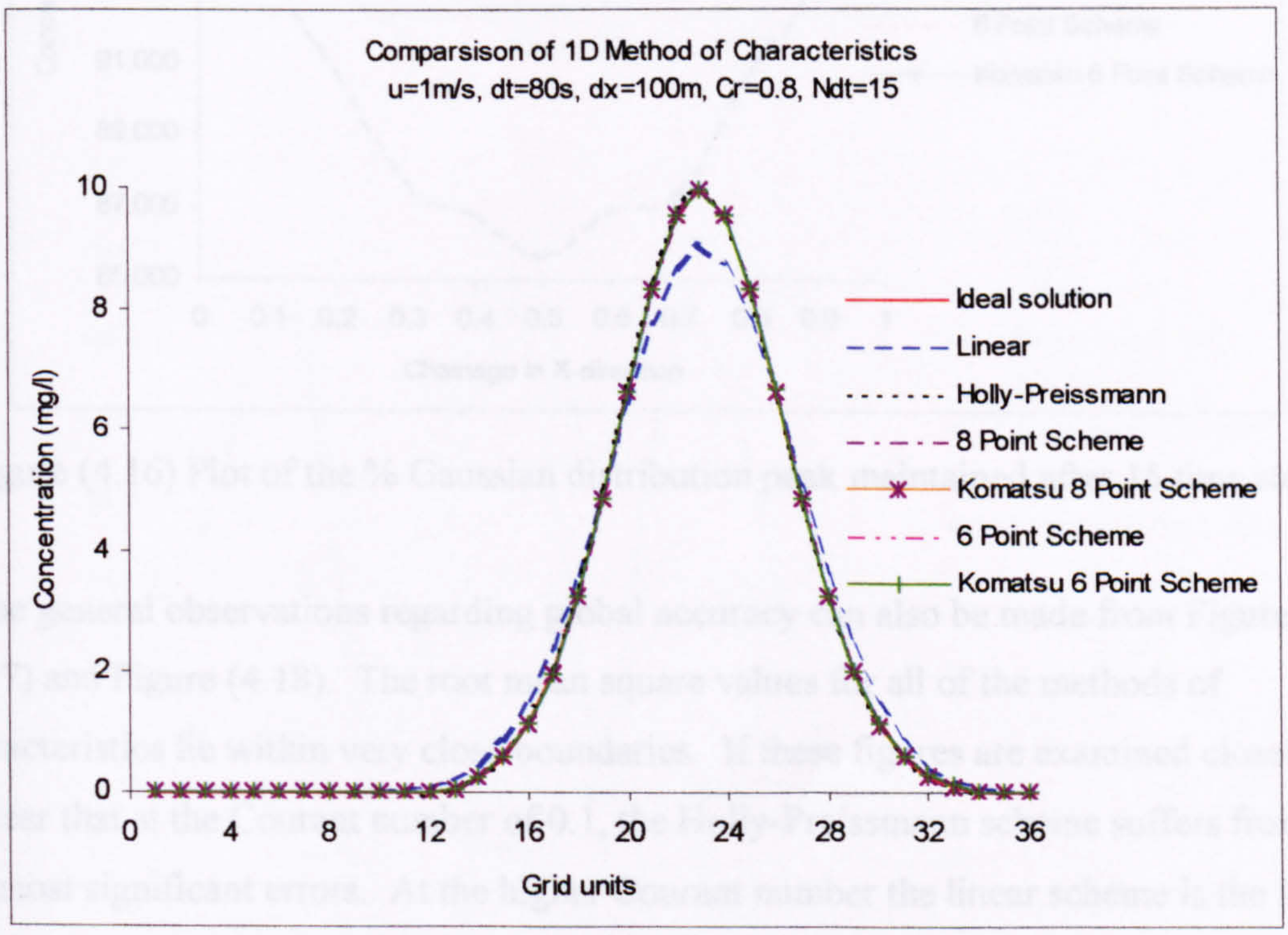

Figure (4.15) Comparison of 1D MOC, using a Gaussian distribution at Cr=0.8

underpredicts the ideal solution by up to 15%.

The solution given by the Holly-Preissmann method varies as the Courant number increases. Initially the values are slightly overpredicted by about 2% and then underpredicted by up to 1%. These values are relatively insignificant.

The multi-point schemes are much more consistent and have a maximum error of –1.5%, which can be thought of as being highly accurate.

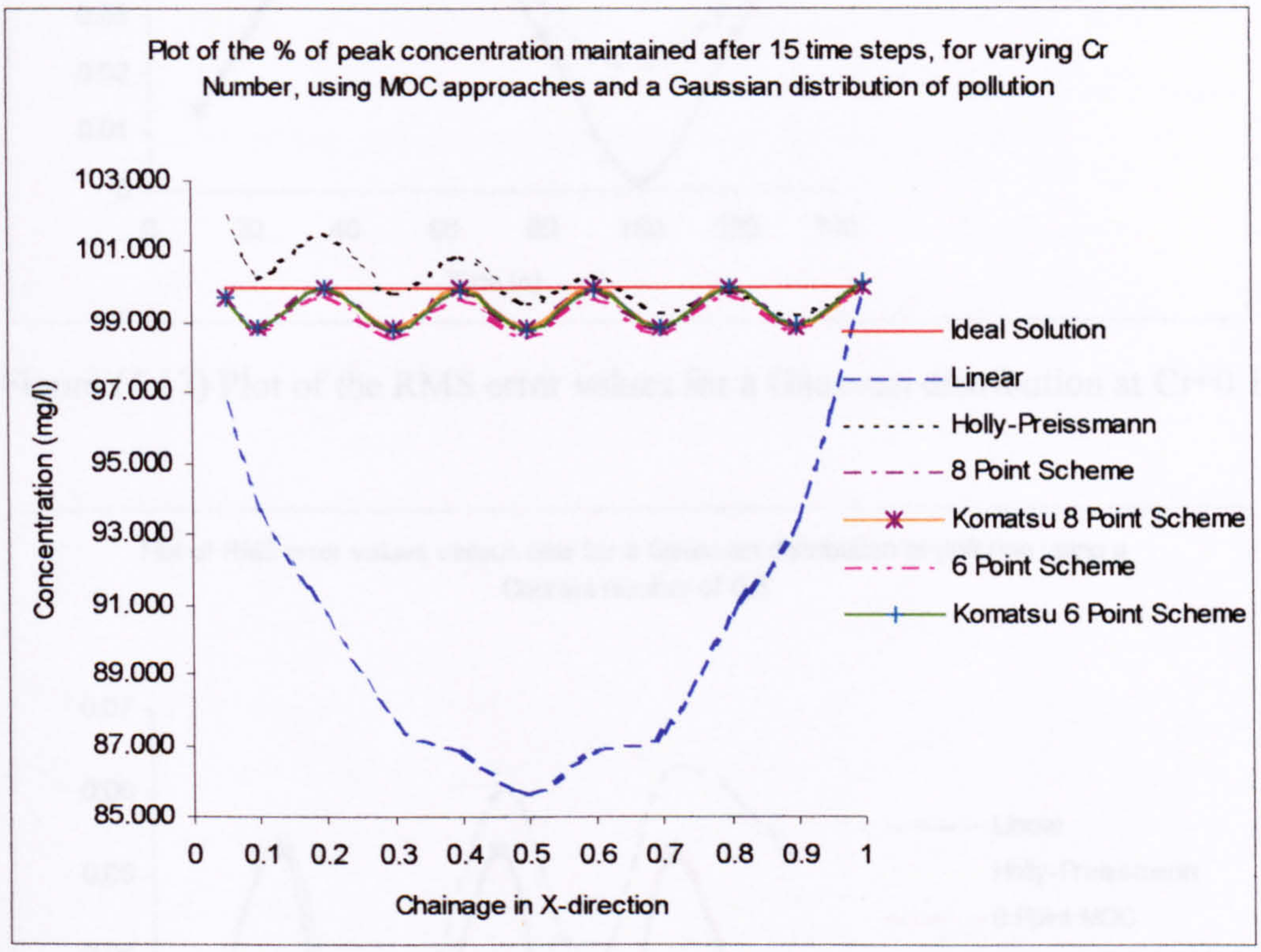

Figure (4.16) Plot of the % Gaussian distribution peak maintained after 15 time steps

Some general observations regarding global accuracy can also be made from Figure (4.17) and Figure (4.18). The root mean square values for all of the methods of characteristics lie within very close boundaries. If these figures are examined closely, it is clear that at the Courant number of 0.1, the Holly-Preissmann scheme suffers from the most significant errors. At the higher Courant number the linear scheme is the least accurate.

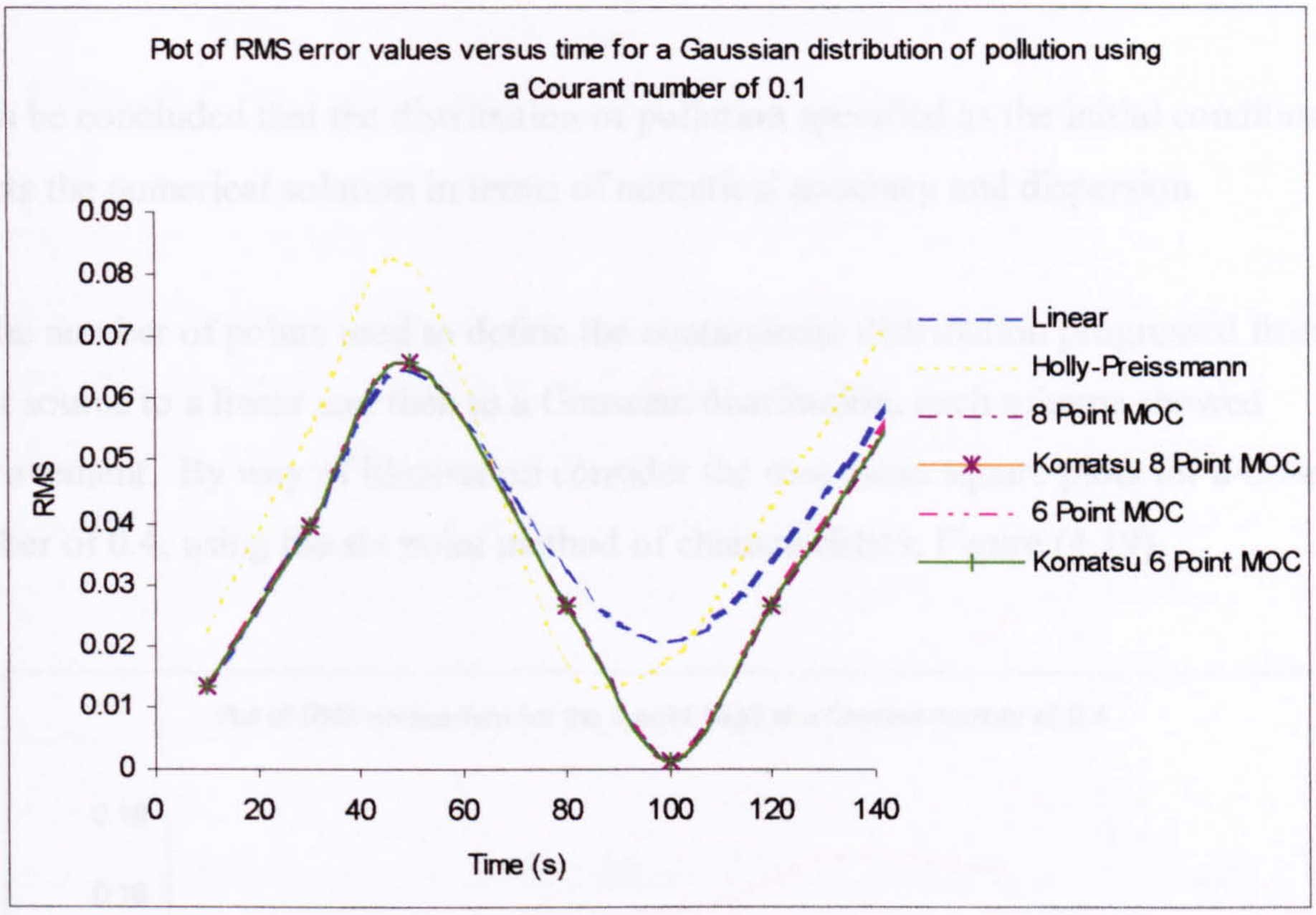

Figure (4.17) Plot of the RMS error values for a Gaussian distribution at Cr=0.1

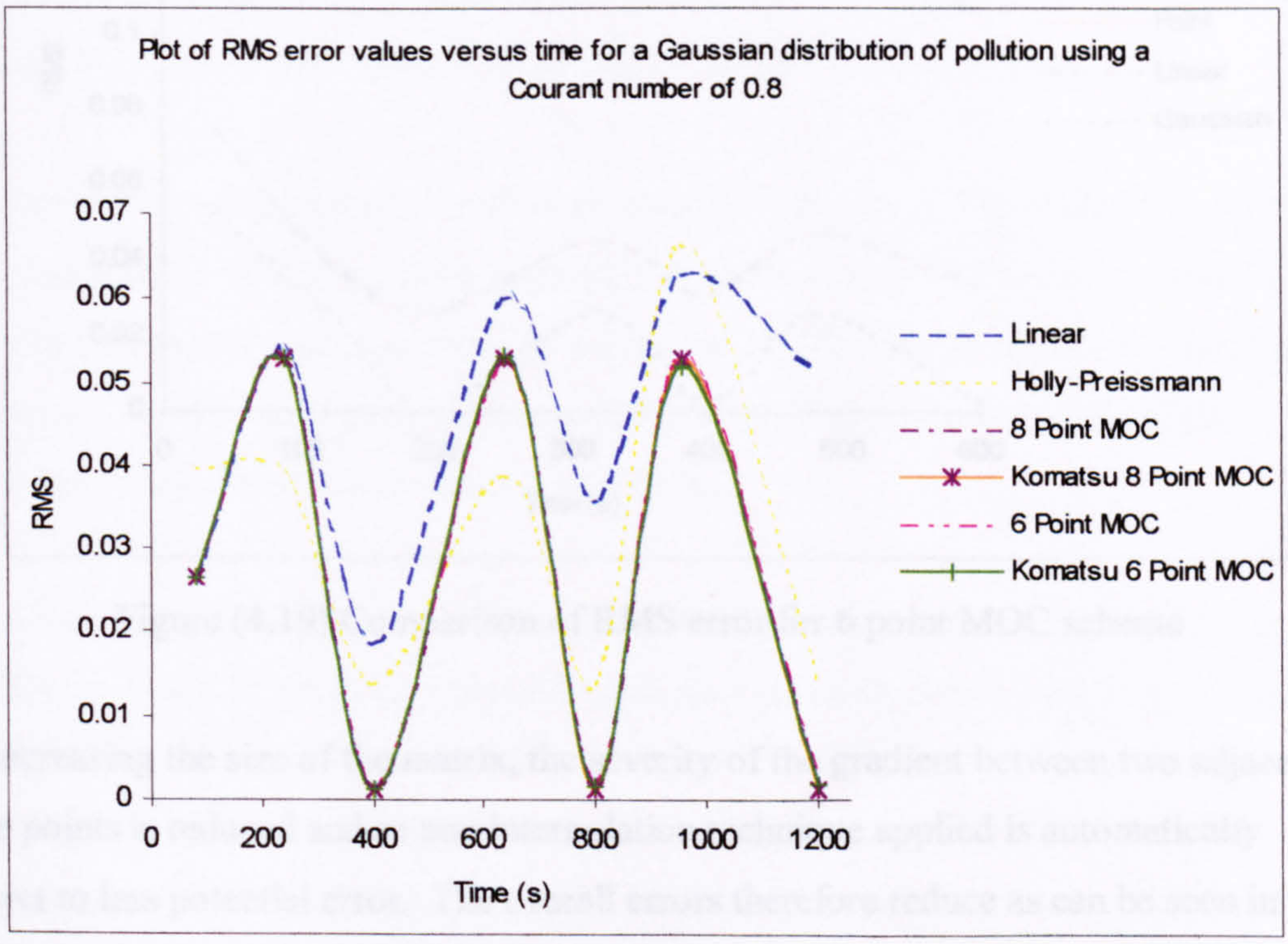

Figure (4.18) Plot of the RMS error values for a Gaussian distribution at Cr=0.8

4.3 Conclusions

It can be concluded that the distribution of pollution specified as the initial conditions affects the numerical solution in terms of numerical accuracy and dispersion.

As the number of points used to define the contaminant distribution progressed from, a point source to a linear and then to a Gaussian distribution, each scheme showed improvement. By way of illustration consider the root mean square plots for a Courant number of 0.4, using the six point method of characteristics, Figure (4.19).

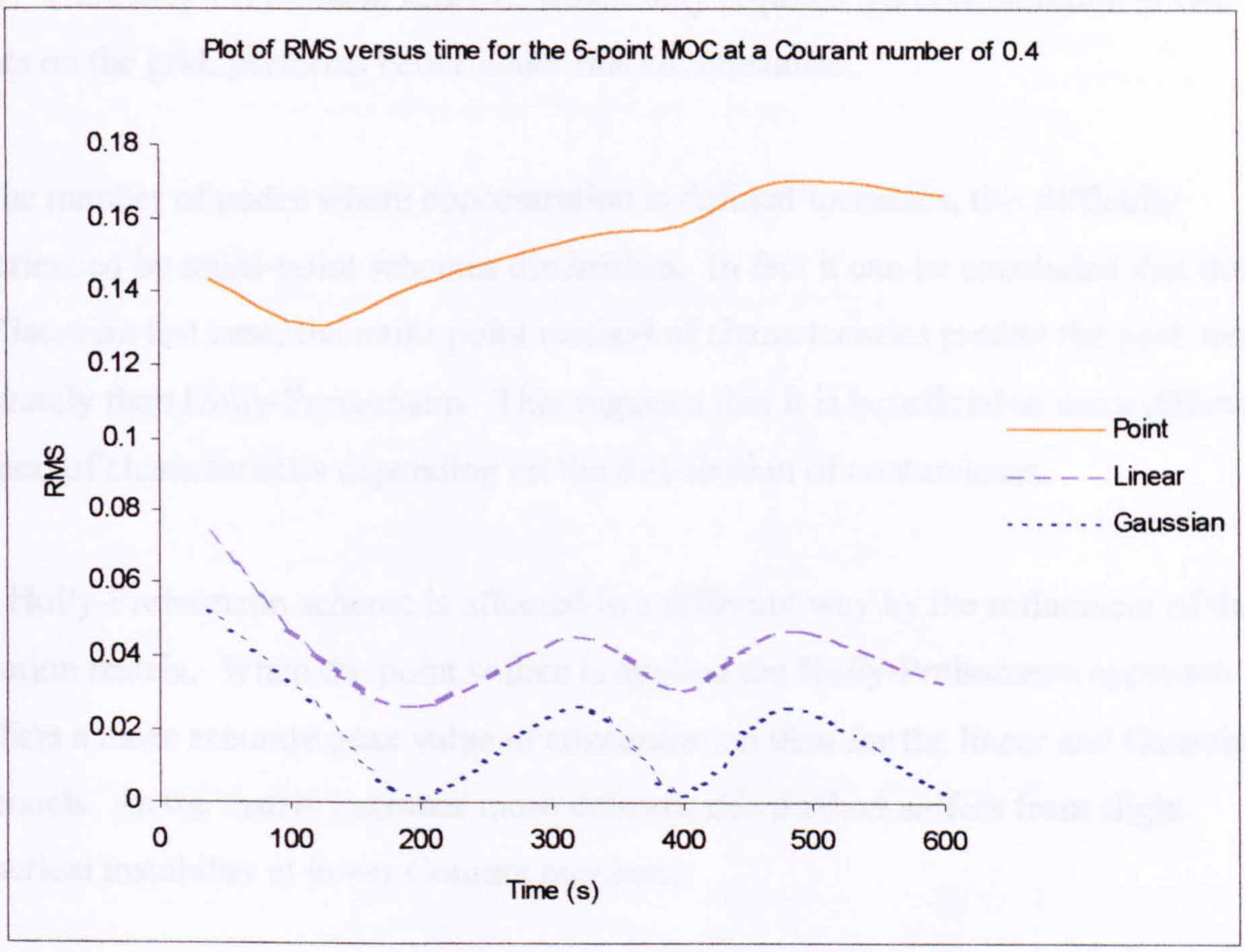

Figure (4.19) Comparison of RMS error for 6 point MOC scheme

By increasing the size of the matrix, the severity of the gradient between two adjacent node points is reduced and so any interpolation technique applied is automatically subject to less potential error. The overall errors therefore reduce as can be seen in the figure. In the case of the point release, the root mean square value increases steadily and has values exceeding 0.14. However, the results for the linear and Gaussian distributions are of magnitudes less than 0.08 and both trends follow very similar

shapes. It is interesting to observe that the numerical dispersion present for the linear and point source testcases is negligible in the results of the Gaussian distribution, Figure (4.4), Figure (4.9) and Figure (4.14).

There is an obvious reason why the multi-point schemes cope less well with the point source of pollution than the linear and Holly-Preissmann approaches. The multi-point schemes use concentrations at locations from i-3 to i+4 to calculate the value at the next time step. If the point source is located at the relative point, i+4, it affects the concentration at the next time step at i, however if there are no concentrations in-between i and i+4, the concentration gradient is very large and a source of significant error. The Holly-Preissmann scheme, which only requires the concentration at two points on the grid, performs better under this circumstance.

As the number of nodes where concentration is defined increases, this difficulty experienced by multi-point schemes diminishes. In fact it can be concluded that during the Gaussian test case, the multi-point method of characteristics predict the peak more accurately than Holly-Preissmann. This suggests that it is beneficial to use a different method of characteristics depending on the distribution of contaminant.

The Holly-Preissmann scheme is affected in a different way by the refinement of the pollution matrix. When the point source is applied the Holly-Preissmann approach predicts a more accurate peak value of concentration than for the linear and Gaussian approach. As the matrix becomes more defined, this method suffers from slight numerical instability at lower Courant numbers.

The effect of the Courant number should also be given some consideration here. In general the Holly-Preissmann approach predicts a gradually lower peak as the Courant number increases. At Courant numbers between 0.8 and 1, the results are the least accurate. The multi-point schemes remain fairly consistent as the Courant number varies in these tests. However, the results of the point source and linear distributions show that peak prediction decreases slightly from 0 to 0.6 and then increases for Courant numbers between 0.7 and 1. This suggests that it would also be more appropriate to use a different approach depending on the value of the Courant number.

4.4 References

1. Vreugdenhil, C.B., *Computational Hydraulics.* 1989, Berlin: Springer- Verlag.

2. Hirsch, C., *Numerical computation of internal and external flows*, ed. Wiley. Vol. 1. 1988: Wiley.

3. Abbott, M.B. and Basco, D.R., *Computational Fluid Dynamics; An Introduction for Engineers.* 1989: Longman Scientific and Technical.

4. Al-Lawatia, M., Sharpley, R.C., and Wang, H., "Second-order characteristic methods for advection-diffusion equations and comparison to other schemes", *Advances in Water Resources*, 1999, **22**(7), 741-768.

5. Croucher, A.E. and O'Sullivan, M.J., "Numerical methods for contaminant transport in rivers and estuaries", *Computers & Fluids*, 1998, **27**(8), 861-878.

6. Makler, S., Marshall, G., and Moledo, L. *Computational aspects of water quality models in estuaries using finite difference and finite element methods.* in *17th Congress of the IAHR; Hydraulic Engineering for Improved Water Management.* 1977. Baden-Baden.

7. Abbott, M.B., *An Introduction to the method of characteristics.* 1966, New York: American Elsevier.

8. Chintu, L., "Comprehensive method of characteristics models for flow simulation", *Journal of Hydraulic Engineering*, 1988, **114**, 1074-1097.

9. Goldberg, D.E. and Wylie, E.B., "Characteristics Method Using Time-Line Interpolations", *Journal of Hydraulic Engineering-Asce*, 1983, **109**(5), 670-683.

10. Holly Jr., F.M. and Preissmann, A., "Accurate calculation of transport in two dimensions", *Journal of the Hydraulics Division*, 1977, **103**(HY11), 1259-1277.

11. Komatsu, T., Ohgushi, K., Asai, K., and Holly Jr., F.M., "Accurate numerical simulation of scalar advective transport", *Journal of Hydroscience and hydraulic Engineering*, 1989, 7(1), 63-73.

12. Glass, J. and Rodi, W., "A higher order numerical scheme for scalar transport", *Computer methods in applied mechanics and engineering*, 1982, **31**, 337-358.

13. Li, C.W., "Advection-Dispersion Simulation By Minimization Characteristics and Alternate Direction Explicit Methods", *Applied Mathematical Modelling*, 1991, **15**(11-12), 616-623.

14. Hervouet, J.M., "Application of the method of characteristics in their weak formulation to solving two-dimensional advection equations on mesh grids", in *Computational Techniques for Fluid Flow, Vol 5: Recent advances in Numerical Methods in Fluids*, C. Taylor, J.A. Johnson, and W.R. Smith, Editors. 1986, Pineridge Press: Swansea. 149-185.

15. Yang, J.C. and Wang, J.Y., "Numerical solution of dispersion equation in one dimension", *Journal of the Chinese Institute of Engineers*, 1988, **11**, 379-383.

16. Kojouharov, H.V. and Chen, B.M., "Nonstandard methods for the convective transport equation with nonlinear reactions", *Numerical Methods For Partial Differential Equations*, 1998, **14**(4), 467-485.

17. Zheng, C., "Extension of the Method of Characteristics For Simulation of Solute Transport in 3 Dimensions", *Ground Water*, 1993, **31**(3), 456-465.

18. Cao, Z. and Wei, L., "An operator-splitting algorithm for advection-diffusion-reaction equation", *Journal of Hydrodynamics*, 1992, **Ser B**(1), 65-73.

19. Bruneau, C.H., Fabrie, P., and Rasetarinera, P., "An accurate finite difference scheme for solving convection- dominated diffusion equations", *International Journal For Numerical Methods in Fluids*, 1997, **24**(2), 169-183.

20. Yang, J.C. and Chiu, K.P., "Use of Characteristics Method With Cubic Interpolation For Unsteady-Flow Computation", *International Journal For Numerical Methods in Fluids*, 1993, **16**(4), 329-345.

21. Lai, C., "Comprehensive Method of Characteristics Models For Flow Simulation", *Journal of Hydraulic Engineering-Asce*, 1988, **114**(9), 1074-1097.

22. Lin, W. and Song, C.C.S. *A multimode scheme of characteristics methos for open channel flows.* in *Proceedings of teh 1990 National Conference: Hydraulic Engineering*. 1990. San-Diego, CA: ASCE.

23. Hinstrup, P.I., Kej, A., and Kroszynski, U. *A high accuracy two-dimensional transport-dispersion model for environmental applications.* in *17th Congress of the IAHR; Hydraulic Engineering for Improved Water Management*. 1977. Baden-Baden.

24. Holly, F.M. and Preissmann, A., "Accurate calculation of transport in two dimensions", *Journal of the Hydraulic Division, ASCE*, 1977, **103**, 1259-1277.

25. Holly Jr., F.M. and Komatsu, T. *Derivative approximations in the two-point fourth order method for pollutant transport.* in *Frontiers in Hydraulic Engineering*. 1983. MIT, MA: ASCE.

26. Komatsu, T., Holly, F.M., Nakashiki, N., and Ohgushi, K., "Numerical calculation of pollutant transport in one and two-dimensions", *Journal of Hydroscience and Hydraulic Engineering*, 1985, **3**, 15-30.

27. Manson, J.R. and Wallis, S.G., "An accurate numerical algorithm for advective transport", *Communications in Numerical Methods in Engineering*, 1995, **11**(12), 1039-1045.

28. Wallis, S.G. and Manson, J.R., "Accurate numerical simulation of advection using large time steps", *International Journal For Numerical Methods in Fluids*, 1997, **24**(2), 127-139.

29. Roberts, D.L. and Selim, M.S., "Comparative-Study of 6 Explicit and 2 Implicit Finite-Difference Schemes For Solving One-Dimensional Parabolic Partial-Differential Equations", *International Journal For Numerical Methods in Engineering*, 1984, **20**(5), 817-844.

30. Towler, B.F. and Yang, R.Y.K., "On comparing the accuracy of some finite difference methods for parabolic partial differential equations", *International Journal for Numerical Methods in Engineering*, 1979, **14**, 1021-1035.

31. Hogarth, W.L., Noye, B.J., Stagnitti, J., Parlange, J.Y., and Bolt, G., "A Comparative-Study of Finite-Difference Methods For Solving the One-Dimensional Transport-Equation With an Initial Boundary-Value Discontinuity", *Computers & Mathematics With Applications*, 1990, **20**(11), 67-82.

32. Wornom, S.F., "Application of 2-Point Implicit Central-Difference Methods to Hyperbolic Systems", *Computers & Fluids*, 1991, **20**(3), 321-331.

Chapter 5

Two-Dimensional Numerical Methods

5.1 Introduction 120

5.1.1 Extension of the upwinding scheme to two-dimensions 120

5.1.2 Extension of the QUICKEST scheme to two-dimensions 123

5.1.3 Extension of the eight point method of characteristics scheme to two-dimensions 134

5.1.4 Extension of the six point method of characteristics scheme to two-dimensions 143

5.2 Comparison of the two-dimensional finite difference schemes and methods of characteristics 149

5.2.1 Diagonal testcase 149

5.2.1.1 Results using a point release 149

5.2.1.2 Results using a linear distribution 155

5.2.1.3 Results using a Gaussian distribution 162

5.2.2 Rotational flow case using a Gaussian distribution 167

5.3 Conclusions 172

5.4 References 176

5.1 Introduction

Four finite difference schemes and six method of characteristics approaches have been derived and examined in one-dimensional testcases in Sections 3.2 and 4.2 respectively. The next stage of this study is to develop these schemes from one to two-dimensions so that they can be applied to more complicated flow patterns. The conclusions from the one-dimensional testcases allow the selection of the most numerically stable and accurate schemes for this development.

5.1.1 Extension of the upwinding scheme to two-dimensions

The upwinding scheme, as applied to the one-dimensional testcases used in Section 3.2, proved to suffer from considerable numerical damping. Despite this, it predicted a numerical solution closest to the actual distribution when compared to the central differencing and QUICK approaches. Its solution was also free from numerical dispersion and instability for all Courant numbers less than or equal to one. In addition, it is a very simple scheme to derive and apply mathematically and highly efficient in terms of computational time.

These attributes plus the fact that upwinding is often used for comparative purposes when testing other numerical schemes, are reasons to develop the approach in two-dimensions.[1-4]

Consider the two-dimensional form of the advection equation, (5.1):

$$\frac{\partial C}{\partial t}+u\frac{\partial C}{\partial x}+v\frac{\partial C}{\partial y}=0 \qquad (5.1)$$

in which C is concentration, t is time, u represents the local velocity in the x-direction and v is the local velocity in the y-direction. This is rearranged in terms of the local rate of change as equation (5.2):

$$\frac{\partial C}{\partial t} = -u\frac{\partial C}{\partial x} - v\frac{\partial C}{\partial y} \tag{5.2}$$

Consider the two-dimensional finite difference grid at the present time step, Figure (5.1).

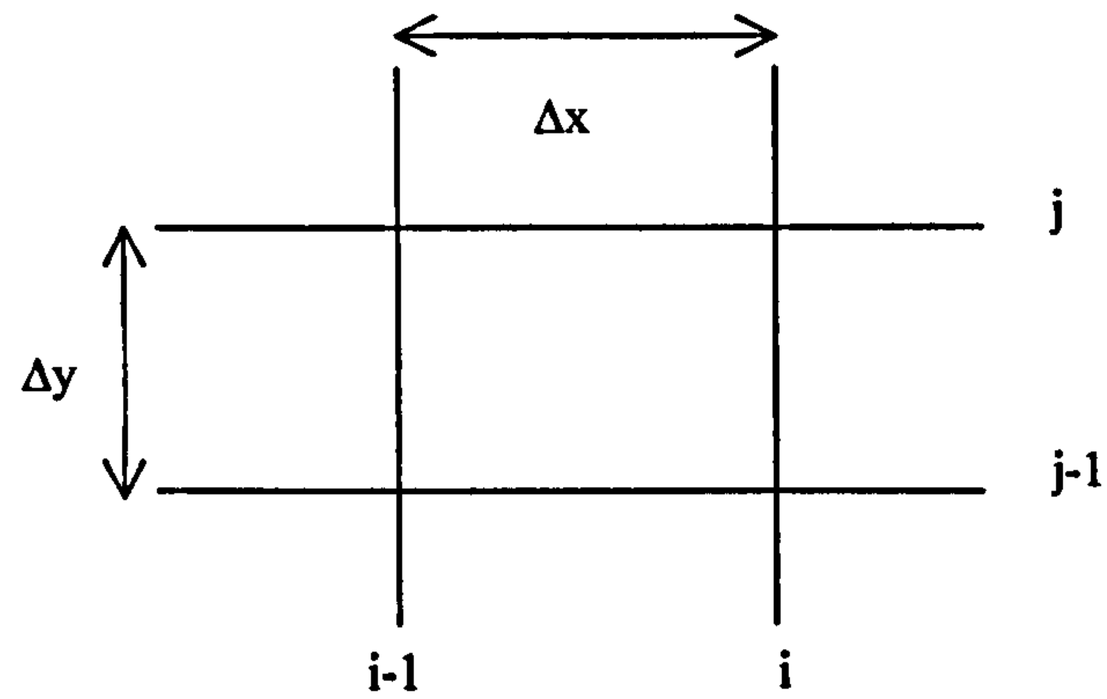

Figure (5.1) Two-dimensional finite difference grid

The Taylor series expansions of (x-Δx,y) and (x,y-Δy) about f(x,y) are given as equations (5.3) and (5.4), in which x=i and y=j:

$$f(x-\Delta x,y) = f(x,y) - f'(x)\frac{\Delta x}{1!} + f''(x)\frac{\Delta x^2}{2!} - f'''(x)\frac{\Delta x^3}{3!} \tag{5.3}$$

$$f(x,y-\Delta y) = f(x,y) - f'(y)\frac{\Delta y}{1!} + f''(y)\frac{\Delta y^2}{2!} - f'''(y)\frac{\Delta y^3}{3!} \tag{5.4}$$

The variables in equations (5.3) and (5.4) are defined as:

$$f(x,y) = C_{i,j}^n \qquad f(x,y-\Delta y) = C_{i,j-1}^n \tag{5.5}$$

$$f(x-\Delta x,y) = C_{i-1,j}^n \qquad f'(y) = \left(\frac{\partial C}{\partial y}\right)_{i,j}^n$$

$$f'(x) = \left(\frac{\partial C}{\partial x}\right)_{i,j}^n$$

$$f''(x)=\left(\frac{\partial^2 C}{\partial x^2}\right)^n_{i,j} \qquad f''(y)=\left(\frac{\partial^2 C}{\partial y^2}\right)^n_{i,j}$$

$$f'''(x)=\left(\frac{\partial^3 C}{\partial x^3}\right)^n_{i,j} \qquad f'''(y)=\left(\frac{\partial^3 C}{\partial y^3}\right)^n_{i,j}$$

Substitution of the variables defined as equation (5.5) into equations (5.3) and (5.4) gives:

$$C^n_{i-1,j}=C^n_{i,j}-\left(\frac{\partial C}{\partial x}\right)^n_{i,j}\frac{\Delta x}{1!}+\left(\frac{\partial^2 C}{\partial x^2}\right)^n_{i,j}\frac{\Delta x^2}{2!}-\left(\frac{\partial^3 C}{\partial x^3}\right)^n_{i,j}\frac{\Delta x^3}{3!}+H.O.T \tag{5.6}$$

$$C^n_{i,j-1}=C^n_{i,j}-\left(\frac{\partial C}{\partial y}\right)^n_{i,j}\frac{\Delta y}{1!}+\left(\frac{\partial^2 C}{\partial y^2}\right)^n_{i,j}\frac{\Delta y^2}{2!}-\left(\frac{\partial^3 C}{\partial y^3}\right)^n_{i,j}\frac{\Delta y^3}{3!}+H.O.T \tag{5.7}$$

in which *H.O.T.* indicates higher order terms which have been neglected. These equations can be rearranged and simplified to produce:

$$\left(\frac{\partial C}{\partial x}\right)^n_{i,j}=\frac{C^n_{i,j}-C^n_{i-1,j}}{\Delta x}+\left(\frac{\partial^2 C}{\partial x^2}\right)^n_{i,j}\frac{\Delta x}{2!}-\left(\frac{\partial^3 C}{\partial x^3}\right)^n_{i,j}\frac{\Delta x^2}{3!} \tag{5.8}$$

$$\left(\frac{\partial C}{\partial y}\right)^n_{i,j}=\frac{C^n_{i,j}-C^n_{i,j-1}}{\Delta y}+\left(\frac{\partial^2 C}{\partial y^2}\right)^n_{i,j}\frac{\Delta y}{2!}-\left(\frac{\partial^3 C}{\partial y^3}\right)^n_{i,j}\frac{\Delta y^2}{3!} \tag{5.9}$$

By neglecting all terms greater than first order accuracy, the first order approximations are obtained:

$$\left(\frac{\partial C}{\partial x}\right)^n_{i,j}=\frac{C^n_{i,j}-C^n_{i-1,j}}{\Delta x} \tag{5.10}$$

$$\left(\frac{\partial C}{\partial y}\right)^n_{i,j} = \frac{C^n_{i,j} - C^n_{i,j-1}}{\Delta y} \tag{5.11}$$

Substituting equations (5.10) and (5.11) into the original equation (5.2):

$$\frac{\partial C}{\partial t} = -u\left(\frac{C^n_{i,j} - C^n_{i-1,j}}{\Delta x}\right) - v\left(\frac{C^n_{i,j} - C^n_{i,j-1}}{\Delta y}\right) \tag{5.12}$$

Using forward in time discretisation of the local rate of change:

$$\frac{C^{n+1}_{i,j} - C^n_{i,j}}{\Delta t} = -u\left(\frac{C^n_{i,j} - C^n_{i-1,j}}{\Delta x}\right) - v\left(\frac{C^n_{i,j} - C^n_{i,j-1}}{\Delta y}\right) \tag{5.13}$$

and rewriting the equation in terms of the required concentration at the next time step gives:

$$C^{n+1}_{i,j} = C^n_{i,j} - \frac{u\Delta t}{\Delta x}\left(C^n_{i,j} - C^n_{i-1,j}\right) - \frac{v\Delta t}{\Delta y}\left(C^n_{i,j} - C^n_{i,j-1}\right) \tag{5.14}$$

which can be reduced to:

$$C^{n+1}_{i,j} = C^n_{i,j} - Cr_x\left(C^n_{i,j} - C^n_{i-1,j}\right) - Cr_y\left(C^n_{i,j} - C^n_{i,j-1}\right) \tag{5.15}$$

where Cr_x and Cr_y are the Courant numbers in the x and y-directions respectively.

Equation (5.15) is the direct extension of the one-dimensional upwinding equation.

5.1.2 Extension of the QUICKEST scheme to two-dimensions

In one-dimension, QUICKEST is a simple equation to derive using third order Taylor series expansions to solve the advection equation. The difficulty in extension to two-dimensions arises when considering the cross derivatives associated with the two-

dimensional advection equation. The cross derivative terms arise from the need to use fully two-dimensional Taylor series expansions, in which, x-y spatial derivatives appear. Specifically these terms are:

$$\frac{\partial^2 C}{\partial x \partial y}$$

$$\frac{\partial^3 C}{\partial x^2 \partial y}$$

$$\frac{\partial^3 C}{\partial x \partial y^2}$$

It has been observed that two-dimensional QUICKEST is inherently unstable when derived by direct extension from the one-dimensional form of Leonard's[5] equation.[6-8] It is only stable if all of the Taylor expansions are included in the derivation. Davies and Moore[9], applied this basic two-dimensional QUICKEST equation neglecting the cross derivatives and found that the temporal accuracy was reduced. However, they used very small time steps of 0.05s and so the omission of these terms have a negligible effect on the stability of the numerical results.

Vested *et al*[4], Ekebjærg and Justesen[10] and Leonard and Niknafs[11], all advocate derivation of this equation using all the Taylor series expansions. Although this greatly increases the complexity of the equation it also improves the numerical accuracy. The full two-dimensional derivation of QUICKEST has been carried out here.

Refer to equation (5.1) which represents the pure advection equation in two-dimensions. Consider the Taylor expansions of the differential terms about the location (i,j) at the current time step.

Equation (5.16) represents the Taylor series expansion in time which is used to determine the finite difference representation of the local rate of change:

$$C_{i,j}^{n+1} = C_{i,j}^{n} + \left(\frac{\partial C}{\partial t}\right)_{i,j}^{n} \frac{\Delta t}{1!} + \left(\frac{\partial^2 C}{\partial t^2}\right)_{i,j}^{n} \frac{\Delta t^2}{2!} + \left(\frac{\partial^3 C}{\partial t^3}\right)_{i,j}^{n} \frac{\Delta t^3}{3!} + H.O.T \tag{5.16}$$

This can be manipulated to give a representation of the differential term:

$$\left(\frac{\partial C}{\partial t}\right)_{i,j}^{n} = \frac{C_{i,j}^{n+1} - C_{i,j}^{n}}{\Delta t} - \left(\frac{\partial^2 C}{\partial t^2}\right)_{i,j}^{n} \frac{\Delta t}{2!} - \left(\frac{\partial^3 C}{\partial t^3}\right)_{i,j}^{n} \frac{\Delta t^2}{3!} + H.O.T \tag{5.17}$$

The spatial derivatives are of second order and so require backward and backward Taylor expansions. In the x-direction the expansions are as given by equations (5.18) and (5.19):

$$C_{i-1,j}^{n} = C_{i,j}^{n} - \left(\frac{\partial C}{\partial x}\right)_{i,j}^{n} \frac{\Delta x}{1!} + \left(\frac{\partial^2 C}{\partial x^2}\right)_{i,j}^{n} \frac{\Delta x^2}{2!} - \left(\frac{\partial^3 C}{\partial x^3}\right)_{i,j}^{n} \frac{\Delta x^3}{3!} + H.O.T \tag{5.18}$$

$$C_{i+1,j}^{n} = C_{i,j}^{n} + \left(\frac{\partial C}{\partial x}\right)_{i,j}^{n} \frac{\Delta x}{1!} + \left(\frac{\partial^2 C}{\partial x^2}\right)_{i,j}^{n} \frac{\Delta x^2}{2!} + \left(\frac{\partial^3 C}{\partial x^3}\right)_{i,j}^{n} \frac{\Delta x^3}{3!} + H.O.T \tag{5.19}$$

Subtraction of equation (5.18) from (5.19) gives:

$$C_{i+1,j}^{n} - C_{i-1,j}^{n} = 2\left(\frac{\partial C}{\partial x}\right)_{i,j}^{n} \frac{\Delta x}{1!} + 2\left(\frac{\partial^3 C}{\partial x^3}\right)_{i,j}^{n} \frac{\Delta x 3}{3!} \tag{5.20}$$

Rewritten in terms of the first spatial derivative:

$$\left(\frac{\partial C}{\partial x}\right)_{i,j}^{n} = \frac{C_{i+1,j}^{n} - C_{i-1,j}^{n}}{2\Delta x} - \left(\frac{\partial^3 C}{\partial x^3}\right)_{i,j}^{n} \frac{\Delta x^2}{3!} \tag{5.21}$$

Similarly the representation in the y-direction is written as:

$$\left(\frac{\partial C}{\partial y}\right)_{i,j}^{n} = \frac{C_{i,j+1}^{n} - C_{i,j-1}^{n}}{2\Delta y} - \left(\frac{\partial^3 C}{\partial y^3}\right)_{i,j}^{n} \frac{\Delta y^2}{3!} \tag{5.22}$$

Substitution of equations (5.17), (5.21) and (5.22) into the two-dimensional advection equation, (5.1), gives:

$$\left[\frac{C_{i,j}^{n+1} - C_{i,j}^{n}}{\Delta t} - \left(\frac{\partial^2 C}{\partial t^2}\right)_{i,j}^{n} \frac{\Delta t}{2!} - \left(\frac{\partial^3 C}{\partial t^3}\right)_{i,j}^{n} \frac{\Delta t^2}{3!}\right] + u\left[\frac{C_{i+1,j}^{n} - C_{i-1,j}^{n}}{2\Delta x} - \left(\frac{\partial^3 C}{\partial x^3}\right)_{i,j}^{n} \frac{\Delta x^2}{3!} - H.O.T\right] + v\left[\frac{C_{i,j+1}^{n} - C_{i,j-1}^{n}}{2\Delta y} - \left(\frac{\partial^3 C}{\partial y^3}\right)_{i,j}^{n} \frac{\Delta y^2}{3!} - H.O.T\right] = 0 \tag{5.23}$$

The full third order expansion representation of the two-dimensional advection equation can therefore be written as:[10, 12]

$$\frac{C_{i,j}^{n+1} - C_{i,j}^{n}}{\Delta t} + u\frac{C_{i+1,j}^{n} - C_{i-1,j}^{n}}{2\Delta x} + v\frac{C_{i,j+1}^{n} - C_{i,j-1}^{n}}{2\Delta y} = \left(\frac{\partial^2 C}{\partial t^2}\right)_{i,j}^{n} \frac{\Delta t}{2!} + \left(\frac{\partial^3 C}{\partial t^3}\right)_{i,j}^{n} \frac{\Delta t^2}{3!} + u\left(\frac{\partial^3 C}{\partial x^3}\right)_{i,j}^{n} \frac{\Delta x^2}{3!} + v\left(\frac{\partial^3 C}{\partial y^3}\right)_{i,j}^{n} \frac{\Delta y^2}{3!} \tag{5.24}$$

All spatial derivatives of greater than third order accuracy are neglected and the temporal derivatives are converted to spatial. The transformation from temporal to spatial derivatives is straightforward.

Consider the first order temporal derivative which can be written as equation (5.25):

$$\frac{\partial C}{\partial t} = -u\frac{\partial C}{\partial x} - v\frac{\partial C}{\partial y} \tag{5.25}$$

The second order derivative is automatically:

$$\frac{\partial^2 C}{\partial t^2} = \left(\frac{\partial C}{\partial t}\right) \times \left(\frac{\partial C}{\partial t}\right) = \left(-u\frac{\partial C}{\partial x} - v\frac{\partial C}{\partial y}\right) \times \left(\frac{\partial C}{\partial t}\right) \tag{5.26}$$

which expands to:

$$\frac{\partial^2 C}{\partial t^2} = -u\frac{\partial C}{\partial x}\left(\frac{\partial C}{\partial t}\right) - v\frac{\partial C}{\partial y} \times \left(\frac{\partial C}{\partial t}\right)$$

and then simplifies to:

$$\frac{\partial^2 C}{\partial t^2} = -u\frac{\partial^2 C}{\partial x \partial t} - v\frac{\partial^2 C}{\partial y \partial t} \tag{5.27}$$

To continue the derivation the spatial-temporal derivatives must also be defined.

Consider the terms in the x-direction:

$$\frac{\partial^2 C}{\partial x \partial t} = \frac{\partial}{\partial x} \times \left(\frac{\partial C}{\partial t}\right)$$

$$\frac{\partial^2 C}{\partial x \partial t} = \left(-u\frac{\partial C}{\partial x} - v\frac{\partial C}{\partial y}\right) \times \left(\frac{\partial}{\partial x}\right)$$

$$\frac{\partial^2 C}{\partial x \partial t} = -u\frac{\partial^2 C}{\partial x^2} - v\frac{\partial^2 C}{\partial x \partial y} \tag{5.28}$$

The y-direction derivatives are obtained in an identical manner:

$$\frac{\partial^2 C}{\partial y \partial t} = -u\frac{\partial^2 C}{\partial x \partial y} - v\frac{\partial^2 C}{\partial y^2} \tag{5.29}$$

Substitution of equations (5.28) and (5.29) into equation (5.27) gives:

$$\frac{\partial^2 C}{\partial t^2} = -u\left(-u\frac{\partial^2 C}{\partial x^2} - v\frac{\partial^2 C}{\partial x \partial y}\right) - v\left(-u\frac{\partial^2 C}{\partial x \partial y} - v\frac{\partial^2 C}{\partial y^2}\right) \tag{5.30}$$

Equation (5.30) is more conveniently written as:

$$\frac{\partial^2 C}{\partial t^2} = u^2\frac{\partial^2 C}{\partial x^2} + 2uv\frac{\partial^2 C}{\partial x \partial y} + v^2\frac{\partial^2 C}{\partial y^2} \tag{5.31}$$

The third order temporal derivatives are calculated in the same manner:

$$\frac{\partial^3 C}{\partial t^3} = \left(\frac{\partial C}{\partial t}\right) \times \left(\frac{\partial^2}{\partial t^2}\right)$$

$$\frac{\partial^3 C}{\partial t^3} = \left(-u\frac{\partial C}{\partial x} - v\frac{\partial C}{\partial y}\right) \times \left(\frac{\partial^2}{\partial t^2}\right)$$

$$\frac{\partial^3 C}{\partial t^3} = -u\frac{\partial C}{\partial x}\left(\frac{\partial^2}{\partial t^2}\right) - v\frac{\partial C}{\partial y}\left(\frac{\partial^2}{\partial t^2}\right)$$

$$\frac{\partial^3 C}{\partial t^3} = -u\frac{\partial^3 C}{\partial x \partial t^2} - v\frac{\partial^3 C}{\partial y \partial t^2} \tag{5.32}$$

Using equation (5.31):

$$\frac{\partial^3 C}{\partial x \partial t^2} = \frac{\partial}{\partial x}\left(u^2\frac{\partial^2 C}{\partial x^2} + 2uv\frac{\partial^2 C}{\partial x \partial y} + v^2\frac{\partial^2 C}{\partial y^2}\right) \tag{5.33}$$

$$\frac{\partial^3 C}{\partial x \partial t^2} = u^2\frac{\partial^3 C}{\partial x^3} + 2uv\frac{\partial^3 C}{\partial x^2 \partial y} + v^2\frac{\partial^3 C}{\partial x \partial y^2} \tag{5.34}$$

Correspondingly for the y-direction:

$$\frac{\partial^3 C}{\partial y \partial t^2} = u^2 \frac{\partial^3 C}{\partial x^2 \partial y} + 2uv \frac{\partial^3 C}{\partial x \partial y^2} + v^2 \frac{\partial^3 C}{\partial y^3} \tag{5.35}$$

Substitution of equations (5.34) and (5.35) into (5.32) leads to:

$$\frac{\partial^3 C}{\partial t^3} = -u\left(u^2 \frac{\partial^3 C}{\partial x^3} + 2uv \frac{\partial^3 C}{\partial x^2 \partial y} + v^2 \frac{\partial^3 C}{\partial x \partial y^2}\right) - v\left(u^2 \frac{\partial^3 C}{\partial x^2 \partial y} + 2uv \frac{\partial^3 C}{\partial x \partial y^2} + v^2 \frac{\partial^3 C}{\partial y^3}\right)$$

which simplifies to:

$$\frac{\partial^3 C}{\partial t^3} = -u^3 \frac{\partial^3 C}{\partial x^3} - 3u^2 v \frac{\partial^3 C}{\partial x^2 \partial y} - 3uv^2 \frac{\partial^3 C}{\partial x \partial y^2} - v^3 \frac{\partial^3 C}{\partial y^3} \tag{5.36}$$

Using these spatial representations of the temporal derivatives, equations (5.31) and (5.36), and substituting them into equation (5.24) gives the fully derived two-dimensional finite difference advection equation (5.37):

$$\begin{aligned}\frac{C_{i,j}^{n+1} - C_{i,j}^{n}}{\Delta t} = &\left(u^2 \frac{\partial^2 C}{\partial x^2} + 2uv \frac{\partial^2 C}{\partial x \partial y} v^2 \frac{\partial^2 C}{\partial y^2}\right)_{i,j}^{n} \frac{\Delta t}{2!} \\ &+\left(-u^3 \frac{\partial^3 C}{\partial x^3} - 3u^2 v \frac{\partial^3 C}{\partial x^2 \partial y} - 3uv^2 \frac{\partial^3 C}{\partial x \partial y^2} - v^3 \frac{\partial^3 C}{\partial y^3}\right)_{i,j}^{n} \frac{\Delta t^2}{3!} \\ &+u\left(\frac{\partial^3 C}{\partial x^3}\right)_{i,j}^{n} \frac{\Delta x^2}{3!} + v\left(\frac{\partial^3 C}{\partial y^3}\right)_{i,j}^{n} \frac{\Delta y^2}{3!} \\ &-u\frac{C_{i+1,j}^{n} - C_{i-1,j}^{n}}{2\Delta x} - v\frac{C_{i,j+1}^{n} - C_{i,j-1}^{n}}{2\Delta y} + H.O.T\end{aligned} \tag{5.37}$$

In order to solve equation (5.37) the spatial derivatives must be discretised and expressed as points on a finite difference grid. Taylor series expansions are again used for this purpose.

Discretised Forms of the Spatial Derivatives

$$\frac{\partial C}{\partial x} = \frac{C^n_{i+1,j} + C^n_{i-1,j}}{2\Delta x} \tag{5.38}$$

$$\frac{\partial C}{\partial y} = \frac{C^n_{i,j+1} + C^n_{i,j-1}}{2\Delta y} \tag{5.39}$$

$$\frac{\partial^2 C}{\partial x^2} = \frac{C^n_{i+1,j} - 2C^n_{i,j} + C^n_{i-1,j}}{\Delta x^2} \tag{5.40}$$

$$\frac{\partial^2 C}{\partial x \partial y} = \frac{C^n_{i,j} + C^n_{i-1,j} - C^n_{i,j-1} - C^n_{i-1,j-1}}{\Delta x \Delta y} \tag{5.41}$$

$$\frac{\partial^2 C}{\partial y^2} = \frac{C^n_{i,j+1} - 2C^n_{i,j} + C^n_{i,j-1}}{\Delta y^2} \tag{5.42}$$

$$\frac{\partial^3 C}{\partial x^3} = \frac{C^n_{i+1,j} - 3C^n_{i,j} + 3C^n_{i-1,j} - C^n_{i-2,j}}{\Delta x^3} \tag{5.43}$$

$$\frac{\partial^3 C}{\partial y^3} = \frac{C^n_{i,j+1} - 3C^n_{i,j} + 3C^n_{i,j-1} - C^n_{i,j-2}}{\Delta y^3} \tag{5.44}$$

$$\frac{\partial^3 C}{\partial x^2 \partial y} = \frac{\left(C^n_{i+1,j} - 2C^n_{i,j} + C^n_{i-1,j}\right) - \left(C^n_{i+1,j-1} - C^n_{i,j-1} + C^n_{i-1,j-1}\right)}{\Delta x^2 \Delta y} \tag{5.45}$$

$$\frac{\partial^3 C}{\partial x \partial y^2} = \frac{\left(C^n_{i,j+1} - 2C^n_{i,j} + C^n_{i,j-1}\right) - \left(C^n_{i-1,j+1} - C^n_{i-1,j} + C^n_{i-1,j-1}\right)}{\Delta x \Delta y^2} \tag{5.46}$$

Substitution of equations (5.40) to (5.46) into equation (5.37) gives the fully discretised form of the two-dimensional advection equation:

$$\frac{\partial C}{\partial t} = \frac{\Delta t}{2}\left[u^2\left(\frac{C^n_{i+1,j} - 2C^n_{i,j} + C^n_{i-1,j}}{\Delta x^2}\right) + 2uv\left(\frac{C^n_{i,j} + C^n_{i-1,j} - C^n_{i,j-1} - C^n_{i-1,j-1}}{\Delta x \Delta y}\right) + v^2\left(\frac{C^n_{i,j+1} - 2C^n_{i,j} + C^n_{i,j-1}}{\Delta y^2}\right)\right]$$

$$+\frac{\Delta t^2}{3!}\left[\begin{array}{l} -u^3\left(\dfrac{C^n_{i+1,j} - 3C^n_{i,j} + 3C^n_{i-1,j} - C^n_{i-2,j}}{\Delta x^3}\right) \\ -3u^2v\left(\dfrac{\left(C^n_{i+1,j} - 2C^n_{i,j} + C^n_{i-1,j}\right) - \left(C^n_{i+1,j-1} - C^n_{i,j-1} + C^n_{i-1,j-1}\right)}{\Delta x^2 \Delta y}\right) \\ -3uv^2\left(\dfrac{\left(C^n_{i,j+1} - 2C^n_{i,j} + C^n_{i,j-1}\right) - \left(C^n_{i-1,j+1} - C^n_{i-1,j} + C^n_{i-1,j-1}\right)}{\Delta x \Delta y^2}\right) \\ -v^3\left(\dfrac{C^n_{i,j+1} - 3C^n_{i,j} + 3C^n_{i,j-1} - C^n_{i,j-2}}{\Delta y^3}\right) \end{array}\right]$$

$$+u\frac{\Delta x^2}{3!}\left(\frac{C^n_{i+1,j} - 3C^n_{i,j} + 3C^n_{i-1,j} - C^n_{i-2,j}}{\Delta x^3}\right)$$

$$+v\frac{\Delta y^2}{3!}\left(\frac{C^n_{i,j+1} - 3C^n_{i,j} + 3C^n_{i,j-1} - C^n_{i,j-2}}{\Delta y^3}\right)$$

$$-u\left(\frac{C^n_{i+1,j} + C^n_{i-1,j}}{2\Delta x}\right) - v\left(\frac{C^n_{i,j+1} + C^n_{i,j-1}}{2\Delta y}\right) \tag{5.47}$$

This is simplified such that it can be more easily included into computer code. The format is changed so that an equation is applied to the four faces of a two-dimensional control volume, as shown in Figure (5.2). These are the forward and backward x and y directional faces, for positive u and v flow. Note that these equations are sensitive to the direction of flow.

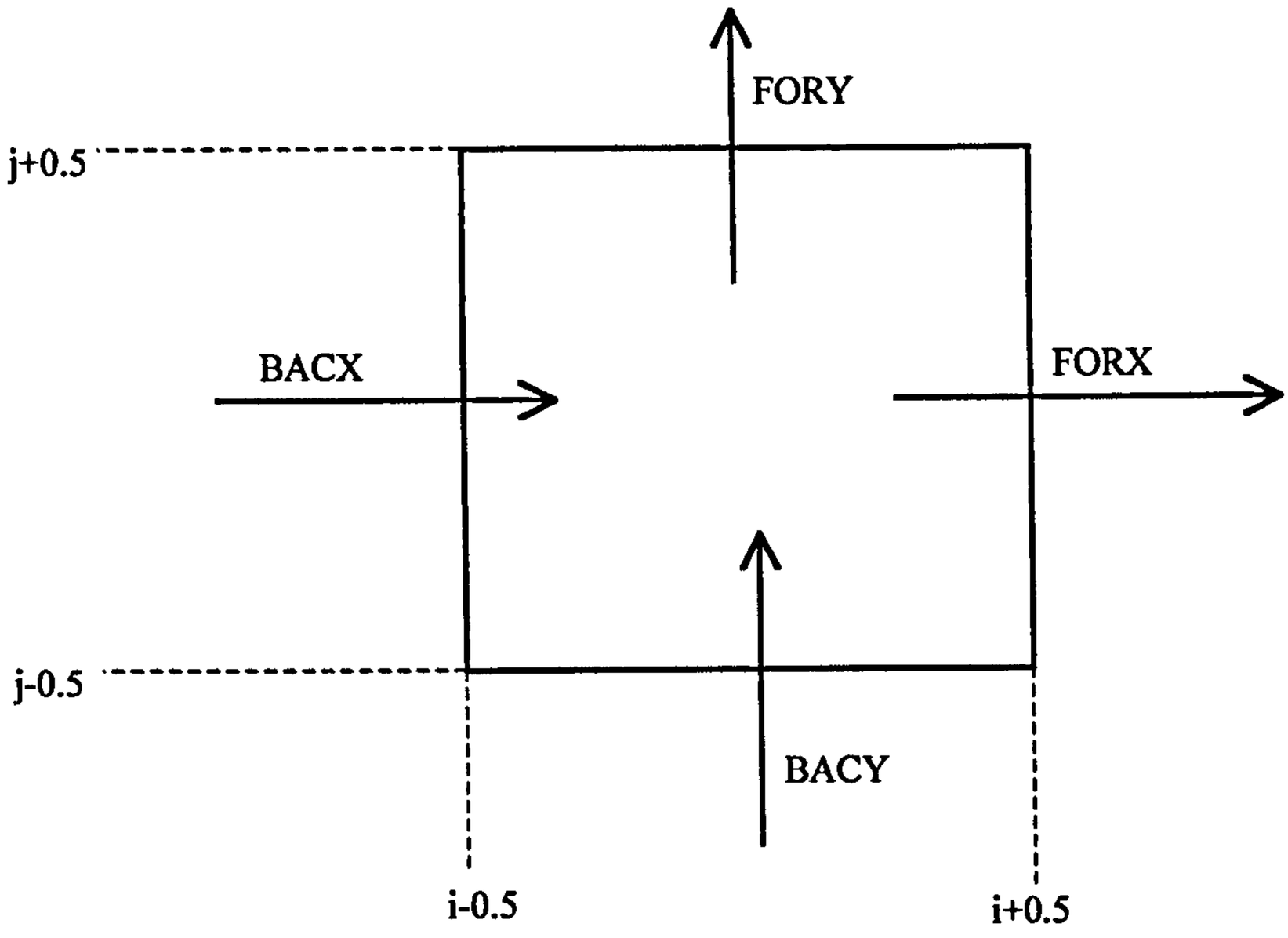

Figure (5.2) Diagram showing the four faces of a control volume

The equations become:

$$FORX = \left(\frac{C^n_{i+1,j}+C^n_{i,j}}{2}\right)-\left(\frac{C^n_{i+1,j}-2C^n_{i,j}+C^n_{i-1,j}}{6}\right)-Cr_x\left(\frac{C^n_{i+1,j}-C^n_{i,j}}{2}\right)$$
$$-Cr_y\left(\frac{C^n_{i,j}-C^n_{i,j-1}}{2}\right)-Cr_y\left(\frac{C^n_{i+1,j}-C^n_{i+1,j-1}-C^n_{i,j}+C^n_{i,j-1}}{4}\right)$$
$$-Cr_y\left(\frac{C^n_{i,j+1}-2C^n_{i,j}+C^n_{i,j-1}}{4}\right)+Cr_xCr_y\left(\frac{C^n_{i+1,j}-C^n_{i+1,j-1}-C^n_{i,j}+C^n_{i,j-1}}{3}\right)$$
$$+Cr_x^2\left(\frac{C^n_{i+1,j}-2C^n_{i,j}+C^n_{i-1,j}}{6}\right)+Cr_y^2\left(\frac{C^n_{i,j+1}-2C^n_{i,j}+C^n_{i,j-1}}{6}\right)$$

$$BACX = \left(\frac{C^n_{i,j}+C^n_{i-1,j}}{2}\right)-\left(\frac{C^n_{i,j}-2C^n_{i-1,j}+C^n_{i-2,j}}{6}\right)-Cr_x\left(\frac{C^n_{i,j}-C^n_{i-1,j}}{2}\right)$$
$$-Cr_y\left(\frac{C^n_{i-1,j}-C^n_{i-1,j-1}}{2}\right)-Cr_y\left(\frac{C^n_{i,j}-C^n_{i,j-1}-C^n_{i-1,j}+C^n_{i-1,j-1}}{4}\right)$$
$$-Cr_y\left(\frac{C^n_{i-1,j+1}-2C^n_{i-1,j}+C^n_{i-1,j-1}}{4}\right)+Cr_xCr_y\left(\frac{C^n_{i,j}-C^n_{i,j-1}-C^n_{i-1,j}+C^n_{i-1,j-1}}{3}\right)$$
$$+Cr_x^2\left(\frac{C^n_{i,j}-2C^n_{i-1,j}+C^n_{i-2,j}}{6}\right)+Cr_y^2\left(\frac{C^n_{i-1,j+1}-2C^n_{i-1,j}+C^n_{i-1,j-1}}{6}\right)$$

$$FORY = \left(\frac{C^n_{i,j+1}+C^n_{i,j}}{2}\right)-\left(\frac{C^n_{i,j+1}-2C^n_{i,j}+C^n_{i,j-1}}{6}\right)-Cr_x\left(\frac{C^n_{i,j}-C^n_{i-1,j}}{2}\right)$$
$$-Cr_y\left(\frac{C^n_{i,j+1}-C^n_{i,j}}{2}\right)-Cr_x\left(\frac{C^n_{i,j+1}-C^n_{i-1,j+1}-C^n_{i,j}+C^n_{i-1,j}}{4}\right)$$
$$-Cr_x\left(\frac{C^n_{i+1,j}-2C^n_{i,j}+C^n_{i-1,j}}{4}\right)+Cr_xCr_y\left(\frac{C^n_{i,j+1}-C^n_{i-1,j+1}-C^n_{i,j}+C^n_{i-1,j}}{3}\right)$$
$$+Cr_x^2\left(\frac{C^n_{i+1,j}-2C^n_{i,j}+C^n_{i-1,j}}{6}\right)+Cr_y^2\left(\frac{C^n_{i,j+1}-2C^n_{i,j}+C^n_{i,j-1}}{6}\right)$$

$$BACY = \left(\frac{C^n_{i,j}+C^n_{i,j-1}}{2}\right)-\left(\frac{C^n_{i,j}-2C^n_{i,j-1}+C^n_{i,j-2}}{6}\right)-Cr_x\left(\frac{C^n_{i,j-1}-C^n_{i-1,j-1}}{2}\right)$$
$$-Cr_y\left(\frac{C^n_{i,j}-C^n_{i,j-1}}{2}\right)-Cr_x\left(\frac{C^n_{i,j}-C^n_{i-1,j}-C^n_{i,j-1}+C^n_{i-1,j-1}}{4}\right)$$
$$-Cr_x\left(\frac{C^n_{i+1,j-1}-2C^n_{i,j}+C^n_{i-1,j-1}}{4}\right)+Cr_xCr_y\left(\frac{C^n_{i,j}-C^n_{i-1,j}-C^n_{i,j-1}+C^n_{i-1,j-1}}{3}\right)$$
$$+Cr_x^2\left(\frac{C^n_{i+1,j-1}-2C^n_{i,j}+C^n_{i-1,j-1}}{6}\right)+Cr_y^2\left(\frac{C^n_{i,j}-2C^n_{i,j-1}+C^n_{i,j-2}}{6}\right)$$

In simple terms this is referred to as:

$$\frac{\partial C}{\partial t} = Cr_x[FORX - BACX]+Cr_y[FORY - BACY]$$

5.1.3 Extension of the eight point method of characteristics schemes to two-dimensions

The extension of this eight point scheme to two-dimensions requires the solution of the double-cubic equation represented by equation (5.48):

$$y = a\alpha^3 + b\alpha^2 + c\alpha + d + e\beta^3 + f\beta^2 + g\beta + h\alpha^2\beta + i\alpha\beta^2 + j\alpha\beta \tag{5.48}$$

where α and β are defined as:

$$\alpha = \frac{x_{i,j} - \xi_x}{x_{i,j} - x_{i-1,j}}$$

$$\beta = \frac{x_{i,j} - \xi_y}{x_{i,j} - x_{i,j-1}}$$

which are equivalent to the Courant numbers in the x and y-directions respectively. The terms, ξ_x and ξ_y, represent the locations at which the characteristic line intersects the x and y spatial planes.

The derivation of the scheme is highly similar to the one-dimensional method, although it is more complicated.[13] The resulting method uses 64 points which does make the scheme computationally cumbersome, however it is also shown to be remarkably accurate. The full derivation of the two-dimensional 8 point method of characteristics is included here.

The identities:

$$\alpha = -x \tag{5.49}$$
$$\beta = -y$$

are used to develop a representation of equation (5.48). This facilitates the mathematical manipulation required to obtain the relevant equations of the spatial derivatives in the x and y-directions:

$$y(x,y) = -ax^3 + bx^2 - cx + d - ey^3 + fy^2 - gy - hx^2y - ixy^2 + jxy \qquad (5.50)$$

The x directional spatial derivative is calculated to be:

$$y'_x(x,y) = -3ax^2 + 2bx - c - 2hxy - iy^2 + jy \qquad (5.51)$$

and correspondingly the y derivative is given as:

$$y'_y(x,y) = -3ey^2 + 2fy - g - hx^2 - 2ixy + jx \qquad (5.52)$$

These are easily rewritten in terms of α and β, as equations (5.53) and (5.54):

$$y'_\alpha(\alpha,\beta) = -3a\alpha^2 - 2b\alpha - c - 2h\alpha\beta - i\beta^2 - j\beta \qquad (5.53)$$

$$y'_\beta(\alpha,y)\beta = -3e\beta^2 - 2f\beta - g - h\alpha^2 - 2i\alpha\beta - j\alpha \qquad (5.54)$$

Using the boundary conditions specified as equation (5.55), equations (5.48), (5.53) and (5.54) can be solved using a system of simultaneous equations. This is identical to the procedure followed in the one-dimensional case.

$$\begin{aligned} Y(0,0) &= C^n_{i,j} \quad Y'_x(0,0) = CX^n_{i,j} \quad Y'_y(0,0) = CY^n_{i,j} \\ Y(1,0) &= C^n_{i-1,j} \quad Y'_x(1,0) = CX^n_{i-1,j} \quad Y'_y(1,0) = CY^n_{i-1,j} \\ Y(0,1) &= C^n_{i,j-1} \quad Y'_x(0,1) = CX^n_{i,j-1} \quad Y'_y(0,1) = CY^n_{i,j-1} \\ Y(1,1) &= C^n_{i-1,j-1} \quad Y'_x(1,1) = CX^n_{i-1,j-1} \quad Y'_y(1,1) = CY^n_{i-1,j-1} \end{aligned} \qquad (5.55)$$

The variables in the two-dimensional polynomial can be easily identified as:

$$a = 2C^n_{i,j} - 2C^n_{i-1,j} - \Delta x CX^n_{i,j} - \Delta x CX^n_{i-1,j} \tag{5.56}$$

$$b = -3C^n_{i,j} + 3C^n_{i-1,j} + 2\Delta x CX^n_{i,j} + 2\Delta x CX^n_{i-1,j}$$

$$c = -\Delta x CX^n_{i,j}$$

$$d = C^n_{i,j}$$

$$e = 2C^n_{i,j} - 2C^n_{i,j-1} - \Delta y CY^n_{i,j} - \Delta y CY^n_{i,j-1}$$

$$f = -3C^n_{i,j} + 3C^n_{i,j-1} + 2\Delta y CY^n_{i,j} + \Delta y CY^n_{i,j-1}$$

$$g = -\Delta y CY^n_{i,j}$$

$$h = -C^n_{i,j} + C^n_{i-1,j} + C^n_{i,j-1} - C^n_{i-1,j-1} + \Delta x CX^n_{i-1,j} - \Delta x CX^n_{i-1,j-1}$$

$$i = -C^n_{i,j} + C^n_{i-1,j} + C^n_{i,j-1} - C^n_{i-1,j-1} + \Delta y CY^n_{i,j-1} - \Delta y CY^n_{i-1,j-1}$$

$$j = 3C^n_{i,j} - 3C^n_{i-1,j} - 3C^n_{i,j-1} + 3C^n_{i-1,j-1} - \Delta x CX^n_{i-1,j} + \Delta x CX^n_{i-1,j-1} - \Delta y CY^n_{i,j-1} + \Delta y CY^n_{i-1,j-1}$$

Substitution of the terms defined as (5.56) into the original form of the equation, (5.48) gives:

$$\begin{aligned} y = {} & \left(2C^n_{i,j} - 2C^n_{i-1,j} - \Delta x CX^n_{i,j} - \Delta x CX^n_{i-1,j}\right)\alpha^3 \\ & + \left(-3C^n_{i,j} + 3C^n_{i-1,j} + 2\Delta x CX^n_{i,j} + 2\Delta x CX^n_{i-1,j}\right)\alpha^2 \\ & + \left(-\Delta x CX^n_{i,j}\right)\alpha + \left(C^n_{i,j}\right) + \left(2C^n_{i,j} - 2C^n_{i,j-1} - \Delta y CY^n_{i,j} - \Delta y CY^n_{i,j-1}\right)\beta^3 \\ & + \left(-3C^n_{i,j} + 3C^n_{i,j-1} + 2\Delta y CY^n_{i,j} + \Delta x CX^n_{i,j-1}\right)\beta^2 + \left(-\Delta y CY^n_{i,j}\right)\beta \\ & + \left(-C^n_{i,j} + C^n_{i-1,j} + C^n_{i,j-1} - C^n_{i-1,j-1} + \Delta x CX^n_{i-1,j} - \Delta x CX^n_{i-1,j-1}\right)\alpha^2\beta \\ & + \left(-C^n_{i,j} + C^n_{i-1,j} + C^n_{i,j-1} - C^n_{i-1,j-1} + \Delta y CY^n_{i,j-1} - \Delta y CY^n_{i-1,j-1}\right)\alpha\beta^2 \\ & + \begin{pmatrix} 3C^n_{i,j} - 3C^n_{i-1,j} - 3C^n_{i,j-1} + 3C^n_{i-1,j-1} - \Delta x CX^n_{i-1,j} \\ + \Delta x CX^n_{i-1,j-1} - \Delta y CY^n_{i,j-1} + \Delta y CY^n_{i-1,j-1} \end{pmatrix}\alpha\beta \end{aligned} \tag{5.57}$$

Equation (5.57) is easily rearranged by grouping terms to form:

$$
\begin{aligned}
Y(\alpha,\beta) = {} & \left(2\alpha^3 - 3\alpha^2 + 1 + 2\beta^3 - 3\beta^2 - \alpha^2\beta - \alpha\beta^2 + 3\alpha\beta\right) C^n_{i,j} \\
& + \left(-2\alpha^3 + 3\alpha^2 + \alpha^2\beta + \alpha\beta^2 - 3\alpha\beta\right) C^n_{i-1,j} \\
& + \left(-2\beta^3 + 3\beta^2 + \alpha^2\beta + \alpha\beta^2 - 3\alpha\beta\right) C^n_{i,j-1} \\
& + \left(-\alpha^2\beta - \alpha\beta^2 + 3\alpha\beta\right) C^n_{i-1,j-1} \\
& + \left(-\alpha^3 + 2\alpha^2 - \alpha\right) \Delta x CX^n_{i,j} + \left(-\beta^3 + 2\beta^2 - \beta\right) \Delta y CY^n_{i,j} \\
& + \left(-\alpha^3 + \alpha^2 + \alpha^2\beta - \alpha\beta\right) \Delta x CX^n_{i-1,j} + \left(-\beta^3 + \beta^2 + \alpha\beta^2 - \alpha\beta\right) \Delta y CY^n_{i,j-1} \\
& + \left(-\alpha^2\beta + \alpha\beta\right) \Delta x CX^n_{i-1,j-1} + \left(-\alpha\beta^2 + \alpha\beta\right) \Delta y CY^n_{i-1,j-1}
\end{aligned}
\tag{5.58}
$$

where $C_{i,j}$, $C_{i-1,j}$, $C_{i,j-1}$ and $C_{i-1,j-1}$ are the concentrations at locations (i,j), (i-1,j), (i,j-1) and (i-1,j-1). $CX_{i,j}$, $CX_{i-1,j}$, $CY_{i,j}$, $CY_{i,j-1}$, $CXY_{i-1,j-1}$ and $CXY_{i-1,j-1}$ are the corresponding spatial derivatives of concentration.

The spatial derivatives are calculated by taking Taylor series expansions about the locations (i,j), (i,j-1), (i-1,j) and (i-1,j-1) in the x and y-directions.

Examples of these expansions are included here about the location (i,j) in both directions.

Expansions about i,j in the x-direction

$$C^n_{i-3,j} = C^n_{i,j} - CX_i(3\Delta x) + \frac{1}{2!}CXX_i(3\Delta x)^2 - \frac{1}{3!}CXXX_i(3\Delta x)^3$$

$$C^n_{i-2,j} = C^n_{i,j} - CX_i(2\Delta x) + \frac{1}{2!}CXX_i(2\Delta x)^2 - \frac{1}{3!}CXXX_i(2\Delta x)^3$$

$$C^n_{i-1,j} = C^n_{i,j} - CX_i(\Delta x) + \frac{1}{2!}CXX_i(\Delta x)^2 - \frac{1}{3!}CXXX_i(\Delta x)^3$$

$$C^n_{i+1,j} = C^n_{i,j} + CX_i(\Delta x) + \frac{1}{2!}CXX_i(\Delta x)^2 + \frac{1}{3!}CXXX_i(\Delta x)^3$$

$$C^n_{i+2,j} = C^n_{i,j} + CX_i(2\Delta x) + \frac{1}{2!}CXX_i(2\Delta x)^2 + \frac{1}{3!}CXXX_i(2\Delta x)^3$$

$$C^n_{i+3,j} = C^n_{i,j} + CX_i(3\Delta x) + \frac{1}{2!}CXX_i(3\Delta x)^2 + \frac{1}{3!}CXXX_i(3\Delta x)^3$$

Expansions about i,j in the y-direction

$$C^n_{i,j-3} = C^n_{i,j} - CY_j(3\Delta y) + \frac{1}{2!}CYY_j(3\Delta y)^2 - \frac{1}{3!}CYYY_j(3\Delta y)^3$$

$$C^n_{i,j-2} = C^n_{i,j} - CY_j(2\Delta y) + \frac{1}{2!}CYY_j(2\Delta y)^2 - \frac{1}{3!}CYYY_j(2\Delta y)^3$$

$$C^n_{i,j-1} = C^n_{i,j} - CY_j(\Delta y) + \frac{1}{2!}CYY_j(\Delta y)^2 - \frac{1}{3!}CYYY_j(\Delta y)^3$$

$$C^n_{i,j+1} = C^n_{i,j} + CYY_j(\Delta y) + \frac{1}{2!}CYY_j(\Delta y)^2 + \frac{1}{3!}CYYY_j(\Delta y)^3$$

$$C^n_{i,j+2} = C^n_{i,j} + CY_j(2\Delta y) + \frac{1}{2!}CYY_j(2\Delta y)^2 + \frac{1}{3!}CYYY_j(2\Delta y)^3$$

$$C^n_{i,j+3} = C^n_{i,j} + CY_j(3\Delta y) + \frac{1}{2!}CYY_j(3\Delta y)^2 + \frac{1}{3!}CYYY_j(3\Delta y)^3$$

The relevant expansions are similarly constructed for all other locations.

As for the one-dimensional case, combinations of Taylor series are derived again using four point consecutive sequences in both directions. These values are averaged and weighting factors are employed, to give final estimates of the spatial derivatives.[16] The weighting factor used is as recommended by Komatsu *et al*[16] and is equal to 9.55.

$$CX^n_{i-1,j} = \frac{1}{2(\ell+1)}\left(CX^1_{i-1,j} + \ell CX^2_{i-1,j} + \ell CX^3_{i-1,j} + CX^4_{i-1,j}\right)$$

$$CX^n_{i,j} = \frac{1}{2(\ell+1)}\left(CX^1_{i,j} + \ell CX^2_{i,j} + \ell CX^3_{i,j} + CX^4_{i,j}\right)$$

similarly for the other spatial derivatives. This results in the definitions:

$$CX^n_{i-1,j} = -\frac{C^n_{i-4,j}}{63.3\Delta x} + \frac{3.1C^n_{i-3,j}}{21.1\Delta x} - \frac{15.73C^n_{i-2,j}}{21.1\Delta x} + \frac{15.73C^n_{i,j}}{21.1\Delta x} - \frac{3.1C^n_{i+1,j}}{21.1\Delta x} + \frac{C^n_{i+2,j}}{63.3\Delta x} \tag{5.59}$$

$$CX^n_{i,j} = -\frac{C^n_{i-3,j}}{63.3\Delta x} + \frac{3.1C^n_{i-2,j}}{21.1\Delta x} - \frac{15.73C^n_{i-1,j}}{21.1\Delta x} + \frac{15.73C^n_{i+1,j}}{21.1\Delta x} - \frac{3.1C^n_{i+2,j}}{21.1\Delta x} + \frac{C^n_{i+3,j}}{63.3\Delta x} \tag{5.60}$$

$$CX^n_{i-1,j-1} = -\frac{C^n_{i-4,j-1}}{63.3\Delta x} + \frac{3.1C^n_{i-3,j-1}}{21.1\Delta x} - \frac{15.73C^n_{i-2,j-1}}{21.1\Delta x} + \frac{15.73C^n_{i,j-1}}{21.1\Delta x} - \frac{3.1C^n_{i+1,j-1}}{21.1\Delta x} + \frac{C^n_{i+2,j-1}}{63.3\Delta x} \tag{5.61}$$

$$CY^n_{i,j-1} = -\frac{C^n_{i,j-4}}{63.3\Delta y} + \frac{3.1C^n_{i,j-3}}{21.1\Delta y} - \frac{15.73C^n_{i,j-2}}{21.1\Delta y} + \frac{15.73C^n_{i,j}}{21.1\Delta y} - \frac{3.1C^n_{i,j+1}}{21.1\Delta y} + \frac{C^n_{i,j+2}}{63.3\Delta y} \tag{5.62}$$

$$CY^n_{i,j} = -\frac{C^n_{i,j-3}}{63.3\Delta y} + \frac{3.1C^n_{i,j-2}}{21.1\Delta y} - \frac{15.73C^n_{i,j-1}}{21.1\Delta y} + \frac{15.73C^n_{i,j+1}}{21.1\Delta y} - \frac{3.1C^n_{i,j+2}}{21.1\Delta y} + \frac{C^n_{i,j+3}}{63.3\Delta y} \tag{5.63}$$

$$CY^n_{i-1,j-1} = -\frac{C^n_{i-1,j-4}}{63.3\Delta y} + \frac{3.1C^n_{i-1,j-3}}{21.1\Delta y} - \frac{15.73C^n_{i-1,j-2}}{21.1\Delta y} + \frac{15.73C^n_{i-1,j}}{21.1\Delta y} - \frac{3.1C^n_{i-1,j+1}}{21.1\Delta y} + \frac{C^n_{i-1,j+2}}{63.3\Delta y} \tag{5.64}$$

These estimated values, equations (5.59) to (5.64), are substituted into the two-dimensional interpolating polynomial, equation (5.58), resulting in:

$$
\begin{aligned}
Y(\alpha,\beta) = {} & \left(2\alpha^3 - 3\alpha^2 + 1 + 2\beta^3 - 3\beta^2 - \alpha^2\beta - \alpha\beta^2 + 3\alpha\beta\right)C_{i,j}^n \\
& + \left(-2\alpha^3 + 3\alpha^2 + \alpha^2\beta + \alpha\beta^2 - 3\alpha\beta\right)C_{i-1,j}^n \\
& + \left(-2\beta^3 + 3\beta^2 + \alpha^2\beta + \alpha\beta^2 - 3\alpha\beta\right)C_{i,j-1}^n + \left(-\alpha^2\beta - \alpha\beta^2 + 3\alpha\beta\right)C_{i-1,j-1}^n \\
& + \left(\begin{array}{l} -\dfrac{C_{i-3,j}^n}{63.3\Delta x} + \dfrac{3.1C_{i-2,j}^n}{21.1\Delta x} - \dfrac{15.73C_{i-1,j}^n}{21.1\Delta x} \\ + \dfrac{15.73C_{i+1,j}^n}{21.1\Delta x} - \dfrac{3.1C_{i+2,j}^n}{21.1\Delta x} + \dfrac{C_{i+3,j}^n}{63.3\Delta x} \end{array}\right)\left(-\alpha^3 + 2\alpha^2 - \alpha\right)\Delta x \\
& + \left(\begin{array}{l} -\dfrac{C_{i,j-3}^n}{63.3\Delta y} + \dfrac{3.1C_{i,j-2}^n}{21.1\Delta y} - \dfrac{15.73C_{i,j-1}^n}{21.1\Delta y} \\ + \dfrac{15.73C_{i,j+1}^n}{21.1\Delta y} - \dfrac{3.1C_{i,j+2}^n}{21.1\Delta y} + \dfrac{C_{i,j+3}^n}{63.3\Delta y} \end{array}\right)\left(-\beta^3 + 2\beta^2 - \beta\right)\Delta y \\
& + \left(\begin{array}{l} -\dfrac{C_{i-4,j}^n}{63.3\Delta x} + \dfrac{3.1C_{i-3,j}^n}{21.1\Delta x} - \dfrac{15.73C_{i-2,j}^n}{21.1\Delta x} \\ + \dfrac{15.73C_{i,j}^n}{21.1\Delta x} - \dfrac{3.1C_{i+1,j}^n}{21.1\Delta x} + \dfrac{C_{i+2,j}^n}{63.3\Delta x} \end{array}\right)\left(-\alpha^3 + \alpha^2 + \alpha^2\beta - \alpha\beta\right)\Delta x \\
& + \left(\begin{array}{l} -\dfrac{C_{i,j-4}^n}{63.3\Delta y} + \dfrac{3.1C_{i,j-3}^n}{21.1\Delta y} - \dfrac{15.73C_{i,j-2}^n}{21.1\Delta y} \\ + \dfrac{15.73C_{i,j}^n}{21.1\Delta y} - \dfrac{3.1C_{i,j+1}^n}{21.1\Delta y} + \dfrac{C_{i,j+2}^n}{63.3\Delta y} \end{array}\right)\left(-\beta^3 + \beta^2 + \alpha\beta^2 - \alpha\beta\right)\Delta y \\
& + \left(\begin{array}{l} -\dfrac{C_{i-4,j-1}^n}{63.3\Delta x} + \dfrac{3.1C_{i-3,j-1}^n}{21.1\Delta x} - \dfrac{15.73C_{i-2,j-1}^n}{21.1\Delta x} \\ + \dfrac{15.73C_{i,j-1}^n}{21.1\Delta x} - \dfrac{3.1C_{i+1,j-1}^n}{21.1\Delta x} + \dfrac{C_{i+2,j-1}^n}{63.3\Delta x} \end{array}\right)\left(-\alpha^2\beta + \alpha\beta\right)\Delta x \\
& + \left(\begin{array}{l} -\dfrac{C_{i-1,j-4}^n}{63.3\Delta y} + \dfrac{3.1C_{i-1,j-3}^n}{21.1\Delta y} - \dfrac{15.73C_{i-1,j-2}^n}{21.1\Delta y} \\ + \dfrac{15.73C_{i-1,j}^n}{21.1\Delta y} - \dfrac{3.1C_{i-1,j+1}^n}{21.1\Delta y} + \dfrac{C_{i-1,j+2}^n}{63.3\Delta y} \end{array}\right)\left(-\alpha\beta^2 + \alpha\beta\right)\Delta y
\end{aligned}
\tag{5.65}
$$

Equation (5.65) can be written more simply as equation (5.66):

$$y(\alpha,\beta) = f1C_{i-4,j} + f2C_{i-3,j} + f3C_{i-2,j} + f4C_{i-1,j} + f5C_{i,j} + f6C_{i+1,j} \quad (5.66)$$
$$+ f7C_{i+2,j} + f8C_{i+3,j} + f9C_{i-4,j-1} + f10C_{i-3,j-1} + f11C_{i-2,j-1}$$
$$+ f12C_{i-1,j-1} + f13C_{i+1,j-1} + f14C_{i+2,j-1} + f15C_{i-1,j-4}$$
$$+ f16C_{i-1,j-3} + f17C_{i-1,j-2} + f18C_{i-1,j+1} + f19C_{i-1,j+2}$$
$$+ f20C_{i,j-4} + f21C_{i,j-3} + f22C_{i,j-2} + f23C_{i,j-1} + f24C_{i,j+1}$$
$$+ f25C_{i,j+2} + f26C_{i,j+3}$$

in which the multiplying variables are defined as:

$$f1 = \frac{\alpha^3 - \alpha^2 - \alpha^2\beta + \alpha\beta}{63.3}$$

$$f2 = \frac{-8.3\alpha^3 + 7.3\alpha^2 + \alpha + 9.3\alpha\beta - 9.3\alpha\beta}{63.3}$$

$$f3 = \frac{12.6\alpha^3 - 9.5\alpha^2 - 3.1\alpha - 15.7\alpha\beta + 15.7\alpha\beta}{21.1}$$

$$f4 = \frac{-26.5\alpha^3 + 31.9\alpha^2 + 21.1\alpha^2\beta + 5.4\alpha\beta^2 - 47.6\alpha\beta + 15.7\alpha}{21.1}$$

$$f5 = \frac{26.5\alpha^3 - 47.6\alpha^2 + 21.1 + 26.5\beta^3 - 47.6\beta^2 - 5.4\alpha^2\beta - 5.4\alpha\beta^2 + 31.9\alpha\beta}{21.1}$$

$$f6 = \frac{-12.6\alpha^3 + 28.3\alpha^2 - 15.7\alpha - 3.1\alpha\beta + 3.1\alpha\beta}{21.1}$$

$$f7 = \frac{8.3\alpha^3 - 17.6\alpha^2 + 9.3\alpha + \alpha^2\beta - \alpha\beta}{63.3}$$

$$f8 = \frac{-\alpha^3 + 2\alpha^2 - \alpha}{63.3}$$

$$f9 = \frac{\alpha^2\beta - \alpha\beta}{63.3}$$

$$f10 = \frac{-3.1(\alpha^2\beta - \alpha\beta)}{21.1}$$

$$f11 = \frac{15.73(\alpha^2\beta - \alpha\beta)}{21.1}$$

$$f12 = -\alpha^2\beta - \alpha\beta^2 + 3\alpha\beta$$

$$f13 = \frac{3.1(\alpha^2\beta - \alpha\beta)}{21.1}$$

$$f14 = \frac{-\alpha^2\beta + \alpha\beta}{63.3}$$

$$f15 = \frac{\alpha\beta^2 - \alpha\beta}{63.3}$$

$$f16 = \frac{-3.1(\alpha\beta^2 - \alpha\beta)}{21.1}$$

$$f17 = \frac{15.73(\alpha\beta^2 - \alpha\beta)}{21.1}$$

$$f18 = \frac{3.1(\alpha\beta^2 - \alpha\beta)}{21.1}$$

$$f19 = \frac{-\alpha\beta^2 + \alpha\beta}{63.3}$$

$$f20 = \frac{\beta^3 - \beta^2 - \alpha\beta^2 + \alpha\beta}{63.3}$$

$$f21 = \frac{-8.3\beta^3 + 7.3\beta^2 + \beta + 9.3\alpha\beta^2 - 9.3\alpha\beta}{63.3}$$

$$f22 = \frac{12.6\beta^3 - 9.5\beta^2 - 3.1\beta - 15.7\alpha\beta^2 + 15.7\alpha\beta}{21.1}$$

$$f23 = \frac{-26.5\beta^3 + 31.9\beta^2 + 5.4\alpha^2\beta - 21.1\alpha\beta^2 - 47.6\alpha\beta + 15.7\beta}{21.1}$$

$$f24 = \frac{-12.6\beta^3 + 28.3\beta^2 - 15.7\beta - 3.1\alpha\beta^2 + 3.1\alpha\beta}{21.1}$$

$$f25 = \frac{8.3\beta^3 - 17.6\beta^2 + 9.3\beta + \alpha\beta^2 - \alpha\beta}{63.3}$$

$$f26 = \frac{-\beta^3 + 2\beta^2 - \beta}{63.3}$$

Note that this derivation is for positive u and v flows. A similar expansion is derived for the other three combinations of flow direction. Hence in two-dimensions this requires computation at 64 points.

This is a very complicated scheme to derive which requires a great deal of implementation time. It would be advantageous to find an alternative, more compact approach which maintains similar accuracy. To this end the six point method of characteristics scheme derived in one-dimension is also extended to two-dimensions.

5.1.4 Extension of the six point method of characteristics scheme to two-dimensions

The derivation of the six point method of characteristics is very closely based on the eight point scheme.[16] However to make the approach more compact some of the terms are removed from the equation by an averaging process which was also carried out in

one-dimension. The six point scheme utilises 36 points in two-dimensions in comparison to the 64 points required for the eight point scheme.

The concentrations at the extremities of the solution domain are estimated in terms of the values at neighbouring points. Linear extrapolation gives the approximations:

$$C^{est}_{i-4,j} = 2C^{n}_{i-3,j} - C^{n}_{i-2,j} \tag{5.67}$$

$$C^{est}_{i+3,j} = 2C^{n}_{i+2,j} - C^{n}_{i+1,j}$$

$$C^{est}_{i,j-4} = 2C^{n}_{i,j-3} - C^{n}_{i,j-2}$$

$$C^{est}_{i,j+3} = 2C^{n}_{i,j+2} - C^{n}_{i,j+1}$$

$$C^{est}_{i-4,j-1} = 2C^{n}_{i-3,j-1} - C^{n}_{i-2,j-1}$$

$$C^{est}_{i-1,j-4} = 2C^{n}_{i-1,j-3} - C^{n}_{i-1,j-2}$$

Substitution of equation (5.67) into equations (5.59) to (5.64) gives:

$$CX^{n}_{i-1,j} = \frac{14.55C^{n}_{i-3,j}}{126.6\Delta x} - \frac{15.4C^{n}_{i-2,j}}{21.1\Delta x} + \frac{15.73C^{n}_{i,j}}{21.1\Delta x} - \frac{3.1C^{n}_{i+1,j}}{21.1\Delta x} + \frac{C^{n}_{i+2,j}}{63.3\Delta x} \tag{5.68}$$

$$CX^{n}_{i,j} = -\frac{C^{n}_{i-3,j}}{63.3\Delta x} + \frac{3.1C^{n}_{i-2,j}}{21.1\Delta x} - \frac{15.73C^{n}_{i-1,j}}{21.1\Delta x} + \frac{15.73C^{n}_{i+1,j}}{21.1\Delta x} - \frac{14.55C^{n}_{i+2,j}}{126.6\Delta x} \tag{5.69}$$

$$CX^{n}_{i-1,j-1} = \frac{14.55C^{n}_{i-3,j-1}}{126.6\Delta x} - \frac{15.4C^{n}_{i-2,j-1}}{21.1\Delta x} + \frac{15.73C^{n}_{i,j-1}}{21.1\Delta x} - \frac{3.1C^{n}_{i+1,j-1}}{21.1\Delta x} + \frac{C^{n}_{i+2,j-1}}{63.3\Delta x} \tag{5.70}$$

$$CY^{n}_{i,j-1} = \frac{14.55C^{n}_{i,j-3}}{126.6\Delta y} - \frac{15.4C^{n}_{i,j-2}}{21.1\Delta y} + \frac{15.73C^{n}_{i,j}}{21.1\Delta y} - \frac{3.1C^{n}_{i,j+1}}{21.1\Delta y} + \frac{C^{n}_{i,j+2}}{63.3\Delta y} \tag{5.71}$$

$$CY^{n}_{i,j} = -\frac{C^{n}_{i,j-3}}{63.3\Delta y} + \frac{3.1C^{n}_{i,j-2}}{21.1\Delta y} - \frac{15.73C^{n}_{i,j-1}}{21.1\Delta y} + \frac{15.73C^{n}_{i,j+1}}{21.1\Delta y} - \frac{14.55C^{n}_{i,j+2}}{126.6\Delta y} \tag{5.72}$$

$$CY^{n}_{i-1,j-1} = \frac{14.55C^{n}_{i-1,j-3}}{126.6\Delta y} - \frac{15.4C^{n}_{i-1,j-2}}{21.1\Delta y} + \frac{15.73C^{n}_{i-1,j}}{21.1\Delta y} - \frac{3.1C^{n}_{i-1,j+1}}{21.1\Delta y} + \frac{C^{n}_{i-1,j+2}}{63.3\Delta y} \qquad (5.73)$$

Inserting equations (5.68) to (5.73) into equation (5.58) gives:

$$
\begin{aligned}
Y(\alpha,\beta) = {} & \left(2\alpha^3 - 3\alpha^2 + 1 + 2\beta^3 - 3\beta^2 - \alpha^2\beta - \alpha\beta^2 + 3\alpha\beta\right)C_{i,j}^n \\
& + \left(-2\alpha^3 + 3\alpha^2 + \alpha^2\beta + \alpha\beta^2 - 3\alpha\beta\right)C_{i-1,j}^n \\
& + \left(-2\beta^3 + 3\beta^2 + \alpha^2\beta + \alpha\beta^2 - 3\alpha\beta\right)C_{i,j-1}^n + \left(-\alpha^2\beta - \alpha\beta^2 + 3\alpha\beta\right)C_{i-1,j-1}^n \\
& + \left(\begin{array}{l} -\dfrac{C_{i-3,j}^n}{63.3\Delta x} + \dfrac{3.1C_{i-2,j}^n}{21.1\Delta x} \\ -\dfrac{15.73C_{i-1,j}^n}{21.1\Delta x} + \dfrac{15.73C_{i+1,j}^n}{21.1\Delta x} - \dfrac{14.55C_{i+2,j}^n}{126.6\Delta x} \end{array}\right)\left(-\alpha^3 + 2\alpha^2 - \alpha\right)\Delta x \\
& + \left(\begin{array}{l} -\dfrac{C_{i,j-3}^n}{63.3\Delta y} + \dfrac{3.1C_{i,j-2}^n}{21.1\Delta y} \\ -\dfrac{15.73C_{i,j-1}^n}{21.1\Delta y} + \dfrac{15.73C_{i,j+1}^n}{21.1\Delta y} - \dfrac{14.55C_{i,j+2}^n}{126.6\Delta y} \end{array}\right)\left(-\beta^3 + 2\beta^2 - \beta\right)\Delta y \\
& + \left(\begin{array}{l} \dfrac{14.55C_{i-3,j}^n}{126.6\Delta x} - \dfrac{15.4C_{i-2,j}^n}{21.1\Delta x} \\ +\dfrac{15.73C_{i,j}^n}{21.1\Delta x} - \dfrac{3.1C_{i+1,j}^n}{21.1\Delta x} + \dfrac{C_{i+2,j}^n}{63.3\Delta x} \end{array}\right)\left(-\alpha^3 + \alpha^2 + \alpha^2\beta - \alpha\beta\right)\Delta x \\
& + \left(\begin{array}{l} \dfrac{14.55C_{i,j-3}^n}{126.6\Delta y} - \dfrac{15.4C_{i,j-2}^n}{21.1\Delta y} \\ +\dfrac{15.73C_{i,j}^n}{21.1\Delta y} - \dfrac{3.1C_{i,j+1}^n}{21.1\Delta y} + \dfrac{C_{i,j+2}^n}{63.3\Delta y} \end{array}\right)\left(-\beta^3 + \beta^2 + \alpha\beta^2 - \alpha\beta\right)\Delta y \\
& + \left(\begin{array}{l} \dfrac{14.55C_{i-3,j-1}^n}{126.6\Delta x} - \dfrac{15.4C_{i-2,j-1}^n}{21.1\Delta x} \\ +\dfrac{15.73C_{i,j-1}^n}{21.1\Delta x} - \dfrac{3.1C_{i+1,j-1}^n}{21.1\Delta x} + \dfrac{C_{i+2,j-1}^n}{63.3\Delta x} \end{array}\right)\left(-\alpha^2\beta + \alpha\beta\right)\Delta x \\
& + \left(\begin{array}{l} \dfrac{14.55C_{i-1,j-3}^n}{126.6\Delta y} - \dfrac{15.4C_{i-1,j-2}^n}{21.1\Delta y} \\ +\dfrac{15.73C_{i-1,j}^n}{21.1\Delta y} - \dfrac{3.1C_{i-1,j+1}^n}{21.1\Delta y} + \dfrac{C_{i-1,j+2}^n}{63.3\Delta y} \end{array}\right)\left(-\alpha\beta^2 + \alpha\beta\right)\Delta y
\end{aligned}
\tag{5.74}
$$

Equation (5.74) reduces to a more manageable format of:

$$\begin{aligned} y(\alpha,\beta) = {} & f1C_{i-3,j-1} + f2C_{i-2,j-1} + f3C_{i-1,j-1} + f4C_{i,j-1} + f5C_{i+1,j-1} \\ & + f6C_{i+2,j-1} + f7C_{i-3,j} + f8C_{i-2,j} + f9C_{i-1,j} + f10C_{i,j} \\ & + f11C_{i+1,j} + f12C_{i+2,j} + f13C_{i,j-3} + f14C_{i,j-2} + f15C_{i,j+1} \\ & + f16C_{i,j+2} + f17C_{i-1,j-3} + f18C_{i-1,j-2} + f19C_{i-1,j+1} \\ & + f20C_{i-1,j+2} \end{aligned} \tag{5.75}$$

in which the multiplying variables are defined as:

$$f1 = \frac{14.55\left(-\alpha^2\beta + \alpha\beta\right)}{126.6}$$

$$f2 = \frac{15.4\left(-\alpha^2\beta + \alpha\beta\right)}{21.1}$$

$$f3 = -\alpha^2\beta - \alpha\beta^2 + 3\alpha\beta$$

$$f4 = \frac{-26.5\beta^3 + 31.9\beta^2 + 5.37\alpha^2\beta + 21.1\alpha\beta^2 - 47.6\alpha\beta + 15.7\beta}{21.1}$$

$$f5 = \frac{-3.1\left(-\alpha^2\beta + \alpha\beta\right)}{21.1}$$

$$f6 = \frac{\left(-\alpha^2\beta + \alpha\beta\right)}{63.3}$$

$$f7 = \frac{-12.55\alpha^3 + 10.55\alpha^2 + 14.55\alpha^2\beta - 14.55\alpha\beta + 2\alpha}{126.6}$$

$$f8 = \frac{12.3\alpha^3 - 9.2\alpha^2 - 15.4\alpha^2\beta + 15.4\alpha\beta - 3.1\alpha}{21.1}$$

$$f9 = \frac{-26.5\alpha^3 + 31.8\alpha^2 + 21.1\alpha^2\beta + 5.4\alpha\beta^2 - 47.6\alpha\beta + 15.7\alpha}{21.1}$$

$$f10=\frac{26.5\alpha^3-47.6\alpha^2+21.1+26.5\beta^3-47.6\beta^2-5.4\alpha^2\beta-5.4\alpha\beta^2+31.8\alpha\beta}{21.1}$$

$$f11=\frac{-12.3\alpha^3+27.7\alpha^2-3.1\alpha^2\beta+3.1\alpha\beta-15.4\alpha}{21.1}$$

$$f12=\frac{12.6\alpha^3-27.1\alpha^2+2\alpha^2\beta-2\alpha\beta+14.6\alpha}{126.6}$$

$$f13=\frac{-12.6\beta^3+10.6\beta^2+14.6\alpha\beta^2-14.6\alpha\beta+2\beta}{126.6}$$

$$f14=\frac{12.3\beta^3-9.2\beta^2-15.4\alpha\beta^2+15.4\alpha\beta-3.1\beta}{21.1}$$

$$f15=\frac{-12.3\beta^3+27.7\beta^2-3.1\alpha\beta^2+3.1\alpha\beta-15.4\beta}{21.1}$$

$$f16=\frac{12.6\beta^3-27.1\beta^2+2\alpha\beta^2-2\alpha\beta+14.6\beta}{126.6}$$

$$f17=\frac{14.55\left(-\alpha\beta^2+\alpha\beta\right)}{126.6}$$

$$f18=\frac{-15.4\left(-\alpha\beta^2+\alpha\beta\right)}{21.1}$$

$$f19=\frac{-3.1\left(-\alpha\beta^2+\alpha\beta\right)}{21.1}$$

$$f20=\frac{-\alpha\beta^2+\alpha\beta}{63.3}$$

This derivation assumes that the velocity is positive in both the x and y-directions. Similar schemes may be derived for the other possible flow fields.

5.2 Comparison of the two-dimensional finite difference schemes and methods of characteristics

These four two-dimensional schemes are tested using two different velocity fields. The first is relatively simple and is used to examine how the methods behave under constant two-dimensional flow conditions. It consists of a diagonal channel constructed on a regular grid with x and y spatial increments of 100m. Velocity in the x and y-directions are +1m/s and –1m/s respectively, resulting in the pollution being advected from the top left corner of the grid to the bottom right. In these cases a time increment of 25 seconds is used to compare the schemes. In addition the effect of varying the time step is examined for the linear distribution testcase.

The second testcase is a rotational flow field, based on a test used by Komatsu *et al*[16]. This provides a more complex flow pattern with which to observe the numerical accuracy and stability of the methods being considered. The flow field lies upon a regular grid of dimensions 100m by 100m and the velocity varies from 0 to ±0.63m/s. The results following one quarter turn are examined.

5.2.1 Diagonal testcase

5.2.1. Results using a point release

The initial 10mg/l point release of concentration, is defined at a single location on the grid, i=14, j=14, as described by Figure (5.3). Although a point release is the most simple of the pollution distributions considered, it is difficult to model as the concentration gradients are very steep.

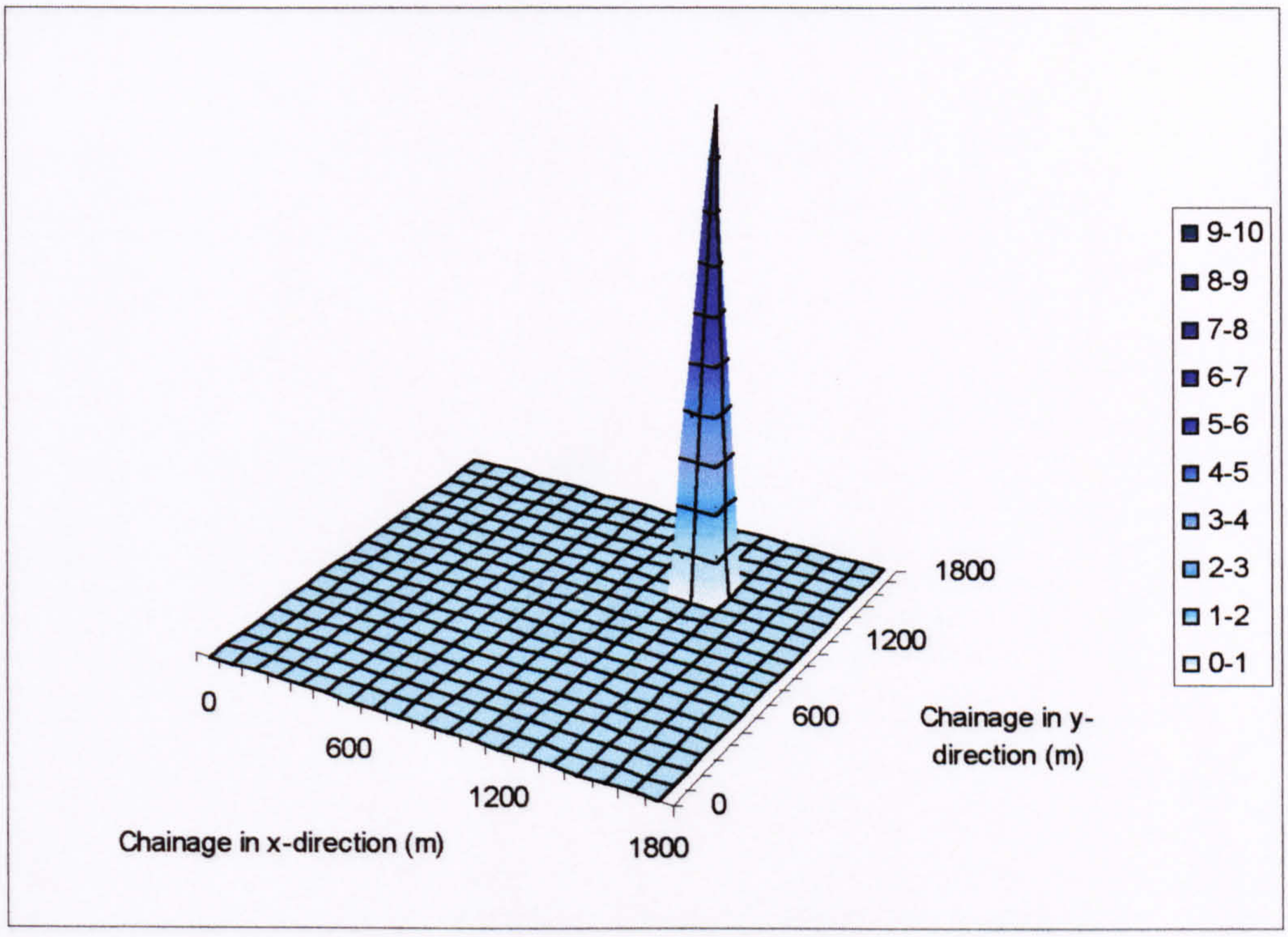

Figure (5.3) Initial conditions using a point release

Due to the sharpness of the gradients it challenges not only the performance of the scheme to advect well but also to cope with sudden extreme concentration changes.

First consider the results of advecting the point source, using each of the four methods, after 400 seconds in Figure (5.4) to Figure (5.7).

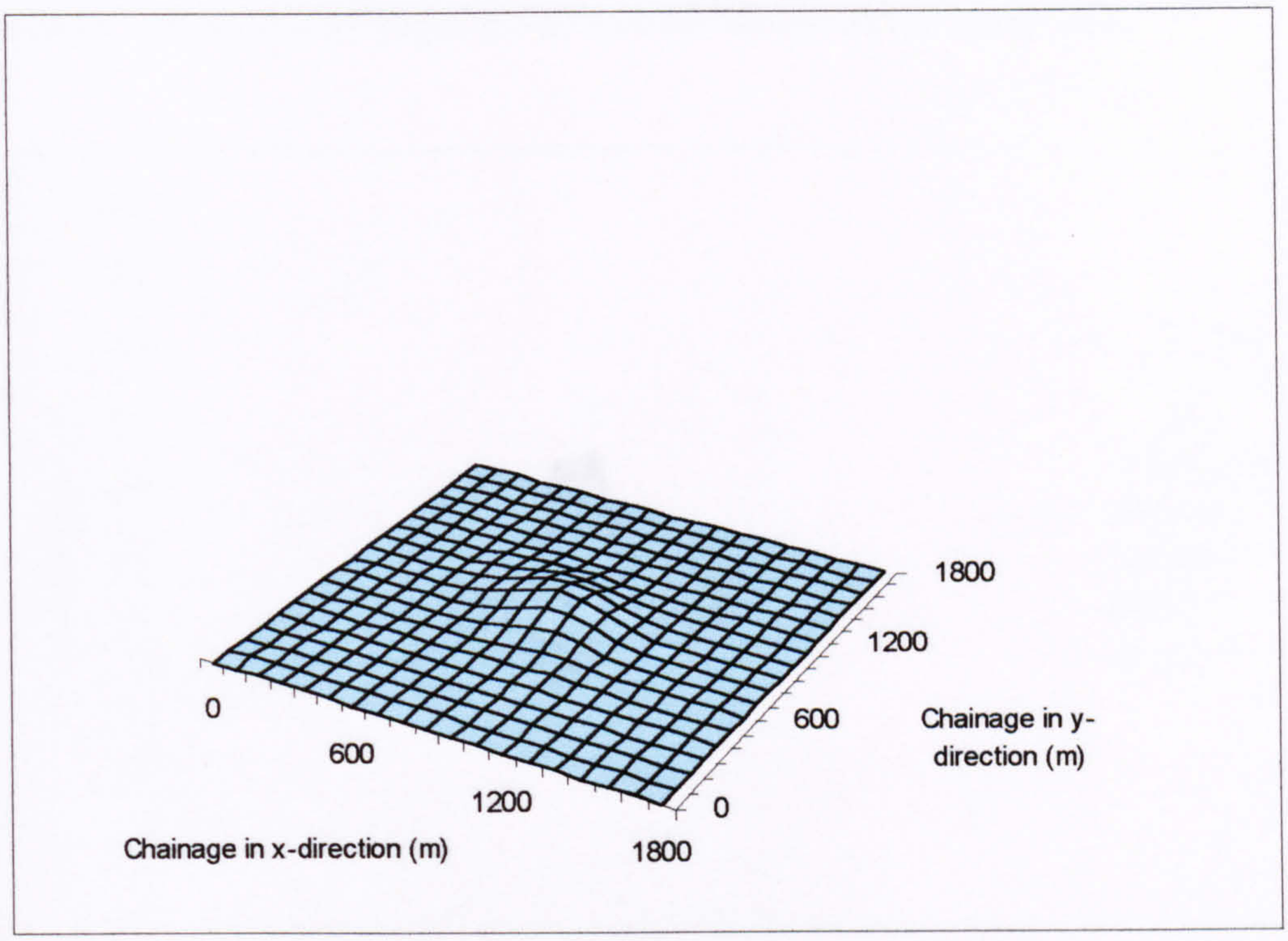

Figure (5.4) Advected point release using 2D Upwinding, Cr=0.25, t=400s

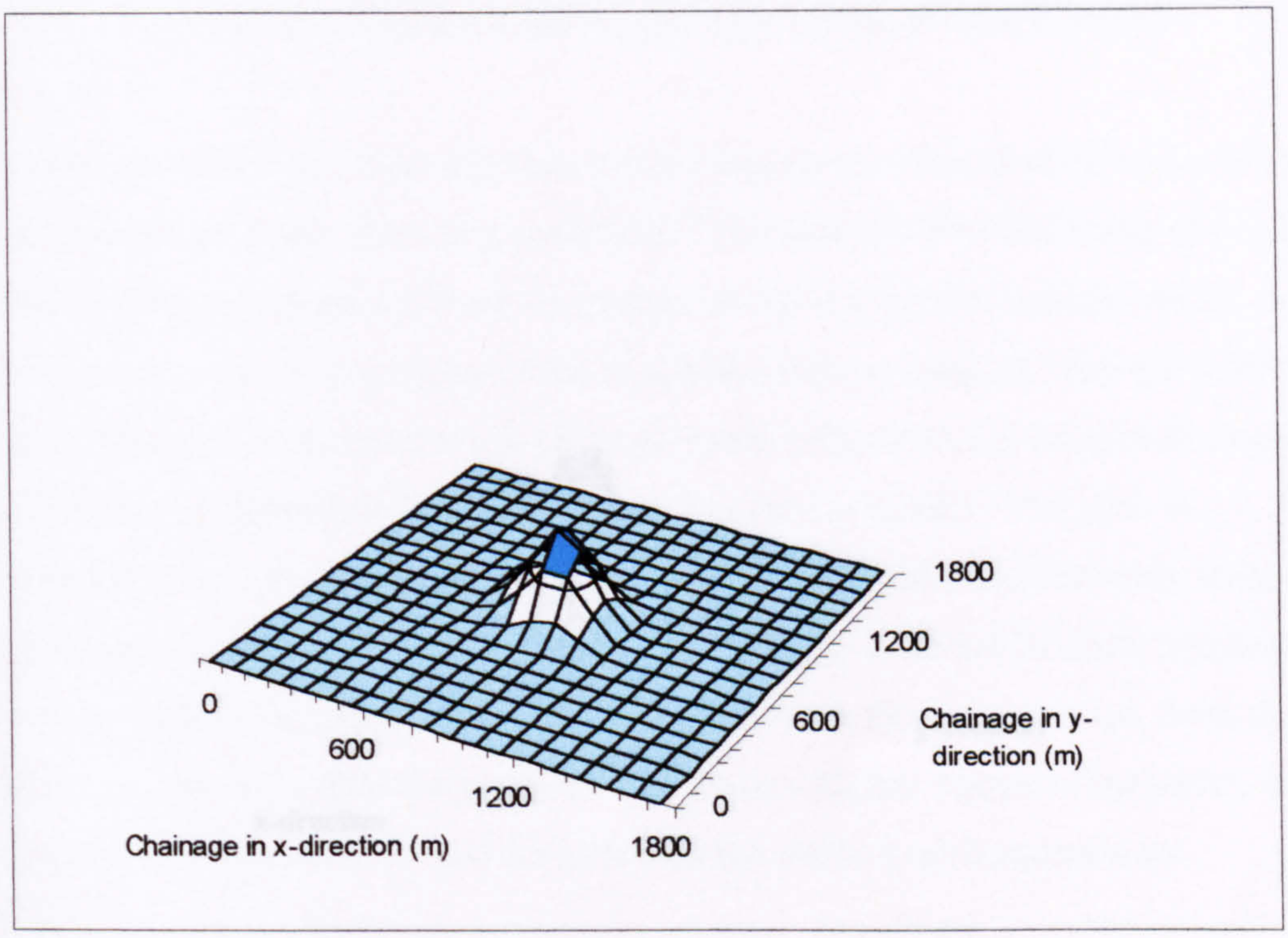

Figure (5.5) Advected point release using 2D QUICKEST, Cr=0.25, t=400s

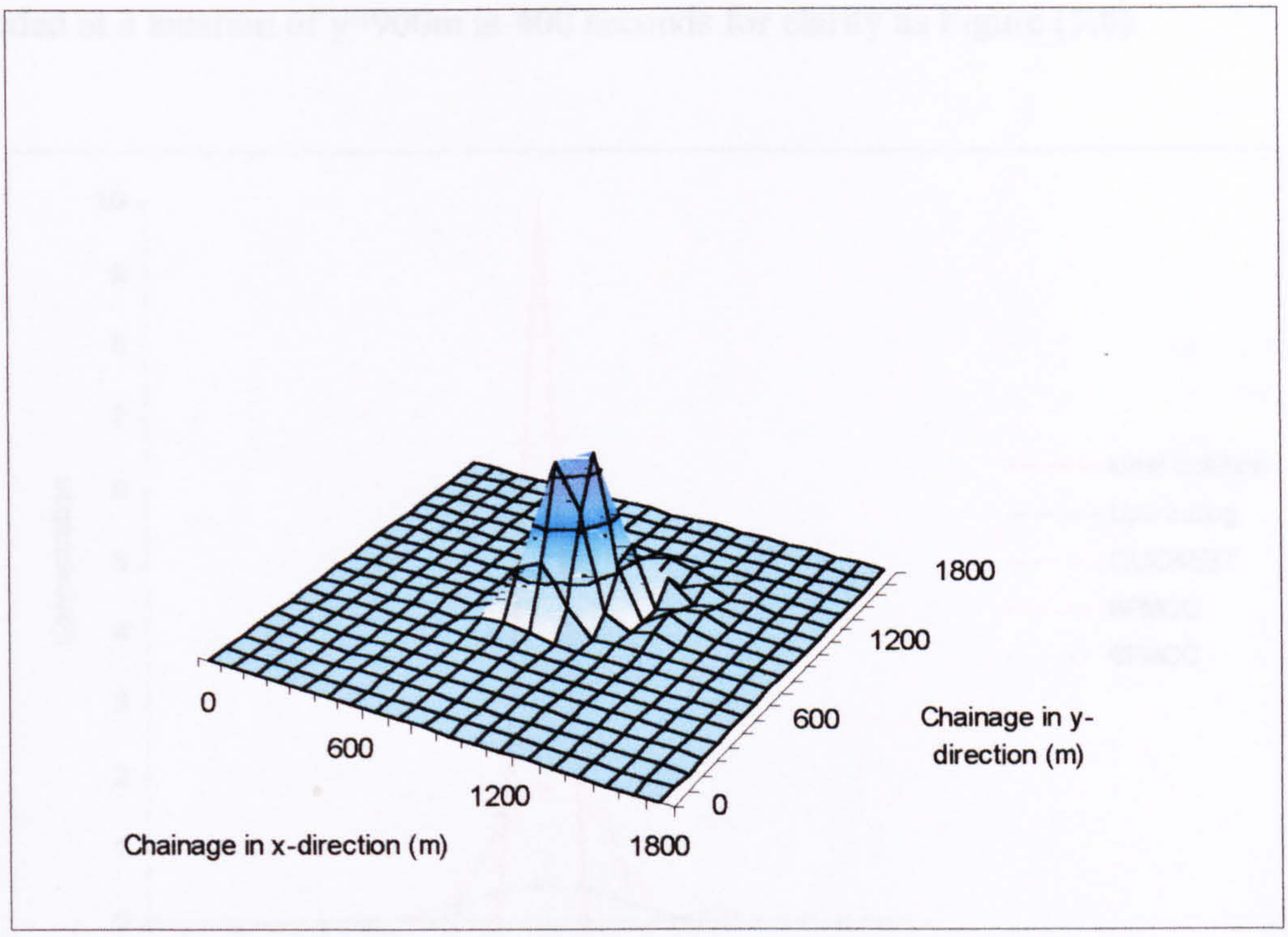

Figure (5.6) Advected point release using 2D 8PMOC, Cr=0.25, t=400s

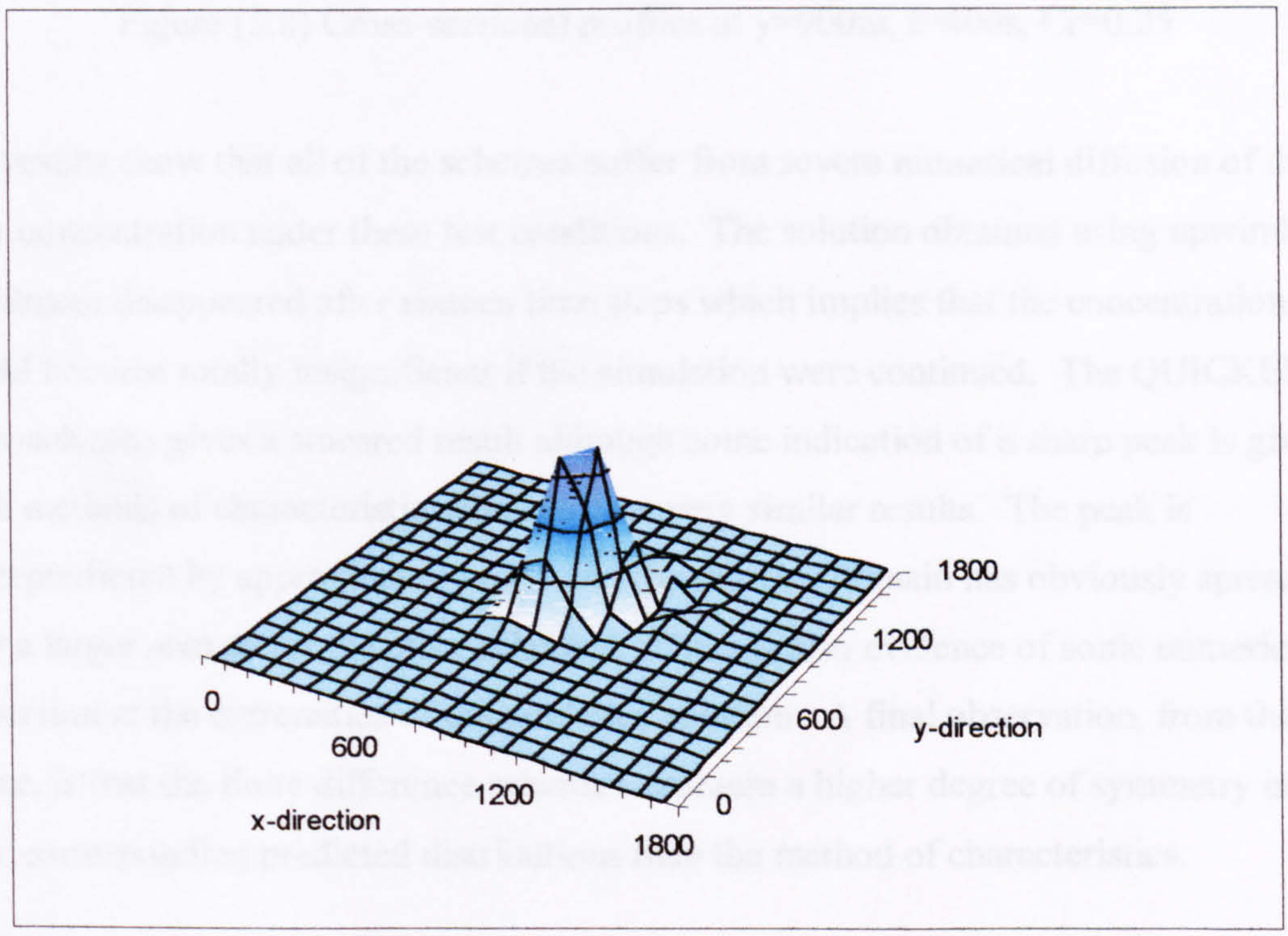

Figure (5.7) Advected point release using 2D 6PMOC, Cr=0.25, t=400s

The results as presented are difficult to interpret easily and so a cross-sectional profile is included at a location of y=900m at 400 seconds for clarity as Figure (5.8).

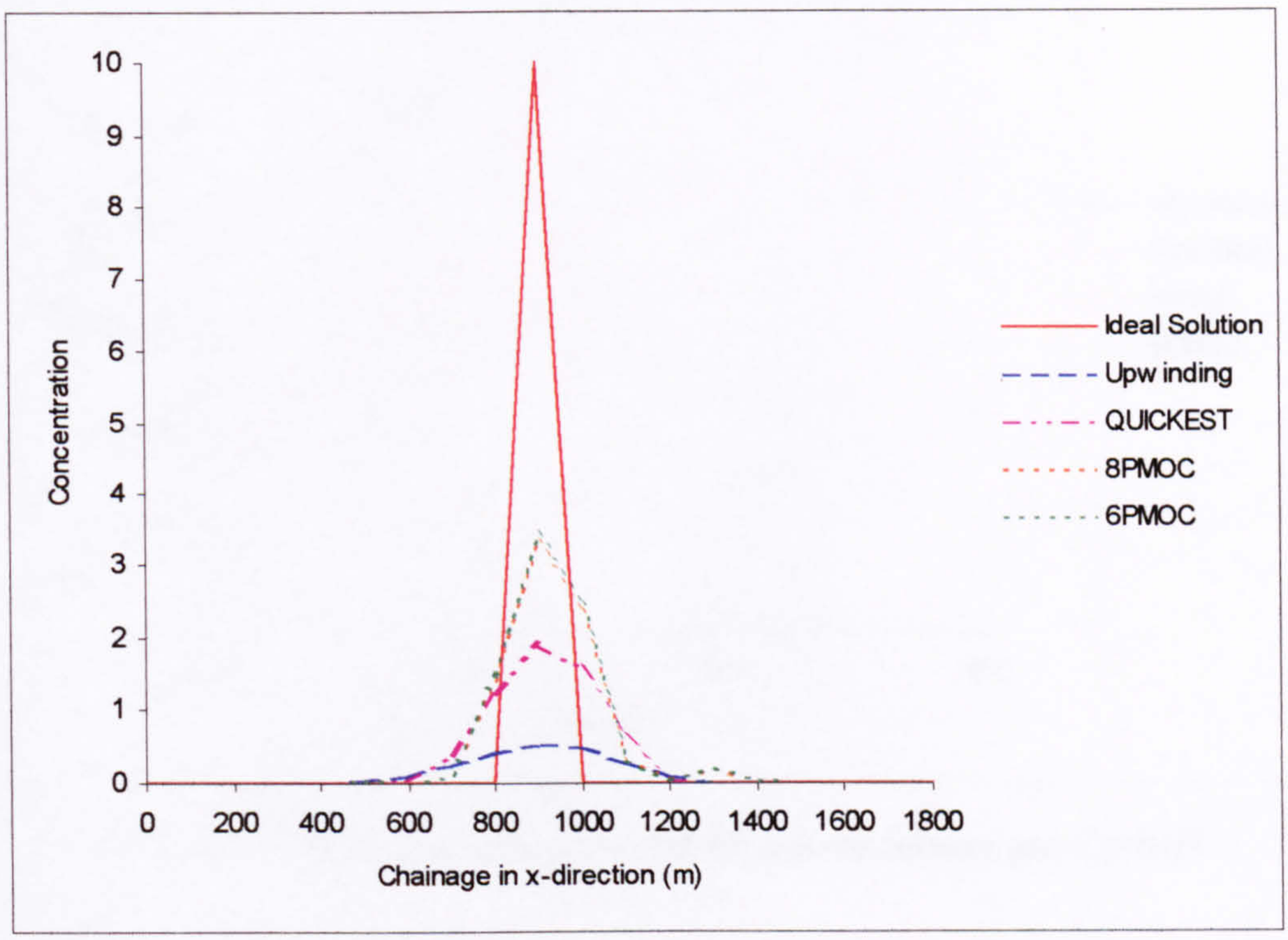

Figure (5.8) Cross-sectional profiles at y=900m, t=400s, Cr=0.25

The results show that all of the schemes suffer from severe numerical diffusion of the peak concentration under these test conditions. The solution obtained using upwinding has almost disappeared after sixteen time steps which implies that the concentration would become totally insignificant if the simulation were continued. The QUICKEST approach also gives a smeared result although some indication of a sharp peak is given. Both methods of characteristic schemes give very similar results. The peak is underpredicted by approximately 67% and the solution domain has obviously spread out over a larger area as for the other schemes. There is also evidence of some numerical dispersion at the extremities of the predicted solution. A final observation, from this figure, is that the finite difference schemes maintain a higher degree of symmetry in their corresponding predicted distributions than the method of characteristics.

The root mean square values are also examined here in Figure (5.9), to give an impression of global accuracy as in the one-dimensional case.

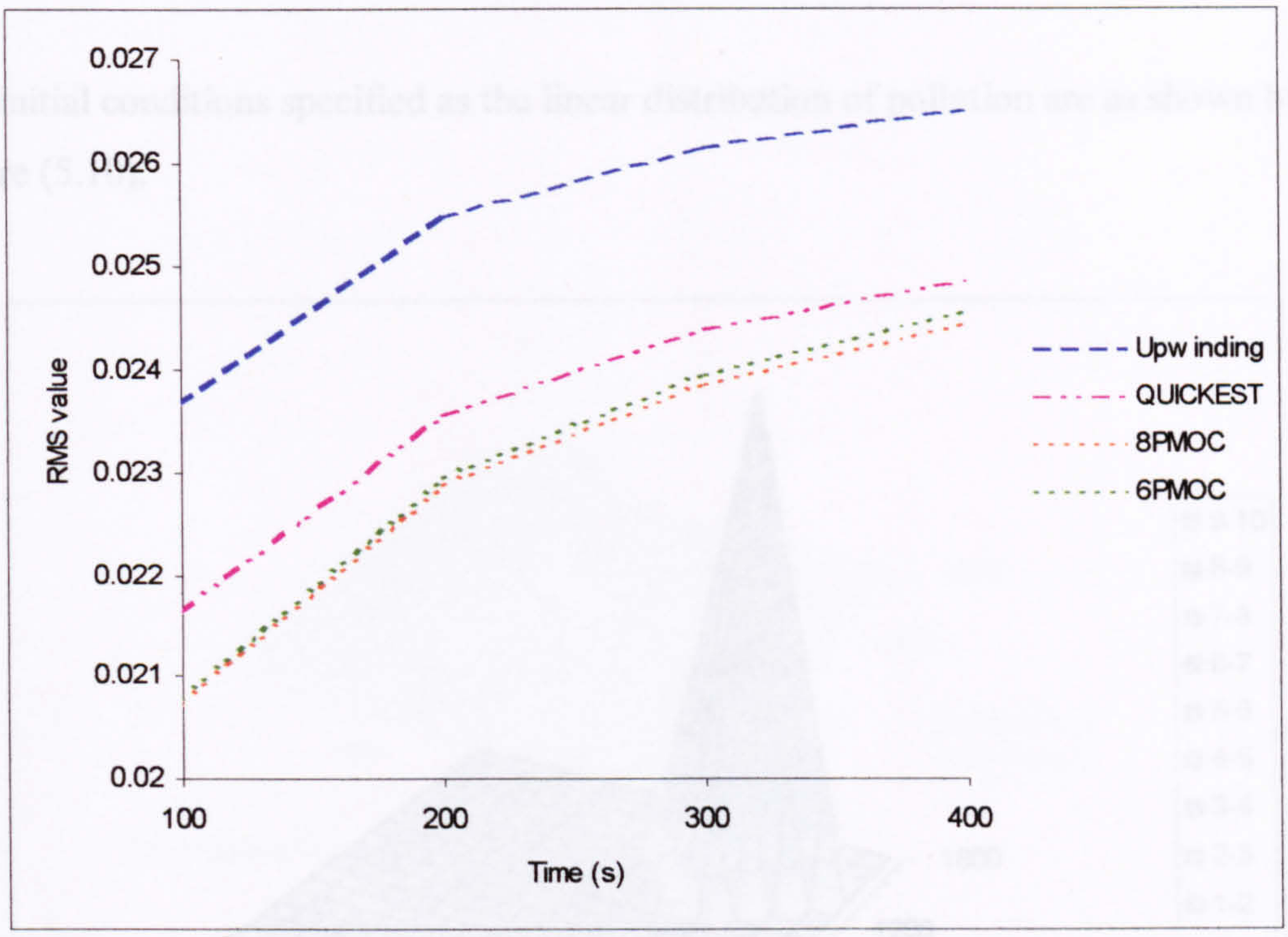

Figure (5.9) Root mean square plot for a point release and Cr=0.25

The root mean square values increase over time indicating that errors in the solution increase as time progresses.

It is interesting to note that, contrary to most other comparisons of this type, the root mean square values for all of the schemes are very close together. This may imply that the error in the solutions has arisen from the same source. It can be concluded that these approaches do not cope well with severe changes in concentration gradient as this is the common factor. This can be confirmed by conducting further tests using a linear and Gaussian distribution. It may also be the case that the schemes perform poorly at a Courant number of 0.25, therefore variation of the Courant number should also be investigated.

5.2.1.2 Results using a linear distribution

The initial conditions specified as the linear distribution of pollution are as shown by Figure (5.10).

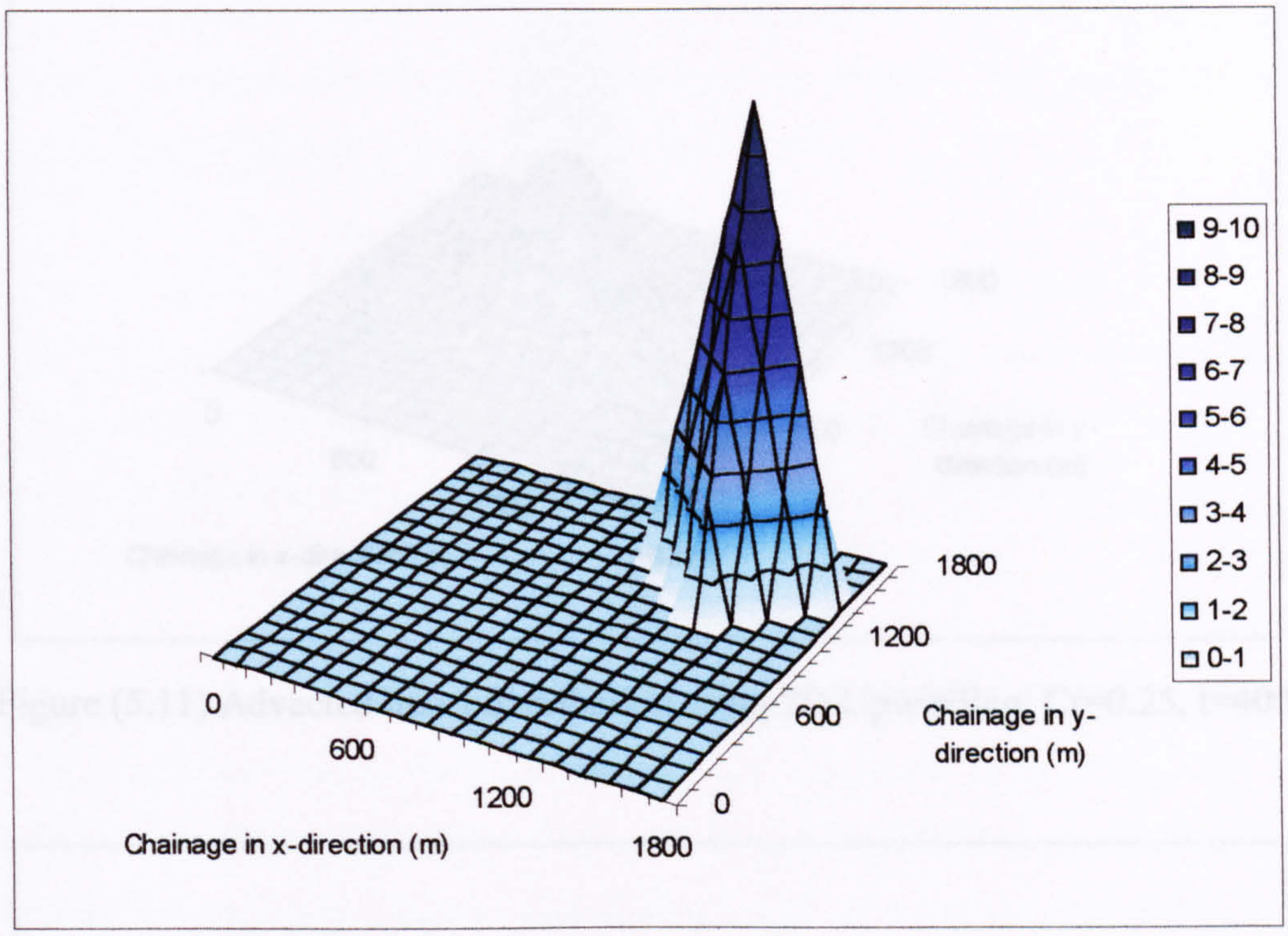

Figure (5.10) Initial conditions using a linear distribution

The peak concentration of 10mg/l is located at the centre of the distribution at i=14, j=14. The pollution is advected downstream using the four numerical schemes and analysed for Courant numbers of 0.25 and 0.5.

Results using a Courant number of 0.25

The results from each scheme were examined after sixteen time steps (400s) and the results included as Figure (5.11) to Figure (5.14).

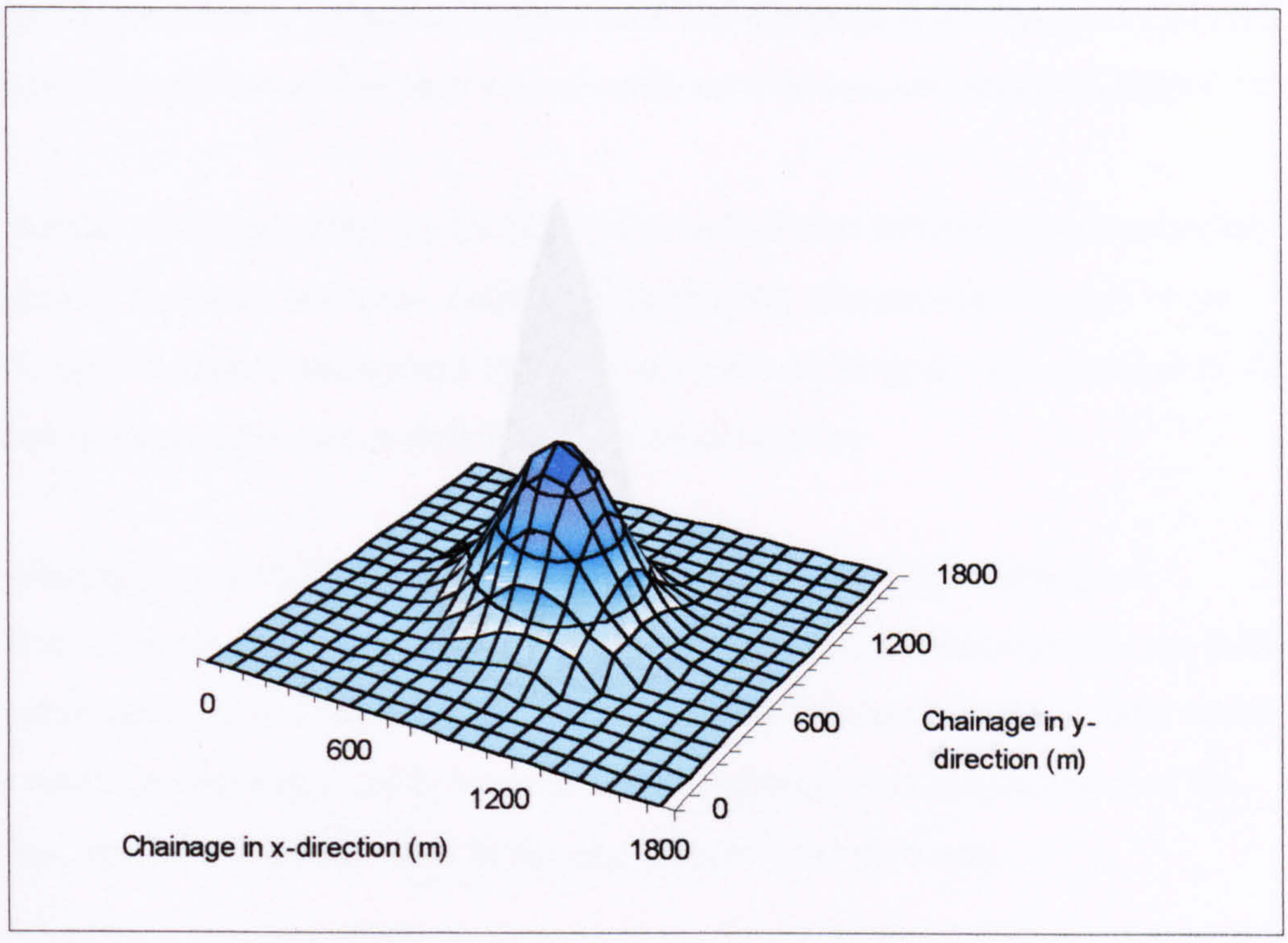

Figure (5.11) Advected linear distribution using 2D Upwinding, Cr=0.25, t=400s

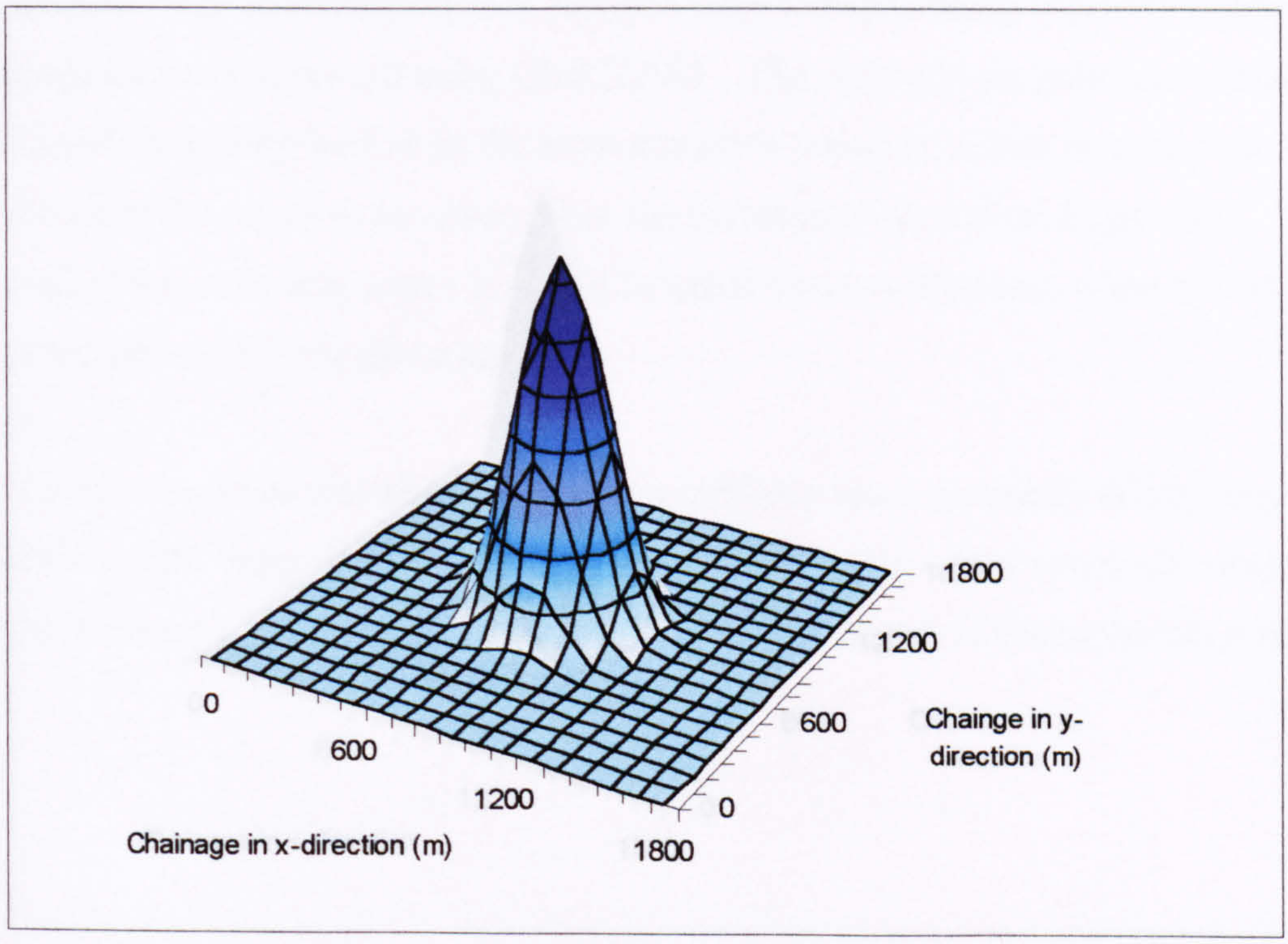

Figure (5.12) Advected linear distribution using 2D QUICKEST, Cr=0.25, t=400s

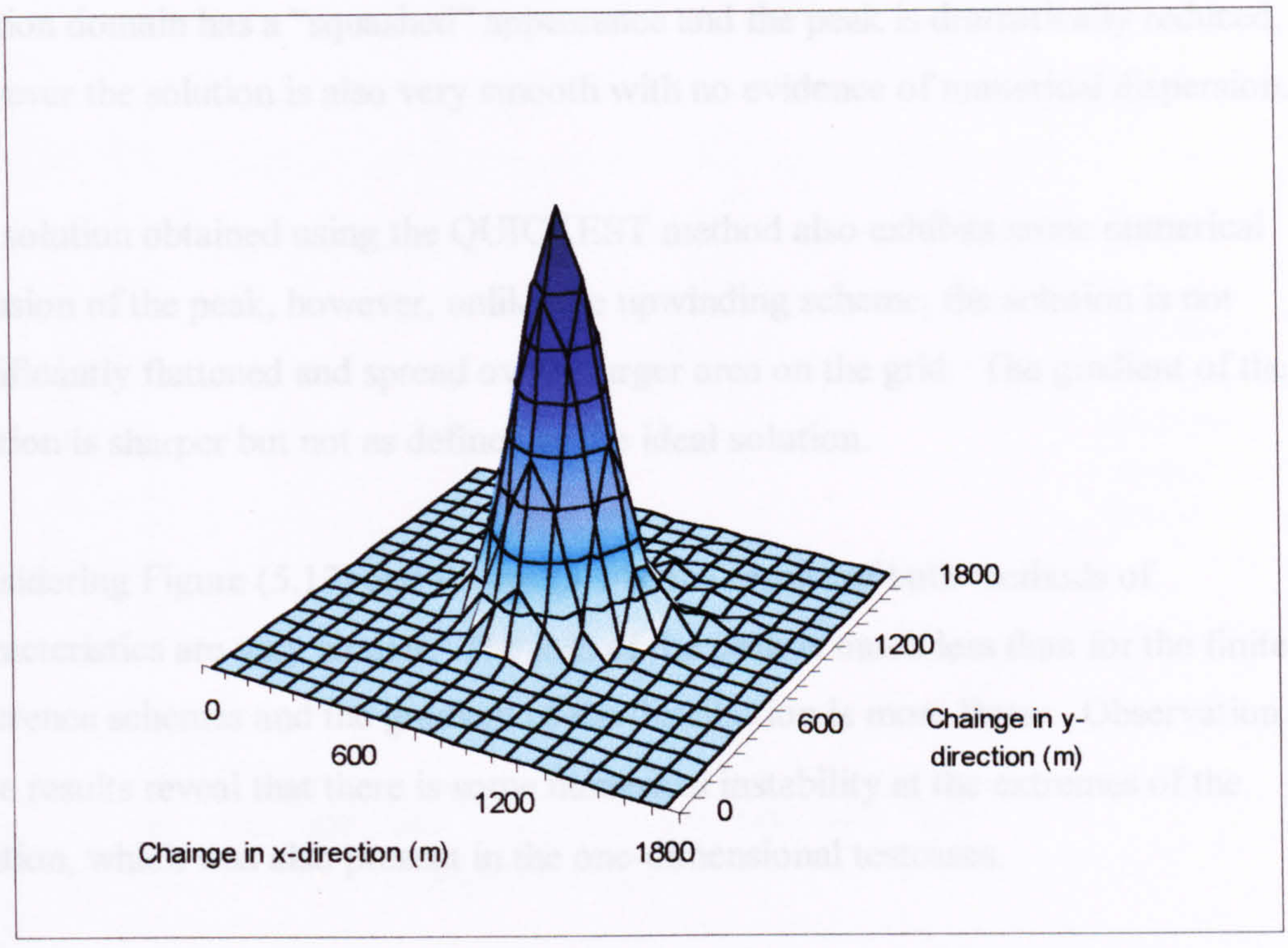

Figure (5.13) Advected linear distribution using 2D 8PMOC, Cr=0.25, t=400s

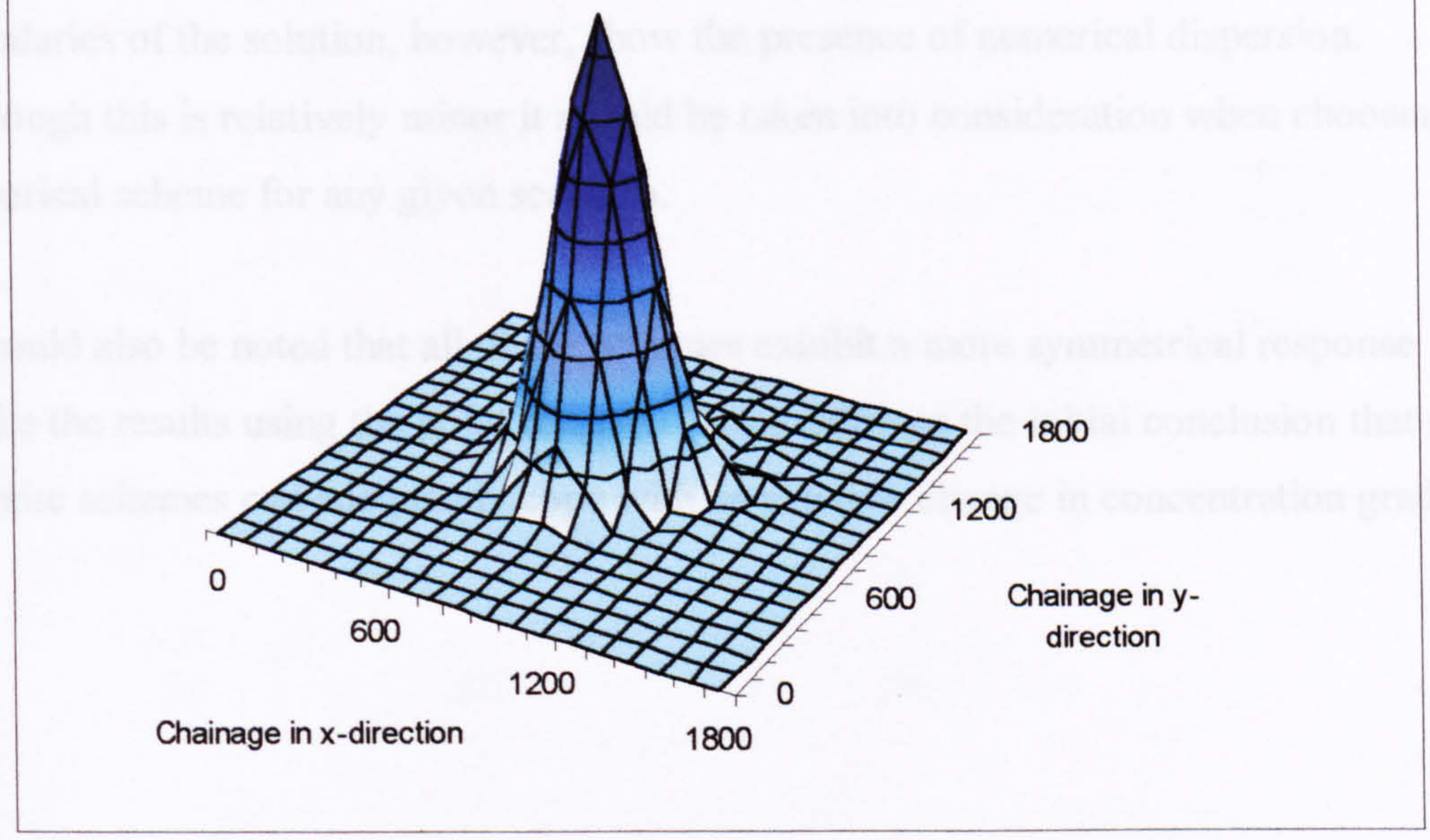

Figure (5.14) Advected linear distribution using 2D 6PMOC, Cr=0.25, t=400s

The upwinding scheme, as expected, suffers from significant numerical diffusion. The solution domain has a "squashed" appearance and the peak is dramatically reduced. However the solution is also very smooth with no evidence of numerical dispersion.

The solution obtained using the QUICKEST method also exhibits some numerical diffusion of the peak, however, unlike the upwinding scheme, the solution is not significantly flattened and spread over a larger area on the grid. The gradient of the solution is sharper but not as defined as the ideal solution.

Considering Figure (5.13) and Figure (5.14), the results of both methods of characteristics are very similar. The loss of the peak is much less than for the finite difference schemes and the gradient of the distribution is more linear. Observation of these results reveal that there is some numerical instability at the extremes of the solution, which was also present in the one-dimensional testcases.

Taking a x-directional cross-section through these results at y=900m, the differences between the schemes can be more clearly observed, Figure (5.15). It is instantly obvious how much the distribution is diffused using the upwinding approach and how this is significantly improved using QUICKEST. The eight and six point methods of characteristics initially look to be the most attractive schemes. Close inspection at the boundaries of the solution, however, show the presence of numerical dispersion. Although this is relatively minor it should be taken into consideration when choosing a numerical scheme for any given scenario.

It should also be noted that all of the schemes exhibit a more symmetrical response unlike the results using the point release. This reinforces the initial conclusion that none of these schemes can adequately cope with an extreme change in concentration gradient.

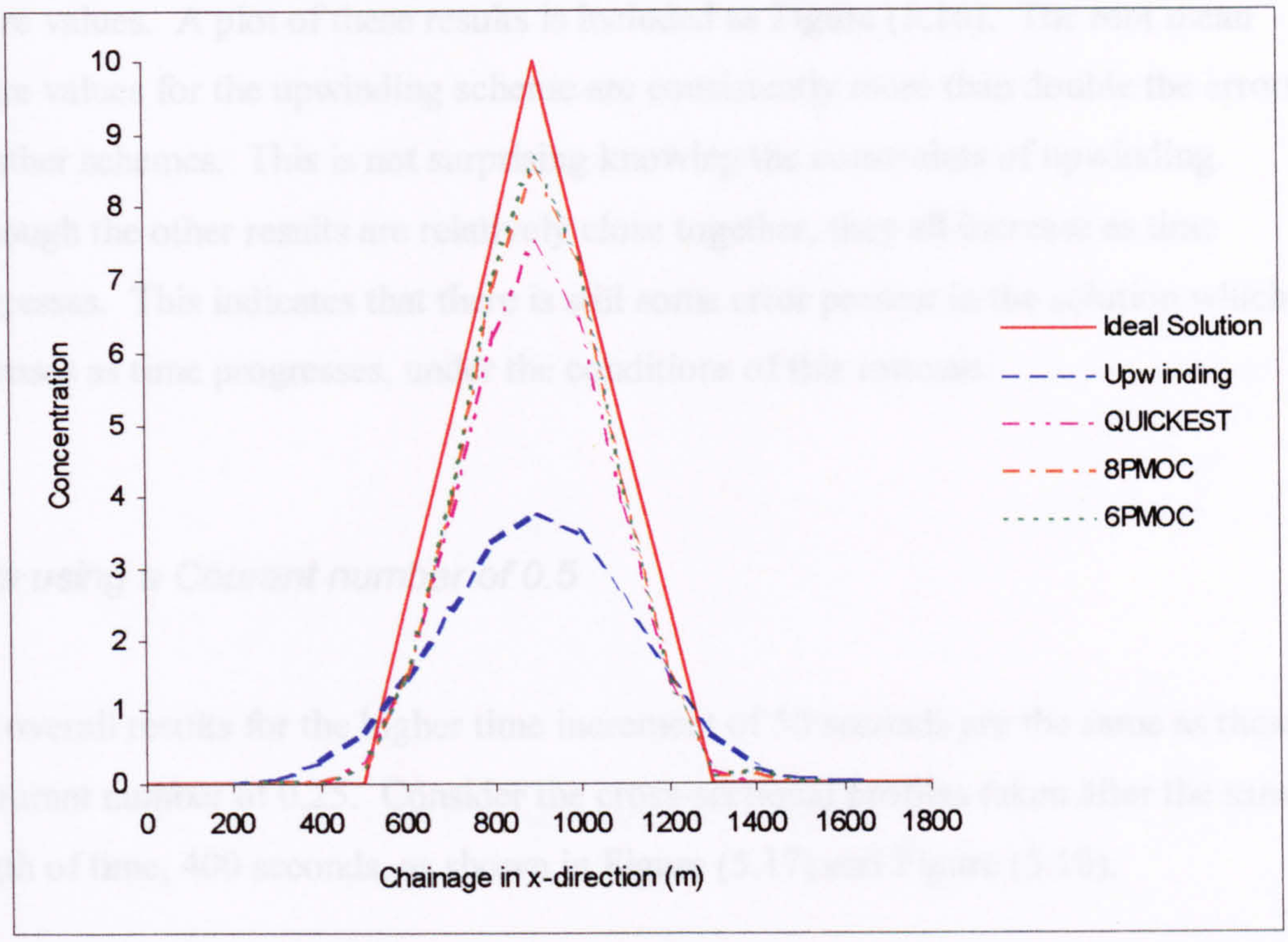

Figure (5.15) Cross-sectional profiles at y=900m, t=400s, Cr=0.25

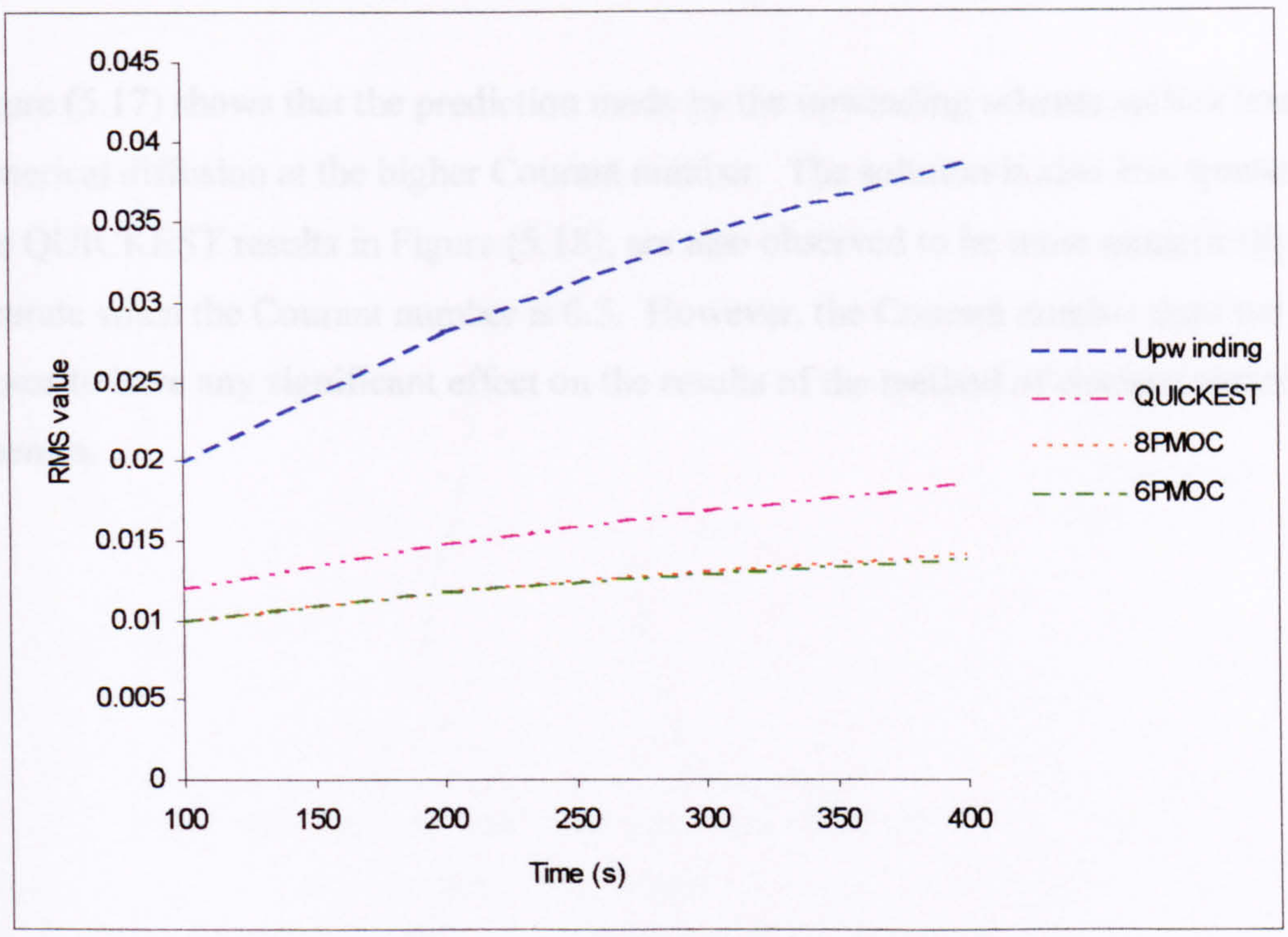

Figure (5.16) Root mean square plot for a linear distribution and Cr=0.25

The global errors may also be examined here using the previously identified root mean square values. A plot of these results is included as Figure (5.16). The root mean square values for the upwinding scheme are consistently more than double the errors of the other schemes. This is not surprising knowing the constraints of upwinding. Although the other results are relatively close together, they all increase as time progresses. This indicates that there is still some error present in the solution which increases as time progresses, under the conditions of this testcase.

Results using a Courant number of 0.5

The overall results for the higher time increment of 50 seconds are the same as those for a Courant number of 0.25. Consider the cross-sectional profiles taken after the same length of time, 400 seconds, as shown in Figure (5.17) and Figure (5.18).

These figures show comparisons between each of the methods using Courant numbers of 0.25 and 0.5. The results have been split into two graphs for clarity.

Figure (5.17) shows that the prediction made by the upwinding scheme suffers less from numerical diffusion at the higher Courant number. The solution is also less spread out. The QUICKEST results in Figure (5.18), are also observed to be more numerically accurate when the Courant number is 0.5. However, the Courant number does not appear to have any significant effect on the results of the method of characteristics schemes.

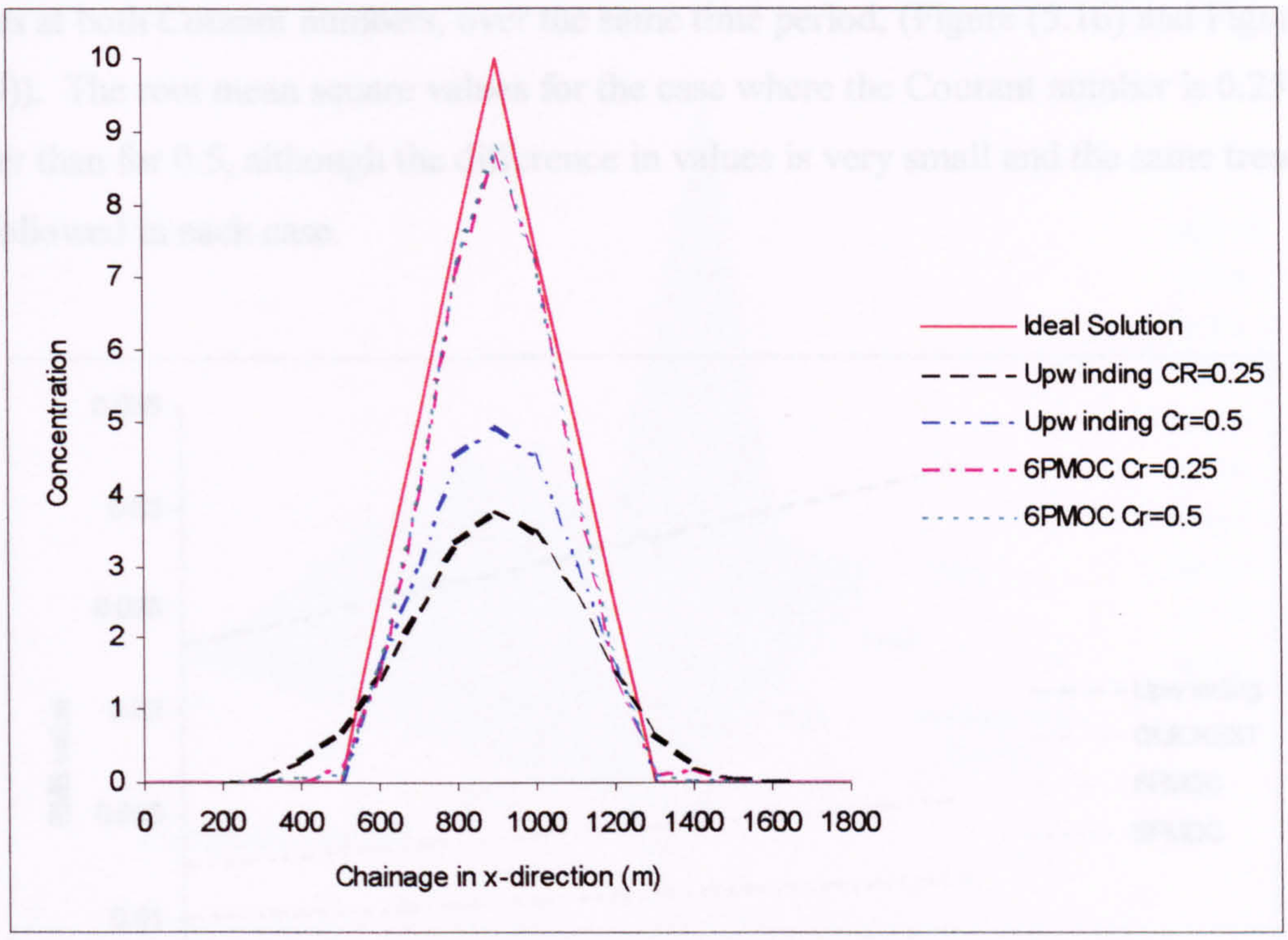

Figure (5.17) Comparison of Upwinding and 6PMOC schemes for Cr=0.25 and 0.5

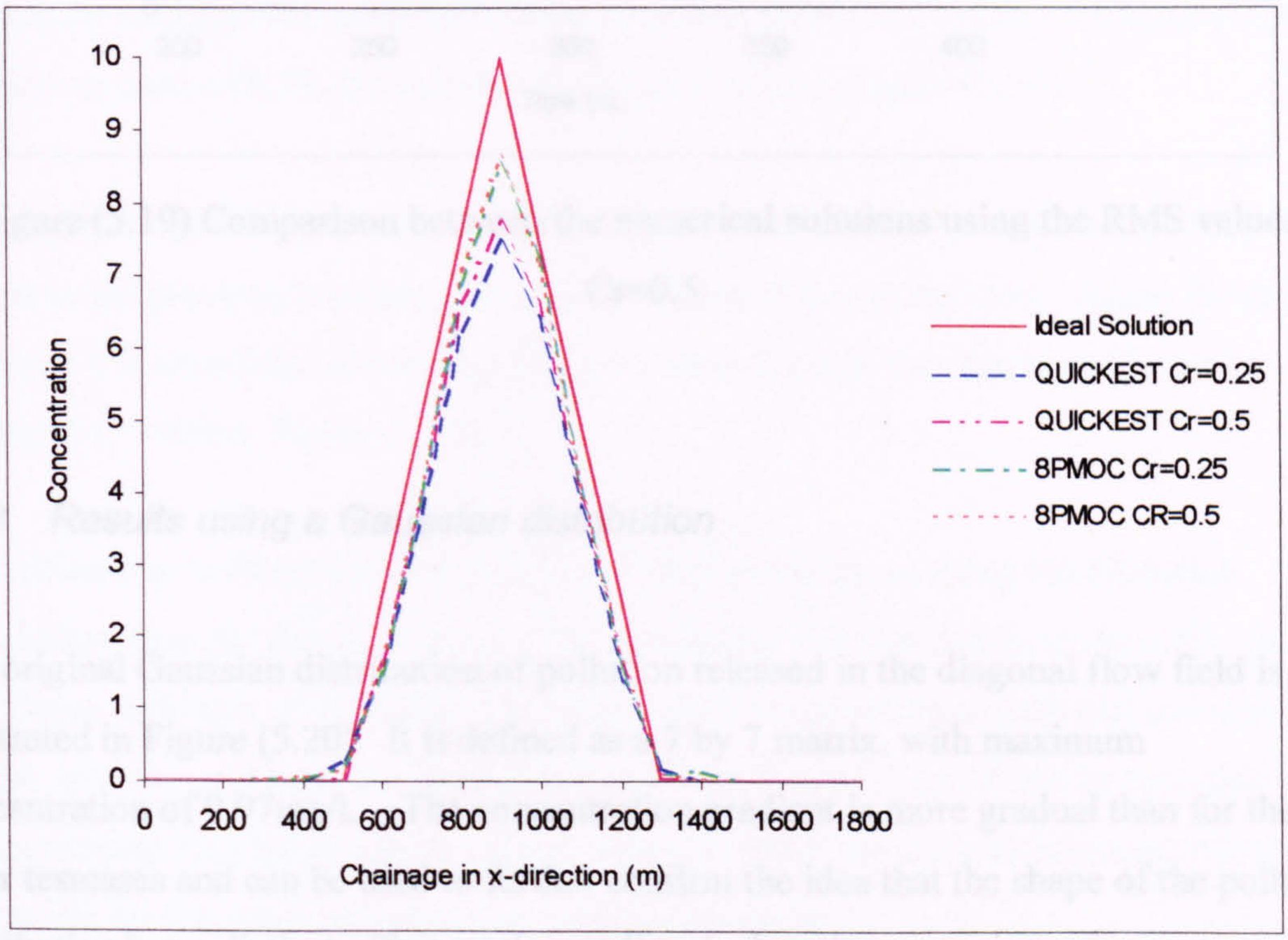

Figure (5.18) Comparison of QUICKEST and 8PMOC schemes for Cr=0.25 and 0.5

This is confirmed by taking account of global errors in terms of the root meant square values at both Courant numbers, over the same time period, (Figure (5.16) and Figure (5.19)). The root mean square values for the case where the Courant number is 0.25 are higher than for 0.5, although the difference in values is very small and the same trends are followed in each case.

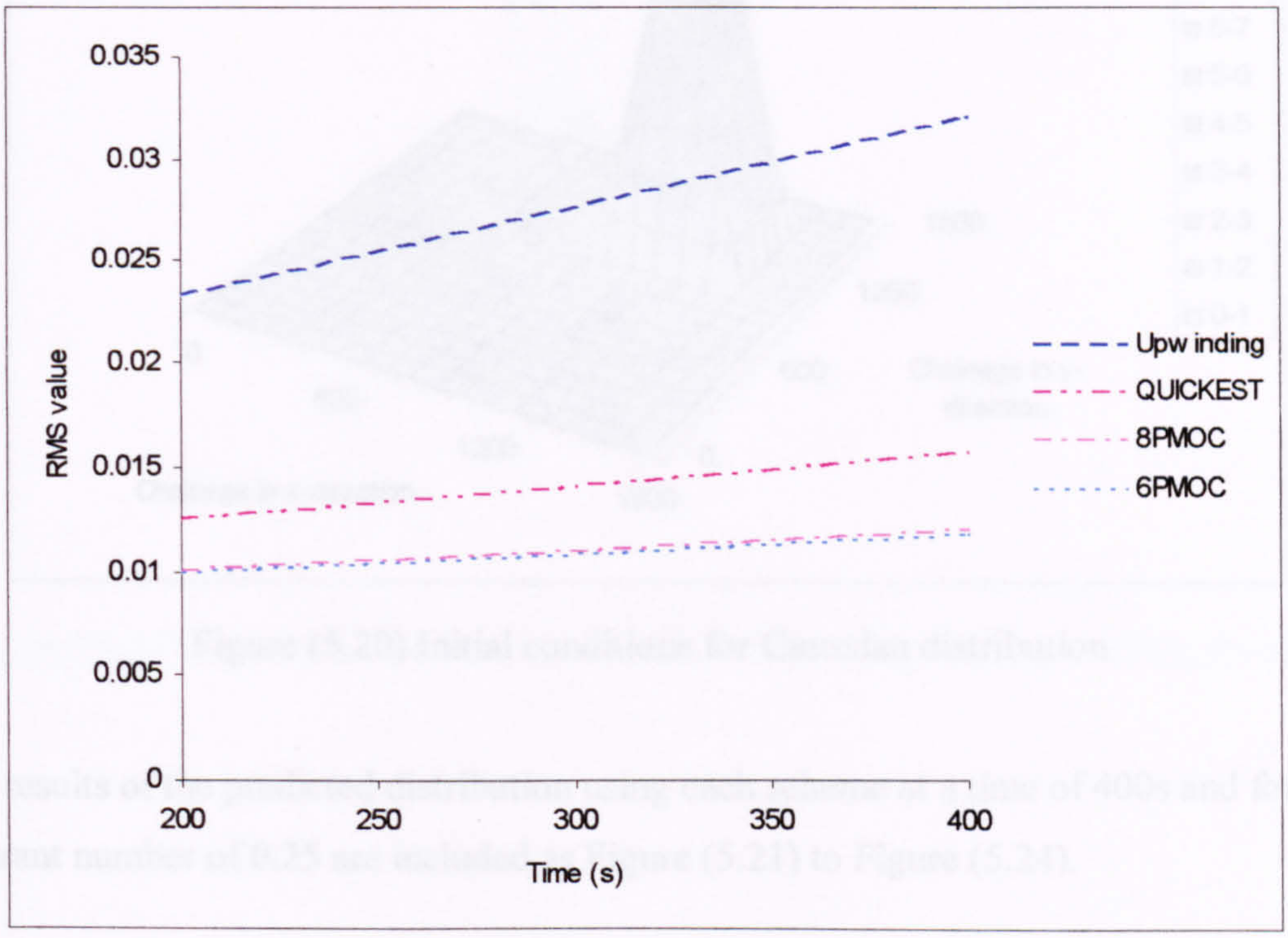

Figure (5.19) Comparison between the numerical solutions using the RMS values, Cr=0.5

5.2.1.3 Results using a Gaussian distribution

The original Gaussian distribution of pollution released in the diagonal flow field is illustrated in Figure (5.20). It is defined as a 7 by 7 matrix, with maximum concentration of 9.97mg/l. The concentration gradient is more gradual than for the other testcases and can be used to further confirm the idea that the shape of the pollution distribution has a distinct effect on the predicted advection.

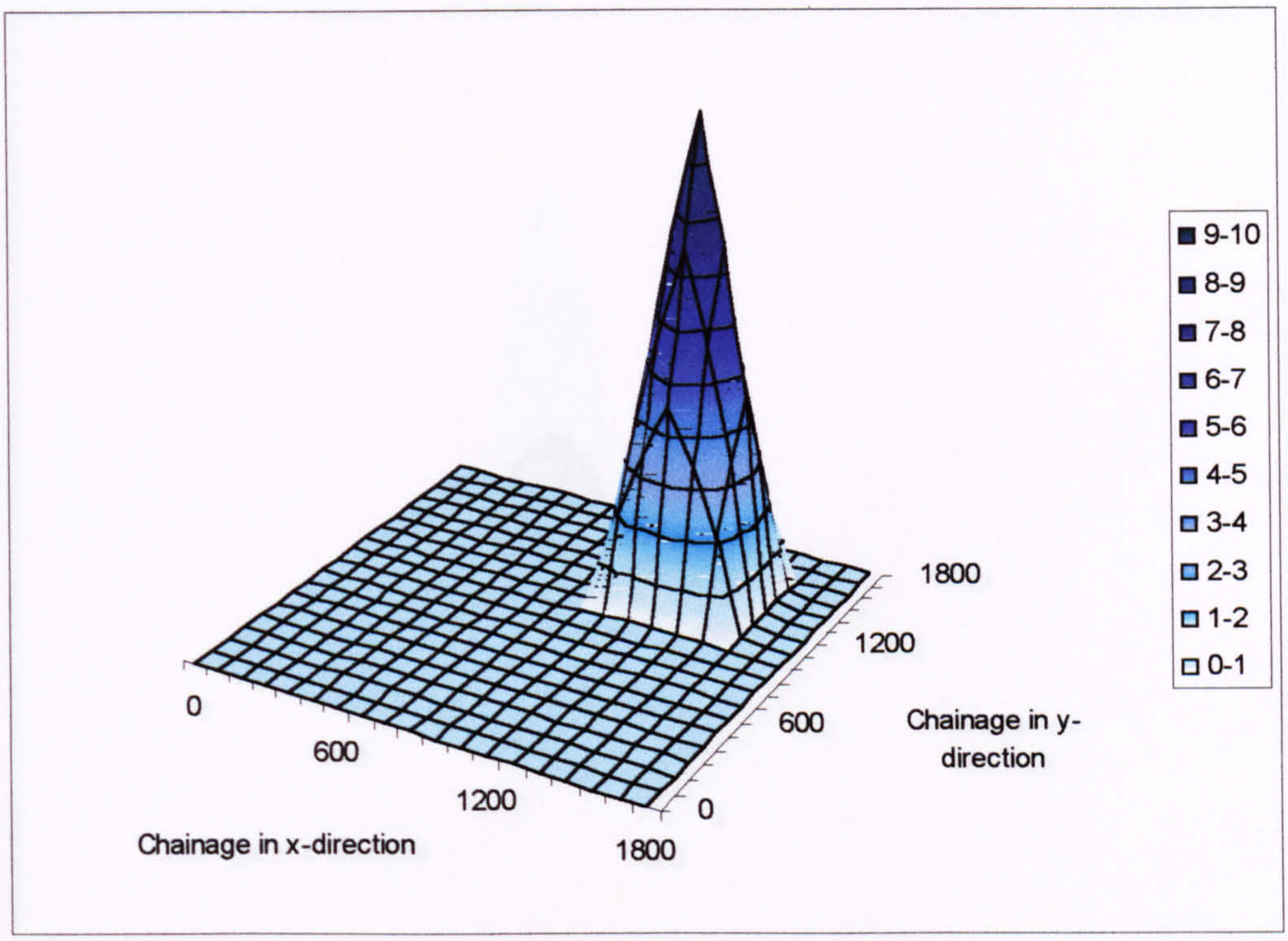

Figure (5.20) Initial conditions for Gaussian distribution

The results of the predicted distribution using each scheme at a time of 400s and for a Courant number of 0.25 are included as Figure (5.21) to Figure (5.24).

The observations which can be made from these results, reiterate what has already been shown in the previous testcases and also in the one-dimensional tests. Again for reasons of clarity it is beneficial to consider cross sections through the results at 400s at a location of y=900m, Figure (5.25).

The difficulties suffered by each scheme are less pronounced using the Gaussian distribution than for the other cases. The upwinding solution continues to suffer from significant diffusion of the peak. The shape of the distribution is flattened and extends further over the grid than the ideal solution. From Figure (5.26) it can be seen that the corresponding root mean square values, although small, do initially increase, whereas the results for the other schemes remain fairly constant.

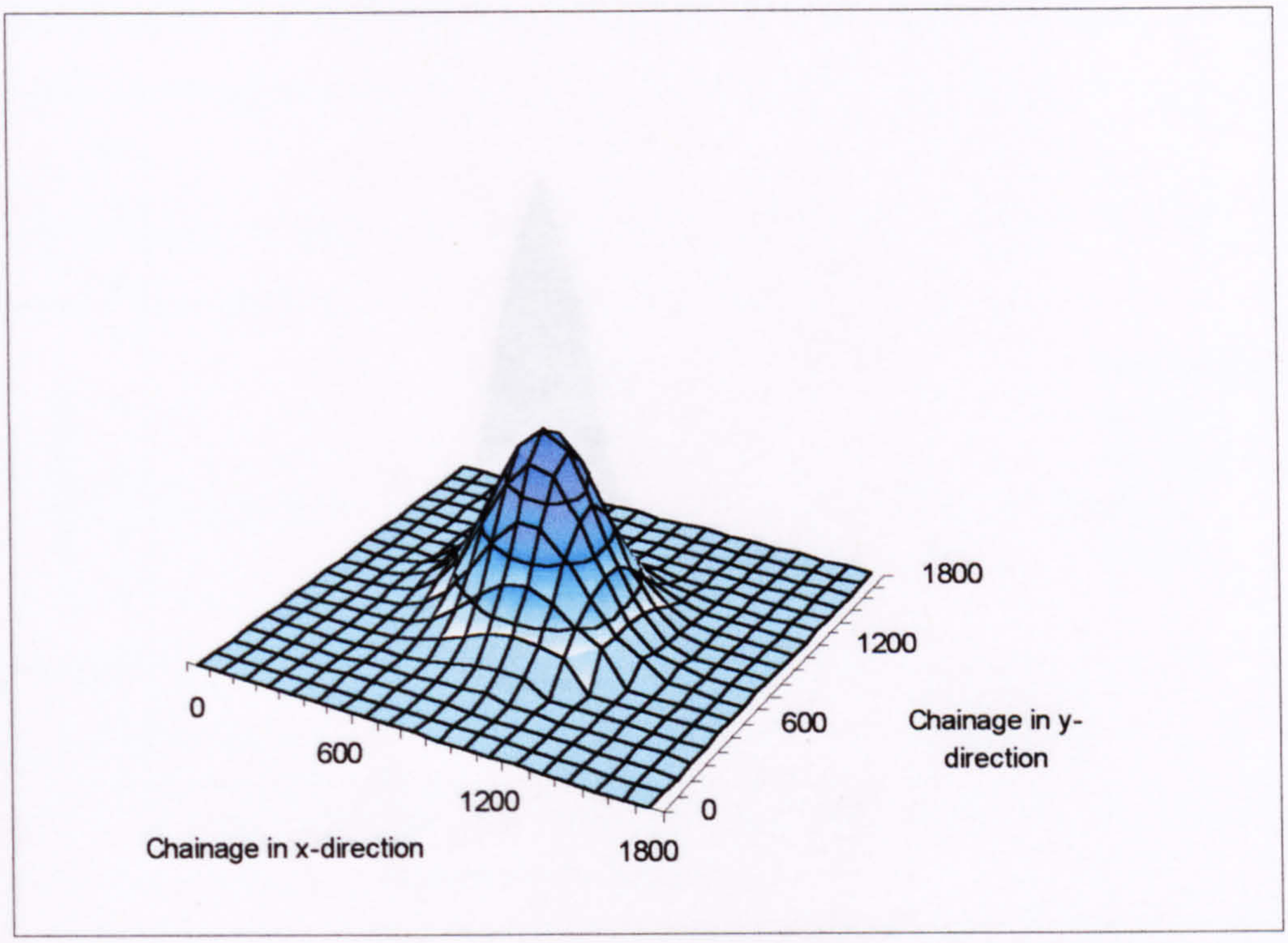

Figure (5.21) Advected Gaussian distribution using 2D Upwinding, t=400s, Cr=0.25

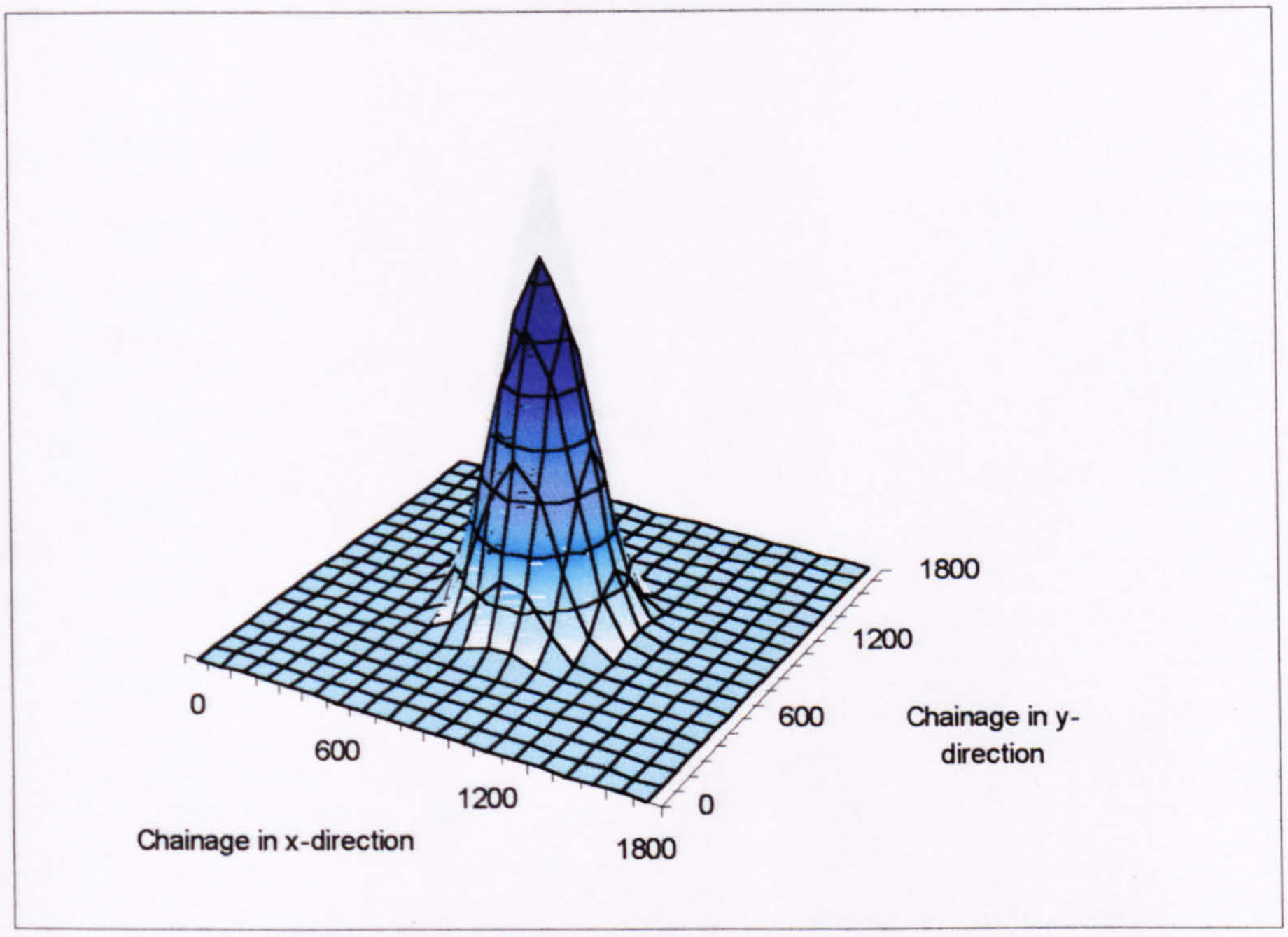

Figure (5.22) Advected Gaussian distribution using 2D QUICKEST, t=400s, Cr=0.25

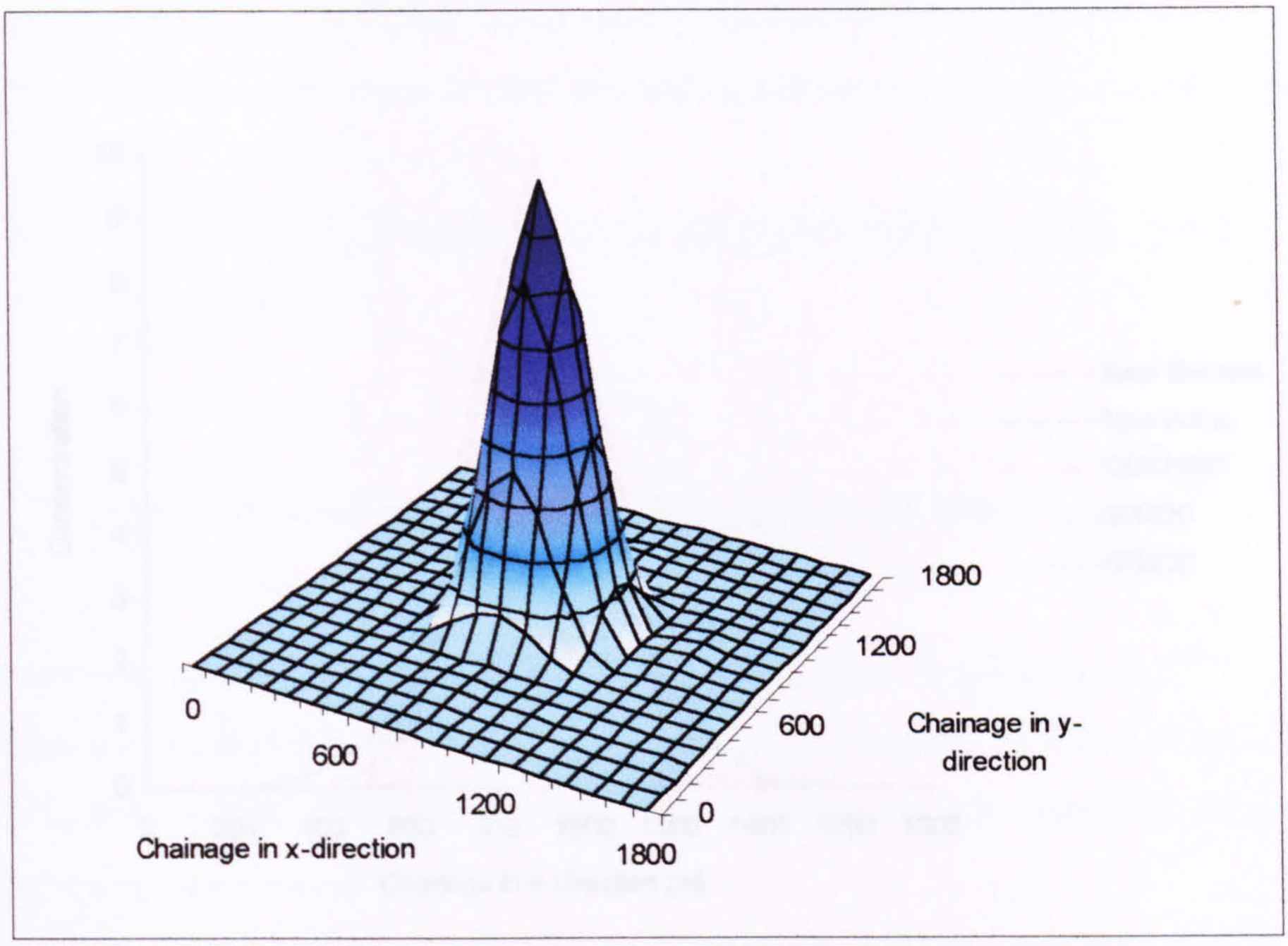

Figure (5.23) Advected Gaussian distribution using 2D 8PMOC, t=400s, Cr=0.25

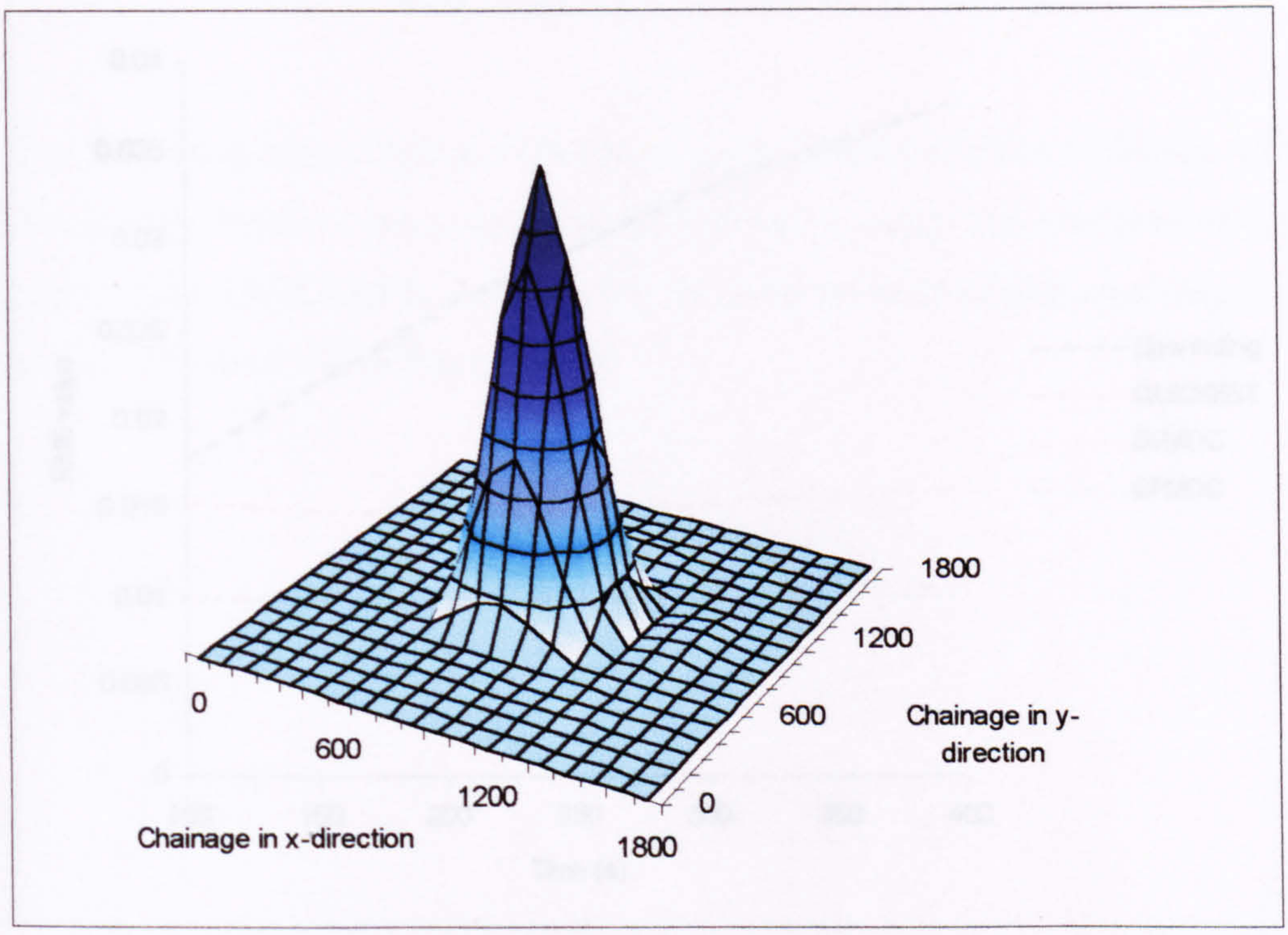

Figure (5.24) Advected Gaussian distribution using 2D 6PMOC=400s, Cr=0.25

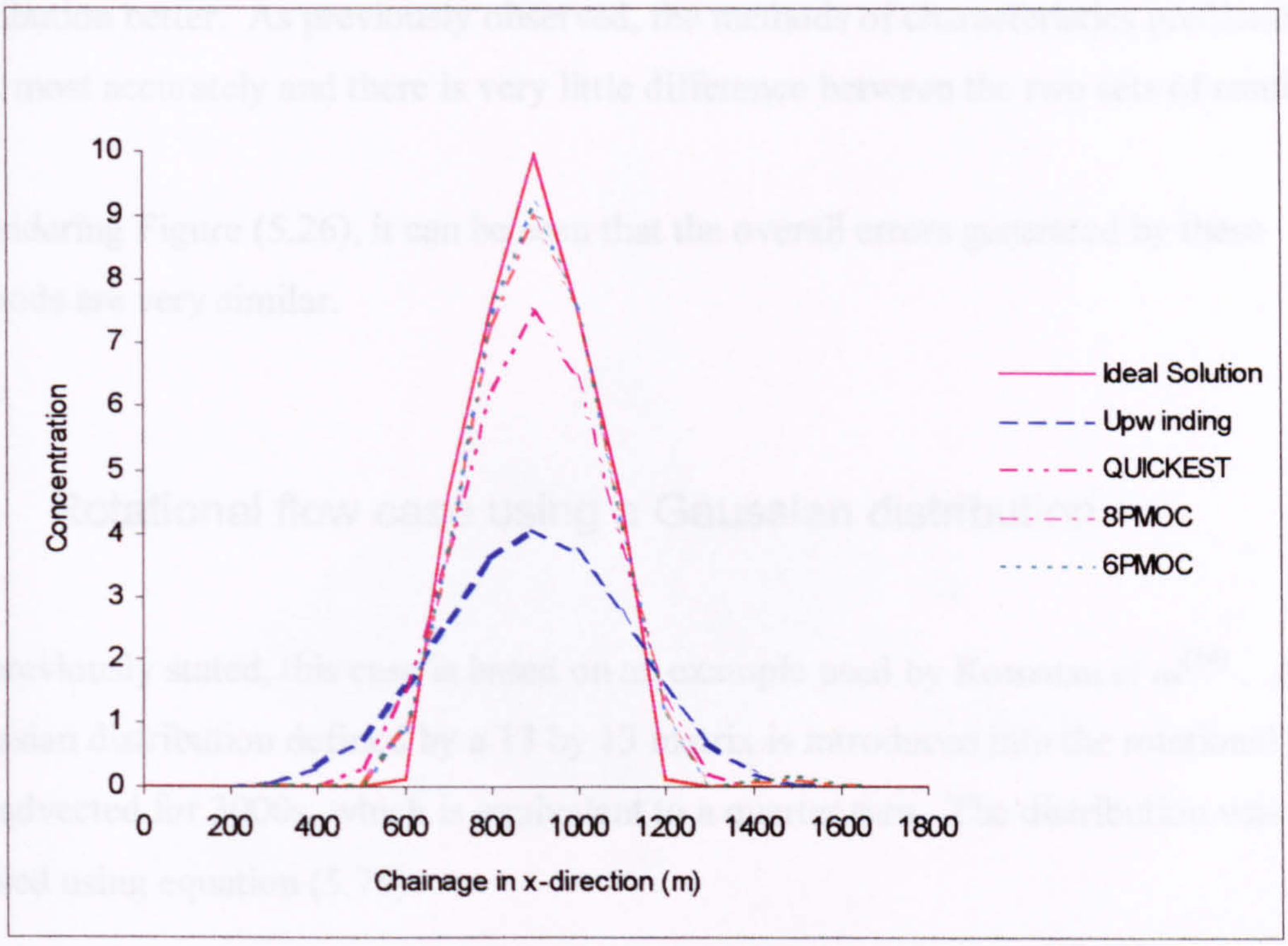

Figure (5.25) Cross-sections through predicted Gaussian distribution, t=400s, y=900m

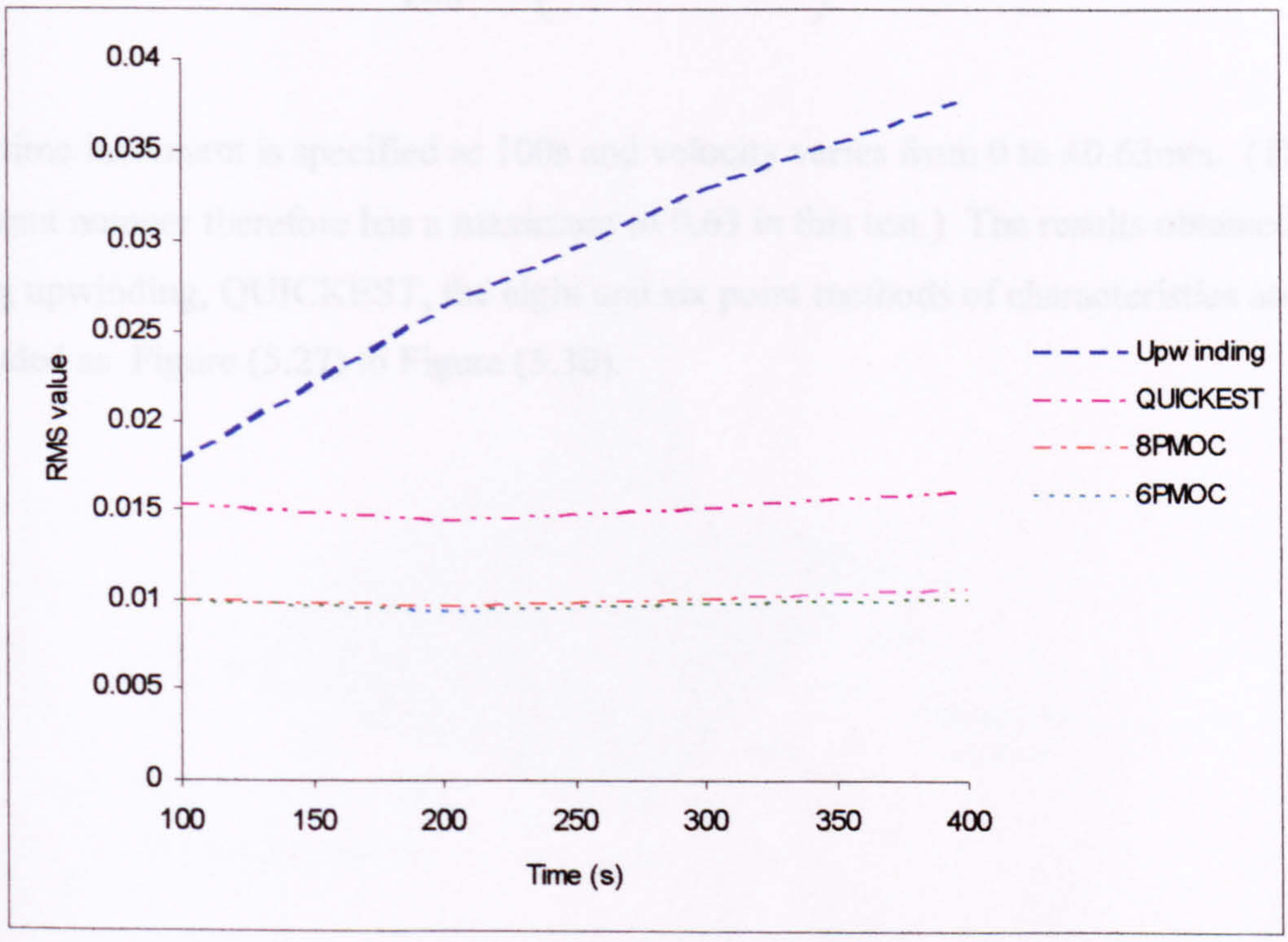

Figure (5.26) Root mean square values using a Gaussian distribution and Cr=0.25

QUICKEST also exhibits numerical diffusion, but maintains the shape of the distribution better. As previously observed, the methods of characteristics predict the peak most accurately and there is very little difference between the two sets of results.

Considering Figure (5.26), it can be seen that the overall errors generated by these methods are very similar.

5.2.2 Rotational flow case using a Gaussian distribution

As previously stated, this case is based on an example used by Komatsu *et al*[14]. A Gaussian distribution defined by a 13 by 13 matrix is introduced into the rotational flow and advected for 3000s, which is equivalent to a quarter turn. The distribution was derived using equation (5.76):

$$C = \frac{M}{\sqrt{2\pi}} \exp\left(-\frac{\Delta X^2}{2} - \frac{\Delta Y^2}{2}\right) \tag{5.76}$$

The time increment is specified as 100s and velocity varies from 0 to ±0.63m/s. (The Courant number therefore has a maximum of 0.63 in this test.) The results obtained using upwinding, QUICKEST, the eight and six point methods of characteristics are included as Figure (5.27) to Figure (5.30).

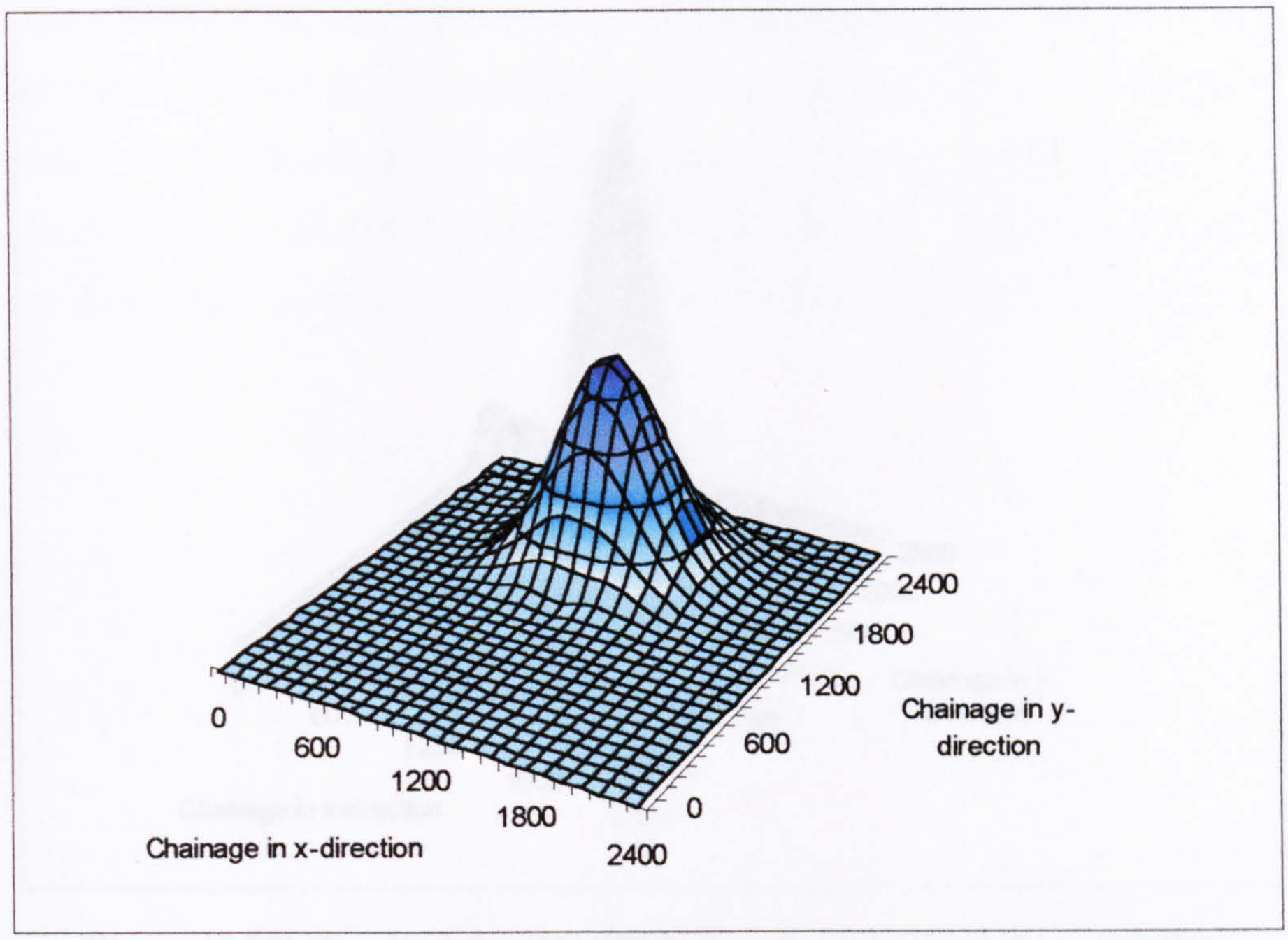

Figure (5.27) Results using 2D Upwinding and a rotational flow, t=3000s

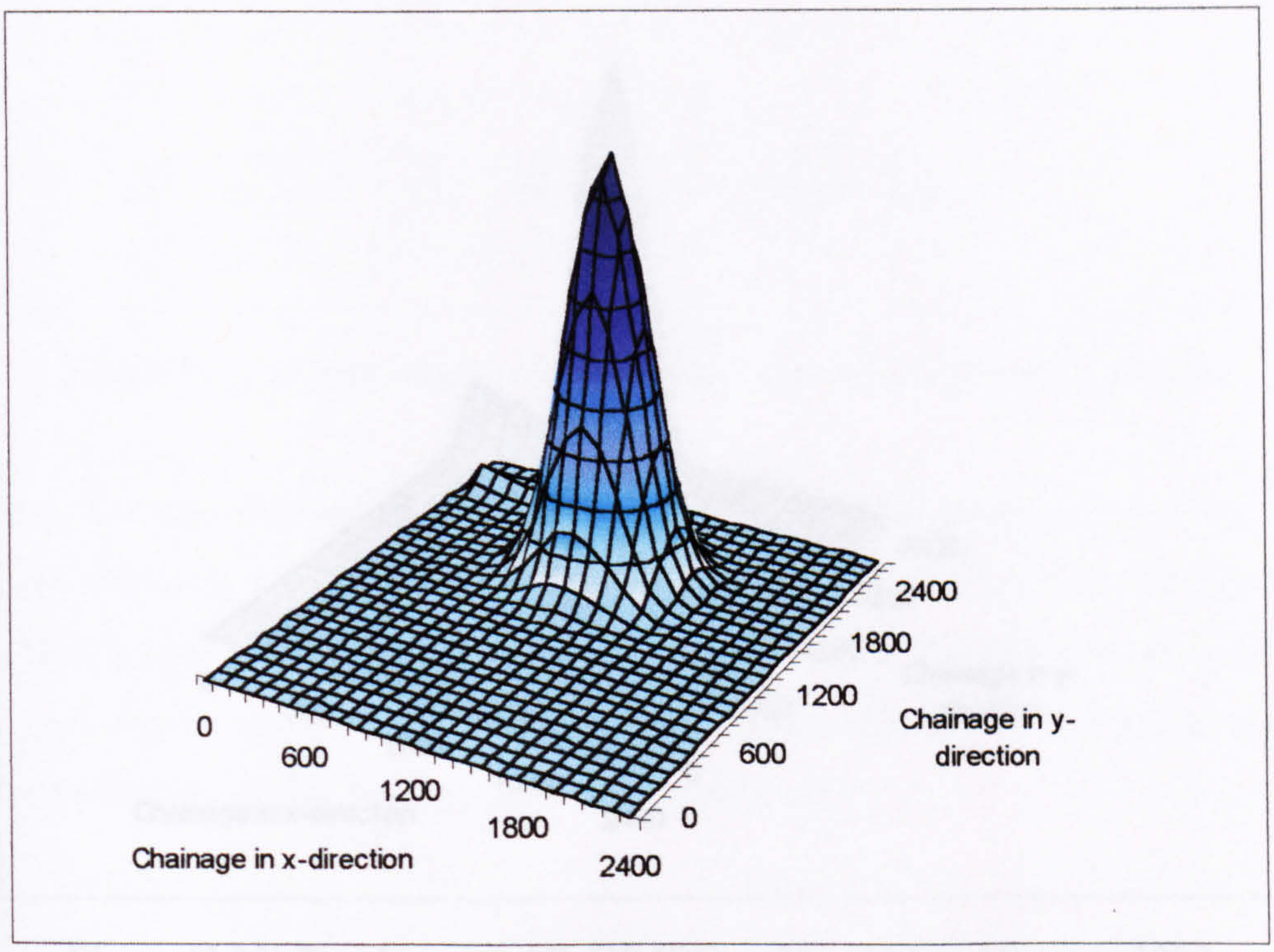

Figure (5.28) Results using 2D QUICKEST and a rotational flow, t=3000s

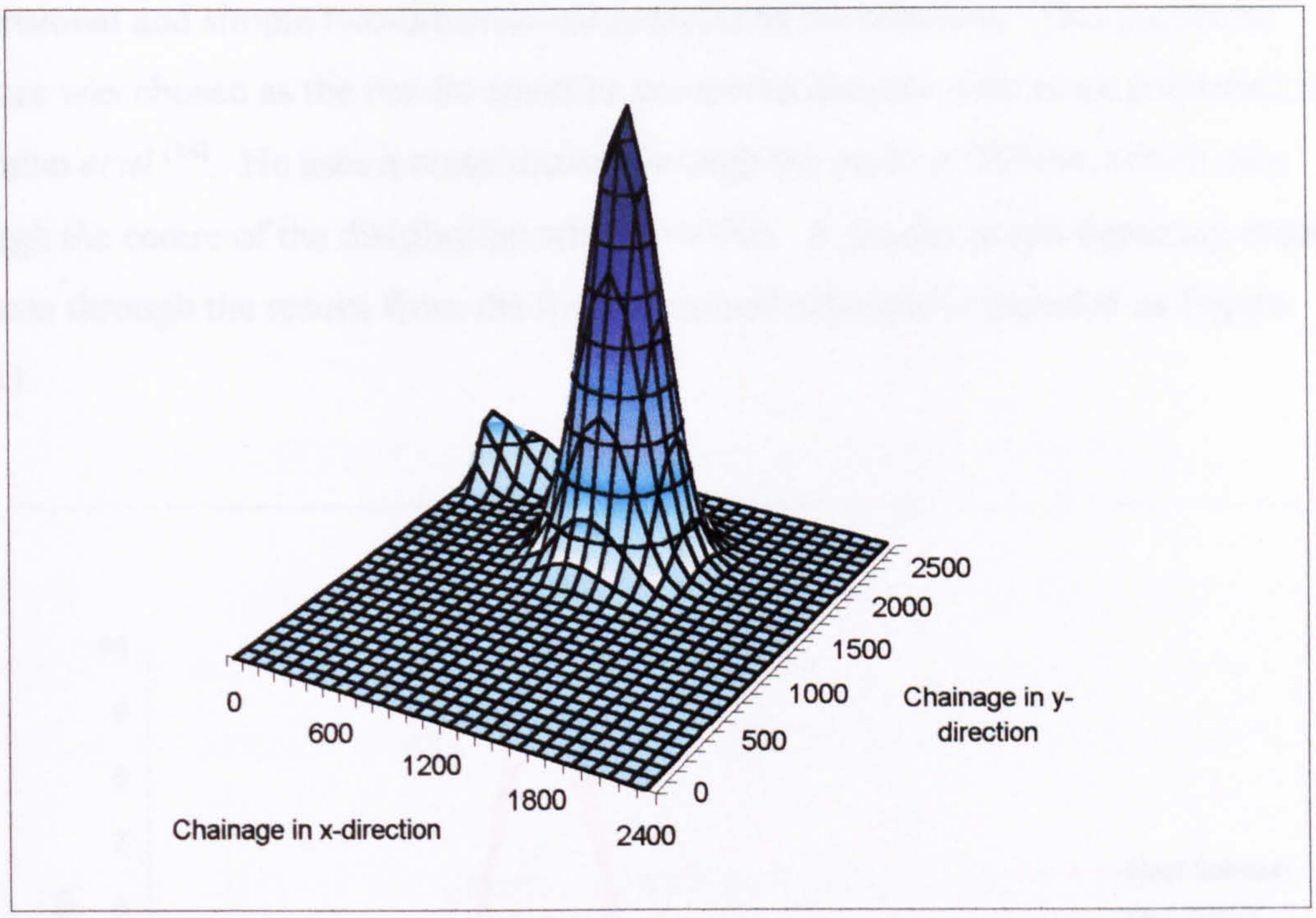

Figure (5.29) Results using 2D 8PMOC and a rotational flow, t=3000s

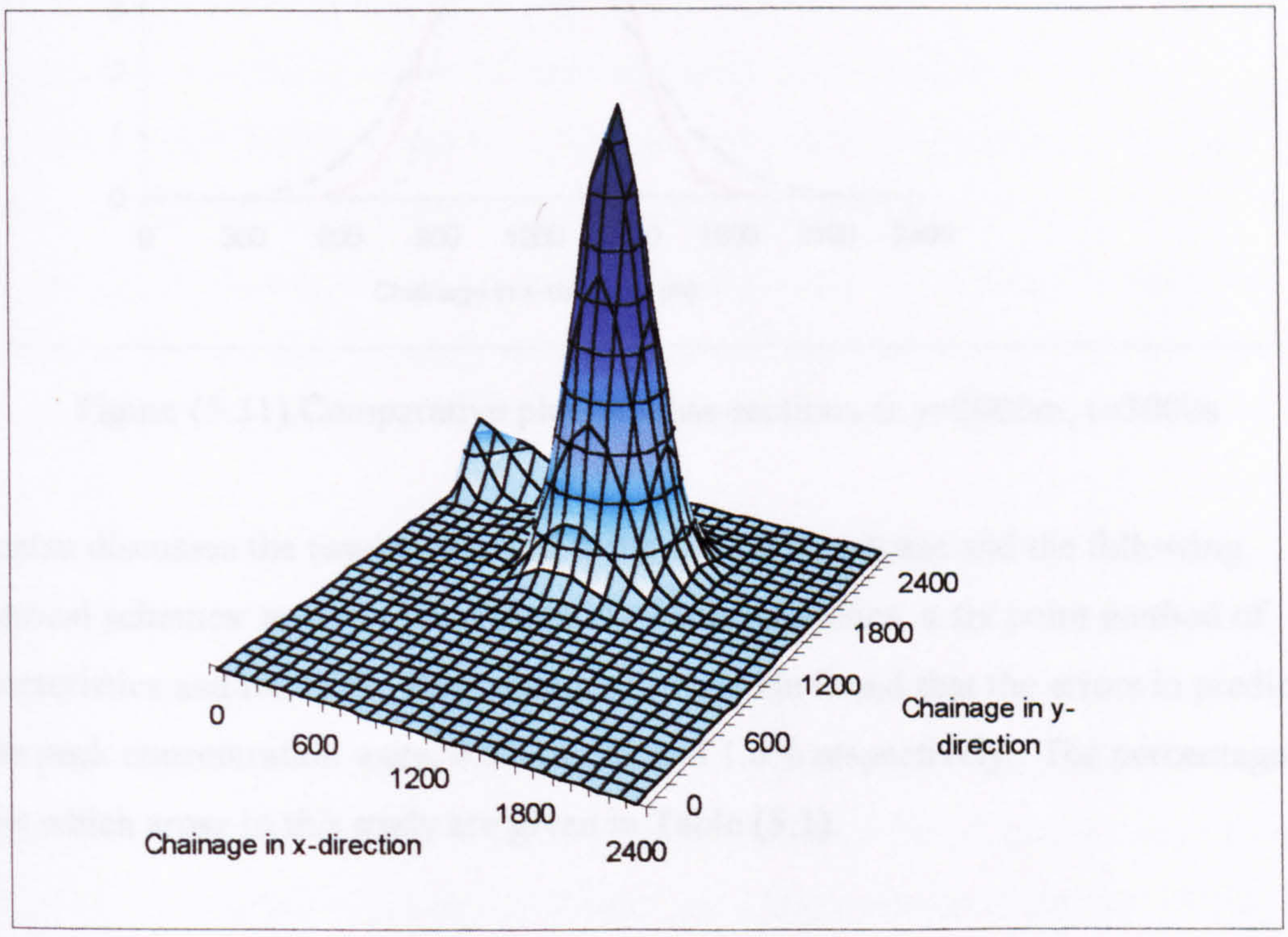

Figure (5.30) Results using 2D 6PMOC and a rotational flow, t=3000s

The general results are as would be expected, given the observations made from one-dimensional and simple two-dimensional analysis of the schemes. This particular testcase was chosen as the results could be compared directly with work published by Komatsu *et al* [14]. He uses a cross section through the point y=2000m, which cuts through the centre of the distribution when t=3000s. A similar graph depicting cross-sections through the results from the four numerical schemes is included as Figure (5.31).

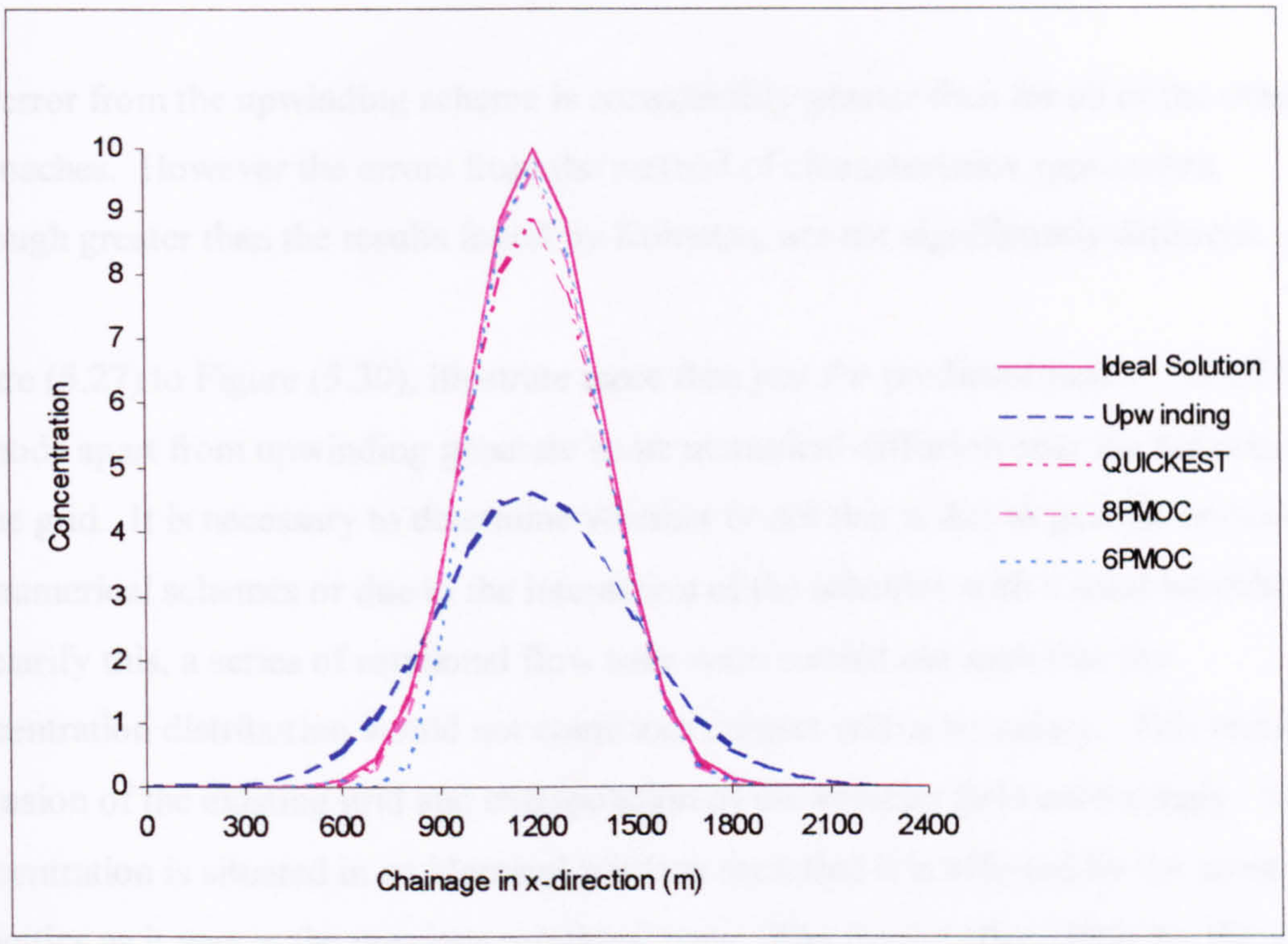

Figure (5.31) Comparative plot of cross-sections at y=2000m, t=3000s

Komatsu discusses the results obtained using the same testcase and the following numerical schemes: an eight point method of characteristics, a six point method of characteristics and the Holly-Preissmann scheme. He found that the errors in prediction of the peak concentration were, 0.5%, 1.1% and 1.8% respectively. The percentage errors which arose in this study are given in Table (5.1).

Numerical Method	% error
Upwinding	53.6
QUICKEST	12.1
8PMOC	4.1
6PMOC	2.9

Table (5.1) Table of percentage error in prediction of the peak

The error from the upwinding scheme is considerably greater than for all of the other approaches. However the errors from the method of characteristics approaches, although greater than the results found by Komatsu, are not significantly different.

Figure (5.27) to Figure (5.30), illustrate more than just the predicted peaks. All of the methods apart from upwinding generate some numerical diffusion near the boundaries of the grid. It is necessary to determine whether or not this is due to generic errors in the numerical schemes or due to the interaction of the schemes with a solid boundary. To clarify this, a series of rotational flow tests were carried out such that the concentration distribution would not come into contact with a boundary. This required extension of the existing grid and extrapolation of the velocity field accordingly. The concentration is situated in an identical position such that it is affected by the same velocities as it was in the previous rotational tests. The results after 3000s for the six point method of characteristics is included here by way of example as Figure (5.32).

The diagram shows that when the concentration does not interact with the boundary, the six point method of characteristics does not predict a solution which includes these numerical inaccuracies. It can therefore be concluded that the numerical scheme is not inherently inaccurate or unstable, but this approach as it stands, does not cope well if it interacts with solid boundaries. This is the same for QUICKEST and the eight point method of characteristics. As these schemes use a large number of points in their solution, five, six or eight, they encounter the boundary at more points than the upwinding scheme which uses only two points. Therefore some further work must include analysis of these schemes at boundaries.

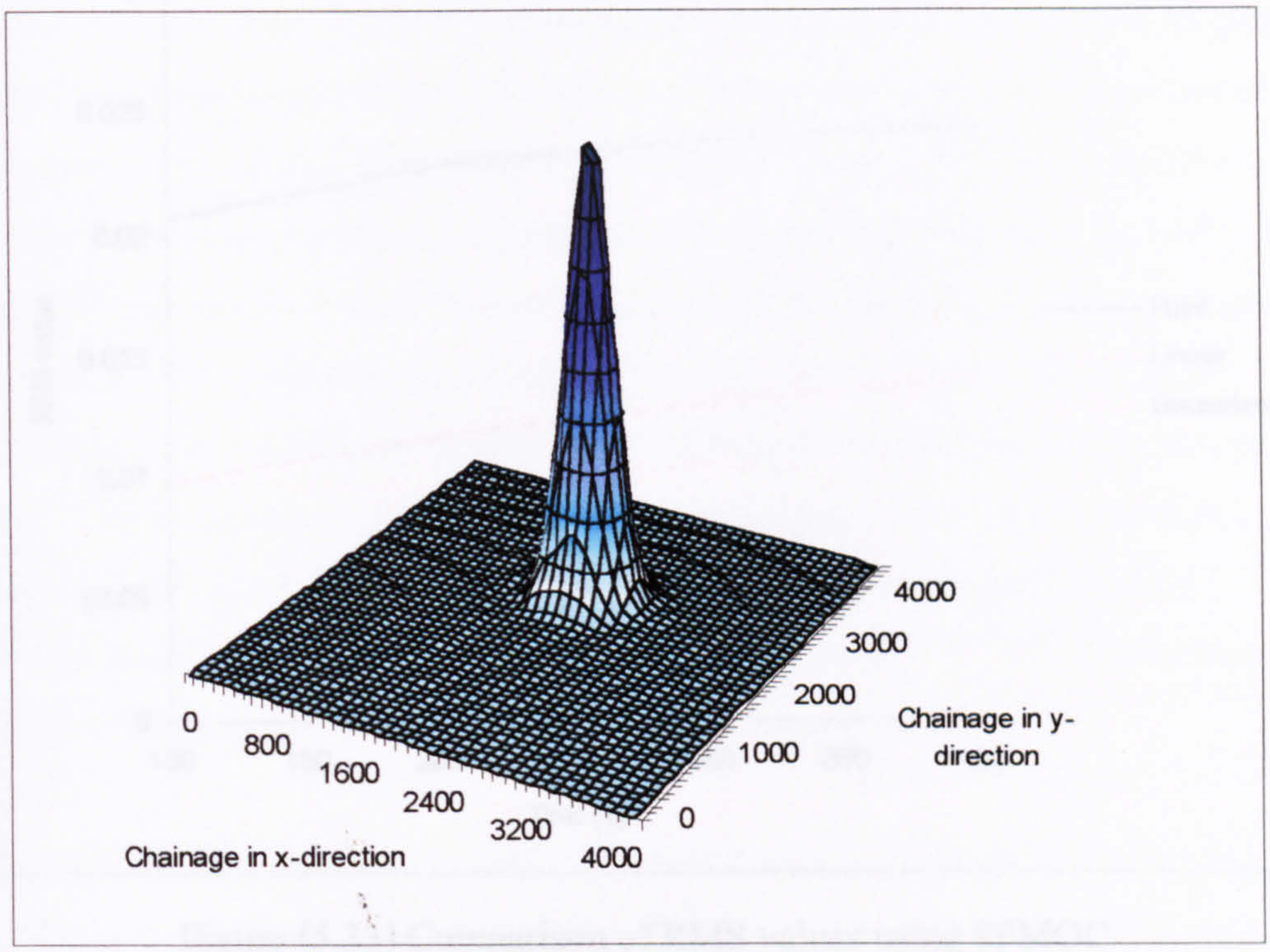

Figure (5.32) Extended rotational case using 6PMOC, t=3000s

5.3 Conclusions

The conclusions made here are corroborated by those made in the chapters discussing one- dimensional finite difference schemes and method of characteristics.

When considering the selection of a numerical scheme many factors must be taken into account. The numerical accuracy of a scheme is very important. The shape of the pollution distribution has a significant effect on the ability of a numerical scheme to accurately predict the advected solution.[15] Consider Figure (5.33), which compares the root mean square values calculated for the eight point method of characteristics, using a time increment of 25 seconds for the three distributions in the diagonal channel.

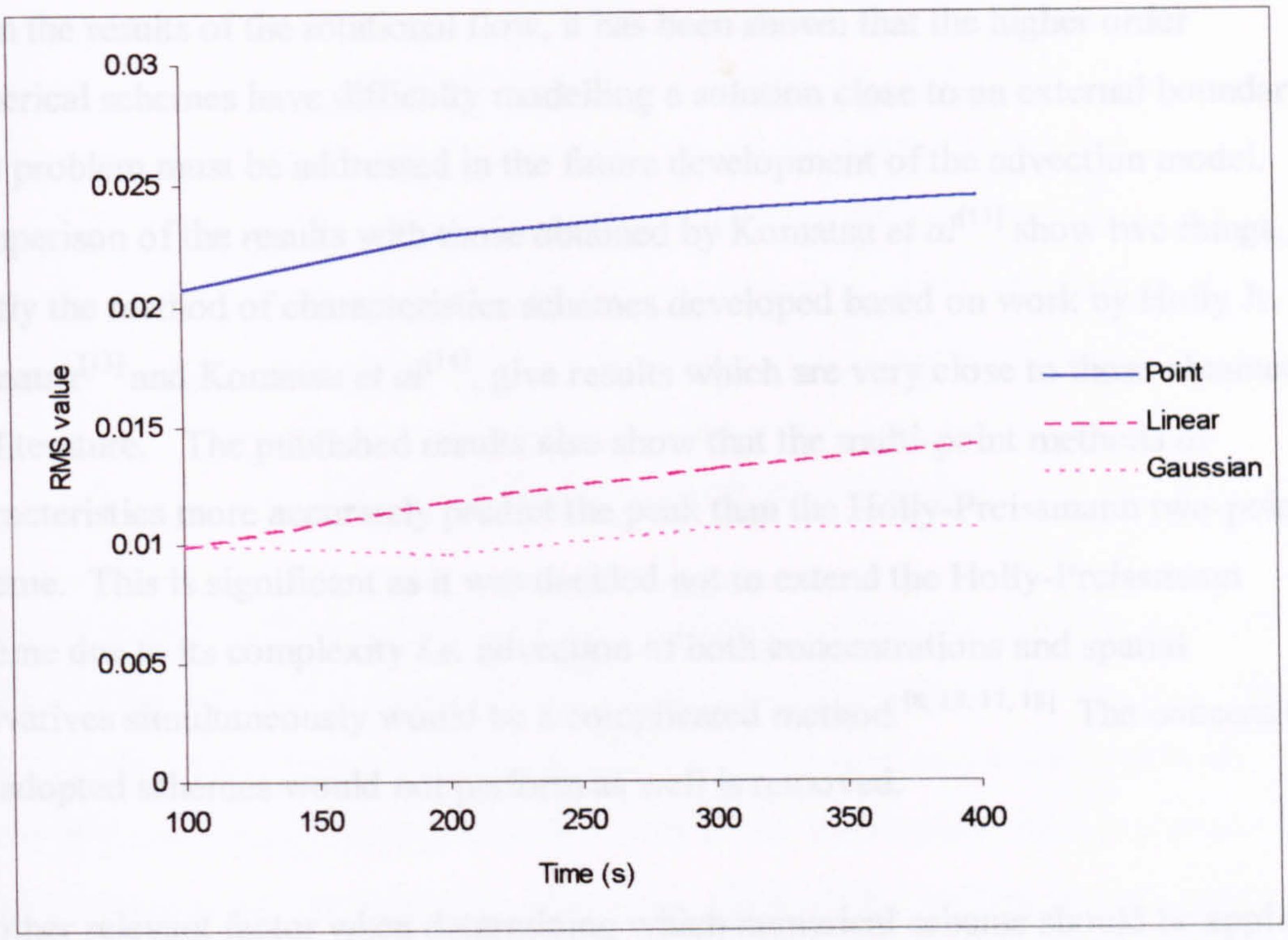

Figure (5.33) Comparison of RMS values using 8PMOC

There is some overlap between the linear and Gaussian distributions in the beginning of the calculation, but as time progresses, they become more distinguishable. The root mean square values decrease as the distribution becomes more refined. This suggests that the methods tested do not cope well with distinct variations in concentration gradients. In practice this is significant for two reasons. Firstly a numerical scheme used in industry should be able to accurately predict a pollutant's motion regardless of its shape. Secondly, it gives rise to the question of how this failing is dealt with. It could be remedied by further developing the numerical scheme by introducing a universal limiter such as used by Leonard[15, 16] in the development of the Ultimate scheme. An alternative is to highly refine the grid where the pollutant is released such that it becomes more defined. The main requirement with this technique is generating nested boundary conditions, which can also be complicated.

The results also confirm that the methods of characteristics predict significantly more accurate solutions than the finite differences considered. However they are also subject to numerical dispersion at the extremities of the solution. This is also important as these can become sources of instabilities as the solution progresses.

From the results of the rotational flow, it has been shown that the higher order numerical schemes have difficulty modelling a solution close to an external boundary. This problem must be addressed in the future development of the advection model. Comparison of the results with those obtained by Komatsu *et al*[14] show two things. Firstly the method of characteristics schemes developed based on work by Holly Jr. and Komatsu[13] and Komatsu *et al*[14], give results which are very close to those obtained in the literature. The published results also show that the multi-point methods of characteristics more accurately predict the peak than the Holly-Preissmann two-point scheme. This is significant as it was decided not to extend the Holly-Preissmann scheme due to its complexity *i.e.* advection of both concentrations and spatial derivatives simultaneously would be a complicated method.[8, 13, 17, 18] The concern that the adopted schemes would not perform as well is removed.

Another relevant factor when determining which numerical scheme should be applied to a specific problem is the complexity of the equations used. In practice numerical schemes are derived and then coded into a computer model. The ease with which they can be derived and inserted must be taken into consideration. In this study each method was coded using Fortran 77 into the pre-existing DIADEM3D model.

The upwinding scheme is very simple to derive and also to transform into Fortran 77.[15] The mathematics associated with the relevant equations are straightforward and easy to understand.[12] The QUICKEST scheme is more complex and takes longer to physically derive and to then apply in the computer model. A great deal of careful manipulation of the equations and their corresponding variables are required as the scheme incorporates 25 points in two-dimensions. The eight and six points methods of characteristics are also difficult to derive and again due to the fact that they utilise 64 and 36 points it is difficult to code these schemes correctly.

The last main concern is the time taken to carry out a simulation using a specific numerical scheme. The times to complete the smaller rotational testcase using a Gaussian distribution were recorded and are included here as Table (5.2). All other conditions were constant, only the method was altered. The computer used in the simulation was an IBM PC clone incorporating an AMD K6-2-380MHZ processor.

Numerical Method	Time (mm:ss)
Upwinding	15:36
QUICKEST	22:57
8PMOC	22:44
6PMOC	22:23

Table (5.2) Times to complete simulation

Using the results of the three main criteria, accuracy, complexity and time, it must be decided which attribute is most valuable under the circumstances.[19] The upwinding scheme suffers from extreme numerical diffusion compared to the other methods. However it takes approximately 30% less time in the simulations and it is considerably easier to develop the corresponding equations. QUICKEST and the two methods of characteristics are all more difficult to derive and to code. Their execution times are also very similar. In terms of accuracy, however, the QUICKEST scheme consistently underpredicts the peak by a greater margin. It should also be noted that the QUICKEST scheme requires fewer points in two-dimensions and so uses less space on the grid, which is significant when considering interaction with external boundaries. Depending on what is most important to the user, these factors must be considered carefully to make the correct choice for any given circumstances.

5.4 References

1. Falconer, R.A., "Flow and Water-Quality Modeling in Coastal and Inland Water", *Journal of Hydraulic Research*, 1992, **30**(4), 437-452.

2. Karpik, S.R. and Crockett, S.R., "Semi-Lagrangian algorithm for two-dimensional advection-diffusion equation on curvilinear coordinate meshes", *Journal of Hydraulic Engineering-Asce*, 1997, **123**(5), 389-401.

3. Komatsu, T., Ohgushi, K., Asai, K., and Holly Jr., F.M., "Accurate numerical simulation of scalar advective transport", *Journal of Hydroscience and hydraulic Engineering*, 1989, **7**(1), 63-73.

4. Vested, H.J., Justesen, P., and Ekebjaerg, L., "Advection-Dispersion Modeling in 3 Dimensions", *Applied Mathematical Modelling*, 1992, **16**(10), 506-519.

5. Leonard, B.P., "A stable and accurate convective modelling procedure based on quadratic upstream interpolation", *Computer methods in applied mechanics and engineering*, 1979, **19**, 59-98.

6. Falconer, R.A., Liu, S.Q., and Chen, Y. *Application of higher order accurate schemes for advective transport in a 2D water quality model.* in *Hydraulic and Environmental Modelling: Coastal waters, Procedings of the 2nd International Conference on Hydraulic and Environmental Modelling of Coastal, Estuarine and River Waters.* 1992.

7. Chen, Y.P. and Falconer, R.A., "Modified Forms of the 3rd-Order Convection, 2nd-Order Diffusion Scheme For the Advection-Diffusion Equation", *Advances in Water Resources*, 1994, **17**(3), 147-170.

8. Chen, Y.P. and Falconer, R.A., "Advection Diffusion Modeling Using the Modified Quick Scheme", *International Journal For Numerical Methods in Fluids*, 1992, **15**(10), 1171-1196.

9. Davis, R.W. and Moore, E.F., "A numerical study of vortex shedding from rectangles", *Journal of Fluid Mechanics*, 1982, **116**, 475-506.

10. Ekebjaerg, L. and Justesen, P., "An Explicit Scheme For Advection Diffusion Modeling in 2 Dimensions", *Computer Methods in Applied Mechanics and Engineering*, 1991, **88**(3), 287-297.

11. Leonard, B.P. and Niknafs, H.S., "Sharp Monotonic Resolution of Discontinuities Without Clipping of Narrow Extrema", *Computers & Fluids*, 1991, **19**(1), 141-154.

12. Abbott, M.B. and Basco, D.R., *Computational Fluid Dynamics; An Introduction for Engineers.* 1989: Longman Scientific and Technical.

13. Holly Jr., F.M. and Komatsu, T. *Derivative approximations in the two-point fourth order method for pollutant transport.* in *Frontiers in Hydraulic Engineering.* 1983. MIT, MA: ASCE.

14. Tamamidis, P. and Assanis, D.N., "Evaluation of various higher-order-accuracy schemes with and without flux limiters", *International Journal of Numerical Methods in Fluids*, 1993, **16**, 931-948.

15. Leonard, B.P., "The Ultimate Conservative Difference Scheme Applied to Unsteady One-Dimensional Advection", *Computer Methods in Applied Mechanics and Engineering*, 1991, **88**(1), 17-74.

16. Komatsu, T., Holly, F.M., Nakashiki, N., and Ohgushi, K., "Numerical calculation of pollutant transport in one and two-dimensions", *Journal of Hydroscience and Hydraulic Engineering*, 1985, **3**, 15-30.

17. Glass, J. and Rodi, W., "A higher order numerical scheme for scalar transport", *Computer methods in applied mechanics and engineering*, 1982, **31**, 337-358.

18. Asai, K., Komatsu, T., Shiomi, H., and Ohgushi, K. *Development of a simple and high-accurate scheme for 1D diffusion simulation.* in *HYDRA 2000*. 1995: Thomas Telford.

19. Croucher, A.E. and O'Sullivan, M.J., "Numerical methods for contaminant transport in rivers and estuaries", *Computers & Fluids*, 1998, **27**(8), 861-878.

Chapter 6

Inclusion of a Spatial Reachout Scheme

6.1 Introduction 179

6.2 The limitations of numerical schemes when Cr>1 180

6.3 Definition of spatial reachout 182

6.4 Testing of the spatial reachout scheme 184

6.5 Conclusions 188

6.6 References 190

6.1 Introduction

It is the ultimate aim of this work to develop a numerical scheme which can be used to accurately model pollution advection. One of the problems in applying a numerical scheme to such a situation is that, for computational efficiency, the time increments used are often large. This directly affects the Courant number, which may exceed unity, the maximum Courant number that has been considered so far.

The spatial reachout scheme is one of several methods which allows the time step to be increased, without causing numerical instability, when applying the method of characteristics.[1-5] Other options include temporal reachback, spatial reachback, multimode and implicit approaches.[6-11]

Early work on spatial reachout was based on research carried out by Lister[12]. He proposed a process in which the characteristic lines intersected the first grid interval on either side of an interior location on a rectangular grid. This was enhanced by Vardy[13], who developed the approach such that the characteristics were able to intersect grids further out than just the first interval. This allowed the use of larger time increments whilst simultaneously meeting the stability criteria required by the Courant condition.

The method proposed by Vardy was implemented by Wiggert and Sundquist[4] in the analysis of pipeline transients using a linear interpolation scheme. It was found that as the time increment increased, both numerical error and computational time were reduced. These are desirable effects in any numerical scheme. The approach has also been adapted for use with the Holly-Preissmann scheme, where similar observations have been made.[1, 9] As yet this approach has not been used in conjunction with multi-point methods of characteristics. This development will be addressed here.

6.2 The limitations of numerical schemes when Cr>1

The upwinding and QUICKEST finite difference schemes and the eight and six point methods of characteristics, have been shown to be numerically stable when using a Courant number less than or equal to one. They all suffer from some form of numerical deficiency, but the schemes tend to be stable. However this is not the case at Courant numbers exceeding one.

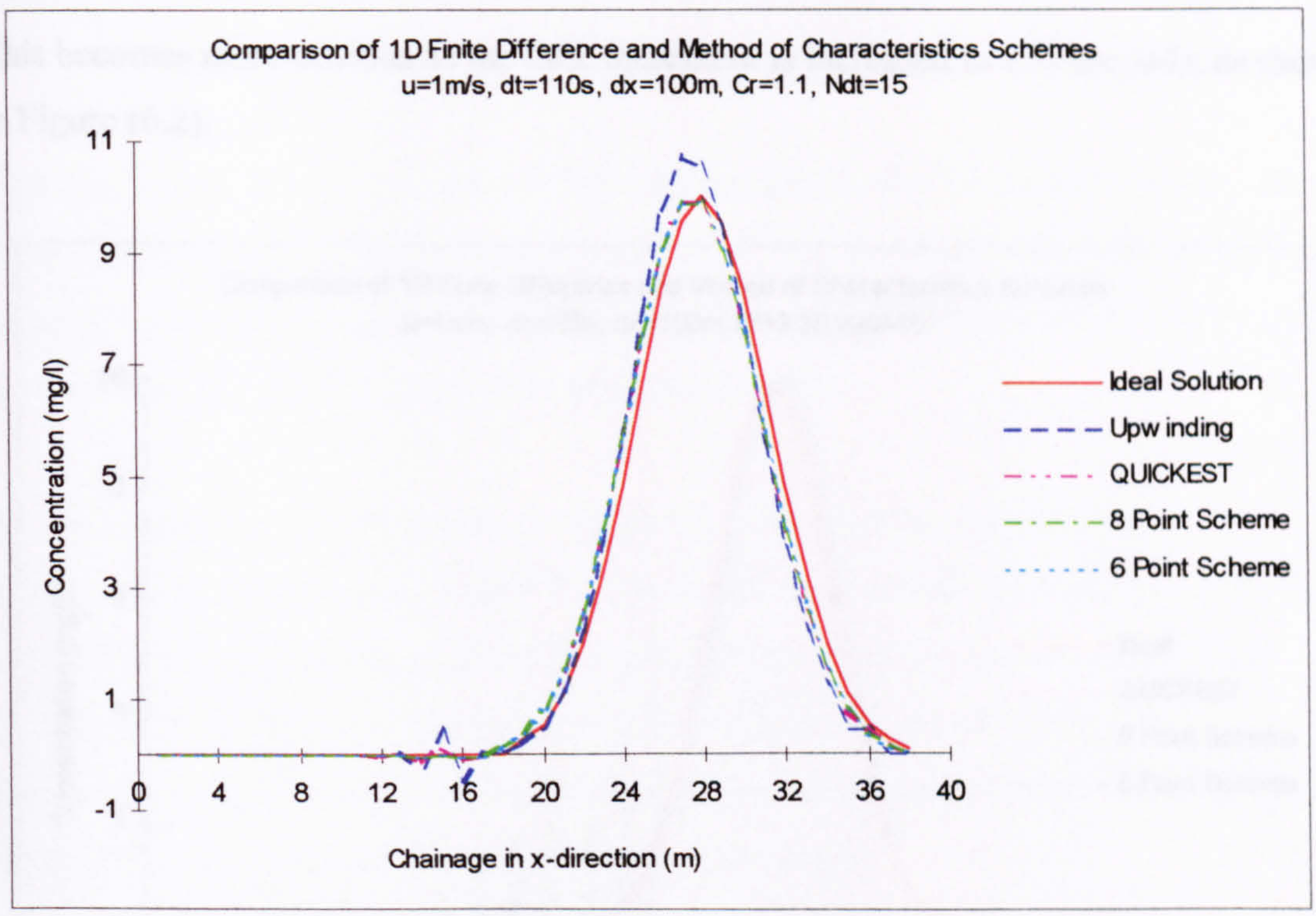

Figure (6.1) Results using a 1D Gaussian distribution and a Courant number of 1.1

A series of one-dimensional tests were carried out to examine the behaviour of the four numerical schemes at Courant numbers greater than one. Figure (6.1) depicts the results of advecting a Gaussian distribution of pollution in the same one-dimensional testcase used in Section 3.2 and 4.2, for a Courant number of 1.1.

The results show that upwinding is subject to numerical dispersion at this slightly higher Courant number. This is contradictory to the results for the situation where the Courant number is less than one: of all the schemes tested upwinding is the only one which has

never displayed signs of dispersion. The peak is also overpredicted which is also in contrast to previous results in which the solution has always been numerically diffused.

Close inspection of the results of the QUICKEST, eight point and six point schemes show that they all produced similar results. Although the overall results demonstrate reasonable correlation with the ideal, there are oscillations present at the left hand extrema of the solution. The solutions also contain phase errors which are located to the left of the exact data.

This becomes more obvious as the time increment is increased to 155 seconds, as shown in Figure (6.2).

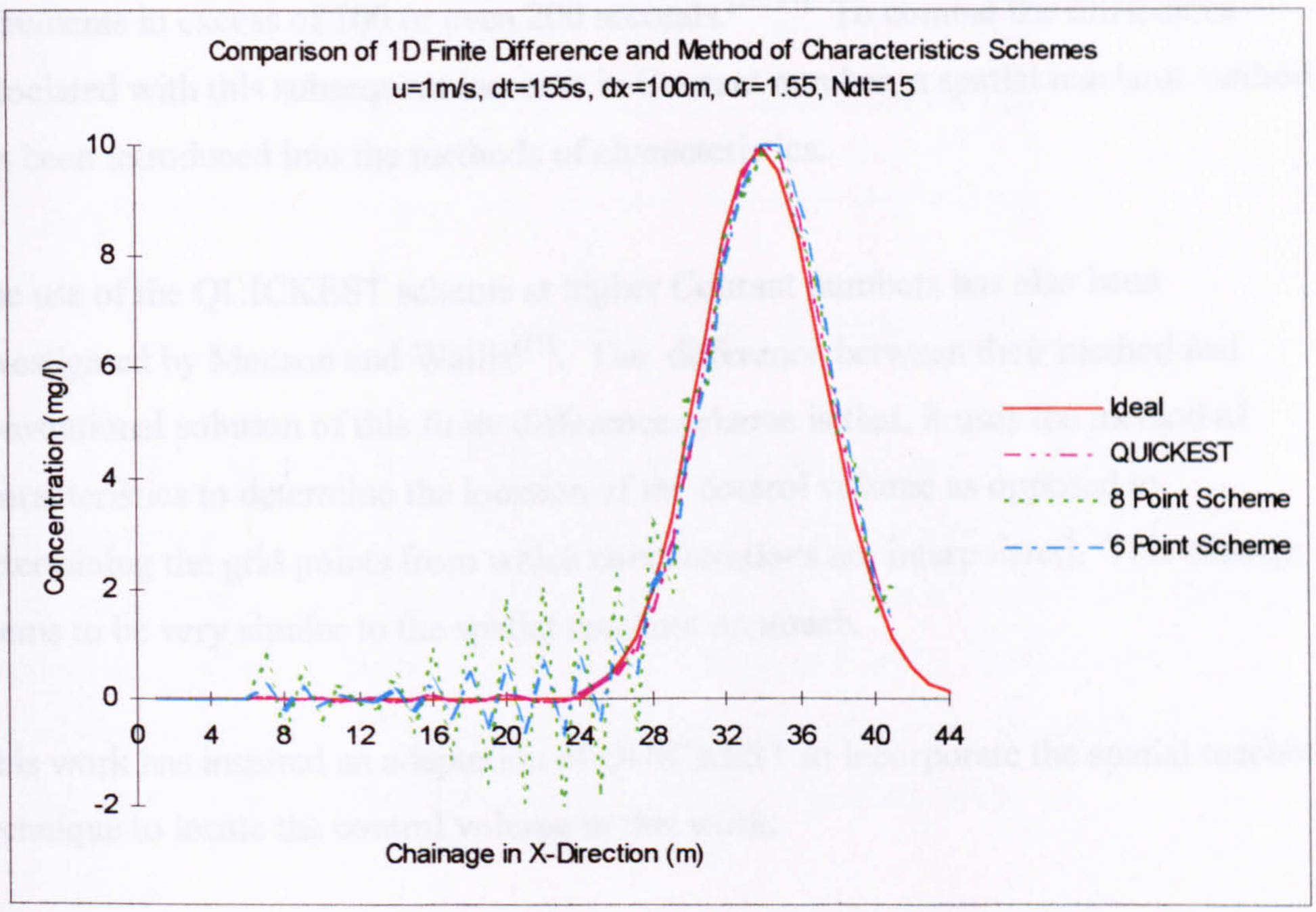

Figure (6.2) Results using a 1D Gaussian distribution and a Courant number of 1.55

There are clear signs of numerical dispersion in the solution under these conditions. The results from the upwinding scheme have been omitted as the scheme becomes highly unstable at Courant numbers exceeding 1.2.

If the Courant number is further increased to 1.6, the results for both methods of characteristics develop the beginnings of numerical instabilities. It may be concluded that the eight and six point methods of characteristics are stable and accurate for Courant numbers less than or equal to one and develop grid scale oscillations if this is increased.

The behaviour of QUICKEST over the range of Courant numbers from one to two has previously been discussed in Section 3.3. It was found that QUICKEST exhibits stability and accuracy at a Courant number of exactly two, but between one and two the scheme is unstable.[14, 15]

If the application is a coastal or estuarine environment, it may be desirable to use time increments in excess of 100 or even 200 seconds.[16, 17] To combat the difficulties associated with this subsequent increase in Courant number, a spatial reachout method has been introduced into the methods of characteristics.

The use of the QUICKEST scheme at higher Courant numbers has also been investigated by Manson and Wallis[17]. The difference between their method and conventional solution of this finite difference scheme is that, it uses the method of characteristics to determine the location of the control volume as opposed to determining the grid points from which concentrations are interpolated. This concept seems to be very similar to the spatial reachout approach.

This work has inspired an adaptation of QUICKEST to incorporate the spatial reachout technique to locate the control volume in this work.

6.3 Definition of spatial reachout

The spatial reachout approach applied here is based on the method used by amongst others, Lai[18] and Yang and Chiu[1]. Consider a simple one-dimensional example for illustrative purposes: an infinitely long channel with spatial increments of 100 metres

and constant velocity of 1m/s, (Figure (6.3)). Assume that the time increment is 350 seconds, thus the Courant number is calculated to be 3.5.

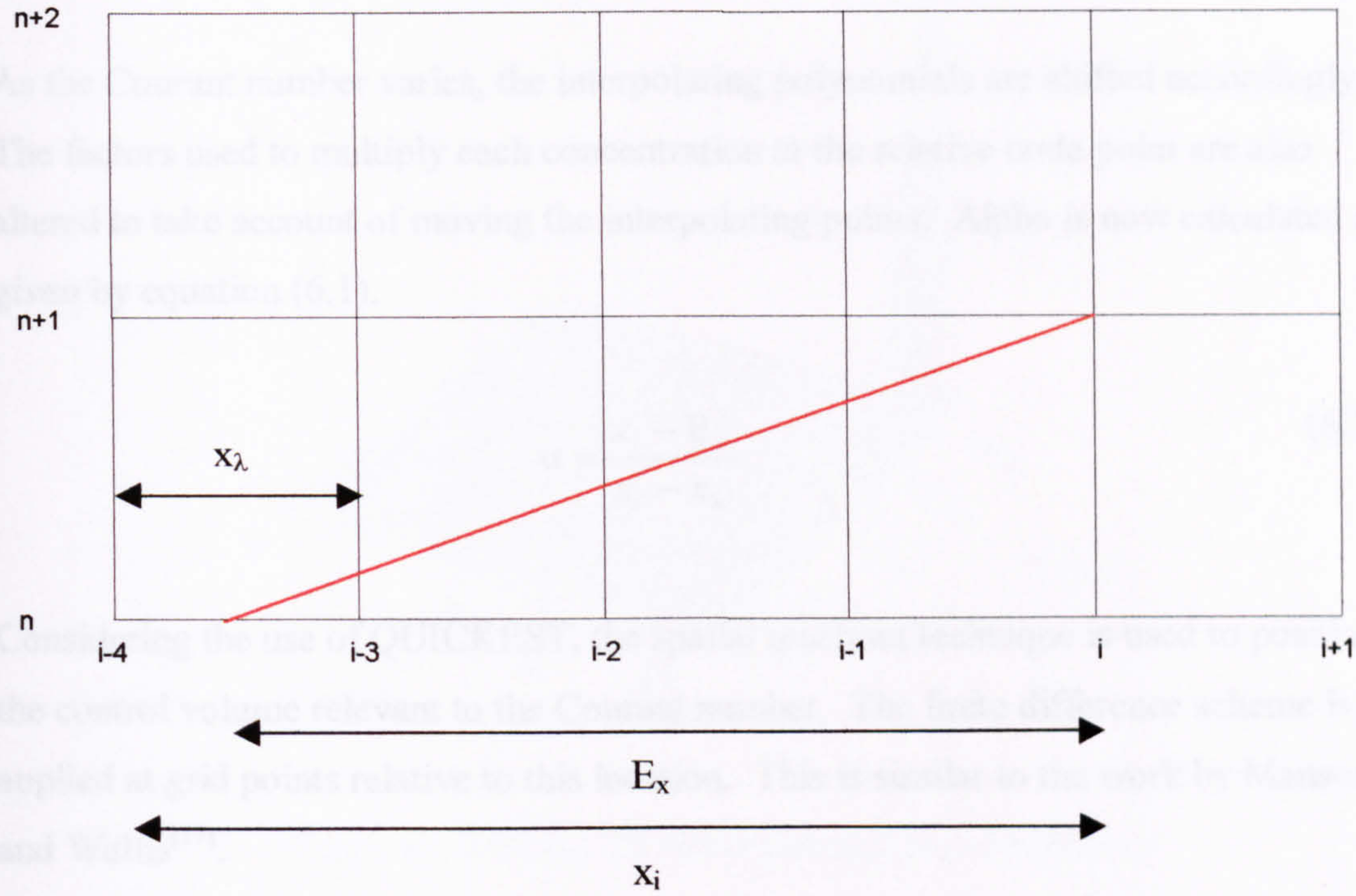

Figure (6.3) Example of a one-dimensional grid

If, for example, the eight point method of characteristics is used to calculate the concentration at location i at the next time step, n+1, the solution would be determined using expansions derived about the locations i and i-1. This is equivalent to the original form of the method of characteristics used in Chapters 4 and 5. Unfortunately it is already know that this will result in a highly unstable solution as the eight point method of characteristics is unstable for Courant numbers exceeding unity.

The spatial reachout scheme can be used to solve this problem. It involves the extension of the characteristics outwith the adjacent time lines, such that they intersect the spatial axis at the current time step.[1, 3] The location of this point of intersection will depend on the Courant number. Yang and Chiu[1] specify this in terms of a reachout number, λ.

In terms of the example, the characteristic will intersect the spatial axis at the current time step between locations i-3 and i-4. The interpolation is then carried out using the two node points on either side of the intersection.

As the Courant number varies, the interpolating polynomials are shifted accordingly. The factors used to multiply each concentration at the relative node point are also altered to take account of moving the interpolating points. Alpha is now calculated as given by equation (6.1).

$$\alpha = \frac{x_i - \mathrm{E}_x}{x_i - x_\lambda} \tag{6.1}$$

Considering the use of QUICKEST, the spatial reachout technique is used to position the control volume relevant to the Courant number. The finite difference scheme is then applied at grid points relative to this location. This is similar to the work by Manson and Wallis[17].

6.4 Testing of the spatial reachout scheme

A two-dimensional testcase is used here to test the inclusion of the spatial reachout scheme to the eight point method of characteristics and also QUICKEST.

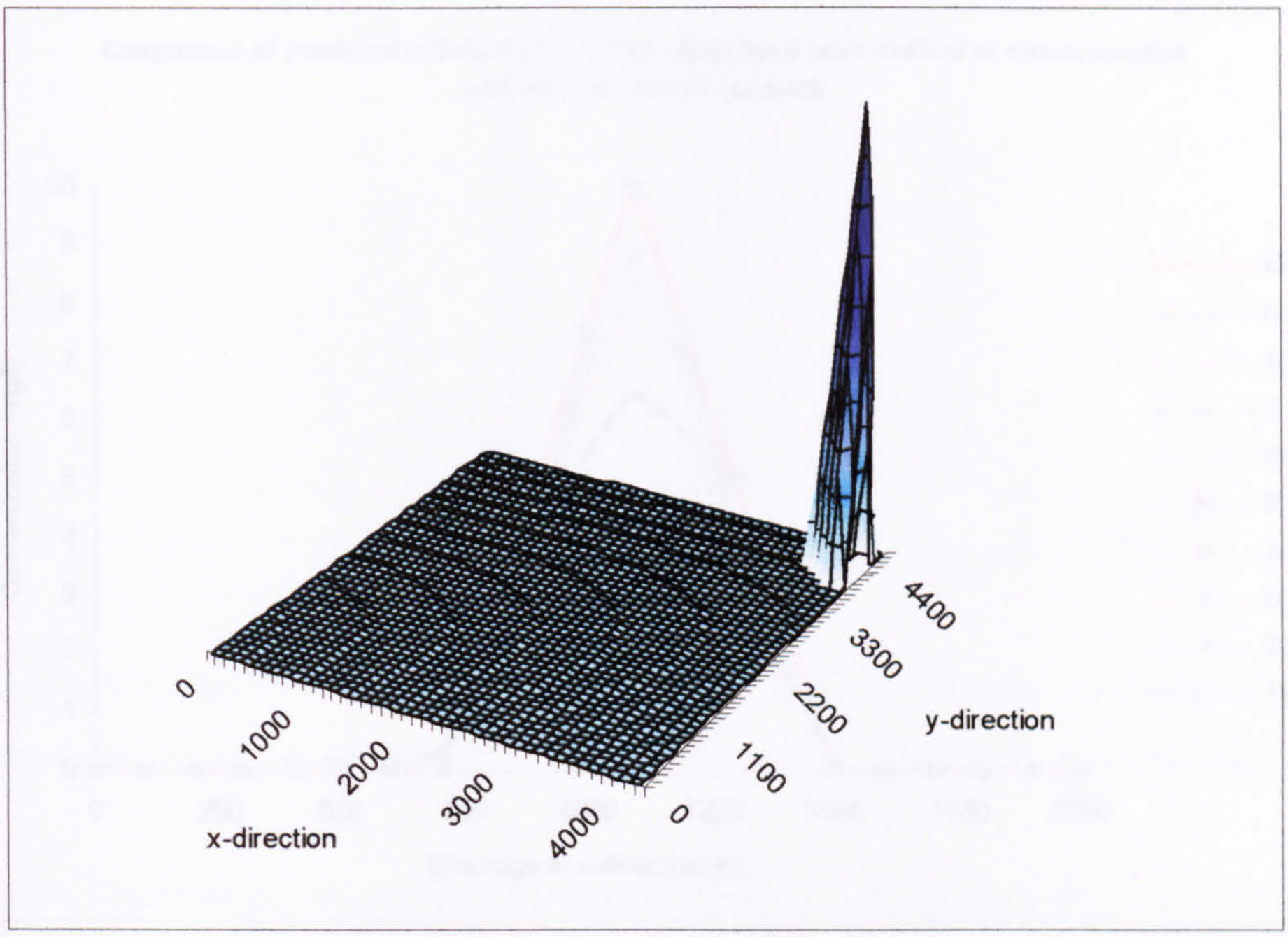

Figure (6.4) Initial 2D linear distribution of pollution

A diagonal channel is located in a 50 by 50 square grid with spatial increment of 100m in both the x and y-directions. The x and y-directional flows are –1m/s. A linear distribution of pollution is introduced into the flow centred at i=42, j=42 as shown in Figure (6.4). The results of advection of the contaminant are observed after 3000s.

Cross-sections of the pollution profiles at y=1100m are included as Figure (6.5) and (6.6). The percentage of the peak calculated using the eight point method of characteristics and QUICKEST, for Courant numbers between 0.5 and 15 is also shown in Table (6.1).

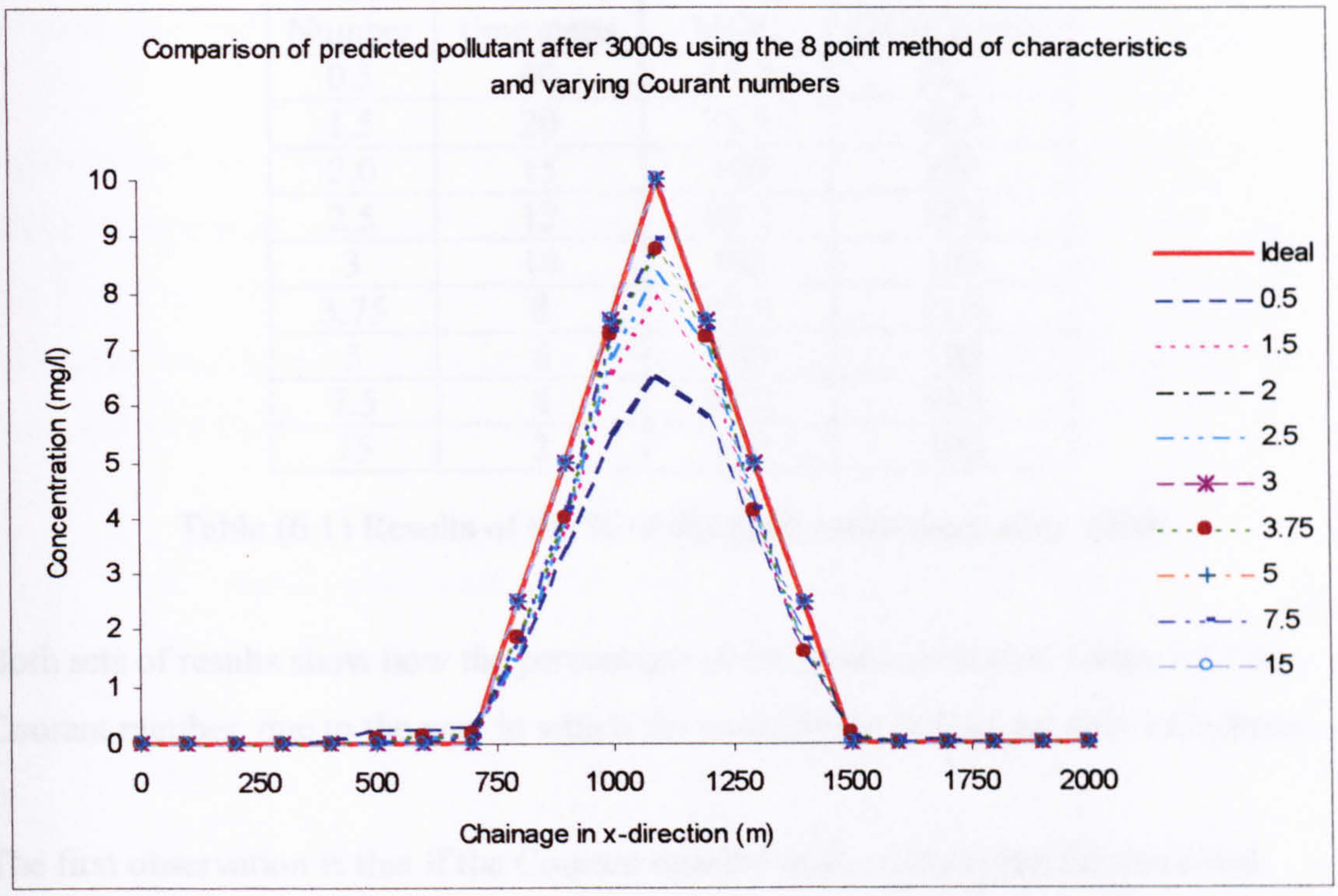

Figure (6.5) Results using a 2D linear distribution using the 8PMOC

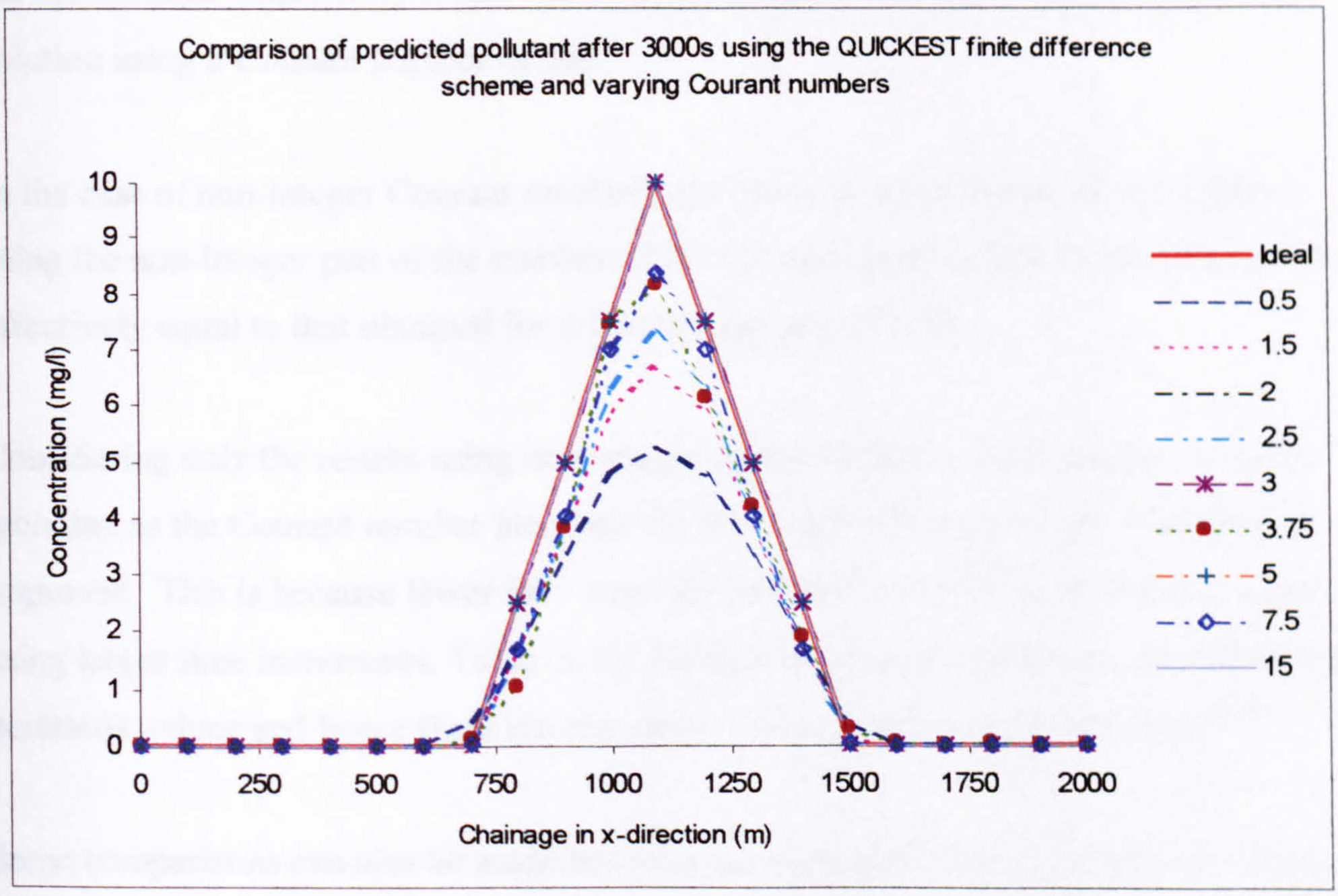

Figure (6.6) Results using a 2D linear distribution using QUICKEST

Courant Number	Number of time steps	% Peak MOC	% Peak QUICKEST
0.5	60	65.2	52.9
1.5	20	78.9	66.8
2.0	15	100	100
2.5	12	83.2	72.9
3	10	100	100
3.75	8	87.4	81.6
5	6	100	100
7.5	4	89.2	83.5
15	2	100	100

Table (6.1) Results of the % of the peak maintained after 3000s

Both sets of results show how the percentage of the peak maintained varies with the Courant number, due to the way in which the multiplying factors are now calculated.

The first observation is that if the Courant number is an integer then the predicted solution is exactly equal to the ideal solution. The reason for this is simple. It has been explained that when using this form of the spatial reachout scheme, the location of i and j, are moved such that they are either side of the location where the characteristics cuts the spatial axis. Effectively if this occurs at an integer point, the result is equal to the solution using a Courant number of one.

In the case of non-integer Courant numbers, the result is equal to that of the solution using the non-integer part of the number: if the Courant number is 3.75, the solution is effectively equal to that obtained for a Courant number of 0.75.

Considering only the results using non-integer forms of the Courant number, it can be seen that as the Courant number increases the numerical accuracy of the solution also improves. This is because fewer time steps are used to travel the same distance when using larger time increments, Table (6.1). Using a larger time increment, the number of iterations reduce and hence there are less errors due to truncation or rounding.[9, 20]

Some comparisons can also be made between the eight point method of characteristics and QUICKEST. Table (6.1) shows that the eight point scheme predicts a peak which

is closer to the ideal solution than QUICKEST. This is consistent with data for Courant numbers less than one.

A plot of the root mean square values for both approaches is also included as Figure (6.7) to compare the accuracy of the two schemes.

As was the case in tests using Courant numbers less than one, the eight point method of characteristics has the lower root mean square error.

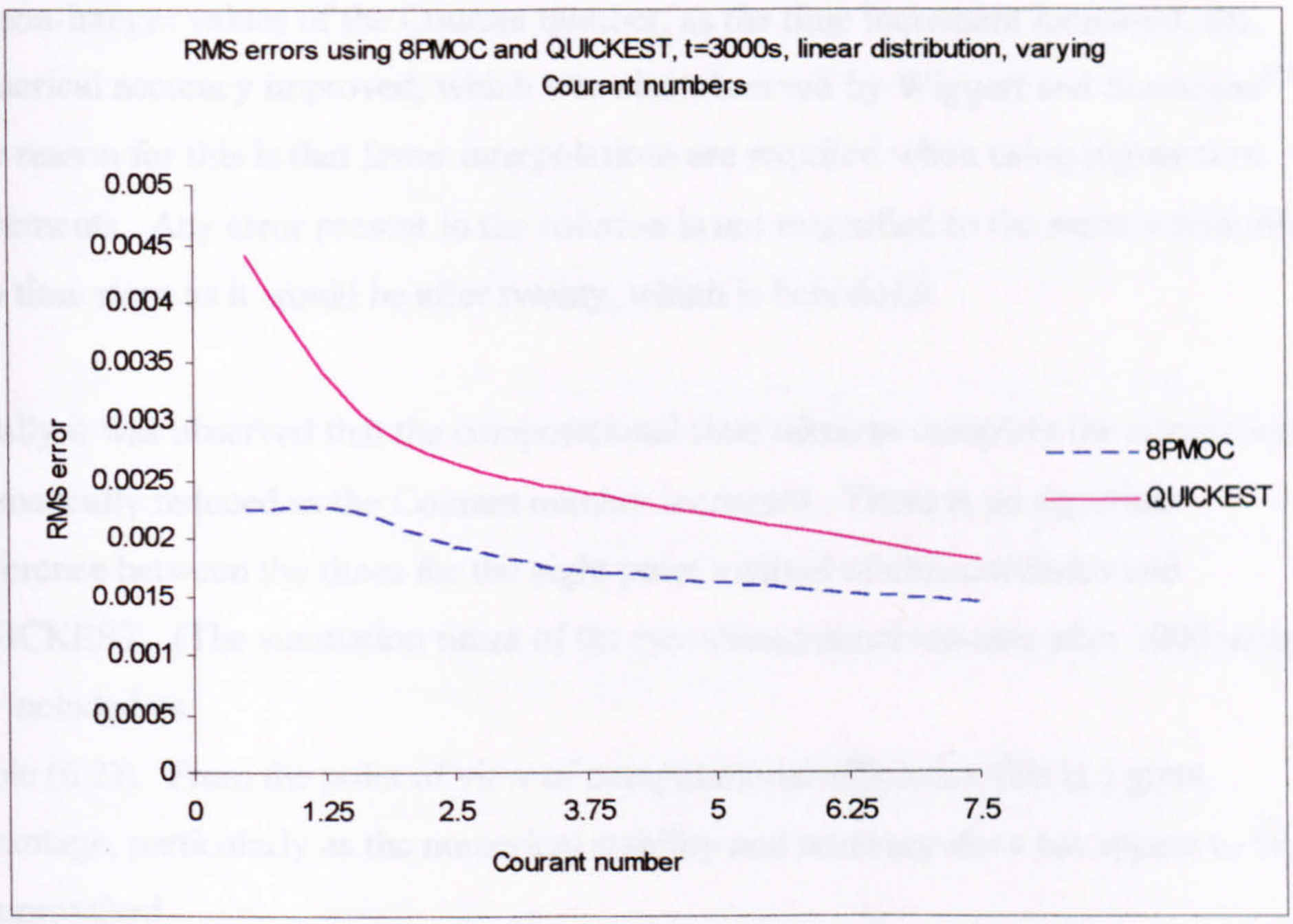

Figure (6.7) Comparison of RMS values for the 2D testcase

6.5 Conclusions

The eight and six point methods of characteristics in their original form cannot predict the pollution distribution to a suitable degree of accuracy, if the Courant number exceeds one. QUICKEST suffers from the same limitation but can also be applied at a Courant number of precisely 2. It can be concluded that in order to solve the advection

equation at greater Courant numbers, using either method, the inclusion of a spatial reachout scheme improves the solution.

The results show that as the time increment is increased, the numerical accuracy of the solutions also improves. When the Courant number is an integer value, the solution is exact and equivalent to the results which would be obtained at a Courant number of one. This is consistent with results observed by Yang and Wang[2] who also ran a series of tests using integer values of the Courant number.

At non-integer values of the Courant number, as the time increment increased, the numerical accuracy improved, which was also observed by Wiggert and Sundquist[4]. The reason for this is that fewer interpolations are required when using higher time increments. Any error present in the solution is not magnified to the same extent after two time steps as it would be after twenty, which is beneficial.

Finally it was observed that the computational time taken to complete the calculations dramatically reduced as the Courant number increased. There is no significant difference between the times for the eight point method of characteristics and QUICKEST. (The simulation times of the two-dimensional testcase after 3000 seconds are included as
Table (6.2)). From the point of view of computational efficiency this is a great advantage, particularly as the numerical stability and accuracy does not appear to be compromised.

Courant Number	Number of time steps	Time MOC (h:m:s)	Time QUICKEST (h:m:s)
0.5	60	1:07:47	1:07:18
1.5	20	0:23:01	0:22:49
2.0	15	0:17:19	0:17:05
2.5	12	0:13:56	0:13:52
3	10	0:11:50	0:11:35
3.75	8	0:09:29	0:09:21
5	6	0:07:08	0:07:07
7.5	4	0:04:52	0:04:55
15	2	0:02:37	0:02:36

Table (6.2) Results of the time taken for a 3000s simulation

6.6 References

1. Yang, J.C. and Chiu, K.P., "Use of Characteristics Method With Cubic Interpolation For Unsteady-Flow Computation", *International Journal For Numerical Methods in Fluids*, 1993, 16(4), 329-345.

2. Yang, J.C. and Wang, J.Y., "Numerical solution of dispersion equation in one dimension", *Journal of the Chinese Institute of Engineers*, 1988, 11, 379-383.

3. Chintu, L., "Comprehensive method of characteristics models for flow simulation", *Journal of Hydraulic Engineering*, 1988, 114, 1074-1097.

4. Wiggert, D.C. and Sundquist, M.J., "Fixed-grid characteristics for pipeline transients", *Journal of the Hydraulics Division*, 1977, 103(HY12), 1403-1416.

5. Chang, F.F.M. and Richards, D.L., "Deposition of sediment in transient flow", *Journal of the Hydraulics Division, Proceedings of the ASCE*, 1971, 97(HY6), 837-849.

6. Chintu, L., "Modelling alluvial-channel flow by multimode characteristic method", *Journal of Engineering Mechanics*, 1991, 117, 32-53.

7. Chintu, L., "Multicomponent-flow analyses by multimode method of characteristics", *Journal of Hydraulic Engineering*, 1994, 120, 378-395.

8. Goldberg, D.E. and Wylie, E.B., "Characteristics Method Using Time-Line Interpolations", *Journal of Hydraulic Engineering-Asce*, 1983, 109(5), 670-683.

9. Lin, W. and Song, C.C.S. *A multimode scheme of characteristics methos for open channel flows.* in *Proceedings of teh 1990 National Conference: Hydraulic Engineering*. 1990. San-Diego, CA: ASCE.

10. Yang, J.C. and Hsu, E.L., "Time-Line Interpolation For Solution of the Dispersion-Equation", *Journal of Hydraulic Research*, 1990, 28(4), 503-520.

11. Yang, J.C. and Hsu, E.L., "On the Use of the Reach-Back Characteristics Method For Calculation of Dispersion", *International Journal For Numerical Methods in Fluids*, 1991, 12(3), 225-235.

12. Lister, M., "The numerical solution of hyperbolic partial difference equations by the method of characteristics", in *Mathematical Methods for Digital Computers*, A. Ralston and H.S. Wilf, Editors. 1960, John Wiley and Sons Inc: New York. 165-179.

13. Vardy, A.E. *On the use of the method of characteristics for the solution of unsteady flows in networks.* in *Proceedings of the Second International Conference on Pressure Surges.* 1977. Cranfield, England.

14. Abbott, M.B. and Basco, D.R., *Computational Fluid Dynamics; An Introduction for Engineers.* 1989: Longman Scientific and Technical.

15. Leonard, B.P., "A stable and accurate convective modelling procedure based on quadratic upstream interpolation", *Computer methods in applied mechanics and engineering*, 1979, 19, 59-98.

16. Croucher, A.E. and O'Sullivan, M.J., "Numerical methods for contaminant transport in rivers and estuaries", *Computers & Fluids*, 1998, 27(8), 861-878.

17. Manson, J.R. and Wallis, S.G., "An accurate numerical algorithm for advective transport", *Communications in Numerical Methods in Engineering*, 1995, **11**(12), 1039-1045.

18. Lai, C., "Comprehensive Method of Characteristics Models For Flow Simulation", *Journal of Hydraulic Engineering-Asce*, 1988, **114**(9), 1074-1097.

19. Wallis, S.G. and Manson, J.R., "Accurate numerical simulation of advection using large time steps", *International Journal For Numerical Methods in Fluids*, 1997, **24**(2), 127-139.

Chapter 7

Implementation of the six point method of characteristics in DIADEM3D

7.1 Introduction 193

7.2 Programming the six point method of characteristics into DIADEM3D 193

7.2.1 General operation of DIADEM3D 194

7.2.2 Implementation of the six point method of characteristics 195

7.3 Application of the six point method of characteristics to the Firth of Clyde 200

7.3.1 Analysis of the model results 211

7.4 References 218

7.1 Introduction

There are two main goals associated with this study:

- To develop a numerical method which accurately solves the advection equation in two-dimensions.
- To program this scheme into an existing numerical model which is used in industry.

The first aim involved the analysis and development of the upwind and QUICKEST finite difference schemes and the eight and six point methods of characteristics, using idealised computational testcases. The comparisons of these schemes in two-dimensions in Section 5.2 indicates that the six point method of characteristics provides the most accurate solution in all of the testcases. With this in mind, the six point method of characteristics is programmed into the, dispersion advection in the environment model in three dimensions, DIADEM3D, which is copyrighted to the Babtie Group Ltd.

This chapter will describe how the scheme was programmed into DIADEM3D and also demonstrate how it can be used to solve an industry based problem.

7.2 Programming the six point method of characteristics into DIADEM3D

The programming of new code into any existing model is a complicated task. It requires detailed analysis of the model to determine the relationship between subroutines and how variables are passed between different functions. This is essential as variables required in the new code must be located and if necessary additional calculations must be inserted to ensure the program will operate correctly.

It also requires knowledge of the programming language, in this case Fortran 77.[1, 2]

7.2.1 General operation of DIADEM3D

DIADEM3D is comprised of two main sections solving the hydrodynamic and water quality equations. The general operation of the program is included as Figure (7.1). Velocities at each grid point are calculated in the hydrodynamic program from which they are transferred to the water quality program, for use in the solution of the advection-diffusion equation.

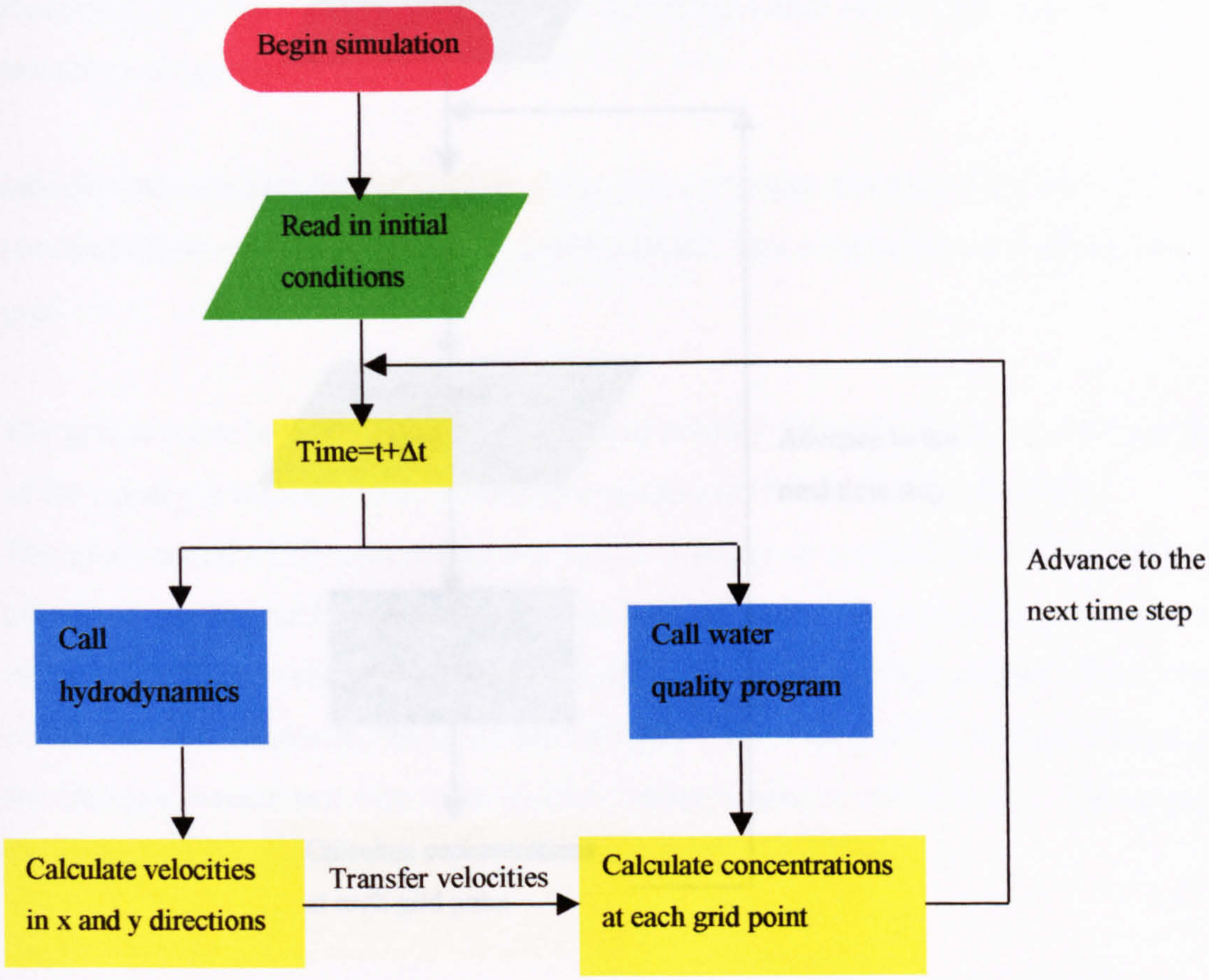

Figure (7.1) Flow chart depicting the general operation of DIADEM3D

If required, the hydrodynamic and water quality programs can be run separately. Initially in this study, the hydrodynamic program was removed from an earlier version of DIADEM3D. Instead of calculating the hydrodynamics, idealised velocity profiles were specified and a new program written to transfer their values to the water quality model, Figure (7.2). This ensured that any errors, which appeared in the solution of the advection equation, were due solely to its numerical solution and not due to any

difficulties in the hydrodynamic simulation. Once the six point method of characteristics was implemented successfully in this version of DIADEM3D, it became simpler to reintegrate it with the hydrodynamic program.

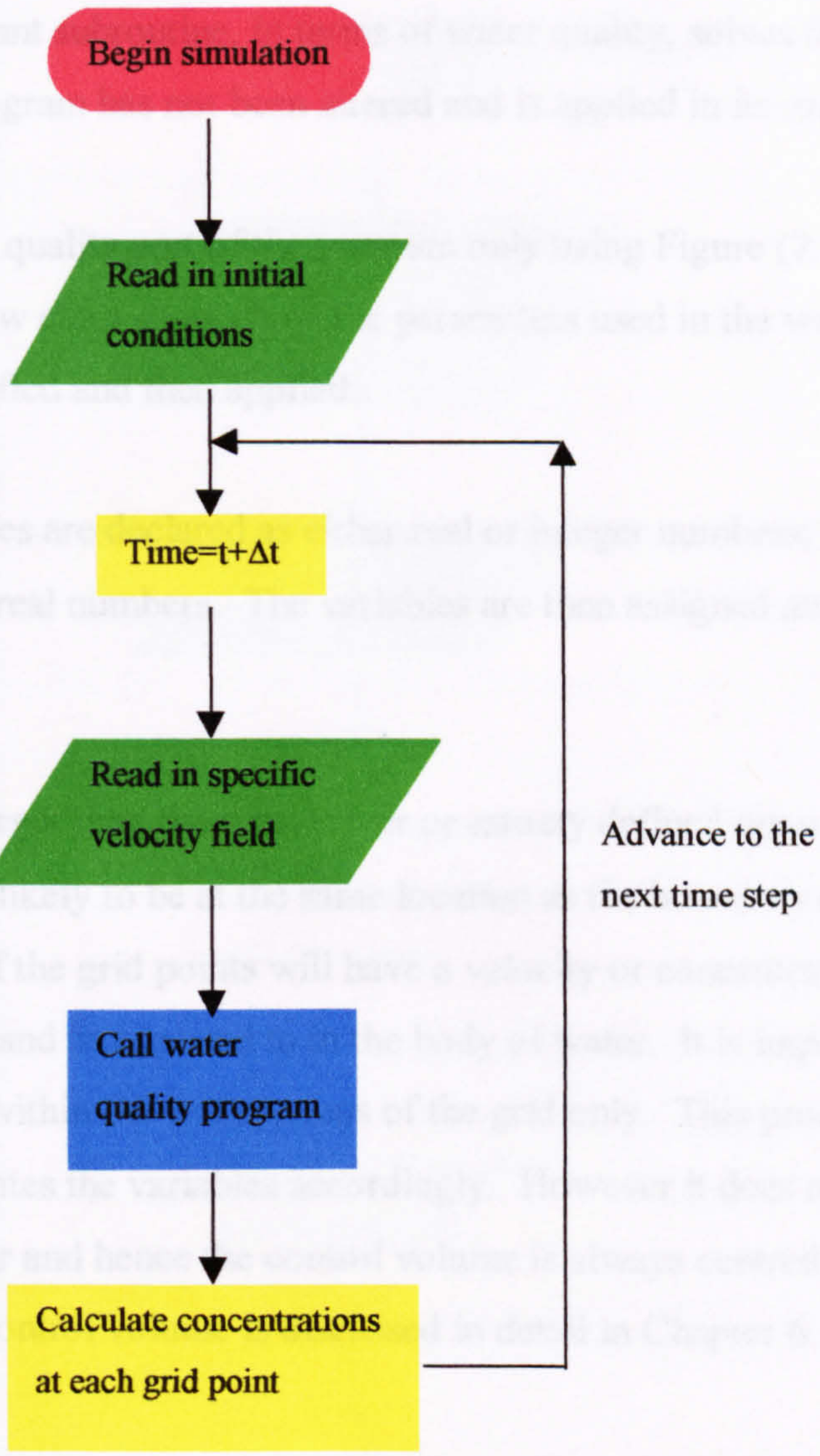

Figure (7.2) Flow chart illustrating the use of a specified velocity field

7.2.2 Implementation of the six point method of characteristics

It is necessary to fully comprehend how the original form of DIADEM3D solves the water quality equations. The main program running DIADEM3D is called Eng4. This is essentially the engine of the model, where all other subroutines pertaining to

hydrodynamics and water quality are called from. The most significant subroutine with respect to water quality is named, Cwqadv. It is here where the calculations associated with the solution of the advection equation are executed.

The second important subroutine, in terms of water quality, solves the diffusion term. This part of the program has not been altered and is applied in its original form.

Consider the water quality part of the program only using Figure (7.3) to illustrate the procedure. The flow chart shows how the parameters used in the water quality equations are specified and then applied.

Initially the variables are declared as either real or integer numbers; velocities and concentrations are real numbers. The variables are then assigned an i,j location on the grid.

The grid is often larger than the actual river or estuary defined upon it, *i.e.* the boundary of the estuary is unlikely to be at the same location as the boundary of the grid. Therefore not all of the grid points will have a velocity or concentration as they are effectively on dry land as opposed to in the body of water. It is important to assign the variable locations within the wet sections of the grid only. This procedure takes account of this fact and locates the variables accordingly. However it does not take account of the Courant number and hence the control volume is always centred at i,j. The reasons for relocating the control volume is discussed in detail in Chapter 6.

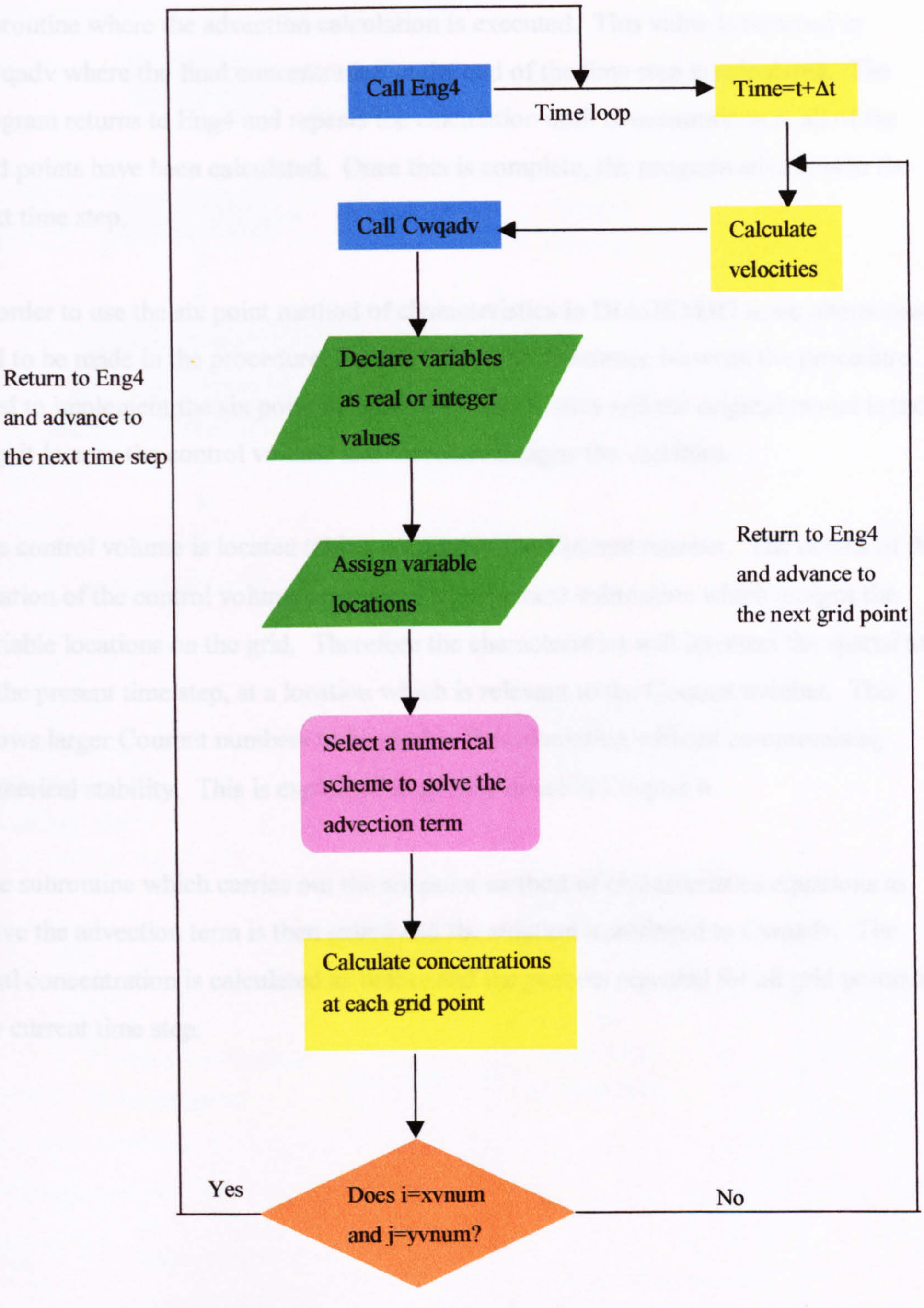

Figure (7.3) Flow chart depicting the original procedure used in the water quality program

Once the variables have assigned locations and thus relative values of velocity and concentration, a numerical scheme, specified in the initial conditions, is used to solve the advection equation. This involves the step of transferring data from Cwqadv to a

subroutine where the advection calculation is executed. This value is returned to Cwqadv where the final concentration at the end of the time step is calculated. The program returns to Eng4 and repeats the calculation until concentrations at all of the grid points have been calculated. Once this is complete, the program advances to the next time step.

In order to use the six point method of characteristics in DIADEM3D some alterations had to be made in the procedure, Figure (7.4). The difference between the procedure used to implement the six point method of characteristics and the original model is the way it locates the control volume and therefore assigns the variables.

The control volume is located taking account of the Courant number. The details of the location of the control volume are passed into the next subroutine which assigns the variable locations on the grid. Therefore the characteristics will intersect the spatial axis at the present time step, at a location which is relevant to the Courant number. This allows larger Courant numbers to be used in the calculation without compromising numerical stability. This is explained in greater detail in Chapter 6.

The subroutine which carries out the six point method of characteristics equations to solve the advection term is then called and the solution transferred to Cwqadv. The final concentration is calculated as before and the process repeated for all grid points at the current time step.

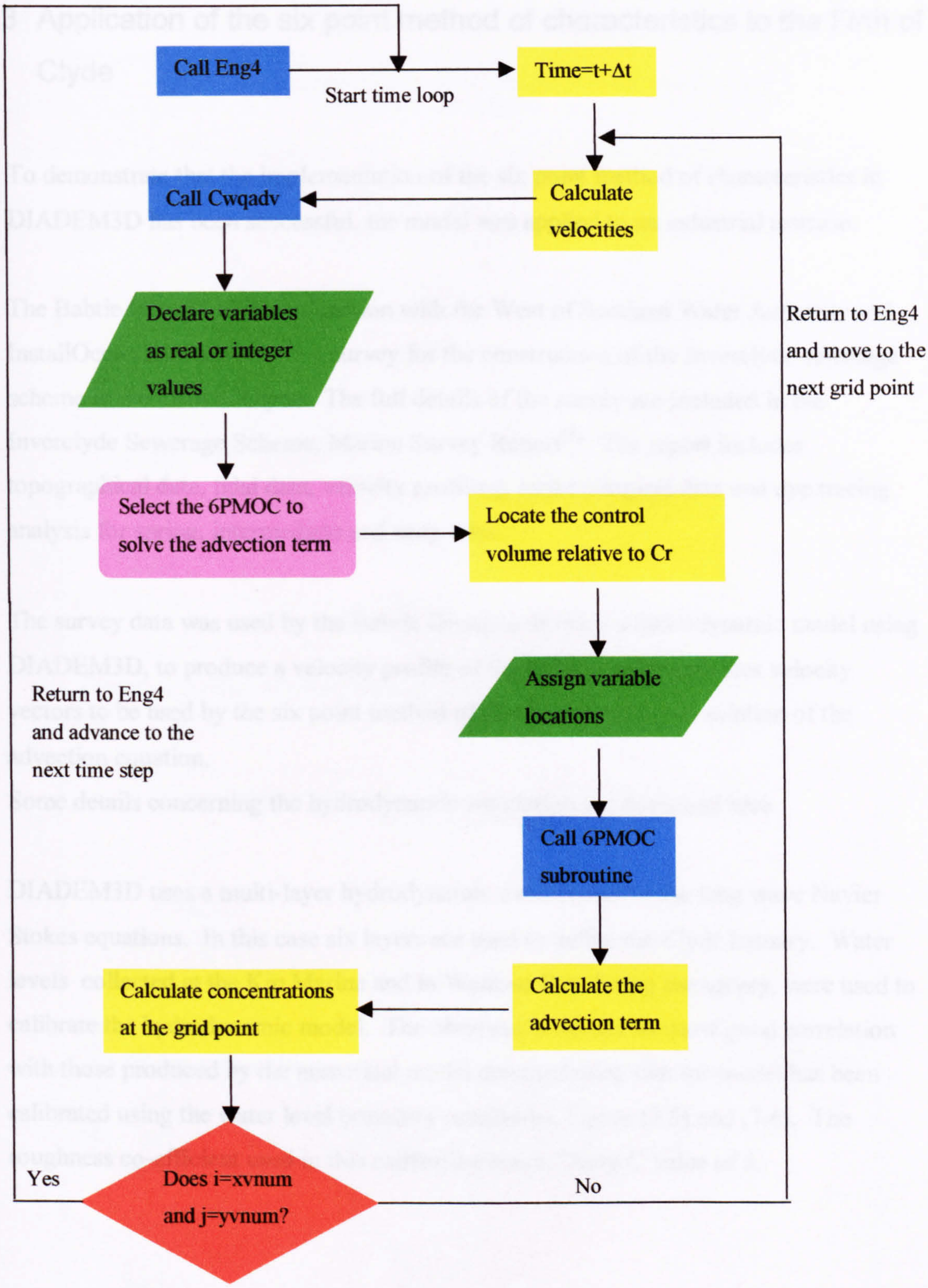

Figure (7.4) Flow chart of the procedure used in the water quality program including the six point method of characteristics

7.3 Application of the six point method of characteristics to the Firth of Clyde

To demonstrate that the implementation of the six point method of characteristics in DIADEM3D has been successful, the model was applied to an industrial testcase.

The Babtie Group Ltd in conjunction with the West of Scotland Water Authority and InstallOcean Ltd, carried out a survey for the construction of the Inverclyde sewerage scheme in the Firth of Clyde. The full details of the survey are included in the Inverclyde Sewerage Scheme, Marine Survey Report[3]. The report includes topographical data, tidal data, velocity profiling, meteorological data and dye tracing analysis for spring, intermediate and neap tides.

The survey data was used by the Babtie Group to develop a hydrodynamic model using DIADEM3D, to produce a velocity profile of the estuary. This provides velocity vectors to be used by the six point method of characteristics in the solution of the advection equation.
Some details concerning the hydrodynamic simulation are discussed here.

DIADEM3D uses a multi-layer hydrodynamic model to solve the long wave Navier Stokes equations. In this case six layers are used to define the Clyde Estuary. Water levels collected at the Kip Marina and in Wemyss Bay during the survey, were used to calibrate the hydrodynamic model. The observed water levels show good correlation with those produced by the numerical model demonstrating that the model has been calibrated using the water level boundary conditions, Figure (7.5) and (7.6). The roughness co-efficient used in this calibration was a Chezy C value of 5.

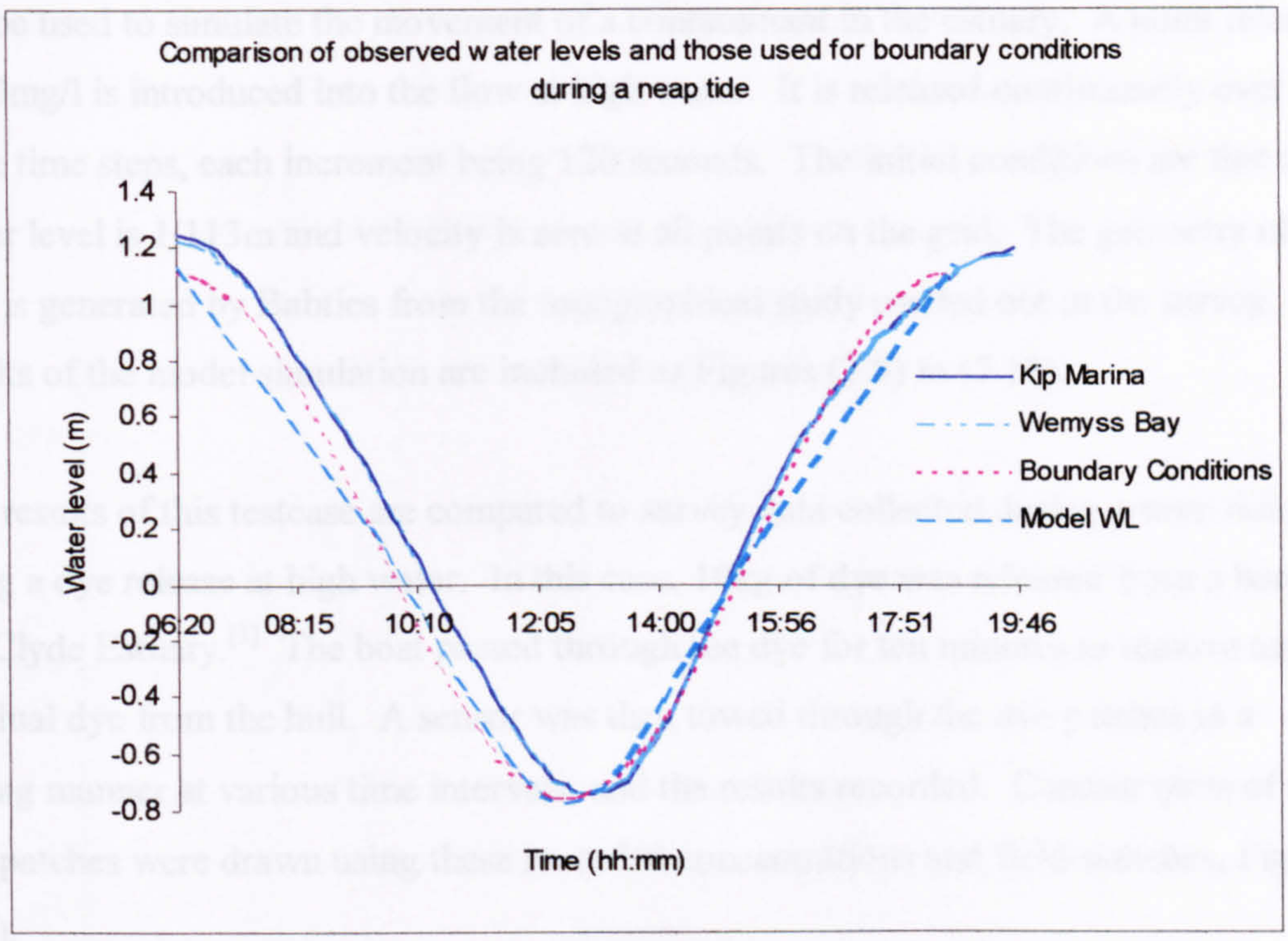

Figure (7.5) Plot of observed and simulated water levels during a neap tide

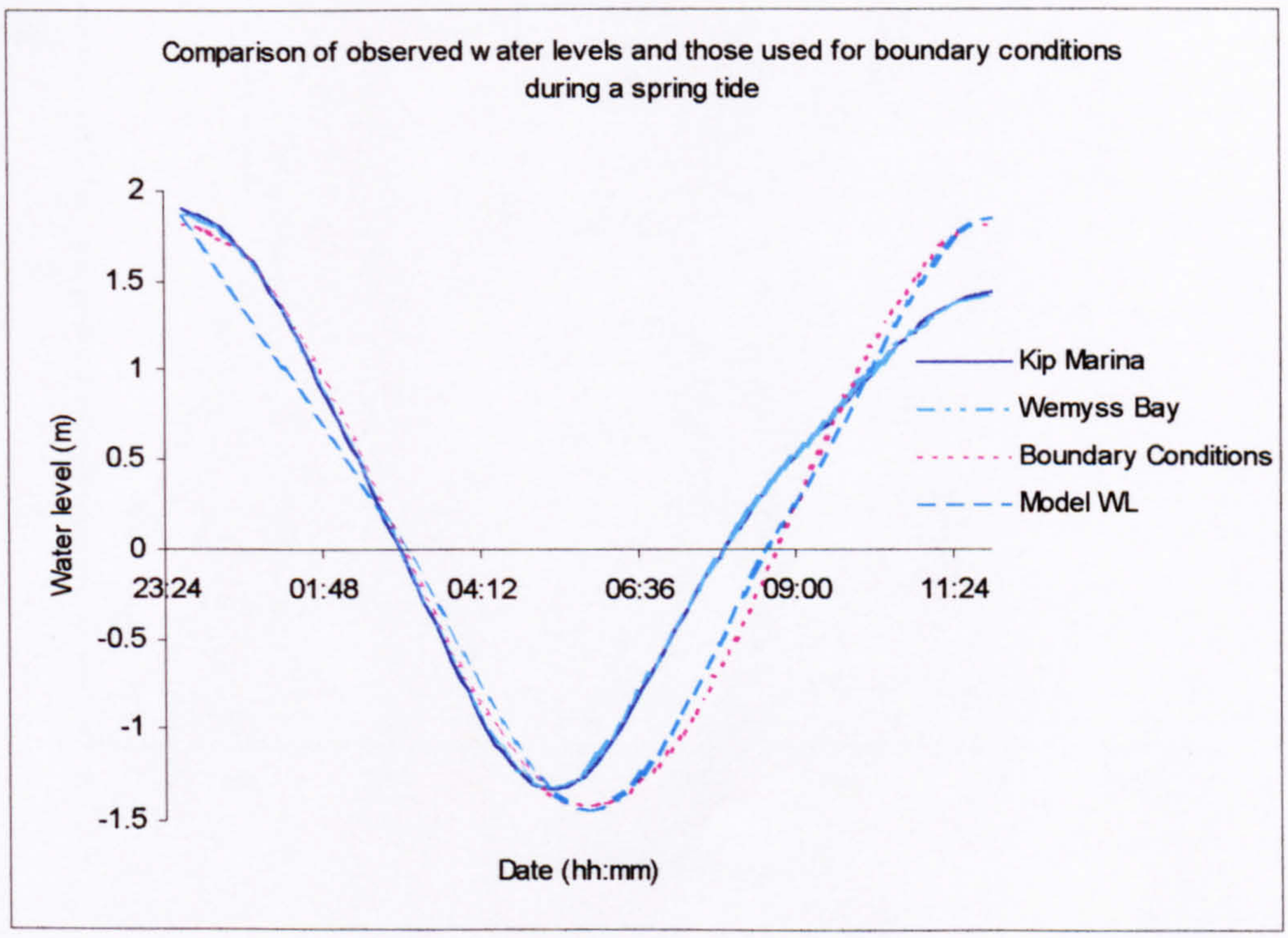

Figure (7.6) Plot of observed and simulated water levels during a spring tide

A testcase using the neap tide conditions, is used to demonstrate how this new method can be used to simulate the movement of a contaminant in the estuary. A point release of 10mg/l is introduced into the flow at high water. It is released continuously over three time steps, each increment being 120 seconds. The initial conditions are that the water level is 1.113m and velocity is zero at all points on the grid. The geometry of this grid is generated by Babties from the topographical study carried out in the survey. The results of the model simulation are included as Figures (7.8) to (7.14).

The results of this testcase are compared to survey data collected during a neap tide, using a dye release at high water. In this case, 10kg of dye was released from a boat in the Clyde Estuary.[3] The boat passed through the dye for ten minutes to remove any residual dye from the hull. A sensor was then towed through the dye patches in a zigzag manner at various time intervals, and the results recorded. Contour plots of the dye patches were drawn using these recorded concentrations and field sketches, Figure (7.7).

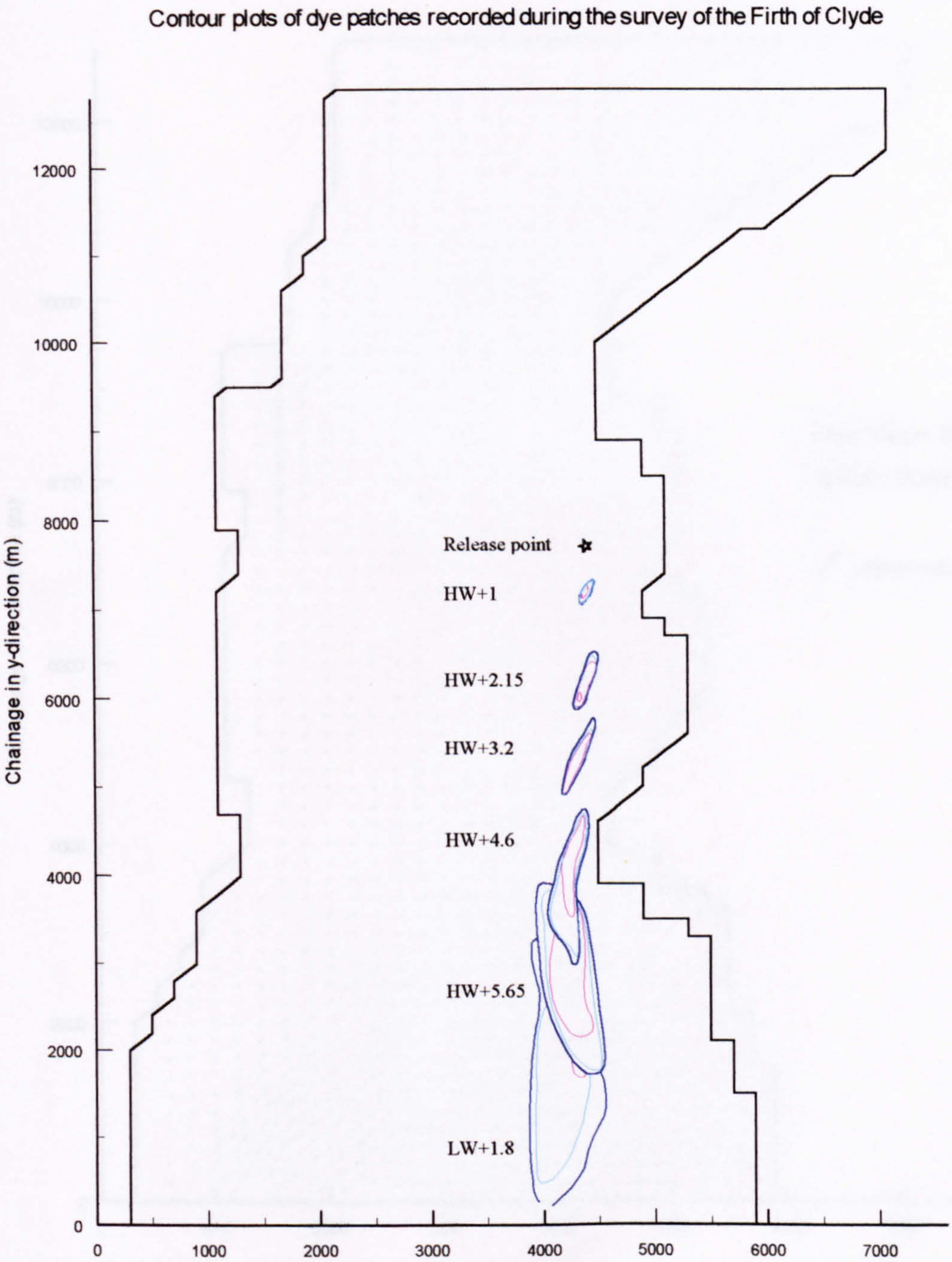

Figure (7.7) Surveyed contour plots

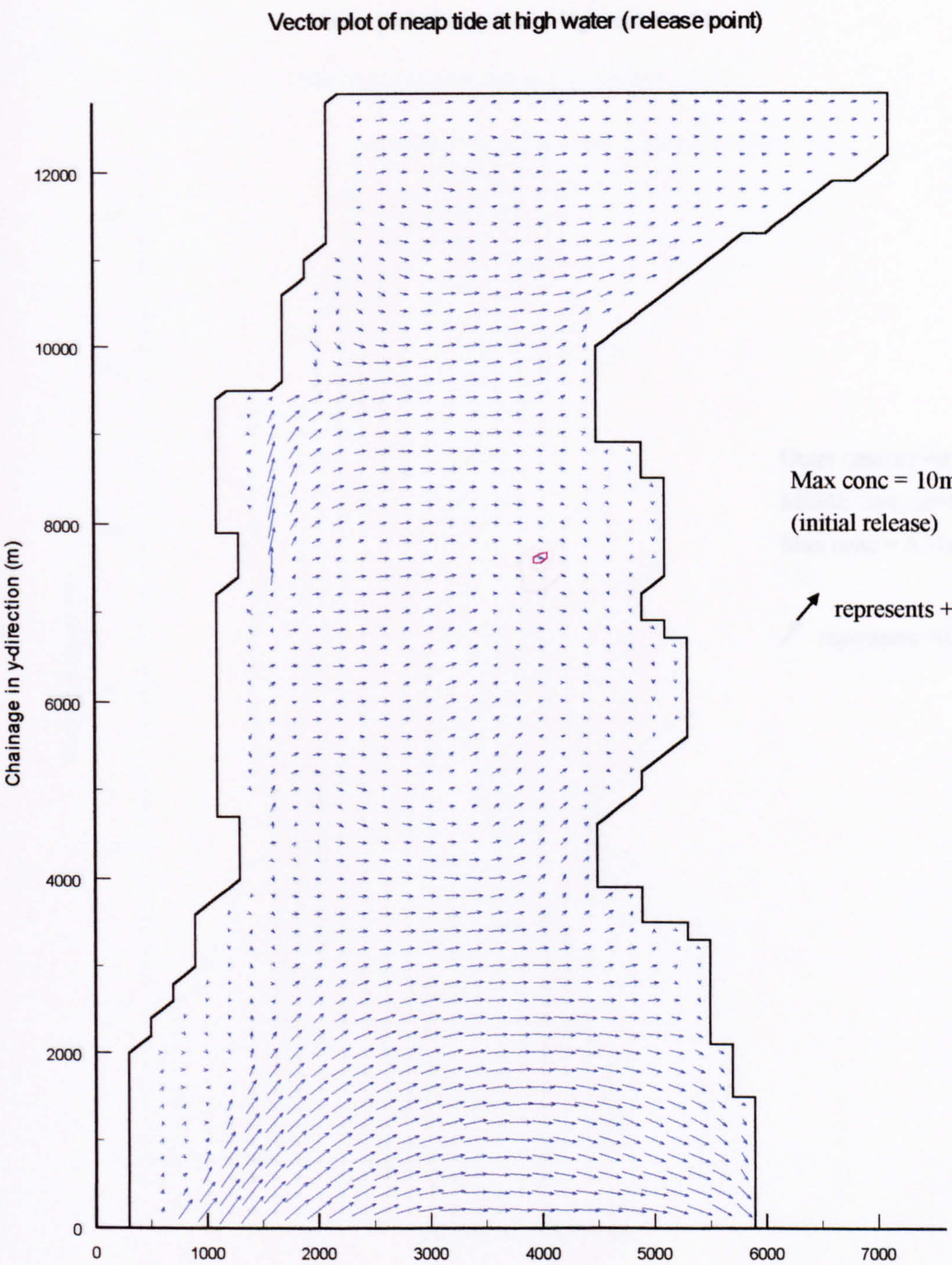

Figure (7.8) Velocity vectors for the neap tide at HW

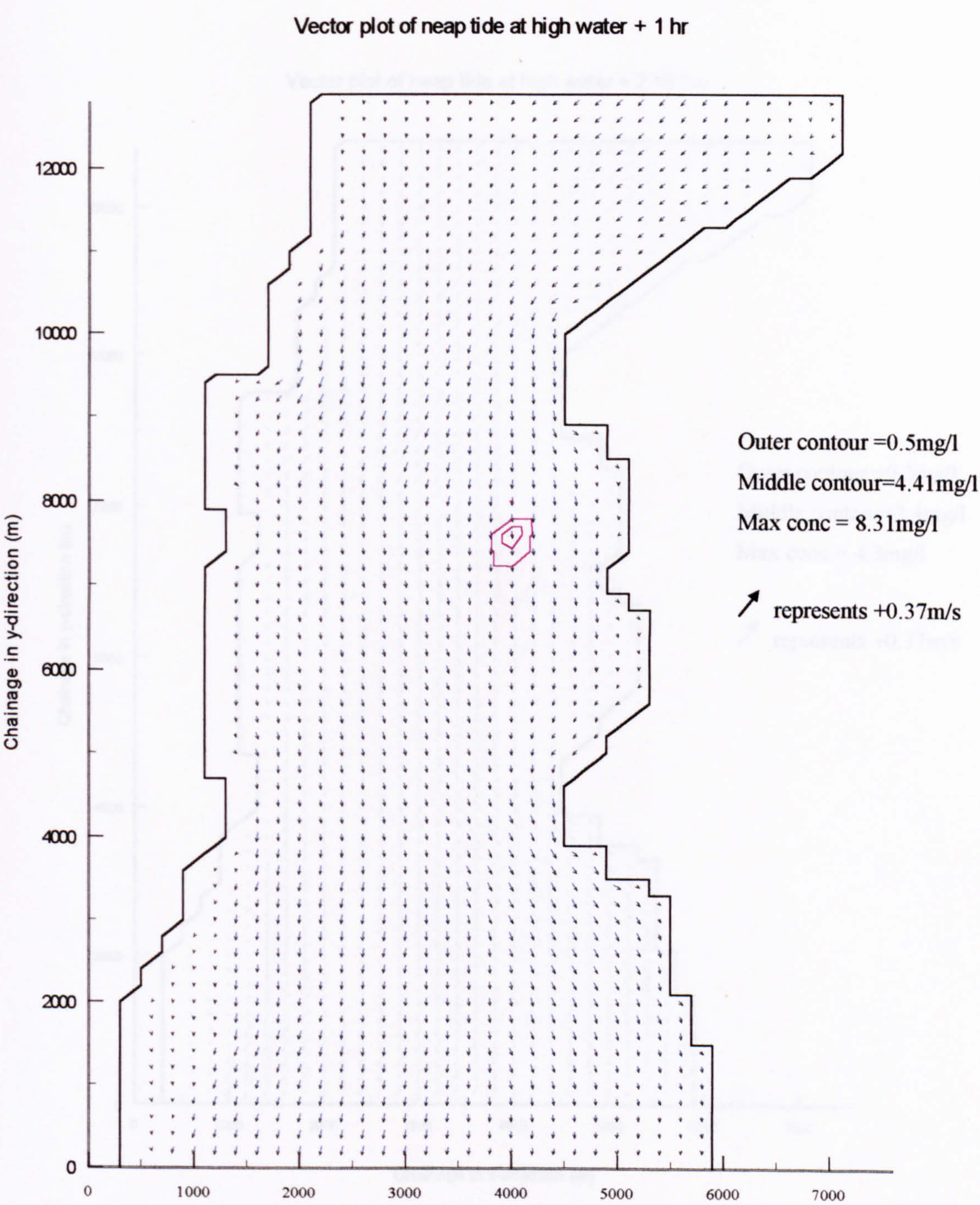

Figure (7.9) Velocity vectors for the neap tide at HW+1hr

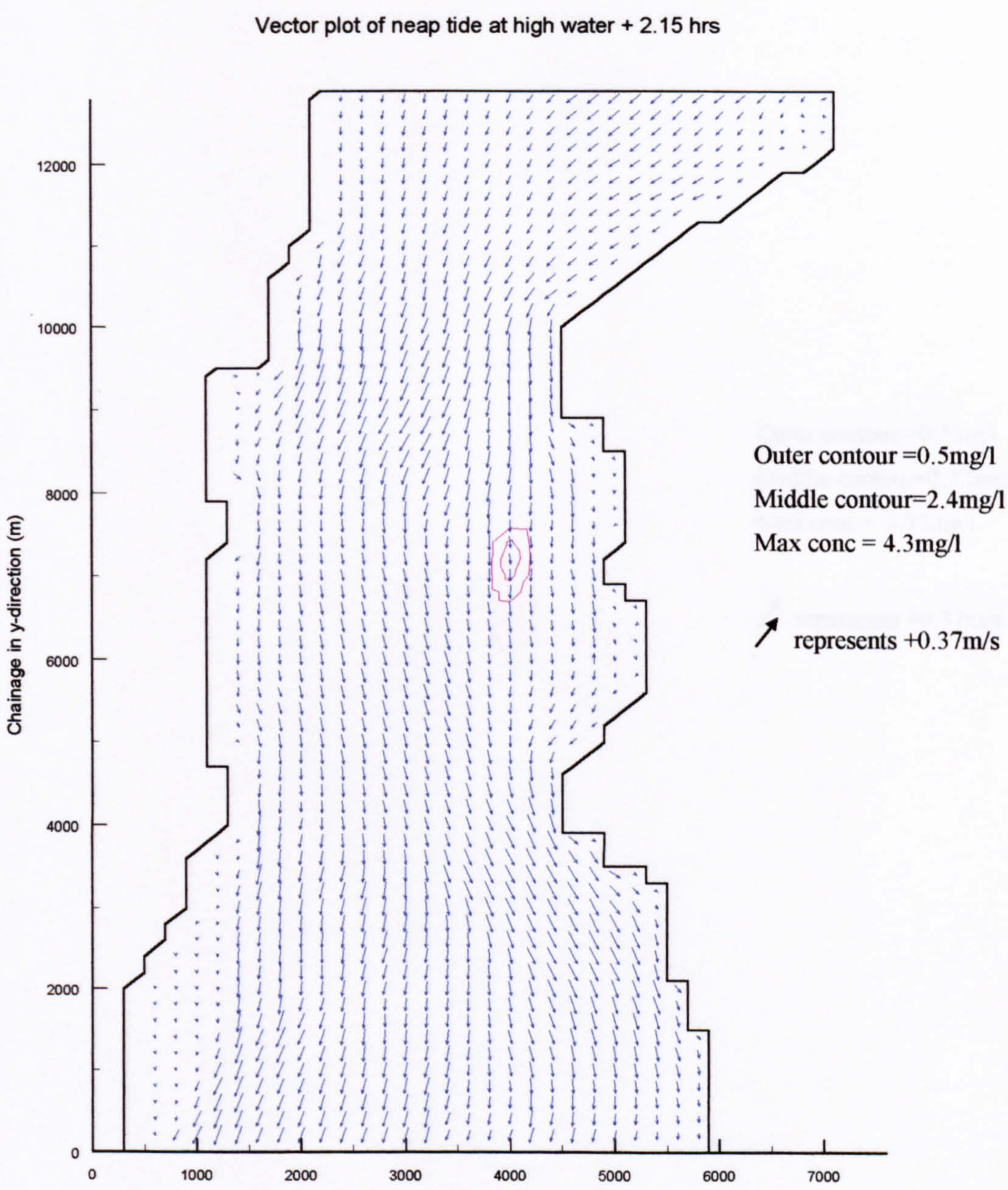

Figure (7.10) Velocity vectors for the neap tide at HW+2.15 hrs

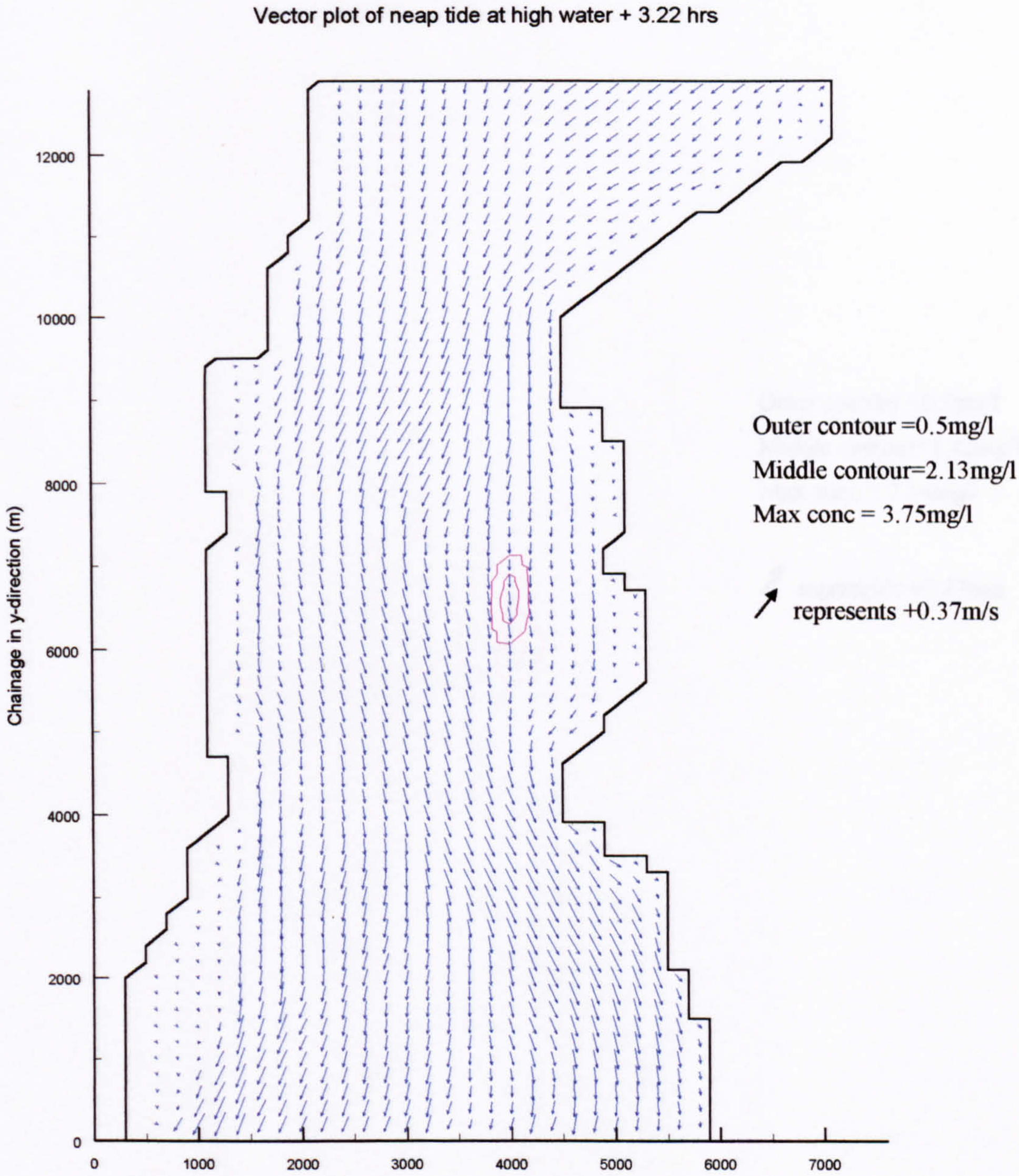

Figure (7.11) Velocity vectors for the neap tide at HW+3.22 hrs

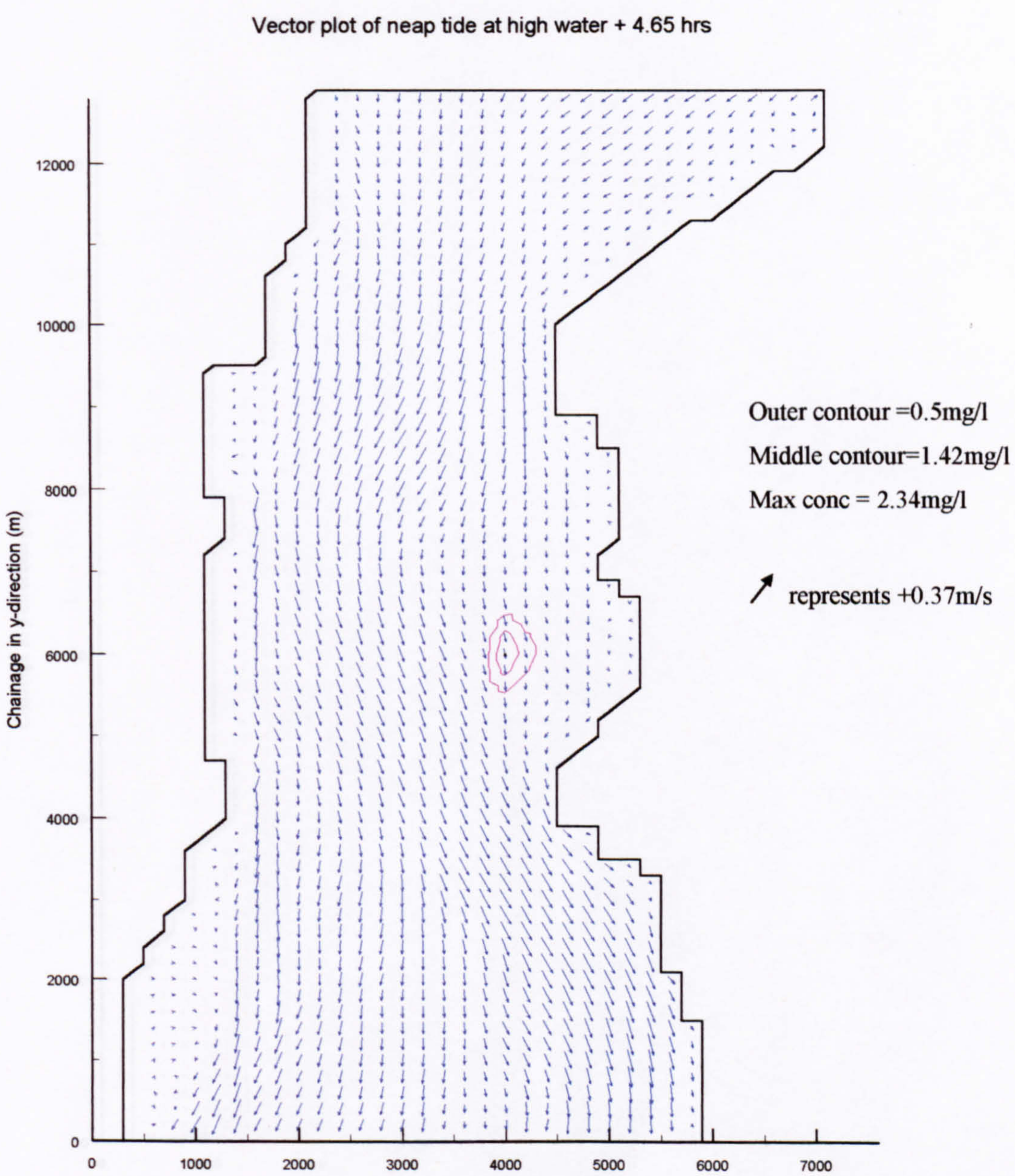

Figure (7.12) Velocity vectors for the neap tide at HW+4.65 hrs

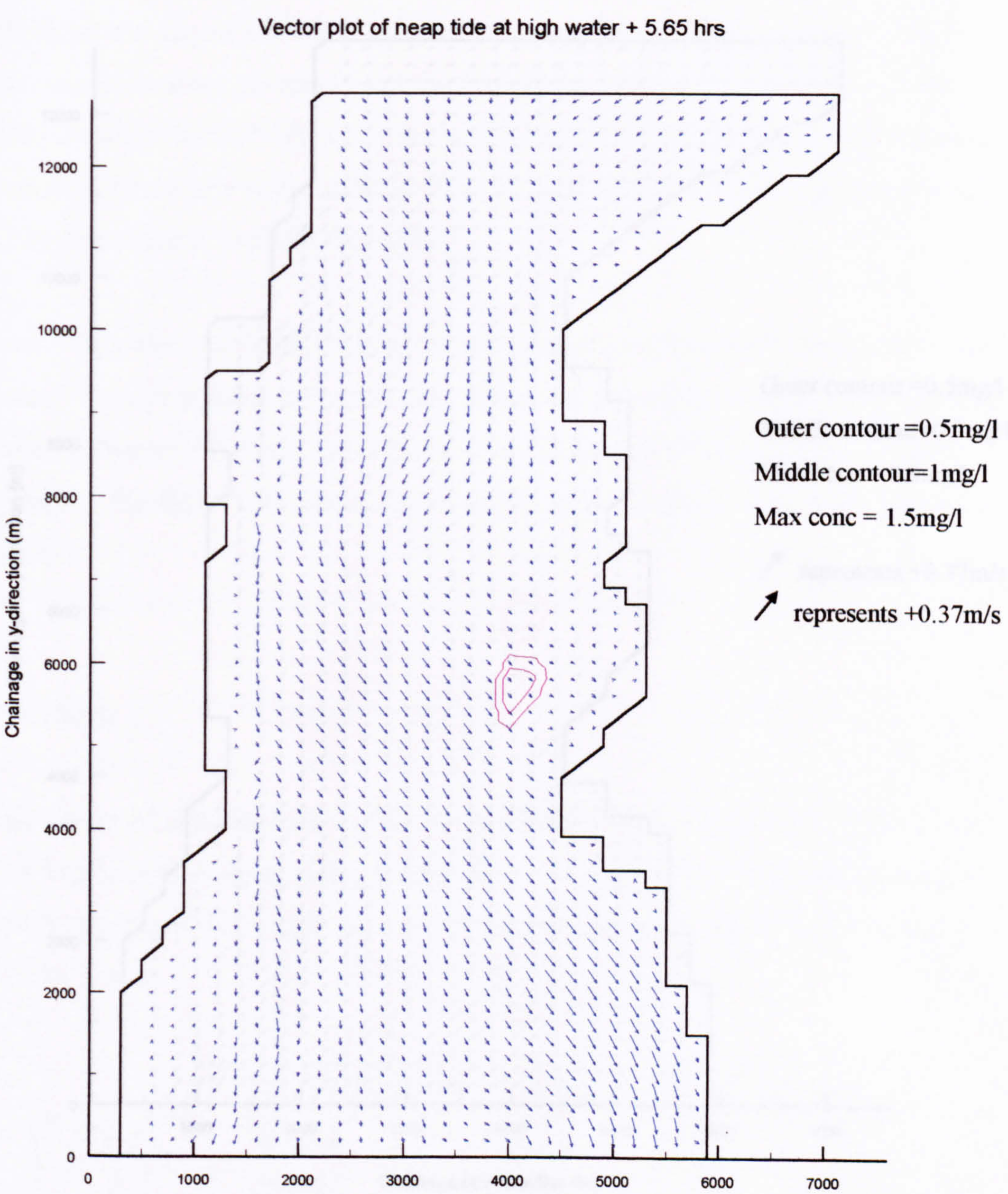

Figure (7.13) Velocity vectors for the neap tide at HW+5.65 hrs

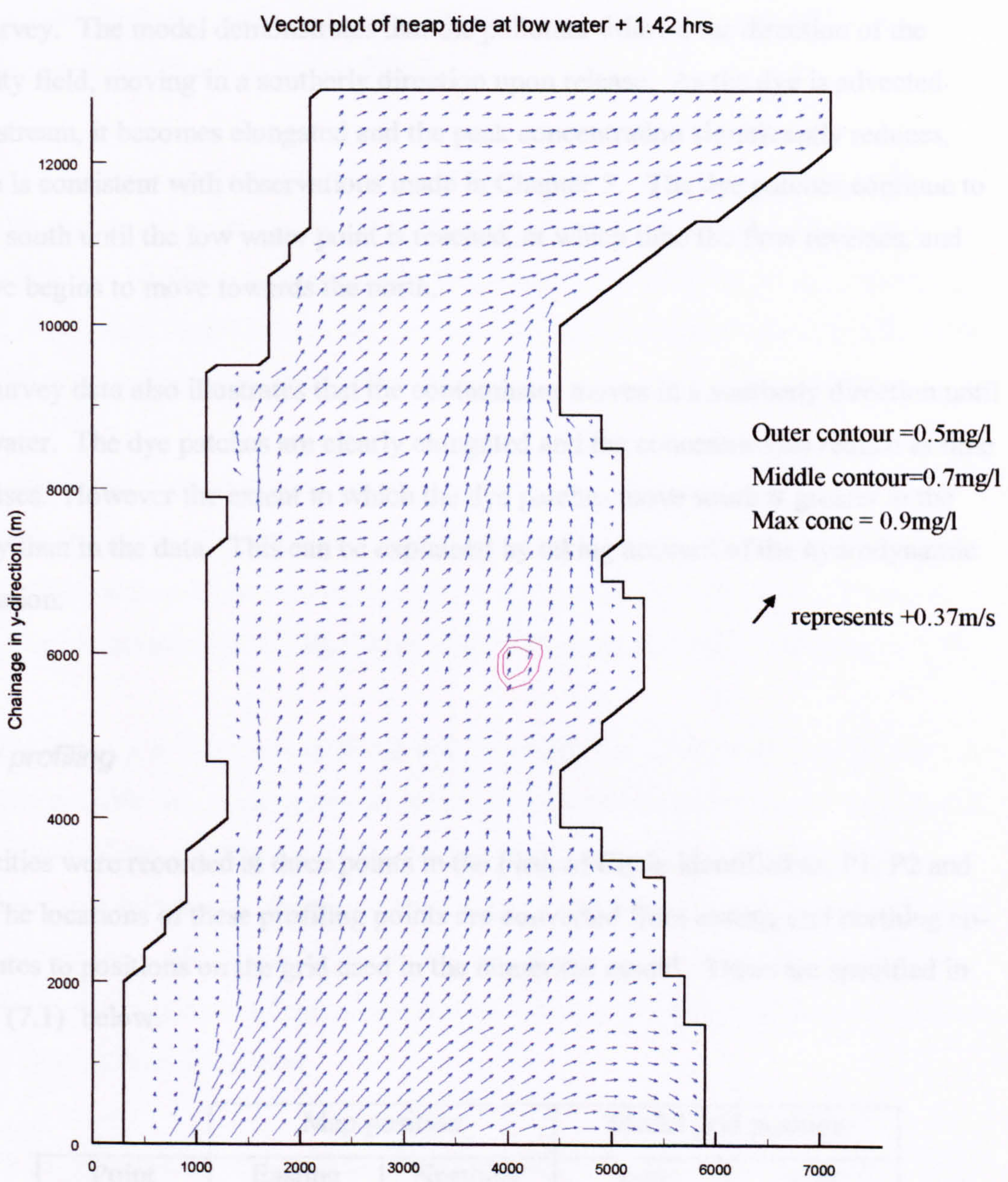

Figure (7.14) Velocity vectors for the neap tide at LW+1.8 hrs

7.3.1 Analysis of the model results

The results show that the numerical model simulates a trend similar to that observed in the survey. The model demonstrates that the pollutant follows the direction of the velocity field, moving in a southerly direction upon release. As the dye is advected downstream, it becomes elongated and the peak concentration significantly reduces, which is consistent with observations made in Chapter 5. The dye patches continue to travel south until the low water point is reached, at which time the flow reverses, and the dye begins to move towards the north.

The survey data also illustrates that the contaminant moves in a southerly direction until low water. The dye patches are clearly elongated and the concentrations reduce as time increases. However the extent to which the dye patches move south is greater in the survey than in the data. This can be explained by taking account of the hydrodynamic simulation.

Velocity profiling

Velocities were recorded at three points in the Firth of Clyde identified as, P1, P2 and P3. The locations of these profiling points are converted from easting and northing co-ordinates to positions on the grid used in the numerical model. These are specified in Table (7.1) below.

	Map position		Model grid position	
Point	Easting	Northing	x-m	y-m
P1	219498	673795	4000	7600
P2	218519	672071	3600	5800
P3	220027	677227	3800	11200

Table (7.1) Relevant positions of profiling points on the grid used in the numerical model

The velocity profiling data was collected using recording current meters, which recorded speed and direction every 12 seconds for one minute. These values were then vector averaged and logged to a computer. Plots depicting the comparison between the surveyed data and the speeds and directions calculated using the numerical model, are included as Figure (7.15) to Figure (7.20).

Comparisons between the observed and simulated velocities show that the predicted neap tide speeds are generally less than those surveyed by up to 50%. The survey also shows that the ebb flows are greater than those associated with the flood, however the model shows little variation between the two. The predicted speed directions do follow a similar trend to those observed in the survey.

This large underprediction of the velocity is significant when considering how far the dye patch will be advected downstream. If the velocity is low the patch will travel a shorter distance than if the velocity is high, as was the case in the survey. There are three possible reasons for this significant difference between model and survey results.

The first is that it is extremely difficult to gather accurate survey data in an estuary. It is therefore possible that some errors were made while collecting the data. The second is that the hydrodynamic model may not be calculating the velocity correctly. The hydrodynamic simulation, like the water quality model, also includes the calculation of an advection term, which has not been analysed in this study. In addition the model velocity is averaged over a depth of ten metres whereas in the survey, the probe records speeds at a depth of one metre.

Finally the presence of wind in the survey is not fully represented in the model. This would have an effect on the velocity field in the estuary.

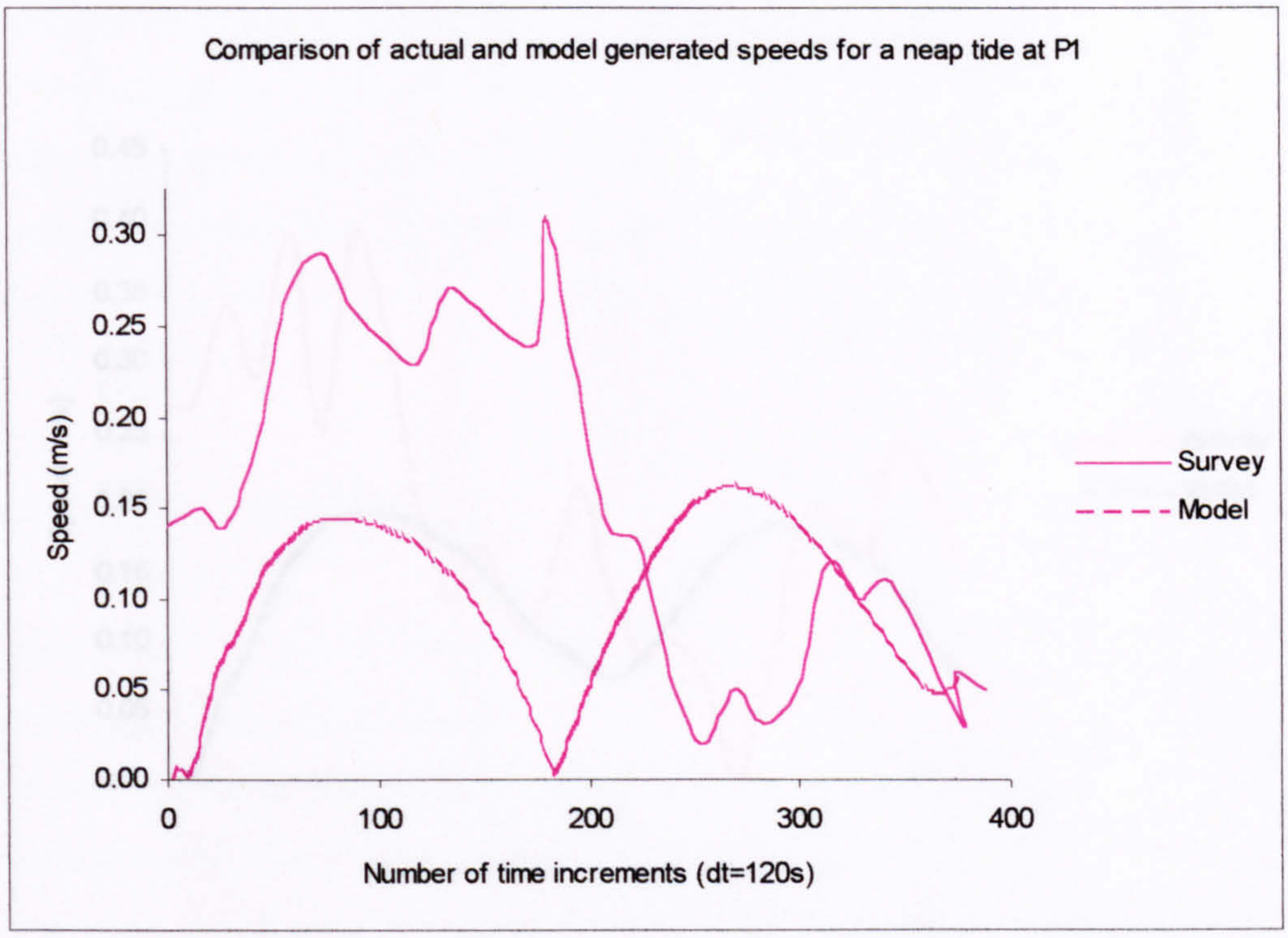

Figure (7.15) Plot of surveyed and calculated speeds at P1

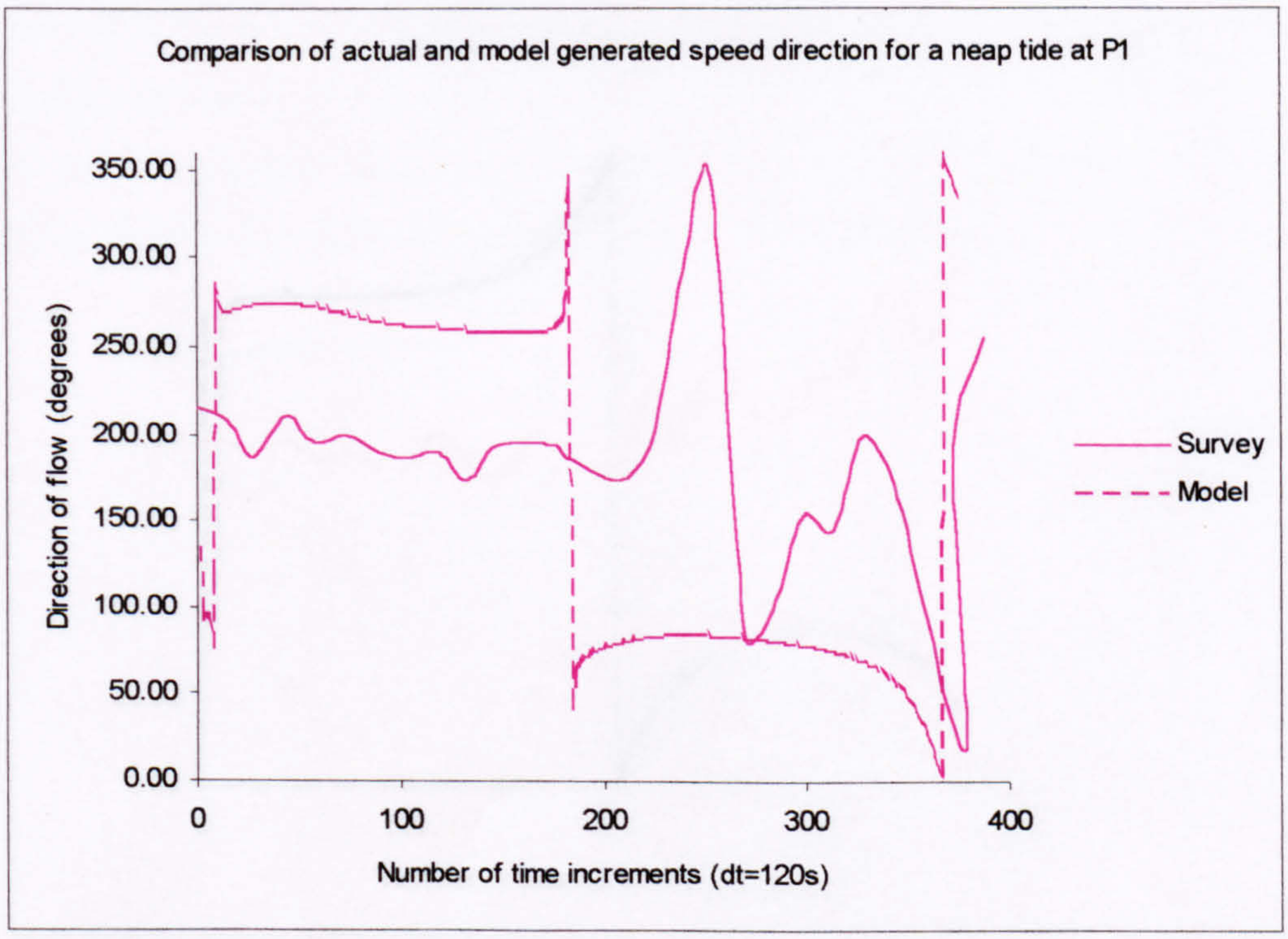

Figure (7.16) Plot of surveyed and calculated directions at P1

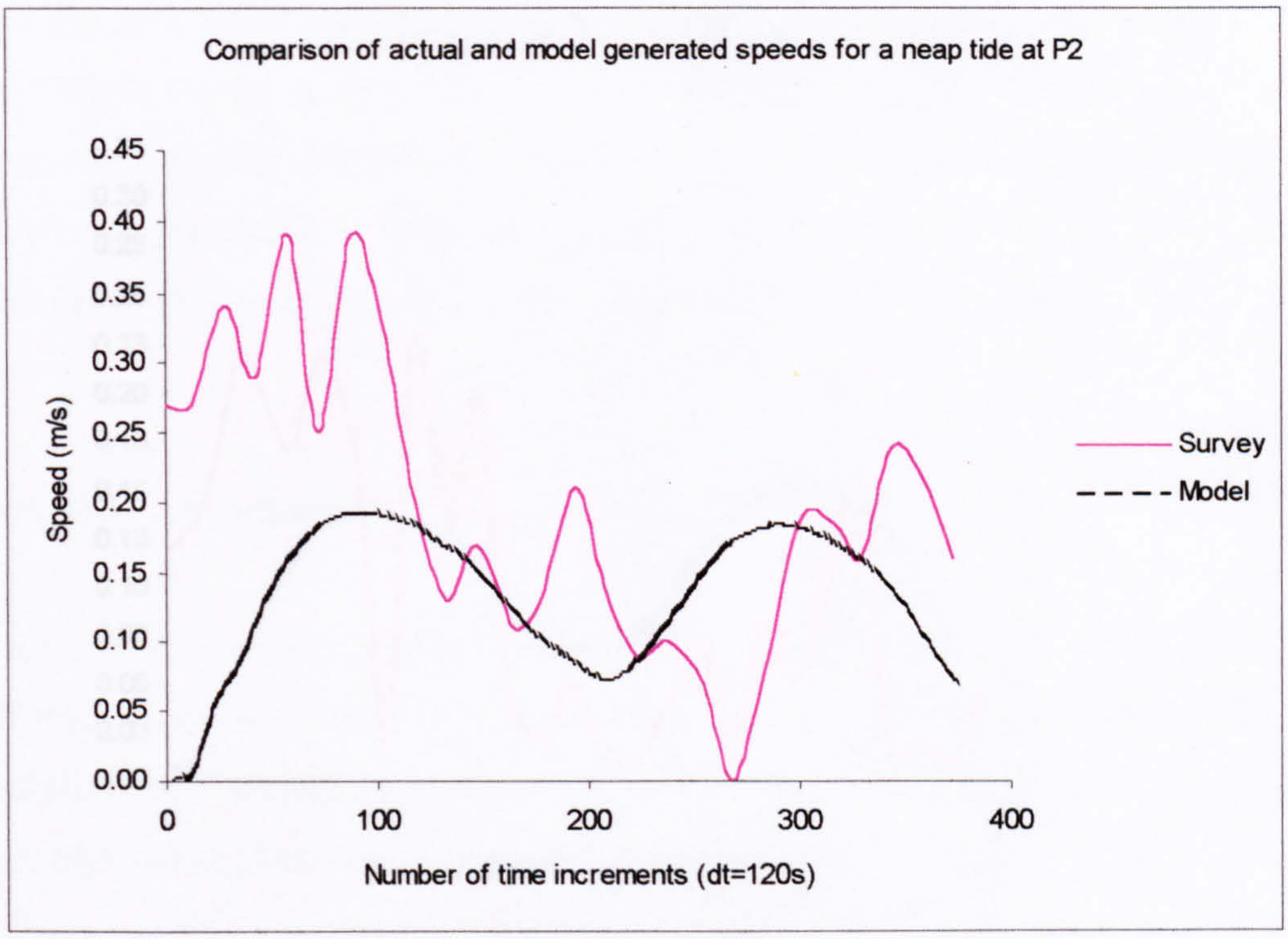

Figure (7.17) Plot of surveyed and calculated speeds at P2

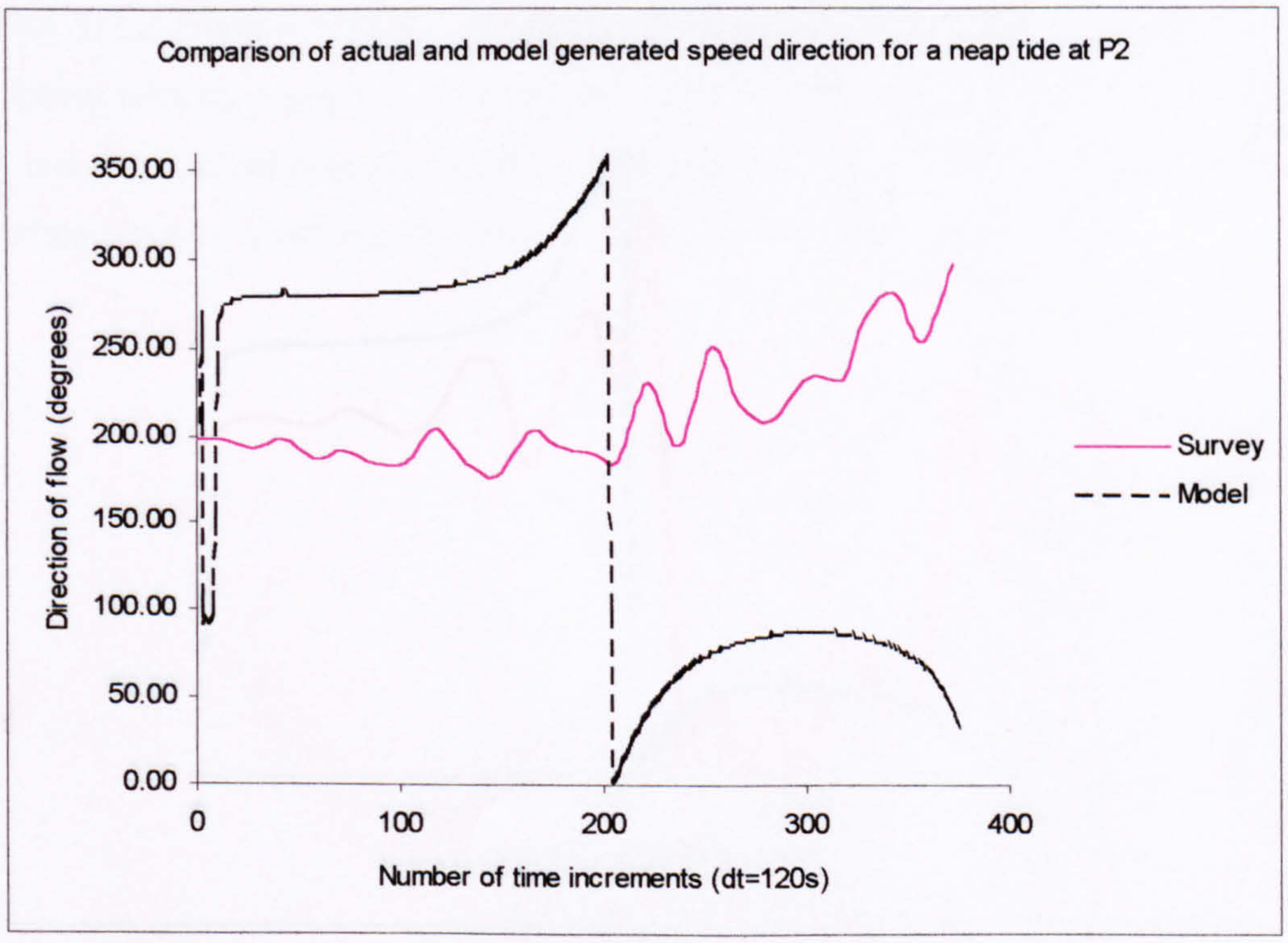

Figure (7.18) Plot of surveyed and calculated directions at P2

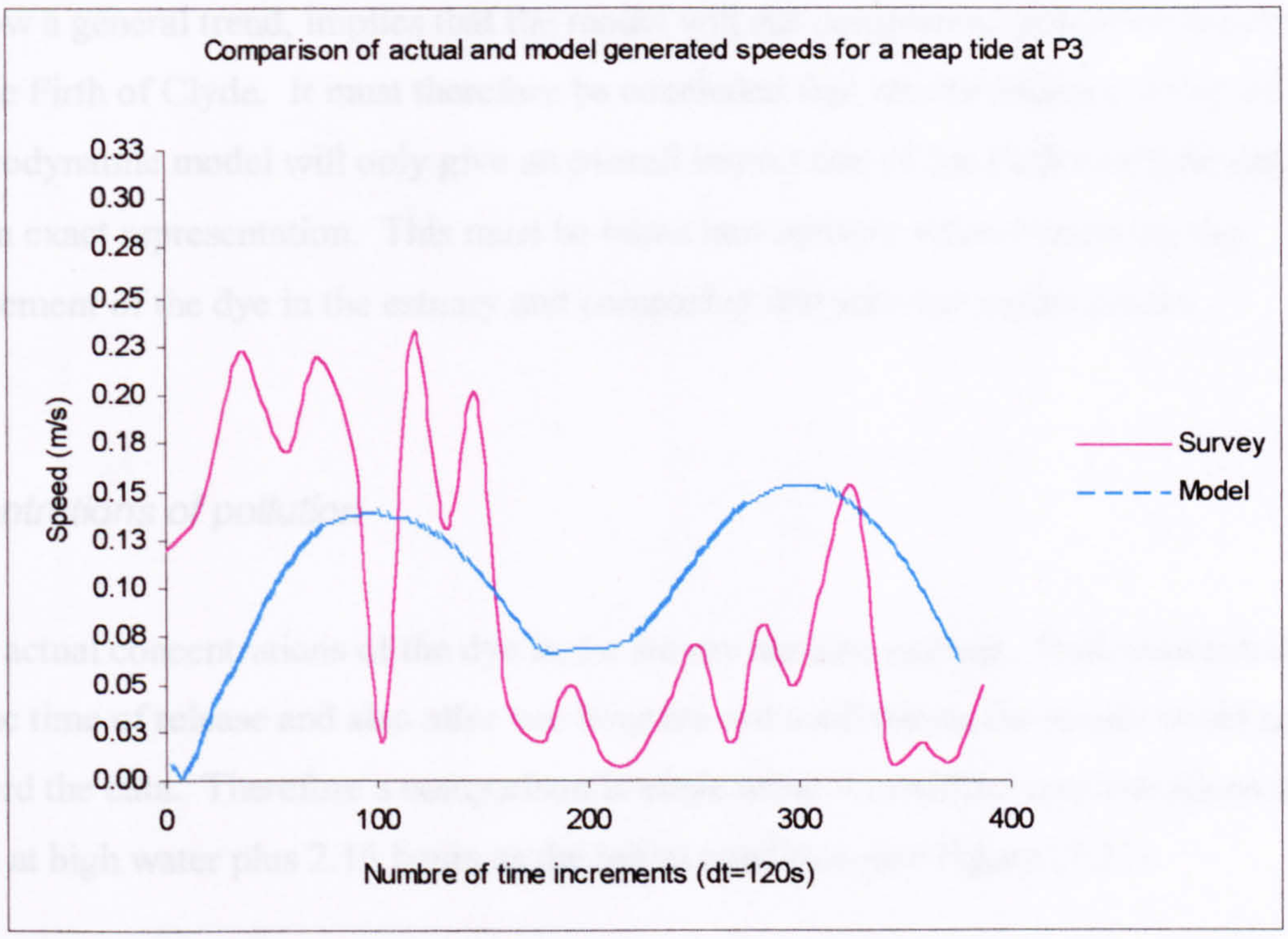

Figure (7.19) Plot of surveyed and calculated speeds at P3

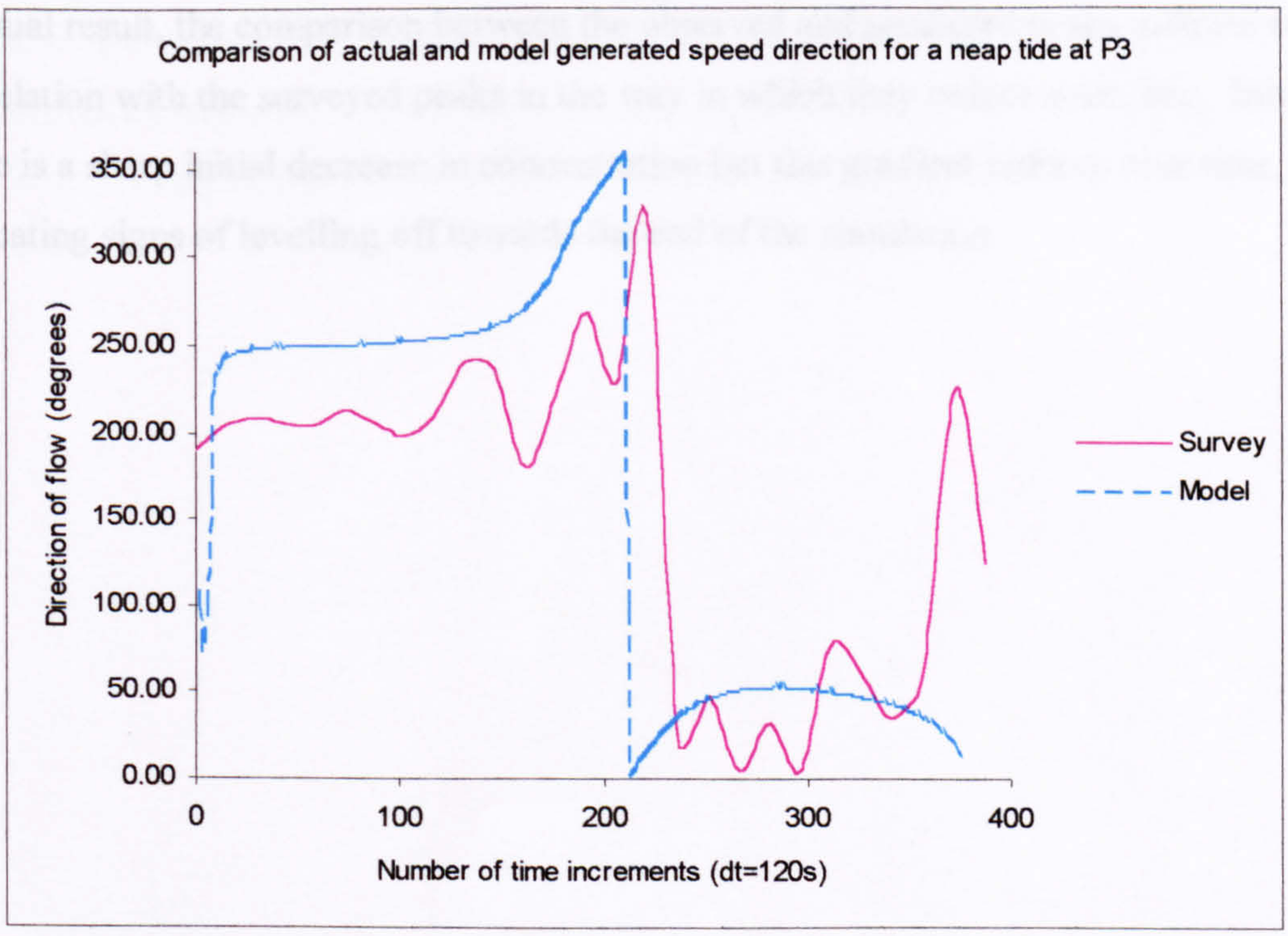

Figure (7.20) Plot of surveyed and calculated directions at P3

The fact that the predicted results do not exactly match the observed data, but only follow a general trend, implies that the model will not completely reproduce conditions in the Firth of Clyde. It must therefore be concluded that results obtained using this hydrodynamic model will only give an overall impression of the Firth of Clyde and not be an exact representation. This must be taken into account when examining the movement of the dye in the estuary and comparing this with the model results.

Concentrations of pollution

The actual concentrations of the dye in the survey are also unclear. Peak concentrations at the time of release and also after one hour are not available as the sensor could not record the data. Therefore a comparison is made using normalised concentrations using data at high water plus 2.15 hours as the initial condition, see Figure (7.21).

These results indicate that some error in recording the survey data was made as there is a sudden increase in concentration at high water plus 4.65 hours. In spite of this unusual result, the comparison between the observed and predicted peaks indicate some correlation with the surveyed peaks in the way in which they reduce over time. Initially there is a sharp initial decrease in concentration but this gradient reduces over time, indicating signs of levelling off towards the end of the simulation.

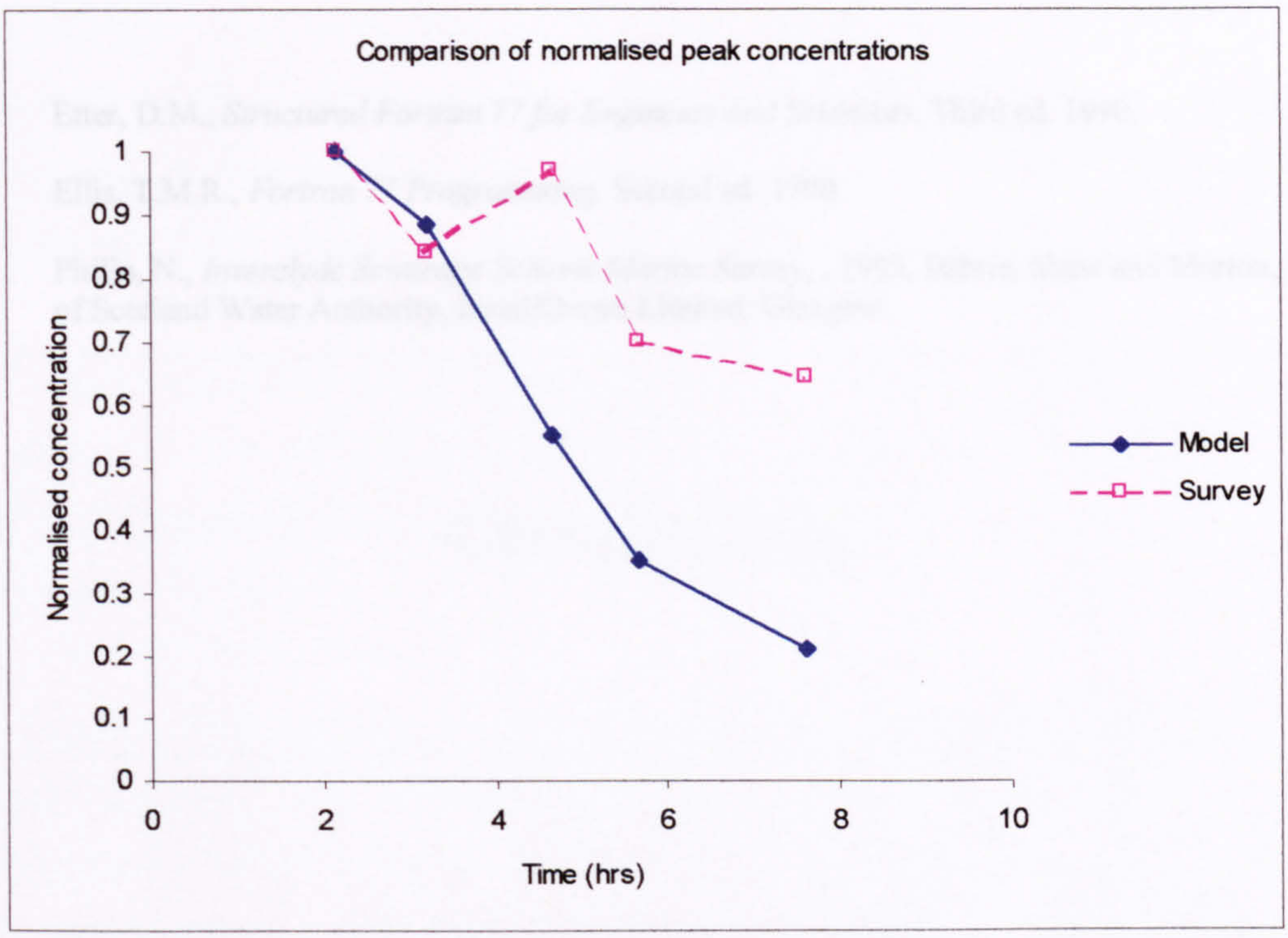

Figure (7.21) Plot of normalised surveyed and simulated peak concentrations

From the analysis of these comparisons it can be concluded that, the six point method of characteristics has been successfully implemented in DIADEM3D. However further field tests are required to evaluate its true value to industry.

7.4 References

1. Etter, D.M., *Structured Fortran 77 for Engineers and Scientists*. Third ed. 1990.

2. Ellis, T.M.R., *Fortran 77 Programming*. Second ed. 1990.

3. Philip, N., *Inverclyde Sewerage Scheme Marine Survey*, . 1995, Babtie, Shaw and Morton, West of Scotland Water Authority, InstallOcean Limited: Glasgow.

Chapter 8

Conclusions

8.1 Discussion 220

8.2 Conclusions 223

8.3 References 224

8.1 Discussion

The solution of the advection equation is shown to be a difficult task. Any numerical scheme used for simulating convection must be both accurate and stable. Time is an additional condition when the application is commercial.

Four popular finite difference schemes were analysed in Chapter 3, upwinding[1], central differencing[2], QUICK[3] and QUICKEST[3]. Of these schemes, upwinding and QUICKEST produced the most stable and numerically accurate results in one-dimension.

The method of characteristics was also considered as a means of solving the advection equation. Chapter 4 investigated the basic linear approach[4], Holly-Preissmann[5] and two multi-point schemes based on work by Holly Jr. and Komatsu[6] and Komatsu *et al*[7]. The eight and six point method of characteristics developed were shown to be highly stable, accurate and easier to extend into two-dimensions than the classical Holly-Preissmann approach.[8]

The four numerical methods, upwinding, QUICKEST, the eight and six point methods of characteristics, were developed into two-dimensions and compared using three different pollution distributions in Chapter 5. All of the schemes suffered from a degree of numerical diffusion and inaccuracy under specific conditions. Upwinding demonstrated significant diffusion for Courant numbers less than one. QUICKEST and the eight and six point methods of characteristics exhibited this to a lesser extent in most cases. However, in testcases using a point release of pollution all of the schemes fared less well, considerably underpredicting the peak.

Tests were also carried out using Courant numbers exceeding unity. Under these circumstances all of the methods showed signs of numerical instability (Chapter 6). This clearly indicates that under the specific circumstances where the Courant number is high, or the pollution distribution has sharp gradients, there are limitations with these numerical schemes.

As the ultimate aim of this work is to derive and implement a numerical scheme into an industrial model, where computational efficiency would be important, the time step issue was tackled. For further developments of the model, the problems associated with modelling sharp changes in concentration should also be addressed in future work.

Chapter 6 is concerned with improving the six point method of characteristics and QUICKEST such that they can be solved using Courant numbers greater than one without compromising accuracy or stability. The spatial reachout technique, used by Yang and Chiu[9] with the Holly-Preissmann scheme, was incorporated into the six point method of characteristics. This novel combination of the two schemes allows a simulation to be run using a wider range of Courant numbers.

The eight point method of characteristics was used to solve the advection term for Courant numbers up to 15. These tests were highly successful as the solutions were numerically stable. They also became more accurate as the Courant number increased as fewer interpolations were required in the simulation.[10] This was an additional benefit to the fact that the computational time could be significantly reduced using larger time increments. This is advantageous in industry as a reduction in computational time will allow many different simulations to be executed quickly, resulting in an improved overall efficiency.

The QUICKEST approach was also improved with respect to computational efficiency. In this case the spatial reachout technique was used to locate the control volume at which QUICKEST solved the advection term. This was based on work by Manson and Wallis[11] who used a method of characteristics to locate the control volume for one-dimensional QUICKEST, solving advection in streamtubes. This is a new approach because the application is fully two-dimensional for the advection term. The same benefits of increased accuracy with a greater Courant number are also observed in this case.

The implementation of the six point method of characteristics into DIADEM3D, in Chapter 7, was also a significant development. Previously DIADEM3D used finite difference schemes, including upwinding and QUICKEST to solve the advection term.

As the six point method of characteristics has been shown to be an improvement on both approaches, this is an important adaptation. The fact that the scheme can also be applied using a large time increment is also beneficial in this commercial model. However, the water quality simulation would have to run independently from the hydrodynamics as this has not been developed to run at Courant numbers exceeding unity.

The application of the scheme to the Firth of Clyde demonstrates that this approach has been implemented successfully.

8.2 Conclusions

- Of the finite difference schemes tested, QUICKEST is the most numerically accurate. When extending this scheme from one to two-dimensions it is important that the full derivation including all cross derivatives should be employed.

- For the test cases considered, the multi-point method of characteristics derived here proved to be more accurate than QUICKEST.

- The six point method of characteristics is shown to be as accurate as the eight point approach. As it is the most compact of the two multi-point schemes it is easier to implement in two-dimensions.

- The flexibility of the six point method of characteristic has been enhanced by the inclusion of the spatial reachout method. It was observed that as the Courant number increased, the predictions made by this scheme with the spatial reachout method, became more accurate, due to the fact that fewer interpolations were required.

- The QUICKEST scheme was also adapted using the spatial reachout technique to locate the control volume for the finite difference scheme. This allows large time increments to be used in this approach.

- The six point method of characteristics was successfully implemented in DIADEM3D, demonstrating its application in an industrially relevant testcase.

8.3 References

1. van Eijkeren, J.C.H., de Haan, B.J., Stelling, G.S., and van Stijn, T.L., "Linear Upwind Biased Methods", in *Numerical Methods for Advection-Diffusion Problems*, C.B. Vreugdenhil and B. Koren, Editors. 1993. 55-88.

2. Koutitas, B., *Mathematical Models in Coastal Engineering*. 1988: Pentech Press, Ltd.

3. Leonard, B.P., "A stable and accurate convective modelling procedure based on quadratic upstream interpolation", *Computer methods in applied mechanics and engineering*, 1979, **19**, 59-98.

4. Abbott, M.B., *An Introduction to the method of characteristics*. 1966, New York: American Elsevier.

5. Holly, F.M. and Preissmann, A., "Accurate calculation of transport in two dimensions", *Journal of the Hydraulic Division, ASCE*, 1977, **103**, 1259-1277.

6. Holly Jr., F.M. and Komatsu, T. *Derivative approximations in the two-point fourth order method for pollutant transport*. in *Frontiers in Hydraulic Engineering*. 1983. MIT, MA: ASCE.

7. Komatsu, T., Holly, F.M., Nakashiki, N., and Ohgushi, K., "Numerical calculation of pollutant transport in one and two-dimensions", *Journal of Hydroscience and Hydraulic Engineering*, 1985, **3**, 15-30.

8. Glass, J. and Rodi, W., "A higher order numerical scheme for scalar transport", *Computer methods in applied mechanics and engineering*, 1982, **31**, 337-358.

9. Yang, J.C. and Chiu, K.P., "Use of Characteristics Method With Cubic Interpolation For Unsteady-Flow Computation", *International Journal For Numerical Methods in Fluids*, 1993, **16**(4), 329-345.

10. Wiggert, D.C. and Sundquist, M.J., "Fixed-grid characteristics for pipeline transients", *Journal of the Hydraulics Division*, 1977, **103**(HY12), 1403-1416.

11. Manson, J.R. and Wallis, S.G., "An accurate numerical algorithm for advective transport", *Communications in Numerical Methods in Engineering*, 1995, **11**(12), 1039-1045.